ABSTRACT

Total Synthesis of (±)-Caesalpinnone A and (-)-Caesalpinflavan B, Progress Toward the Total Synthesis of (+)-Alterbrassicicene C and (-)-Alterbrassicicene B

Noah J. Sims, Ph.D.

Mentor: John L. Wood, Ph.D.

In 2017, caesalpinnone A was isolated alongside three congeners, caesalpinflavans A-C. Caesalpinnone A possesses an unprecedented oxa-bridged ring system and displays modest cytotoxicity against a variety of cancer cell lines including MFC-7. To explore the structural features and the aforementioned bioactivity, a synthesis of these natural products was developed. The latter entails an early stage Barluenga coupling to convergently cross-couple two hindered, functionalized arenes. The derived material was advanced by reduction, protecting group interchange, and a Claisen Schmidt condensation to furnish the remainder of the carbon skeleton. A late-stage allyl deprotection leads to a spontaneous, chemoselective oxa-Michael to complete the synthesis of (±)-caesalpinnone A in 7 steps from known materials.

Alterbrassicicene C and B were isolated alongside a number of family members in 2019 from *Alternaria brassicola.* The alterbrassicicenes belong to the brassicene family, which is part of the even larger fusicoccane terpenoid family. Several investigations of the fusicoccane family have revealed that numerous members possess remarkable biological

activity. Structurally, alterbrassicicene C manifests an unprecedented tetracyclic 5/6/6/5 ring system that features three quaternary centers. In developing an asymmetric synthesis of the alterbrassicicene, we designed a reductive enzymatic desymmetrization that effectively delivers a versatile early intermediate. The route employed to advance this latter intermediate features a lithium-halogen exchange and ring closing metathesis to assemble the 5/8/5 parent scaffold in only 7-steps from known materials. A silver promoted, oxiranium-stabilized rearrangement serves to transfer stereochemistry across the 8-membered ring. While this latter chemistry was employed in efforts to complete alterbrassicicene B, the transannular ethereal bridge this rearrangement produces can also serve as a precursor from which one can initiate an oxa-Michael/retro-oxa-Michael cascade to deliver the alterbrassicicene C oxygen/carbon scaffold.

Total Synthesis of (±)-Caesalpinnone A and (-)-Caesalpinflavan B, Progress Toward the Total Synthesis of (+)-Alterbrassicicene C and (-)-Alterbrassicicene B

by

Noah J. Sims, B.S.

A Dissertation

Approved by the Department of Chemistry and Biochemistry

_____

John L. Wood, Ph.D., Chairperson

Submitted to the Graduate Faculty of
Baylor University in Partial Fulfillment of the
Requirements for the Degree
of

Doctor of Philosophy

Approved by the Dissertation Committee

_____

John L. Wood, Ph.D., Chairperson

_____

Kevin G. Pinney, Ph.D.

_____

Caleb D. Martin, Ph.D.

_____

Daniel Romo, Ph.D.

_____

Leigh Greathouse, Ph.D.

Accepted by the Graduate School

December 2022

_____

J. Larry Lyon, Ph.D., Dean

Page bearing signatures is kept on file in the Graduate School.

TABLE OF CONTENTS

LIST OF FIGURES

LIST OF TABLES

LIST OF SCHEMES

ABBREVIATIONS

Ac	acetyl
AIBN	2,2'-azobis(2-methylpropionitrile)
Ar	aromatic
Bn	benzyl
Bu	butyl
Cat.	Catalytic
CD	circular dichroism
DCM	dichloromethane
DBU	1,8-Diazoabicyclo[5.4.0]undec-7-ene
DIPEA	diisopropylethylamine
DMAP	4-(dimethylamino)pyridine
DMDO	dimethyldioxirane
DMF	*N,N*-dimethylformamide
DMP	Dess-Marin Periodinane
dr	diastereomeric ratio
ent	enantiomer(ic)
epi	epimer(ic)
equiv	equivalent(s)
er	enantiomeric ratio
ESI	electrospray ionization
Et	ethyl
EtOAc	ethyl acetate
FT	fourier transform
HAT	hydrogen atom transfer
Hex	hexanes
HPLC	high pressure liquid chromatography
HRMS	high resolution mass spectrometry
IPA	isopropanol
KHMDS	potassium bis(trimethylsilyl)amide
LDA	lithium diisopropylamine
LiHMDS	lithium bis(trimethylsilyl)amide
mCPBA	meta-chloroperbenzoic acid
Me	Methyl
MeCN	acetonitrile
MS	molecular sieves
NBS	*N*-bromosuccinamide
NMR	nuclear magnetic resonance
Nu	nucleophile
Ph	phenyl
PIDA	phenyl iodo-diacetate

PTSA	4-toluenesulfonic acid
py	pyridine
SCXRD	single crystal X-ray diffraction
TBAF	tetrabutylammonium fluoride
TBS	*tert*-butyldimethylsilyl
*t*Bu	*tert*-butyl
TEA	triethylamine
Tf	trifluoromethylsulfonyl
TFA	trifluoroacetate
THF	tetrahydrofuran
TLC	thin-layer chromatography
TMS	trimethylsilyl
UV	ultraviolet

ACKNOWLEDGMENTS

"I can do all this through Him who gives me strength."

Philippians 4:13 NIV

The number of times I have said this verse throughout my graduate career is extraordinarily high, but the verse says it all. God is good.

I would be remiss if I didn't give John the credit he deserves. He has been extraordinary supportive and understanding through the many trials and tribulations I have experienced in my time at Baylor. Beyond this, thank you for being supportive in letting me try the egregious number of 'bad' ideas that, at the time, I thought would be revolutionary. Clearly most of them weren't, and I am sure he knew that ahead of time… Thank you for being an amazing advisor, and I am glad to be able to call you a colleague in the future.

To the lab, I want to say thank you as well. To Jacob, thank you so much for being patient with me while I earned the necessary fundamental techniques and skills. JGTFC. You are a great chemist and friend. To Ricky, I will forever miss your insight about getting hosed. To Lin, I am glad we could experience this together, and thank you for keeping the lab a 'safer' place. To Amy, thank you for your X-ray skills and getting coffee with me. To Tae, I appreciated your level-headedness throughout our time and your great chemical intuition, it has helped me many times.

Beyond the lab, I need to thank my amazing wife, Bea. I am forever thankful that during my graduate career, despite the weird schedule and stress, you were always there

and made the day-to-day so much more pleasant. From listening to my non-sensical practice presentations to proofreading my gibberish, you did it all. Without you, I can not imagine having gotten through it. I am eternally grateful for you.

Finally, I would like to thank my family, especially my parents. From a young age, I always remember mixing random foods, chemicals, and objects to see if anything would happen, and even when I tried melting a rock with mustard, you guys always supported me. Thank you for fostering my curious nature. Most of all, thank you for always being there when I needed a pick-me-up or a call. I love you all.

DEDICATION

To my amazing wife, Bea and to my supportive parents, Jeffrey and Stacey. Thank you.

CHAPTER ONE

Total Synthesis of (±)-Caesalpinnone A and (-)-Caesalpinflavan B

1.1 Isolation of Caesalpinnone A and the Caesalpinflavans A-C

In 2017, Wang and coworkers isolated caesalpinnone A and the caesalpinflavans A-C from the twigs and leaves of *Caesalpinia enneaphylla*.[1] This plant can be found in China, India, Sri Lanka, Burma and other Asian countries. Structural elucidation revealed that caesalpinnone A (**1.01**, Figure 1.1) has an intriguing bicyclic structure; it possesses a 10,11-dioxatricyclic-[5.3.3.$0^{1,6}$]tridecane bridged system. This bridged ring-system was completely unprecedented in the literature. Additionally, **1.01** contains two alpha-beta unsaturated ketone moieties, a substituted chalcone, and a bridged acetal. Although the isolation chemists report extensive spectroscopic support for the assigned structure, the crystalline nature of **1.01** eventually allowed confirmation of the structural assignment by X-ray analysis. The caesalpinflavans (**1.02-1.04**) are clearly structurally related but lack the bridged ring-system.

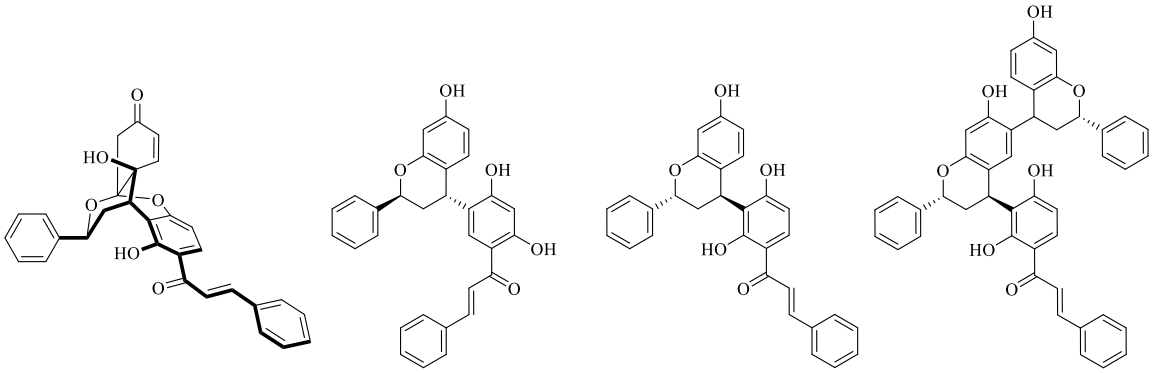

Figure 1.1 Reported structures of caesalpinnone A and caesalpinflavan A-C

Upon obtaining milligram quantities of the natural products, the isolation chemists performed biological studies to probe any pharmacological potential. Against a variety of cancer cell-lines it was found that **1.01**-**1.04** all possess biological activity, with that of caesalpinnone A being the most potent displaying activity in the sub-micromolar IC_{50} range. Specifically, caesalpinnone A had an IC_{50} = 0.87 μM against MCF-7, a human breast cancer cell line. The structural features alongside the biological activity made caesalpinnone A an attractive target for synthesis.

1.2 Retrosynthetic Analysis of Caesalpinnone A and Caesalpinflavan B

1.2.1 Biosynthetic Hypothesis

In determining the most suitable approach for a synthesis of caesalpinnone A, we noted a potential a connection between the natural products that was not addressed by the isolation chemists. We theorized that caesalpinflavan B may actually be the precursor to caesalpinnone A via selective oxidation of the "A- ring" followed by a conjugate addition of the bisphenol (Scheme 1.1). Furthermore, it was hypothesized that caesalpinflavan B derives from flavanone **1.05** and the chalcone **1.06** by a covalent connection between the 'C' and 'D' rings.[2,3] This interesting connection would eventually lead to inspiration for our retrosynthetic analysis.

However, one problem with this hypothesis is that the absolute stereochemistry assigned by the isolation chemists to the two natural products (**1.01** and **1.03**) is antipodal at carbons-2" and -4". We reasoned that it would be unlikely for both centers to undergo epimerization during biosynthesis thus, we conjectured that the isolation chemists had misassigned the absolute stereochemistry of caesalpinflavan B. This is likely due to the

fact that the isolation chemists assigned the absolute stereochemistry based on comparison of CD spectra to analogous natural products, a strategy that has led to incorrect assignment in the past.[4] Notably, caesalpinnone A's absolute stereochemistry is based on high quality single-crystal X-ray diffraction (SCXRD). In order to validate this hypothesis, we concluded that we would need to develop an enantioselective synthesis of caesalpinflavan B and compare the optical rotation data derived from the natural and synthetic products.

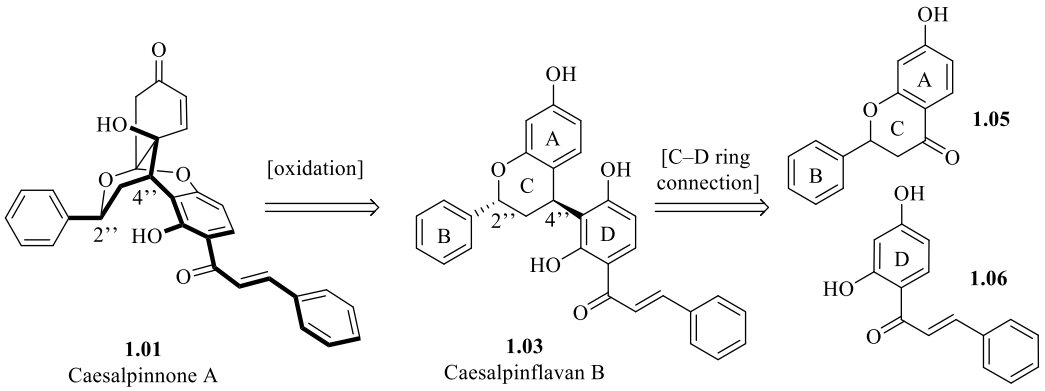

Scheme 1.1 Putative biosynthesis of caesalpinnone A from caesalpinflavan B

1.2.2 A General Unified Approach

In accord with the hypothesis mentioned above, we turned toward developing a route to caesalpinnone A wherein caesalpinflavan B would serve as an advanced intermediate. As illustrated retrosynthetically in Scheme 1.2, we envisioned that late stage de-allylation of **1.07**, followed by oxa-Michael would furnish the natural product. Dienone **1.07** would arise from aromatic oxidation of phenol **1.08** which, notably, is a protected variant of caesalpinflavan B (**1.03**). We hypothesized that protected-caesalpinflavan B could be synthesized from reduction of pyran **1.09**. To furnish the sterically encumbered pyran, we surmised that the underutilized Barluenga cross-coupling would be a worthwhile

strategy to investigate.[5] The latter would allow us to start our synthesis with a simple tosyl hydrazone (**1.10**) and aryl iodide (**1.11**).

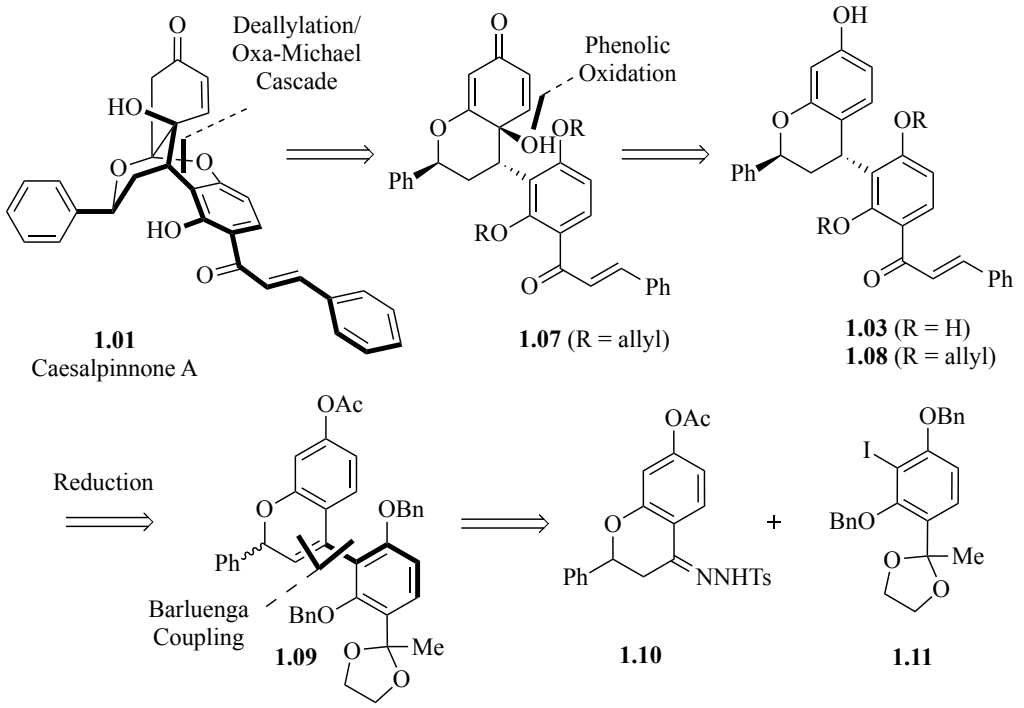

Scheme 1.2 Retrosynthetic Approach to caesalpinnone A

1.3 Evolution of a Concise Approach to (±)-*Caesalpinnone A*

1.3.1 Synthesis of Coupling Partners

To prepare the aryl iodide component for the Barluenga cross-coupling, we began with commercially available 2',4'-dihydroxyacetophenone (Scheme 1.3 top, **1.12**) and performed a mono-iodination which regioselectively delivered the illustrated product wherein the iodine resides in a meta position relative to the methyl ketone. This was followed bis-benzyl protection to give ketone **1.13**. Finally, acetal protection with ethylene

glycol using traditional Dean-Stark conditions gave aryl iodide **1.11** in an overall yield of 89% for the 3-steps.

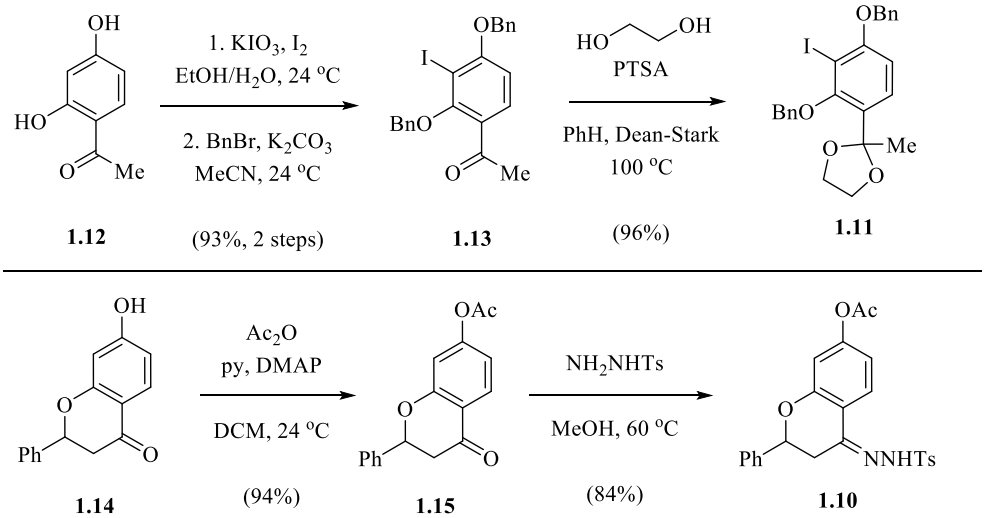

Scheme 1.3 Synthesis of coupling partners

To construct the desired tosyl hydrazone (**1.10**, Scheme 1.3, bottom), we began from 7-hydroxyflavanone **1.14** which, upon treatment with acetic anhydride, pyridine, and catalytic DMAP in DCM produced the protected phenol **1.15** in 94% yield. Exposure of the derived acylated ketone to tosyl hydrazine in hot methanol produced hydrazone **1.10** in 84% yield after recrystallization from MeOH.

1.3.2 Employing the Barluenga Cross-Coupling

Having developed efficient and robust routes to both coupling partners **1.10** and **1.11**, we were ready to explore the Barluenga cross coupling (Table 1.1).[5] In addition to the ease with which the coupling partners could be prepared, in particular the tosyl hydrazone as compared to a vinyl boronic ester or stannane, the Barluenga reaction held

promise due to the intermediate Pd-carbenoid's ability to smoothly undergo very hindered migratory insertions. Mechanistically the latter carbenoid derives from an initially formed diazo species produced upon *in situ* exposure of the hydrazone to base. Although literature precedents provided some guidance to or efforts to apply the Barluenga coupling, we employed automatic high throughput screening to explore a number of the reaction variables. This study eventually led to our finding that the Buchwald pre-catalyst, XPhos Pd G3, is uniquely effective in promoting this transformation. Fluorobenzene was found to give the highest yields after a moderate solvent screen. Although fluorinated solvents often have mysteriously positive effects on various transformations, in this particular reaction we attribute at least some of the improved efficiency to increased solubility of the tosylhydrazone. In terms of reagent stoichiometry, nearly equivalent amounts of both coupling partners were found to result in complete consumption of the starting materials but only a modest 37% yield of the desired benzopyran (**1.09**) as a 1.8: 1 mixture of inconsequential atropisomers (Table 1.1, entry 1).

Table 1.1. Optimization of Barluenga Cross-Coupling

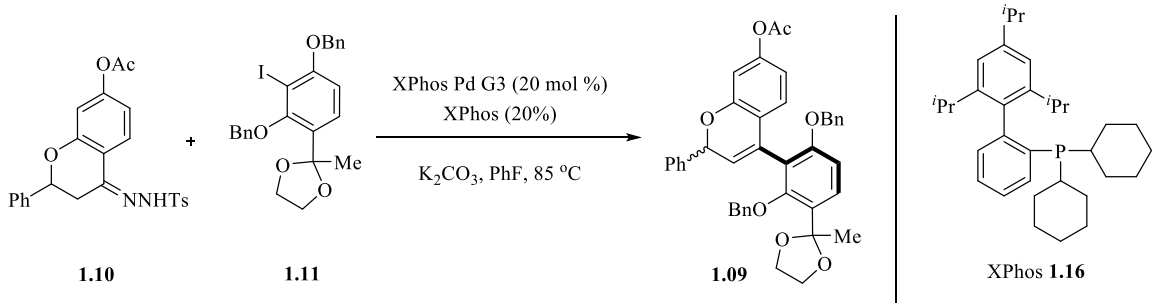

1.10 **1.11** **1.09** XPhos **1.16**

Entry	Conditions	Equiv. **1.10**/**1.11**	Equiv. K_2CO_3	Time (h)	Yield (%)
1	Excess **1.10**	1.2/1.0	2.8	4	37
2		2.5/1.0	4.0	12	44
3	Excess **1.11**	1.0/2.0	3.0	12	67
4		1.0/2.5	3.0	22	68
5	Slow addition **1.10**[a,b]	2.5/1.0	5.0	16	91

[a]10h of addition, 6h of additional time [b]1:2.2 v/v PhF:1,4-dioxane

In efforts to improve the yield, our attention turned to the likelihood that the intermediate diazo compound was undergoing deleterious side reactions. Diazo compounds are known to be promiscuous functional groups that can do many types of reactions, such as the Bamford-Stevens elimination, dimerizations, etc.[6] Given numerous possible deleterious fates for the diazo intermediate we opted to explore increasing the equivalents of tosyl hydrazone. While these efforts were rewarded with some initial yield increases, the levels were not sufficient for significant material throughput. Eventually, through intensive screening, we found that slow addition of the tosyl hydrazone was crucial for high yields (91%).

1.3.3 Conformation Analysis and Preliminary Studies of Benzopyran Reduction

After combining the two coupling partners (**1.10** and **1.11**), we next needed to reduce pyran **1.09**. We suspected from the outset that the latter transformation would be a challenge due to the potential difficulties with both chemo- (benzylic vs. alkene reduction) and stereo-selectivity (syn vs. anti) issues (Scheme 1.4). With regard to the latter, from a kinetic perspective one would predict that hydrogenation-type reductions would preferably deliver H_2 from the least hindered face, opposite the phenyl ring attached to the stereogenic carbon at position 2'' (Scheme 1.14A), thus resulting in syn-arenes (**1.17b**). Thermodynamically, based on literature precedent,[7] one would predict that a 1,3-diaxial interaction between the phenyl ring and the benzylic methine would lead to a preference for both arenes to be pseudo-equatorial, thereby also leading to the undesired syn-diastereomer. Despite the anticipated challenge, we attempted to reduce the olefin directly. In the event, we found that hydrogenation of pyran **1.09** suffers from sluggish olefin reduction and results in products derived benzylic hydrogenolysis and cleavage of the benzylic ether within the benzopyran. In turning next to reductions that would be expected to deliver thermodynamic-type products, we attempted a slew of dissolving metal conditions. Typically, the only isolable products from these latter conditions appeared to derive from either benzyl deprotection or fragmentation-type reactions. Based on the failures we were experiencing with direct reductions, we opted to next explore stepwise approaches to set the desired trans-stereochemistry.

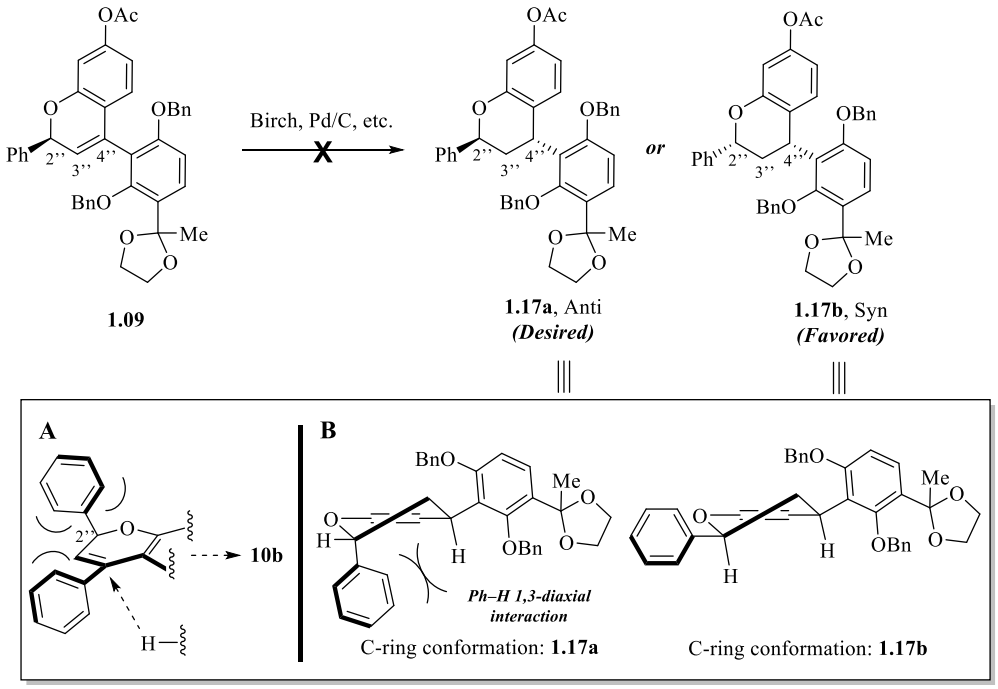

Scheme 1.4 Conformational analysis of benzopyran reduction

1.3.4 Stepwise Approach to Achieve the Trans-Diastereomer

In considering alternative approaches to the correct trans-diastereomer (**1.17a**), we explored a route wherein the stereochemistry would be introduced on an intermediate possessing a different substitution pattern about the benzopyran, thus potentially changing the stereochemical preference. Toward this latter end, we began by exposing pyran **1.09** to mCPBA in the presence in $NaHCO_3$. These conditions cleanly furnished an intermediate epoxide (**1.18**, Scheme 1.5) which, followed by spontaneous epoxide opening, formed the *p*-quinone methide **1.19** in 69% yield. Going forward, the hope was that the diastereotopic face selectivity observed upon reduction of the quinone methide by treatment with $NaBH_4$ would be biased toward delivery of the hydride from the β-face, thereby giving the desired trans-stereochemistry relative to the arenes. Unfortunately, the rection produced a 1.7:1 mixture of diastereomers, favoring the illustrated syn isomer (**1.20**) in a ratio of 1.7:1. The

illustrated stereochemistry of **1.20** and the preceding intermediates was supported by low-quality X-ray analysis of the major diastereomer. Although this initial result was disappointing, we recognized there were other options for advancing the *p*-quinone methide.

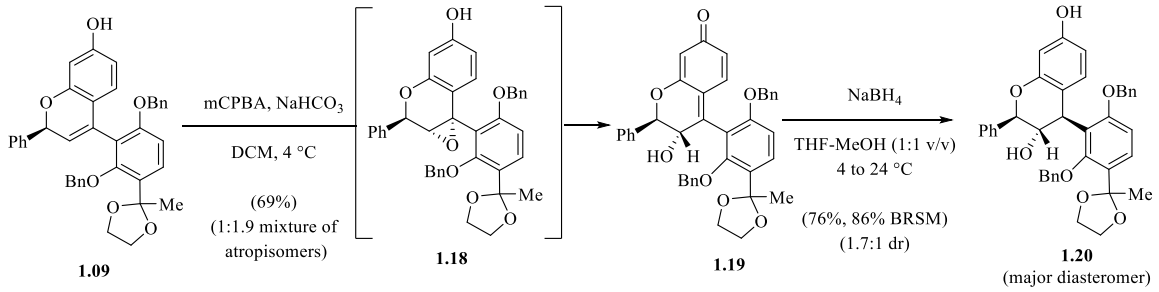

Scheme 1.5 Access to *p*-quinone methide

In exploring alternatives for advancing **1.19** we turned next toward the intramolecular transfer of hydride. Based on the stereochemistry of the intermediate there was a possibility that suprafacial 1,2-hydride shift could directly deliver the desired stereochemistry. However, as illustrated in Scheme 1.6, exposure of **1.19** to BF_3•OEt_2 effected clean 1,2-hydride shift, but unfortunately the resultant ketone rapidly tautomerized to furnish the corresponding enol (**1.21**, Scheme 1.6) in 94% yield. Interestingly, we found that exposure of the keto/enol mixture of **1.21** and **1.22** to borane *t*-butylamine complex gave a good yield of corresponding alcohol diastereomer **1.23** in 42% yield. Other hydride sources gave generally lower yields and poor diastereomeric mixtures.

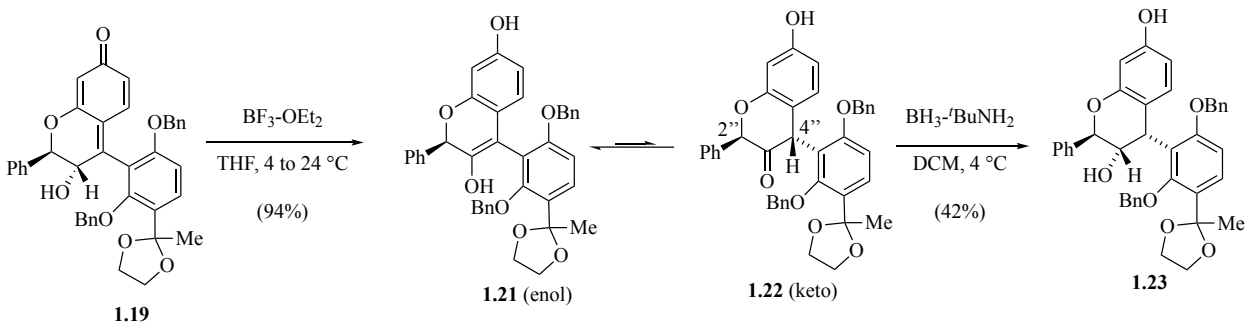

Scheme 1.6 Elaboration of quinone methide to anti-arenes

Although at this point we had set the requisite stereochemistry at C-2" and -4", deoxygenation of the secondary alcohol was required to complete construction of the desired intermediate. To this end, considering the functionality present in the molecule, it was decided that the Barton-McCombie reaction would be the most suitable deoxygenation method.[8] After considerable experimentation, it was found that treatment of diol **1.23** with KH and CS_2, followed by methylation, gave bis-xanthate **1.24** (Scheme 1.7). Typical deoxygenation conditions resulted in the desired product (**1.17**). Although this approach gave us the desired trans-selectivity for the first time, it was horrendously inefficient with 3 redox manipulations and 5-steps to affect the overall single reduction of **1.09**. Not comfortable with this route, we began considering alternative approaches to access **1.17**.

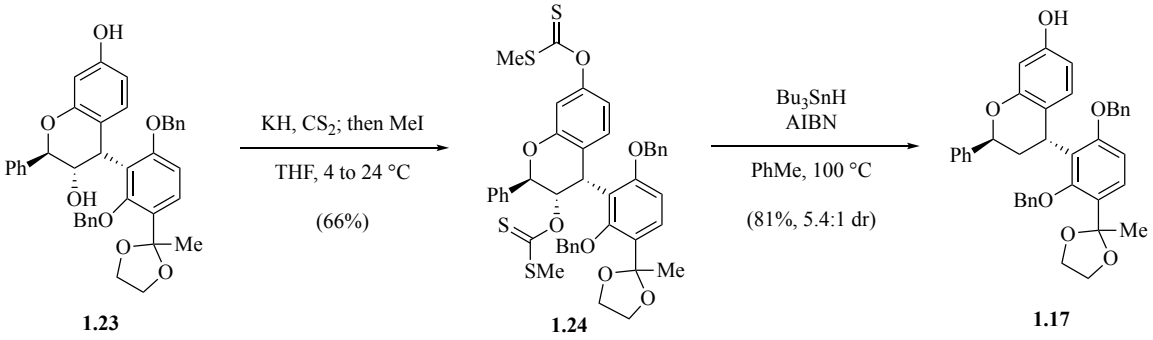

Scheme 1.7 Deoxygenation of secondary alcohol

1.3.5 Utilization of Hydrogen Atom Transfer

In search of a more direct route to dihydropyran **1.17**, we turned to Shenvi's very recently developed hydrogen atom transfer (HAT) chemistry.[9] Shenvi has demonstrated that this latter method is quite robust and displays excellent chemoselectivity for olefins. Due to the radical intermediates produced in this reaction, the stereochemical outcome would potentially be thermodynamically controlled and thus this method held the possibility of providing at least some of our desired trans-stereoisomer **1.17a** in a single step. Excited about the potential, we began by attempting this transformation employing only a slight modification of the reported conditions (Entry 1, Table 1.2), which entailed adding DCM to help solubilize the starting material. To our delight, under these conditions, we observed a clean and efficient reduction (84% yield) but unfortunately the resultant mixture of diastereomers (1:2.2) significantly favored the undesired diastereomer (**1.17b**).

Table 1.2 Optimization of Shenvi HAT

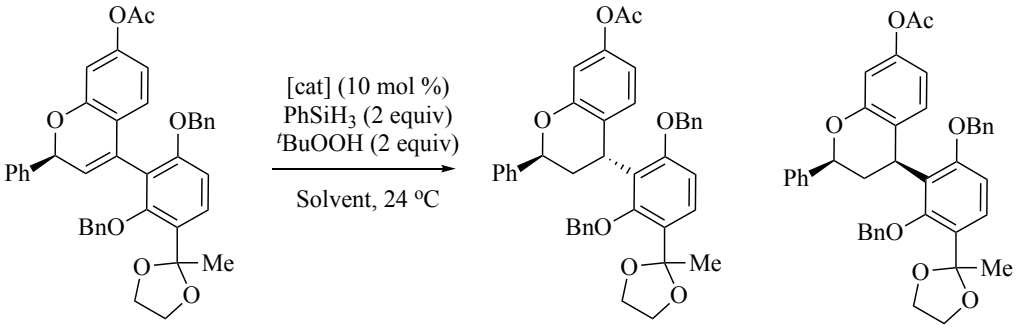

1.09 | **1.17a** (Desired) | **1.17b**

Entry	Catalyst	Solvent	Time (h)	Yield (%)[a]	1.17a:b[b]
1	$Mn(dpm)_3$	DCM/IPA (1:1)	2	84	1:2.2
2	$Fe(acac)_3$	DCM/IPA (1:1)	18	<5	
3	(R,R)-$Mn(Salen^{tBu,tBu})Cl$	DCM/IPA (1:1)	18	<5	
4	$Mn(dpm)_3$[c]	DCM/IPA (1:1)	4	(68)	1:2.5
5	$Mn(dpm)_3$	THF/IPA (1:1)	24	<5	
6	$Mn(dpm)_3$	PhH/IPA (1:1)	22	(74)	1:1.1
7	$Mn(dpm)_3$	PhMe/IPA (1:1)	5	67	1.5:1
8	$Mn(dpm)_3$	PhF/IPA (1:1)	4	82	1.3:1
9	$Mn(dpm)_3$	$PhCF_3$/IPA (3:1)	1.5	85	1.5:1

[a]Isolated yields, yields in parentheses are ^1H NMR yields. [b]Ratio determined by ^1H NMR. [c]^{i}IPrO(Ph)SiH_2 was used instead

Encouraged by the efficiency of this approach, we began screening various conditions. Two other catalysts known to promote HAT chemistry (i.e., Mn(salen) and $Fe(acac)_2$), were tested with no success (Entries 2 and 3). Manipulating the silane to one that has been reported to be a more reactive variant (i.e., ^{i}IPrO(Ph)SiH_2) resulted in diminished selectivity for the desired product (Entry 4). A final round of optimization studies focused on solvent. To this end, ethereal solvents gave no product, while aromatic

solvents showed promising results. Reactions run in benzene produced, for the first time, product mixtures comprised of nearly equivalent amount of both diastereomers (dr 1:1.1, entry 6). Further screening of aromatic solvents continued to result in improved drs and eventually led to the discovery of conditions favoring the desired product (Entry 7). Finally, it was found that employing trifluorotoluene as a co-solvent with iso-propanol (IPA) gave the best result, providing an 85% yield of diastereomers (1.5:1 dr) favoring the desired isomer (**1.17a**). Fortunately, we were able to cleanly separate the diastereomers using preparative reverse-phase HPLC.

1.3.6 Completion of (±)-*Caesalpinflavan B*

Having an acceptable approach to the reduced benzopyran **1.17a**, our focus shifted to accessing caesalpinflavan B, en route to caesalpinnone A. Overall, we needed to effect global deprotection and assemble the chalcone moiety. To this end, as illustrated in Scheme 1.8, the acetal moiety in **1.17a** was removed by exposure to methanolic HCl and the intermediate ketone was then subjected to hydrogenolytic debenzylation by the addition, in the same pot, of Pearlman's Catalyst.[10.] The derived bis-phenol (**1.25**) was then exposed to a one-pot three-step transformation involving re-protection as the corresponding bis-allyl ether, de-acylation with MeOH, and Claisen-Schmidt condensation employing benzaldehyde and LiOH. Exposure of the resultant chalcone (**1.08**) to allyl deprotection with Pd in the presence of dimethyl barbituric acid (**1.26**), employed to trap the intermediate pi-allyl complex, then afforded the natural product caesalpinflavan B (**1.03**) in 40% over the 3-steps. Overall, the synthesis required only 6-steps from known materials and is the first and only synthesis of caesalpinflavan B (**1.03**) reported to date.

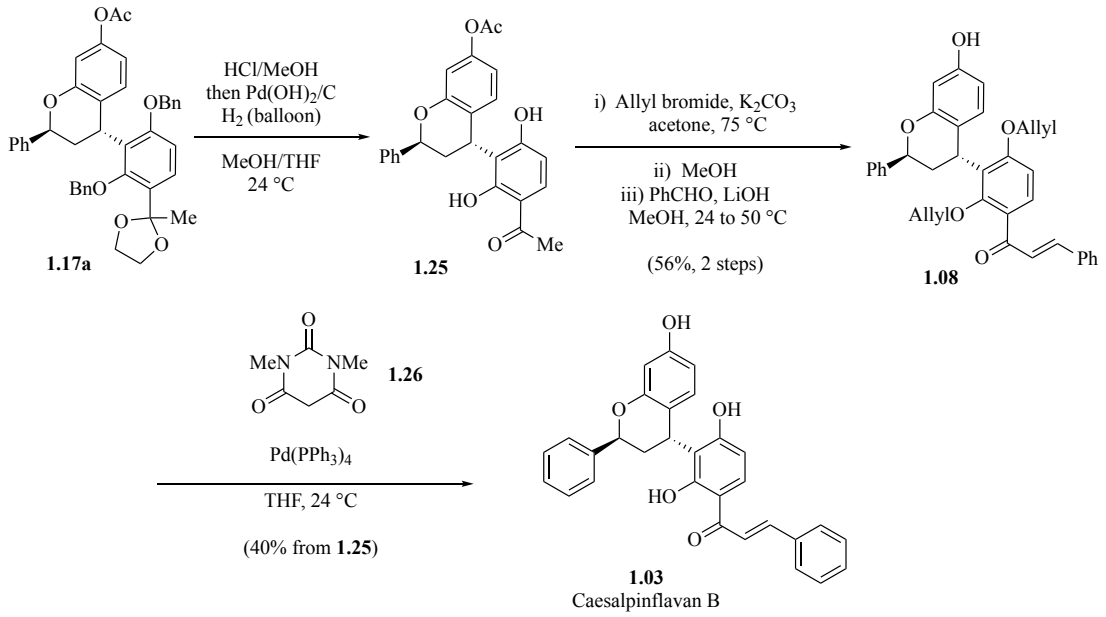

Scheme 1.8 Completion of caesalpinflavan B

1.3.7 End-Game Approach to (±)-*Caesalpinnone A*

Following completion of caesalpinflavan, we were excited to turn our efforts to the more complex caesalpinnone A (**1.01**). In terms of our biosynthetic hypothesis, we believed that nature produces caesalpinflavan A directly from caesalpinflavan B via a selective A-ring oxidation followed by spontaneous oxa-Michael (Scheme 1.9). From a synthetic perspective, we sought to achieve this transformation in the laboratory by applying one of many known reagents capable of oxidizing phenols. However, numerous oxidation attempts under a multitude of conditions, such as metal catalyzed oxidation and organic oxidations, never resulted in direct conversion of caesalpinflavan B to caesalpinnone A. Based on crude NMR data collected on reaction mixtures, these failures were attributed to the deleterious effects of the free bis-phenol that is also prone to oxidation.

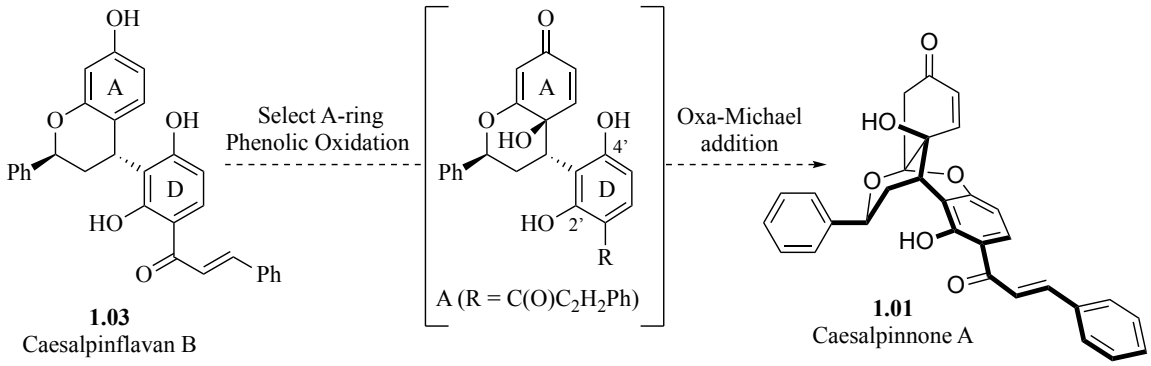

Scheme 1.9 Direct conversion to caesalpinnone A

To avoid undesired oxidation of the bis-phenol ring, we decided to revisit a late-stage intermediate in the synthesis of caesalpinflavan B, bis-allylphenol **1.08**. To our delight, initial attempts to oxidize **1.08** with Doyle's dearomative phenolic oxidation conditions (i.e., $Rh_2(cap)_4$ and TBHP) led to the desired product, albeit in only 15% yield. Further screening (Scheme 1.10A) showed that PIDA was more effective and capable of delivering nearly double the yield (29%) of oxidized material. However, as illustrated this reaction produced an interesting mixture of diastereomers about carbon 2" and 4" (**1.07a** and **1.07b**). Although the mechanism leading to the epimerization of C-2" is not clear, acetic acid by products produced under these conditions could set the stage for epimerization via transient formation of a benzylic cation at C2". Regardless, the transformation provided a quantity of material sufficient for further advancement. To this end, the mixture of diastereomers **1.07** was subject to conditions similar to those employed in the route to caesalpinflavan B. Gratifyingly, the desired diastereomer produced the natural product directly by way of deprotection and then intramolecular oxa-Michael addition. Importantly, the oxa-Michael was completely chemoselective and only engaged the vinylogous ester (Scheme 1.10B).[11] Interestingly, the undesired diastereomer (**1.07b**)

also underwent de-allylation and oxa-Michael, however it furnished the opposite regioselectivity to form tricycle **1.01A** (Scheme 1.10C). Overall, we completed the total synthesis of racemic caesalpinnone A in only 7 steps from known materials.[12]

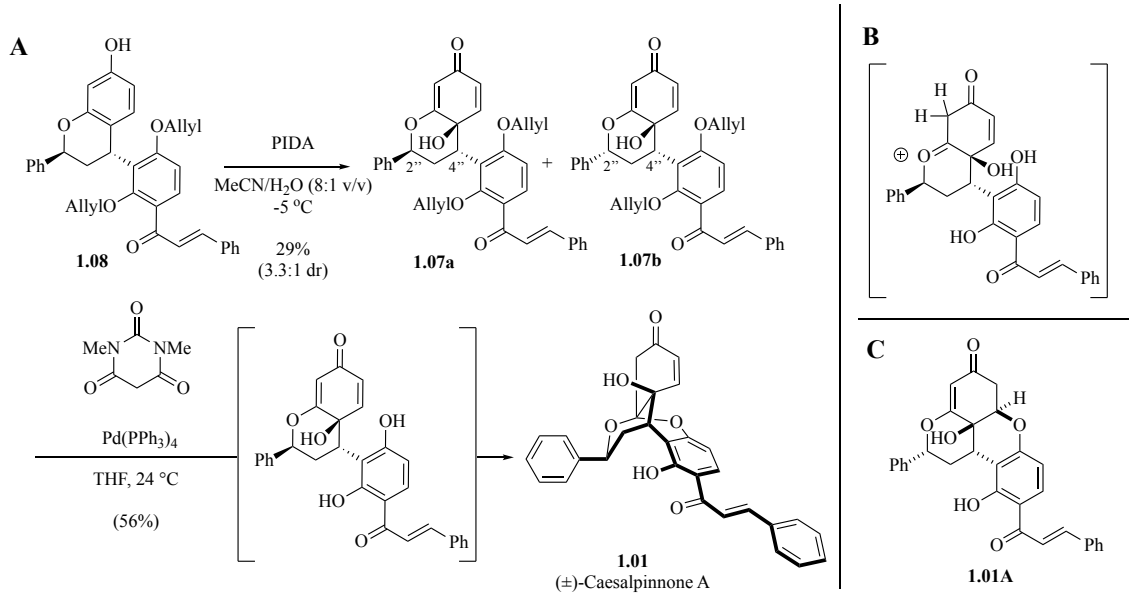

Scheme 1.10 Synthesis of caesalpinnone A

1.4 Asymmetric Synthesis of Caesalpinflavan B

Although the racemic synthesis validated the route to produce caesalpinnone A, it had not addressed the underlying question of our biosynthetic hypothesis – whether or not caesalpinflavan B could serve as the biosynthetic precursor to caesalpinnone A. A question that would need to be addressed based on the absolute stereochemistry of the two natural products. An asymmetric synthesis of caesalpinnone A was thus needed to address this question (Scheme 1.11).

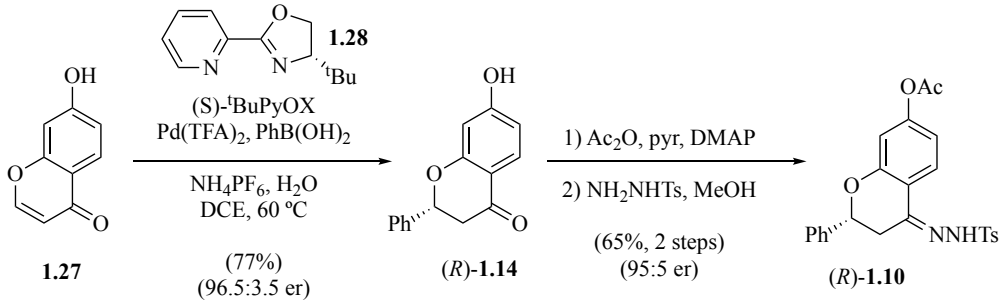

Scheme 1.11 Synthesis of asymmetric hydrazone

In order to prepare enantioenriched caesalpinflavan B, we needed to revise the tosyl hydrazone synthesis (Scheme 1.11). In searching the literature for relevant transformations, we found that the Stoltz group had developed a stereoselective synthesis of (*R*)-**1.14** using an asymmetric conjugate addition into 7-chromenone (**1.27**).[13] In our hands, this conjugate addition provided a 77% yield with 96.5:3.5 er of the desired product. From this point (*R*)-**1.14** was advanced to (*R*)-**1.10** employing the conditions used previously.

With the asymmetric hydrazone in hand, we advanced further by employing conditions for the Barluenga coupling that were similar to those used on racemic material (Scheme 1.12A). However, there were two distinct changes. First, we employed an excess of the aryl iodide in comparison to the hydrazone. This was switched made due to the precious nature of the enantioenriched material. Secondly, the addition time was greatly shortened from 8 to 1 hour(s). This latter modification was critical for preventing severe enantioerosion, due to the benzopyran (**1.09**) likely reacting in a Tsuji-Trost type mechanism where the resulting phenol would indiscriminately add back to the palladium-pi-allyl complex (Scheme 1.12B).[14] Having completed the coupling on enantioselective material we turned to the Shenvi HAT chemistry by employing the optimized conditions

developed in the racemic series. As in the coupling reaction we noted a minor decrease in er. Fortunately, recrystallization allowed the er to be upgraded to 99:1.

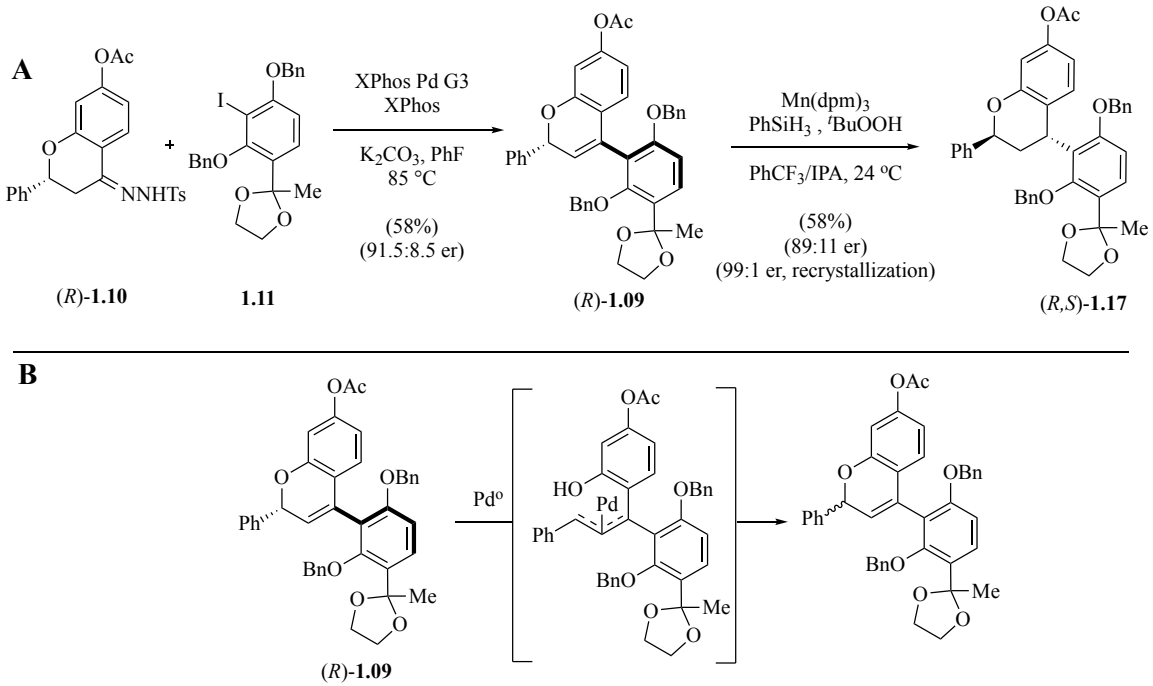

Scheme 1.12 Asymmetric route to dihydropyran and Tsuji-Trost proposal

With highly enantioenriched material in-hand , we next turned to completion of (?)-caesalpinflavan B. To this end, we employed the same sequence of functional group interconversion, as well as allyl deprotection to arrive at enantioenriched caesalpinflavan B (Scheme 1.13). Importantly, based on the known absolute configuration of the synthetic material, this product possesses the same absolute stereochemistry that the isolation chemists assigned to natural (+)-caesalpinflavan B (i.e., *R, S*). Upon taking the optical rotation of synthetic material using parameters similar those employed by the isolation chemists', we observe a levarotatory value. Given that the natural product is dextrarotatory, this result indicates that the isolation chemists had indeed misassigned the stereochemistry by using CD. Moreover, this reassignment of absolute stereochemistry is

consistent with that of caesalpinnone A, thereby supporting our hypothesis that caesalpinflavan B is the likely biosynthetic precursor to caesalpinnone A.

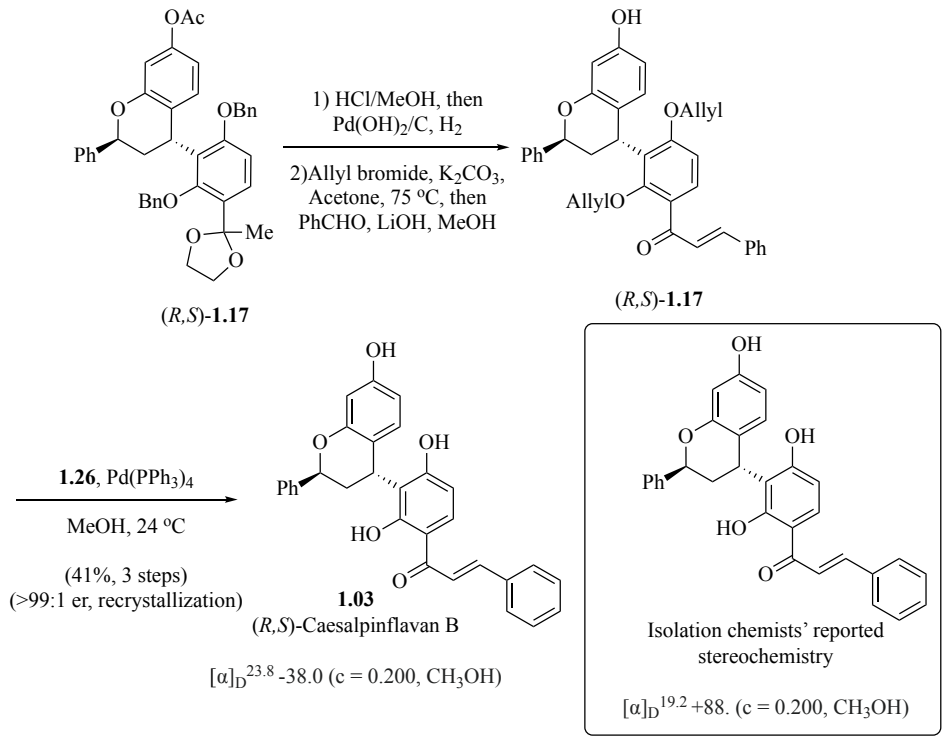

Scheme 1.13 Asymmetric synthesis of (-)-caesalpinflavan B

1.4 Conclusion and Summary

Overall, we were able to complete the total syntheses of (±)-caesalpinnone A and (±)-caesalpinflavan B in 7 and 6 steps, respectively. Upon completing the racemic series we then utilized an enantioselective conjugate addition to furnish enantioenriched hydrazone which enabled access (-)-caesalpinflavan B in high enantiopurity following recrystallization. These synthetic efforts enabled the determination that the wrong absolute stereochemistry had been initially assigned to caesalpinflavan B. Additionally, to our knowledge, this synthesis marks the first use of the Barluenga cross-coupling in a completed total synthesis, thus further demonstrating the utility of this powerful reaction.

Acetal **1.11**

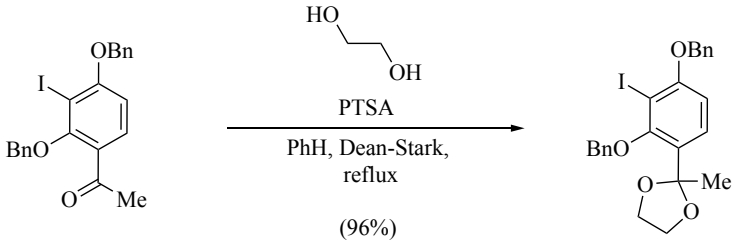

1.13 **1.11**

Experimental: In a 1 L round-bottom flask containing a magnetic stir-bar was added 2,4-bis(benzyloxy)-3-iodoacetopenone **1.13** (13.8 g, 30.0 mmol, 1 equiv), *p*-toluenesulfonic acid monohydrate (282 mg, 1.5 mmol, 5 mol %) and dry benzene (210 mL). To this stirred solution was added ethylene glycol (8.5 mL, 120 mmol, 4.0 equiv). The flask was then equipped with a Dean-Stark trap (25 mL reservoir filled with dry benzene) and reflux condenser. The apparatus was purged with an atmosphere of argon, left under a static atmosphere of argon and heated to 105 °C for 14 hours. The flask was then cooled to 4 °C and a chilled solution of saturated $NaHCO_3$ was added with vigorous stirring. The suspension was transferred to a 2 L separatory funnel and the organic and aqueous layers separated. The aqueous layer was washed with EtOAc (3 x 150 mL) and the combined organic layers washed with saturated brine (1 x 200 mL). The combined organic layers were then dried over Na_2SO_4 and concentrated *in vacuo* to afford **1.11** (14.5 g, 96 %) as a light-pink microcrystalline solid. Product could be used as is in the next step.

^{1}H NMR: (600 MHz, Chloroform-*d*): δ 7.74 (d, *J* = 7.8 Hz, 2 H), 7.65 –7.32 (m, 9 H), 6.67 (dd, J = 8.5, 1.3, 1 H), 5.20 (s, 2 H), 5.18 (s, 2 H), 4.25 – 4.05 (m, 2 H), 3.98 – 3.84 (m, 2 H), 1.83 (s, 3 H). **^{13}C NMR (151 MHz, $CDCl_3$)**: δ 158.6, 157.4, 137.5, 135.4, 130.3,

128.7, 128.5, 128.3, 128.0, 127.9, 127.9, 127.0, 106.3, 107.6, 87.6, 75.3, 71.09, 64.49, 26.2. **HRMS (ESI$^+$)**: Calcd. for $C_{24}H_{23}IO_4Na$. $[M+Na]^+$: 525.0529. Found: 525.0530. **IR (ATR)**: ν_{max} (cm^{-1}) = 3064 (w), 3031 (w), 2985 (m), 2377 (w), 1671 (w), 1585 (m), 1497 (m), 1388 (s), 1251 (m), 1198 (s), 1148 (w), 1067 (m), 1041 (s), 950 (m), 886 (w), 762 (w), 735 (s), 674 (s), 599 (w). **TLC** (EtOAc–hexanes–Et_3N = 10:90:1): R_f = 0.26.

Tosyl Hydrazone **1.10**

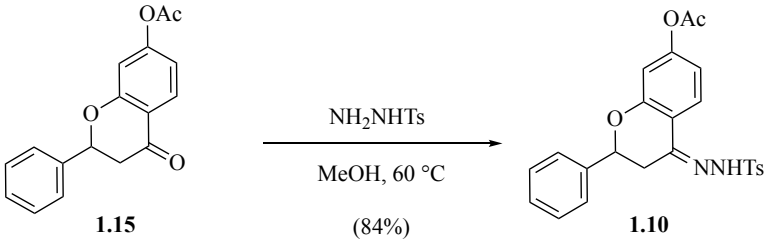

1.15 **1.10**

Experimental: In a 250 mL round-bottom flask containing a magnetic stir-bar was added **1.15** (2.75 g, 9.75 mmol, 1 equiv) and MeOH (120 mL). To the stirred solution was added *p*-tosylhydrazide (3.60 g, 19.7 mmol, 2.0 equiv) and the flask then heated to 60 °C under a static atmosphere of nitrogen. After 14 h, the solution slowly cooled to 4 °C over the course of 1 hour. The precipitate was collected in a large Kiriyama filter to yield **1.10** (3.41 g) as a colorless microcrystalline solid. The filtrate was evaporated to ca. half volume and cooled to 4 C for 1 hour before being re-filtered to give additional **1.10** (261 mg, 3.67 g total, 84%). The material was azeotropically-dried from benzene (3 x 100 mL) before being used in the next step.

^{1}H NMR (600 MHz, DMSO-d_6) δ 10.63 – 10.55 (m, 1H), 7.82 (dd, J = 8.2, 1.4 Hz, 2H), 7.79 – 7.74 (m, 1H), 7.54 – 7.47 (m, 2H), 7.42 (ddd, J = 8.8, 6.1, 1.2 Hz, 4H), 7.40 – 7.36 (m, 1H), 6.83 – 6.76 (m, 2H), 5.25 (dd, J = 12.0, 3.1 Hz, 1H), 3.22 – 3.18 (m, 1H), 2.74 (dd, J = 17.1, 12.0 Hz, 1H), 2.38 (s, 3H), 2.25 (s, 3H). **^{13}C NMR (151 MHz, DMSO-d_6)** δ

168.7, 157.1, 152.6, 146.6, 143.4, 139.3, 136.0, 129.5, 128.4, 128.3, 127.5, 126.3, 125.0, 117.2, 115.6, 111.0, 76.5, 32.0, 21.0, 20.8. **IR (ATR)**: ν_{max} (cm^{-1}) = 3214 (m), 1762 (s), 1623 (m), 1600 (m), 1433 (s), 1340 (m), 1205 (s), 1167 (s), 1082 (m), 913 (m), 739 (m), 699 (m), 567 (m). **HRMS (ESI$^+$)** Calcd. for $C_{24}H_{22}N_2O_5SNa$. $[M+Na]^+$: 473.1147, found: 473.1141

Benzopyran **1.09**

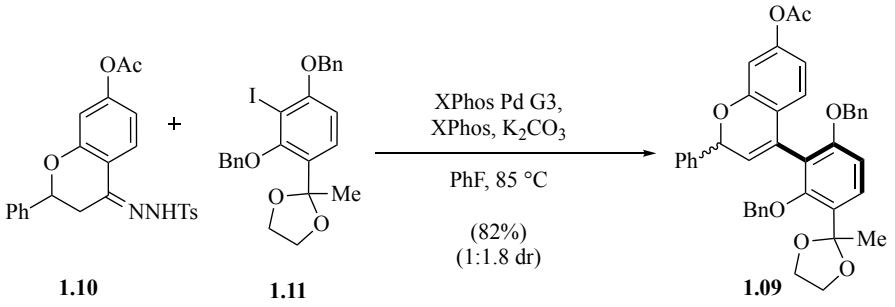

1.10 **1.11** **1.09**

Experimental: In a dry 100 mL round-bottomed flask containing a magnetic stir-bar was charged with **1.11** (398 mg, 0.79 mmol, 1 equiv), XPhos Pd G3 (140 mg, 0.16 mmol, 20 mol %), XPhos (76 mg, 0.16 mmol, 20 mol %), and K_2CO_3 (552 mg, 4.0 mmol, 5 equiv), followed by dry PhF (16 mL). The flask was sealed and resulting suspension sparged with argon for 15 minutes before being left under a static atmosphere of argon. The flask was then warmed to 85 °C. To a separate, dry 50 mL Erlenmeyer flask equipped with a 14/20 ground-glass joint was added **1.10** (900 mg, 2.0 mmol, 2.5 equiv). The flask was then sealed and purged with an atmosphere of argon before 1,4-dioxane (23 mL) was added via syringe. The resulting suspension was swirled until complete dissolution (ca. 15 minutes) and subsequently sparged with dry argon. The solution of **1.10** was then added slowly (ca. 2.3 mL/h) to the suspension containing **1.11** at 85 °C. After the addition was complete, the reaction let to stir for 7 hours before being cooled to 24 °C, filtered over a pad of silica gel.

The silica gel pad was washed with EtOAc (5 x 30 mL) and the washes combined with the filtrate before being concentrated in vacuo to give a sticky orange oil. The oil was chromatographed (MPLC, 40 g column, 30 mL/min, 10 % to 40% EtOAc/hexanes) to give **1.09** as a light-yellow foam (425 mg, 82%, 1:1.8 mixture of atropisomers).

^{1}H NMR (600 MHz, Chloroform-*d*, both atropisomers): δ 7.56 – 7.54 (m, 2.9), 7.41 – 7.40 (m, 7.4H), 7.38 – 7.35 (m, 3.9H), 7.33 – 7.31 (m, 5.9H), 7.29 – 7.26 (m, 9.9H, overlap with $CHCl_3$), 7.24 – 7.18 (m, 6.9H), 7.16 –7.10 (m, 9.1H), 6.90 (d, J = 8.3 Hz, 1.8 H), 6.85 (d, J = 8.4 Hz, 1.0H), 6.81 – 6.77 (m, 2.8H), 6.72 (d, J = 2.2 Hz, 1.0H), 6.63 (d, J = 2.2 Hz, 1.7H), 6.60 – 6.58 (m, 2.8H), 6.06 (d, J = 3.3 Hz, 1.0H), 5.85 (d, J = 3.4 Hz, 1H), 5.80 (d, J = 3.5 Hz, 1.7H), 5.77 (d, J = 3.6 Hz, 1.8H), 5.06 – 5.03 (m, 5.7H), 4.98 (d, J = 10.0 Hz, 1.8H), 4.88 (d, J = 10.3 Hz, 1.0H), 4.78 (d, J = 10.3 Hz, 1.0H), 4.74 (d, J = 10.0 Hz, 1.8H), 4.14 – 4.04 (m, 5.7H), 3.99 –3.96 (m, 1.8H), 3.94 – 3.87 (3.9H), 2.29 (s, 3.1H), 2.26 (s, 5.3H), 1.83 – 1.80 (m, 8.2H). **^{13}C NMR (151 MHz, $CDCl_3$, both atropisomers):** δ 169.2, 169.1, 157.5, 157.5, 156.2, 155.9, 154.4, 153.9, 151.2, 140.7, 139.9, 138.0, 138.0, 137.0, 136.7, 129.4, 128.6, 128.5, 128.5, 128.5, 128.4, 128.4, 128.3, 128.3, 128.2, 128.2, 128.2, 127.8, 127.8, 127.7, 127.7, 127.7, 127.3, 127.3, 127.2, 127.0, 126.8, 126.0, 125.8, 125.5, 125.3, 122.5, 122.1, 120.8, 120.6, 114.1, 114.0, 109.9, 109.7, 108.9, 108.8, 107.5, 106.9, 77.7, 77.5, 76.0, 75.6, 70.4, 70.3, 64.6, 64.5, 64.5, 26.4, 26.4, 21.3. (8 overlapping ^{13}C resonances) **IR (ATR)**: ν_{max} (cm^{-1}) = 3031 (w), 2933 (m), 2884 (m), 2359 (w), 1762 (s), 1608 (m), 1589 (m), 1465 (m), 1454 (m), 1371 (m), 1201 (s), 1143 (m), 1129 (m), 1072 (m), 1043 (m), 811 (m), 737 (m), 693 (m). **HRMS (ESI$^+$)** Calcd. for $C_{41}H_{36}O_7Na$. $[M+Na]^+$: 663.2359, found: 663.2354. **TLC** (EtOAc–hexanes = 25:75): R_f = 0.38.

p-Quinone Methide **1.19**

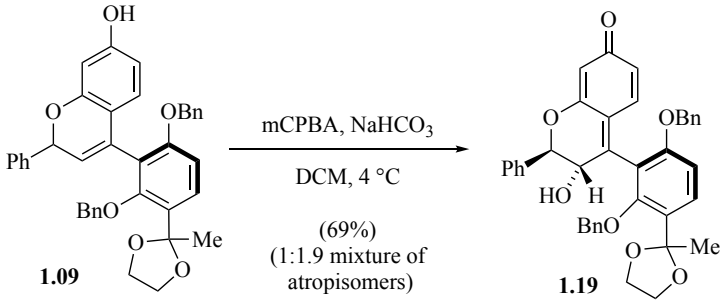

Experimental: In a 100 mL round bottom flask containing a magnetic stir-bar was added **1.09** (548 mg, 0.916 mmol) and DCM (13 mL). The stirred solution was cooled to 4 ºC and a solid mixture containing mCPBA (514 mg, 77% purity, 2.30 mmol) and $NaHCO_3$ (761 mg, 9.05 mmol) were added in one portion. The suspension vigorously stirred at 4 ºC for 45 minutes before being diluted with DCM (25 mL) and saturated brine (50 mL). The contents were then transferred to a separatory funnel and layers separated. The aqueous phase washed with DCM (5 x 25 mL) and combined organic phases washed with saturated brine (3 x 50 mL) before being dried over Na_2SO_4, filtered. Silica gel (ca 10 g) was added and the suspension concentrated in vacuo. The free-flowing solid then chromatographed directly (33% to 50% EtOAc/hexanes) to give **1.19** as a yellow foam (385 mg, 69% yield) and as a 1:1.9 mixture of atropisomers.

^{1}H NMR (600 MHz, Chloroform-*d*, both atropisomers): δ 7.63 – 7.55 (m, 2H), 7.03 (d, *J* = 9.8 Hz, 1H), 6.93 (d, *J* = 9.9 Hz, 1H), 6.87 (d, *J* = 8.8 Hz, 1H), 6.79 (d, *J* = 8.9 Hz, 1H), 6.34 (dd, *J* = 9.8, 1.8 Hz, 1H), 6.27 (dd, *J* = 9.9, 1.9Hz, 1H), 6.04 (d, *J* = 1.8 Hz, 1H), 5.96 (dd, *J* = 6.2, 1.8 Hz, 1H), 5.41 (d, *J* = 10.8 Hz, 1H), 5.18 – 4.99 (m, 6H), 4.88 – 4.78 (m, 2H), 4.54 – 4.40 (m, 3H), 4.17 – 4.04 (m, 5H), 4.03 –3.82 (m, 5H), 1.85 (s, 2H), 1.77 (s, 4H). **^{13}C NMR (151 MHz, $CDCl_3$, both atropisomers):** δ 188.3, 188.2, 161.2, 161.0,

156.7, 156.3, 156.0, 155.5, 150.7, 145.7, 137.6, 137.0, 136.9, 136.1, 136.0, 135.74 134.2, 133.9, 133.8, 130.0, 129.94 129.5, 129.2, 129.1, 129.1, 129.0, 128.9, 128.7, 128.7, 128.7, 128.6, 128.5, 128.5, 128.4, 128.4, 128.4, 128.3, 128.3, 128.3, 128.2, 128.2, 128.1, 128.0, 127.7, 127.7, 127.4, 127.4, 127.2, 127.2, 127.0, 126.9, 126.6, 126.4, 125.2, 121.0, 118.6, 109.0, 108.9, 108.8, 108.4, 108.3, 108.2, 108.1, 83.0, 82.6, 80.4, 77.5, 77.5, 71.0, 70.7, 70.1, 69.0, 64.7, 64.6, 64.5, 64.5, 26.5, 26.3. **IR (ATR)**: ν_{max} (cm^{-1}) = 3373 (s), 2926 (m), 1761 (s), 1736 (m), 1617 (s), 1593 (s), 1496 (m), 1370 (m), 1284 (s), 1212 (s), 1110 (m), 966 (m), 805 (m), 753 (w). **HRMS (ESI$^+$)** Calcd. for $C_{39}H_{34}NaO_7$. $[M+Na]^+$: 637.2202. found: 637.2198. **TLC** (EtOAc–hexanes = 1:1): R_f = 0.24.

Aliphatic Alcohol **1.20**

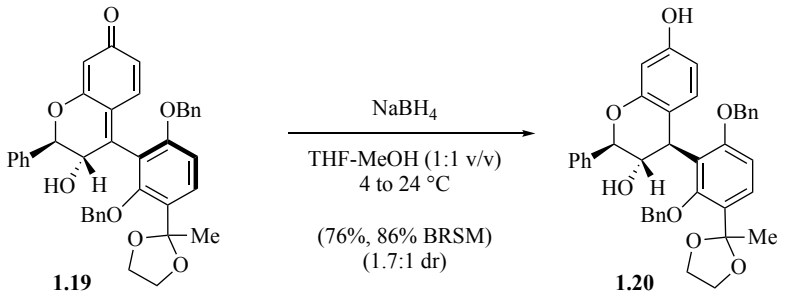

Experimental: In a scintillation vial containing a magnetic stir-bar was added of *p*-quinone methide **1.19** (0.298 mg, 0.485 mmol). The starting material was dissolved in a mixture of THF and MeOH (6 mL, 1:1 v/v) at 4 ºC was added portion wise $NaBH_4$ (3 portions over 45 mins, 48.6 mg, 1.28 mmol). After the reaction was complete by TLC, EtOAc (10 mL) and saturated ammonium chloride (10 mL) was added and the contents transferred to a separatory funnel. The phases were separated, and the aqueous phase washed with EtOAc (5 x 10 mL). The combined organics were washed with brine (3 x 10 mL), dried over Na_2SO_4, and filtered. Silica gel (ca. 5 g) was added and the solvents removed in vacuo. The

free flowing solid was then chromatographed directly (20% to 50% EtOAc/hexanes) to give **1.20** as a 1.7:1 mixture of diastereomers (228.3 mg, 76%). The major diastereomer is illustrated and the minor diastereomer was not assigned.

^{1}H NMR (600 MHz, Chloroform-*d*): δ 7.63 – 7.57 (m, 4 H), 7.52 – 7.47 (m, 3H), 7.43 – 7.38 (m, 4H), 7.38 – 7.28 (m, 16H), 7.26 – 7.21 (m, 14H), 7.20 – 7.15 (m, 2H), 7.02 – 6.95 (m, 4H), 6.85 (s, 2H), 6.76 – 6.70 (m, 3H), 6.59 (d, J = 8.4 Hz, 1H), 6.56 (dd, J = 8.4, 1.1 Hz, 2H), 6.45 (d, J = 2.5 Hz, 1H), 6.35 (d, J = 2.5 Hz, 2H), 6.33 (dd, J = 8.4, 2.6 Hz, 1H), 6.29 (dd, J = 8.4, 2.6 Hz, 2H), 5.47 (d, J = 4.1 Hz, 1H), 5.35 (d, J = 10.2 Hz, 2H), 5.11 (d, J = 10.3 Hz, 2H), 4.92 – 4.84 (m, 4H), 4.84 – 4.75 (m, 6H), 4.75 – 4.69 (m, 5H), 4.63 (td, J = 9.4, 3.1 Hz, 2H), 4.53 (d, J = 7.5 Hz, 1H), 4.17 – 4.06 (m, 6H), 4.03 – 3.90 (m, 5H), 1.89 (s, 5H), 1.79 (s, 3H). **^{13}C NMR (151 MHz, $CDCl_3$):** δ 157.7, 157.7, 155.1, 155.0, 154.9, 154.6, 138.3, 138.1, 137.7, 136.4, 128.9, 128.8, 128.6, 128.6, 128.6, 128.5, 128.4, 128.3, 128.3, 128.2, 127.9, 127.8, 127.8, 127.7, 127.4, 127.3, 127.2, 126.9, 126.7, 124.5, 124.1, 118.1, 108.9, 108.4, 108.3, 108.1, 107.7, 103.0, 102.9, 82.8, 78.5, 70.2, 70.0, 69.8, 69.7, 64.4, 64.4, 64.4, 41.3, 37.9, 26.4, 26.2. **IR (ATR)**: ν_{max} (cm^{-1}) = 3307 (m), 3246 (m), 2924 (m), 2888 (m), 1622 (s), 1510 (m), 1455 (s), 1388 (m), 1208 (vs), 1170 (vs), 1081 (vs), 1000 (m), 847 (s), 695 (s). **HRMS (ESI$^+$)** Calcd. for $C_{39}H_{36}NaO_7$. $[M+Na]^+$: 639.2359. found: 639.2348 **TLC** (EtOAc–hexanes = 1:1): R_f = 0.48.

Enol **1.21**

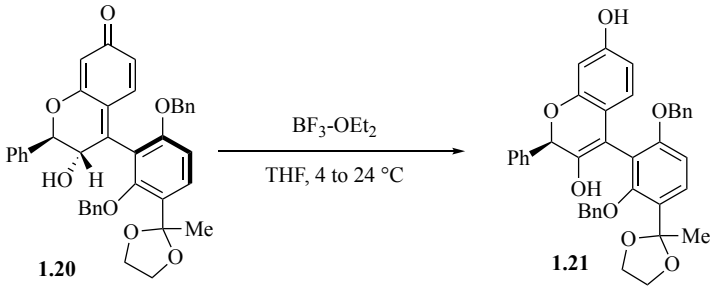

Experimental: To a solution of quinone methide **14** (220 mg, 0.35 mmol) in THF (8 mL) at 4 ºC was added boron trifluoride diethyl etherate (51 μL, 0.39 mmol). The solution stirred at 4 ºC for 15 mins before being warmed slowly to room temperature over the course of 30 minutes. After 2 h, saturated sodium acetate (10 mL) was added, followed by DCM. The contents were transferred to a separatory funnel and an additional 10 mL DCM added. The aqueous phase was extracted with DCM (3 x 5 mL) and the combined organics washed with saturated brine (2 x 10 mL) before being dried over Na_2SO_4, filtered, and concentrated in vacuo. The light purple foam was sensitive to oxygen was carried forward as is; presumably as a 1:1.1 mixture of atropisomers.

Alcohol **1.23**

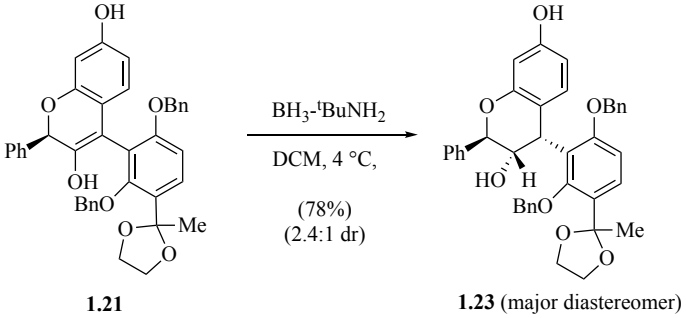

Experimental: In a vial containing a magnetic stir-bar was added a solution of **1.21** (502 mg, 0.818 mmol) in DCM at 4 ºC. BH_3-^{t}BuNH$_2$ (4 portions over 3 hours, 336 mg, 3.86 mmol, 4.7 equiv) was added. The solution was stirred at 4 ºC for 6 hours before being

quenched with saturated aqueous ammonium chloride (20 mL). The contents transferred to a separatory funnel and aqueous phase washed with DCM (4 x 20 mL). The combined organics washed with brine (4 x 20 mL), dried over Na_2SO_4, filtered, and concentrated in vacuo. Crude ^{1}H NMR showed a 2.4:1 dr. The residue was dissolved in DCM (ca. 40 mL), and silica gel added (ca 5 g), before being concentrated to dryness and chromatographed directly (10% to 50 % EtOAc/hexanes). The fractions containing the pure major diastereomer were combined while the fractions containing a mixture diastereomers were combined and chromatographed again. This process was carried out three times to eventually yield 238.2 mg pure **1.23** (42%, major diastereomer) and a ca. 1:2 mixture of diastereomers, favoring the undesired diastereomer (153 mg).

^{1}H NMR (600 MHz, Chloroform-*d*), 12: 7.53 (d, *J* = 8.7 Hz, 1H), 7.29 – 7.27 (m, 3H), 7.25 – 7.12 (m, 6H), 6.97 – 6.90 (m, 2H), 6.87 (dd, *J* = 6.6, 2.9 Hz, 2H), 6.81 (d, *J* = 8.8 Hz, 1H), 6.64 – 6.56 (m, 1H), 6.52 (d, *J* = 2.6 Hz, 1H), 6.34 (dd, *J* = 8.4, 2.6 Hz, 1H), 5.42 (d, *J* = 3.1 Hz, 1H), 4.94 (d, *J* = 11.1 Hz, 1H), 4.82 – 4.58 (m, 5H), 4.52 – 4.38 (m, 2H), 4.07 (td, *J* = 4.9, 4.0, 2.2 Hz, 2H), 3.99 – 3.85 (m, 2H), 1.74 (s, 3H).**^{13}C NMR (151 MHz, $CDCl_3$):** 157.8, 156.9, 155.2, 154.3, 139.3, 136.9, 135.3, 130.1, 128.7, 128.7, 128.5, 128.2, 128.1, 128.1, 127.6, 127.5, 127.2, 127.2, 125.2, 123.7, 115.3, 108.7, 108.7, 108.2, 103.2, 81.3, 77.1, 72.1, 71.1, 64.4, 64.4, 33.4, 26.1. **IR (ATR)**: ν_{max} (cm^{-1}) = 3307 (m), 3246 (m), 2924 (m), 2888 (m), 1622 (s), 1510 (m), 1455 (s), 1388 (m), 1208 (vs), 1170 (vs), 1081 (vs), 1000 (m), 847 (s), 695 (s). **HRMS (ESI$^+$)** Calcd. for $C_{39}H_{36}NaO_7$. $[M+Na]^+$: 639.2359. found: 639.2349 **TLC** (EtOAc–hexanes = 1:1): R_f = 0.43.

Bis-Xanthate **1.24**

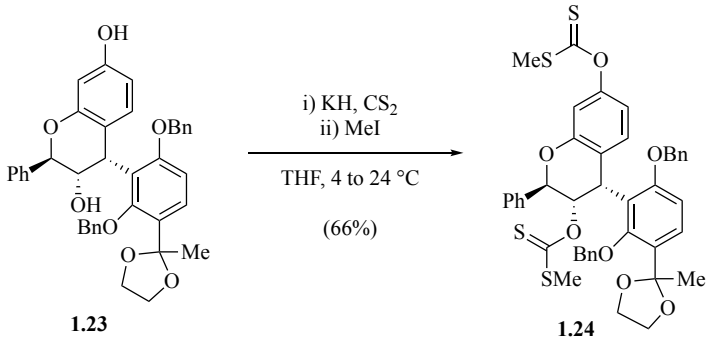

Experimental: In a scintillation vial containing a magnetic stir-bar was added KH (30% in oil, 333 mg, 2.55 mmol) followed by THF (2.9 mL) at 4 ºC. A solution of alcohol **1.23** (105 mg, 0.170 mmol) in THF (6 mL). The mixture was warmed to 24 ºC and stirred for 40 min before being cooled back down to 4 ºC. Carbon disulfide (213 μL, 3.02 mmol) was added and the mixture was stirred for 1 h at 4 ºC before being warmed to 24 ºC for 2 h before an additional 120 μL CS_2 was added. After 7 h the reaction was then cooled to 4 ºC and MeI (414 μL, 6.04 mmol) was added and the reaction stirred for 30 min before being quenched by addition of saturated sodium bicarbonate (10 mL) and diluted with EtOAc (10 mL. The suspension was extracted with EtOAc (5 x 10 mL), combined organic extracts washed with brine (20 mL). The combined organic extracted were then dried over Na_2SO_4, filtered, and evaporated in vacuo. The residue was chromatographed (10% to 33% EtOAc/hexanes) to give **1.24** as a yellow oil (80.5 mg, 66% yield)

^{1}H NMR (600 MHz, Chloroform-*d*): 7.54 (d, *J* = 8.7 Hz, 1H), 7.37 – 7.20 (m, 14H), 7.09 – 7.03 (m, 2H), 6.97 (dd, *J* = 8.4, 1.1 Hz, 1H), 6.77 (d, *J* = 8.8 Hz, 1H), 6.73 (d, *J* = 2.4 Hz, 1H), 6.66 – 6.62 (m, 2H), 5.57 (d, *J* = 6.3 Hz, 1H), 5.17 – 5.08 (m, 2H), 4.98 (d, *J* = 11.5 Hz, 1H), 4.80 (dd, *J* = 10.9, 4.8 Hz, 2H), 4.16 – 4.05 (m, 2H), 4.04 – 3.96 (m, 1H), 3.96 – 3.88 (m, 1H), 2.70 (s, 3H), 2.25 (s, 3H), 1.82 (s, 3H). **^{13}C NMR (151 MHz, $CDCl_3$):** 215.5,

214.8, 158.7, 156.9, 154.6, 153.6, 137.6, 137.3, 136.4, 128.9, 128.6, 128.6, 128.6, 128.4, 128.3, 128.3, 127.9, 127.8, 127.7, 127.6, 127.5, 126.5, 122.8, 121.7, 114.7, 110.7, 108.9, 108.1, 79.7, 77.0, 70.6, 64.5, 64.4, 33.8, 26.3, 20.1, 18.6. **IR (ATR)**: ν_{max} (cm^{-1}) = 2922 (m), 2882 (m), 1592 (s), 1494 (s), 1421 (m), 1253 (vs), 1131 (s), 1060 (vs), 1041 (s), 979 (m). **HRMS (ESI$^+$)** Calcd. for $C_{43}H_{40}O_7S_4Na$. $[M+Na]^+$: 819.1555, found: 819.1545. **TLC** (EtOAc–hexanes = 1:10, 3 developments): R_f = 0.47.

Deoxygenated **1.17**

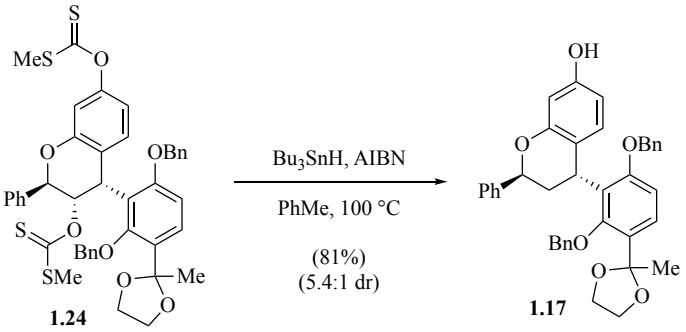

Experimental: In a vial containing magnetic stirring was added xanthate **1.24** (80.5 mg, 0.10 mmol) followed by degassed PhMe (4 mL), Bu_4SnH (136 μL, 0.5 mmol) and AIBN (7.9 mg, 0.044 mmol), consecutively. The solution was then heated to 100 ºC for 3 hours before being cooled to 24 ºC and concentrated *in vacuo*. The resulting oily residue was chromatographed directly (0% to 50% EtOAc/hexanes) to give phenol **1.17** (44.6 mg, 81%, 5.4:1 dr) as a colorless foam.

^{1}H NMR (600 MHz, Chloroform-*d*): 7.51 – 7.42 (m, 1H), 7.34 – 7.17 (m, 12H), 7.05 – 6.97 (m, 2H), 6.91 (d, *J* = 7.2 Hz, 2H), 6.79 – 6.68 (m, 2H), 6.57 (d, *J* = 8.3 Hz, 1H), 6.28 (ddd, *J* = 13.6, 8.3, 2.6 Hz, 1H), 5.54 (t, *J* = 4.1 Hz, 1H), 4.99 – 4.84 (m, 2H), 4.82 – 4.61 (m, 4H), 4.51 (dd, *J* = 11.1, 5.8 Hz, 1H), 4.14 – 4.06 (m, 3H), 4.00 – 3.87 (m, 3H), 3.06 (ddd, *J* = 13.3, 10.8, 4.7 Hz, 1H), 2.29 (ddd, *J* = 13.5, 5.9, 3.5 Hz, 1H), 1.79 (s, 3H). **^{13}C**

NMR (151 MHz, $CDCl_3$): 158.4, 156.3, 155.0, 154.9, 142.0, 137.2, 136.7, 128.7, 128.6, 128.3, 128.3, 128.2, 127.8, 127.7, 127.2, 127.1, 126.2, 125.4, 119.1, 109.0, 108.1, 107.7, 103.2, 75.8, 70.1, 64.5, 32.4, 27.7, 26.3. note: 2 overlapping aliphatic Cs. **IR (ATR)**: ν_{max} (cm^{-1}) = 3389 (br), 3031 (m), 2934 (m), 2880 (m), 1591 (s), 1503 (s), 1478 (s), 1304 (m), 1263 (s), 1209 (s), 1152 (s), 1041 (s), 965 (m), 842 (m). **HRMS (ESI^+)** Calcd. for $C_{39}H_{36}NaO_6$. $[M+Na]^+$: 623.2410. Found: 623.2407. **TLC** (EtOAc–hexanes = 1:3): R_f = 0.29.

Dihydropyran **1.17a/b**

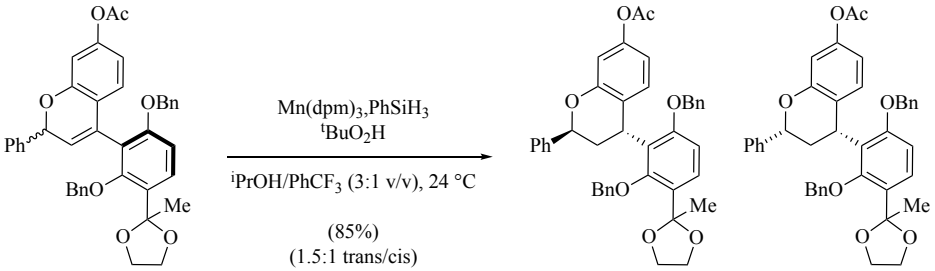

Experimental: In a scintillation vial containing a magnetic stir-bar was added a stirred solution of **1.09** (200 mg, 0.312 mmol, 1 equiv) in dry $PhCF_3$/*i*PrOH (8.0 mL, 3:1 v/v) and $PhSiH_3$ (67 μL, 0.624 mmol, 2 equiv) was added, followed by *t*butyl hydroperoxide (220 μL, 5.5 M in decane, 1.21 mmol, 3.9 equiv). The solution was sparged for 5 minutes with dry argon before $Mn(dpm)_3$ (38.0 mg, 0.062 mmol, 0.2 equiv) was added in one portion. The solution was then sparged for 10 seconds with dry argon before being left under a static atmosphere of argon and stirred at 24 °C for 19 h. After completion (as judged by ESI-MS), silica gel (ca. 2.5 g) was added and the suspension concentrated to a free-flowing powder, which was chromatographed directly by MPLC (12 g column, 20 mL/min, 10% to 40% EtOAc/hexane) to give **1.17a** and **1.17b** (170 mg, 85%) as a 1.5:1 mixture of

trans/cis isomers and as a colorless oil. The mixture was separated by iterative, preparative reverse-phase HPLC (21.2 x 100 mm Phenomenex Gemini column (5 μm C_{18} 110 Å, 21.2 x 100 mm), 65% MeCN in H_2O to 100% MeCN over 15 minutes, 20 mL/min, ca. 30 mg injections) to give **1.17a** (41 mg) and **1.17b** (39 mg), both as colorless foams (47% HPLC recovery). The relative stereochemistry of **1.17a** and **1.17b** was assigned both by analogy to similar compounds.

1.17a: **^{1}H NMR (600 MHz, Chloroform-*d*):** δ 7.47 (d, *J* = 8.6 Hz, 1H), 7.30 – 7.20 (m, 13H), 7.03 (d, *J* = 7.0 Hz, 2H), 6.88 (d, *J* = 6.9 Hz, 2H), 6.75 (d, *J* = 2.4 Hz, 1H), 6.74 – 6.70 (m, 2H), 6.52 (dd, *J* = 8.4, 2.4 Hz, 1H), 5.51 (t, *J* = 4.2 Hz, 1H), 4.88 (d, *J* = 11.4 Hz, 1H), 4.76 (dd, *J* = 18.7, 10.4 Hz, 2H), 4.72 – 4.63 (m, 1H), 4.55 (dd, *J* = 10.5, 6.0 Hz, 1H), 4.15 – 4.04 (m, 2H), 4.00 – 3.88 (m, 2H), 3.00 (ddd, *J* = 14.4, 10.4, 4.6 Hz, 1H), 2.36 – 2.24 (m, 4H), 1.78 (s, 3H). **^{13}C NMR (151 MHz, $CDCl_3$)** δ 169.4, 158.2, 156.3, 154.9, 149.7, 141.8, 137.2, 136.5, 128.7, 128.6, 128.5, 128.3, 127.8, 127.8, 127.3, 127.3, 126.8, 126.4, 125.4, 124.3, 113.4, 109.8, 109.0, 108.0, 100.1, 97.1, 77.2, 75.8, 70.3, 64.5, 64.5, 32.5, 28.1, 26.3, 21.3. **IR (ATR)**: ν_{max} (cm^{-1}) = 3031 (w), 2934 (m), 2887 (m), 2361 (w), 1752 (s), 1583 (s), 1585 (s) ,1472 (m), 1370 (s), 1252 (w), 1209 (Vs), 1143 (s), 1110 (s), 1087 (s), 1081 (m), 1043 (s), 1016 (m), 906 (w), 811 (w), 736 (m), 698 (m), 676 (m). **HRMS (ESI^+)** Calcd. for $C_{41}H_{38}O_7Na$ (Both isomers). $[M+Na]^+$: 665.2515. Found: 665.2509. **TLC** (EtOAc–hexanes = 50:50): both isomers, R_f = 0.50

1.17b: ^{1}H NMR (600 MHz, Chloroform-*d*): δ 7.60 – 7.54 (m, 2H), 7.48 (d, *J* = 8.6 Hz, 1H), 7.43 (t, *J* = 7.5 Hz, 2H), 7.39 – 7.35 (m, 1H), 7.33 – 7.24 (m, 7H), 7.23 – 7.16 (m, 2H), 6.99 – 6.91 (m, 2H), 6.82 (dd, *J* = 8.4, 1.1 Hz, 1H), 6.71 (d, *J* = 8.7 Hz, 1H), 6.63 (d, *J* = 2.4 Hz, 1H), 6.54 (dd, *J* = 8.4, 2.4 Hz, 1H), 5.09 (d, *J* = 10.4 Hz, 1H), 5.04 (dd, *J* =

11.3, 2.4 Hz, 2H), 4.92 (dd, *J* = 11.9, 5.7 Hz, 1H), 4.84 (d, *J* = 11.2 Hz, 1H), 4.75 (d, *J* = 11.2 Hz, 1H), 4.20 – 4.07 (m, 2H), 4.03 – 3.87 (m, 2H), 2.77 (d, *J* = 11.8 Hz, 1H), 2.29 (s, 3H), 2.04 (ddd, *J* = 13.4, 5.8, 2.1 Hz, 1H), 1.88 (s, 3H). **^{13}C NMR (151 MHz, $CDCl_3$):** δ 169.5, 158.0, 156.6, 155.8, 149.5, 141.5, 137.8, 136.5, 128.7, 128.7, 128.5, 128.3, 128.2, 128.1, 127.9, 127.8, 127.8, 127.4, 126.4, 126.4, 126.2, 124.0, 113.5, 110.0, 109.0, 107.8, 78.8, 77.8, 70.1, 64.6, 64.5, 35.0, 33.8, 26.5, 21.3. **HRMS (ESI$^+$)** Calcd. for $C_{41}H_{38}O_7Na$ (Both isomers). $[M+Na]^+$: 665.2515. Found: 665.2509. **TLC** (EtOAc–hexanes = 1:1): both isomers, R_f = 0.50

Caesalpinflavan B **1.03**

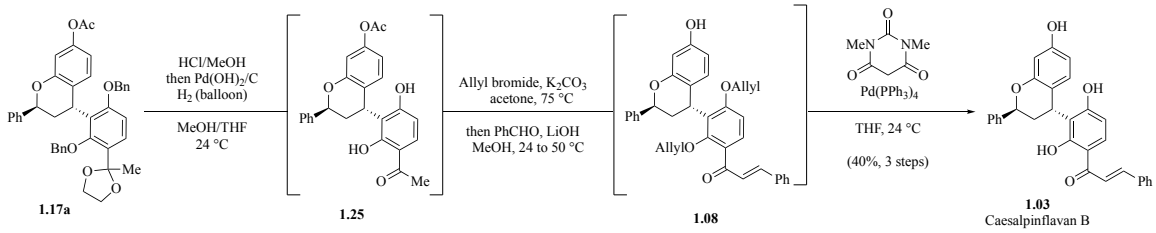

Experimental: In a 1.5 dr vial was added dihydropyran **1.17a** (19.1 mg, 0.029 mmol), diluted with MeOH (1.5 mL) and 10% aq. HCl (5 μL) was added. The solution stirred at 24 °C for 15 minutes before being sparged with dry argon for 10 minutes, followed by evacuation under vacuum (ca. 15 torr) for 5 minutes. THF (1.5 mL) was then added and the solution then sparged with hydrogen gas for 5 minutes before being placed under a static atmosphere of hydrogen gas. To the resulting solution was added Pearlman's catalyst (11.2 mg). The resulting suspension was sparged with hydrogen gas for 5 minutes before being placed under an atmosphere of static hydrogen and stirred vigorously for 75 minutes. After the reaction was complete, it was rapidly filtered through a plug of Celite, eluting

with ethyl acetate (5 mL). The resulting solution was concentrated under vacuum to give bisphenol **1.25** (35.7 mg), which was used crude in the next step.

In a 10 ml microwave tube with magnetic stirring was added a solution of crude bisphenol **1.25** (35.7 mg) in acetone (0.5 mL). Allyl bromide (10.6 μL, 0.12 mmol) and potassium carbonate 12.6 mg, 0.091 mmol) were added, in that order. The tube was then sealed and placed under an atmosphere of dry nitrogen before being heated in a microwave at 85 °C for 3 hours. The suspension was then cooled to 24 °C and volatiles removed under vacuum, thoroughly. MeOH (0.5 mL) was then added to the tube and the suspension stirred for 10 minutes before benzaldehyde (12.5 μL, 0.12 mmol) and lithium hydroxide monohydrate (10 mg, 0.24 mmol) were added. The tube was then heated in an aluminum heating block at 50 °C for 30 minutes. After being cooled to 24 °C, the suspension was quenched with 5 mL saturated aqueous ammonium chloride. The mixture was extracted with ethyl acetate (5 x 5 mL) and the combined organic phases washed with saturated brine (5 mL), dried over sodium sulfate, filtered, and concentrated *in vacuo*. After drying under high vacuum overnight, the crude phenol **1.08** (16.1 mg) was used crude in the next step.

In a dry 20 mL vial containing a magnetic stir-bar was added 1,3-dimethyl barbituric acid (11.2 mg, 0.072 mmol), [$Pd(PPh_3)_4$] (3.4 mg, 0.0029 mmol), crude phenol **1.08** (14.7 mg) and dry THF (4.5 mL). The bright yellow solution was stirred for 15 mins before being rapidly filtered through a short plug of silica gel, which was eluted with ethyl acetate (10 mL). The resulting solution as concentrated under vacuum and purified by reverse-phase preparative TLC (1:7 water/acetonitrile) followed by normal-phase preparative TLC (5% MeOH/ DCM). The yellow band was collected affording caesalpinflavan B (4.9 mg, 40% over 3 steps) as a yellow amorphous solid.

^{1}H NMR (600 MHz, MeOH-d_4): δ 7.94 (d, J = 8.9 Hz, 1H), 7.85 – 7.79 (m, 2H), 7.76 – 7.71 (m, 2H), 7.46 –7.39 (m, 3H), 7.38 – 7.33 (m, 2H), 7.35 – 7.29 (m, 3H), 7.25 (t, J = 7.2 Hz, 1H), 6.52 (dd, J = 8.4, 1.0 Hz, 1H), 6.46 (d, J = 8.9 Hz, 1H), 6.40 (d, J = 2.5 Hz, 1H), 6.21 (dd, J = 8.3, 2.5 Hz, 1H), 5.54 (dd, J = 5.8, 3.9 Hz, 1H), 4.49 (t, J = 7.3 Hz, 1H), 2.74 (ddd, J = 13.6, 8.3, 3.9 Hz, 1H), 2.25 (dt, J = 13.6, 6.1 Hz, 1H). **^{13}C NMR (151 MHz, MeOH-d_4):** δ 192.1, 164.6, 163.2, 155.8, 155.0, 143.6, 142.3, 135.0, 130.2, 130.1, 128.6, 128.3, 128.1, 127.9, 126.7, 125.2, 120.5, 117.3, 116.8, 113.2, 107.5, 107.4, 102.4, 75.4, 32.9, 26.6.**TLC** (C_{18} silica: water–acetonitrile = 1:7), R_f = 0.72. **IR (ATR)**: ν_{max} (cm^{-1}) = 3407 (br), 2925 (w), 1586 (s), 1495 (m), 1449 (m), 1288 (s), 1228 (s), 1156 (s), 1118 (m), 977 (w), 759 (m), 697 (m). **HRMS (ESI$^+$)** Calcd. for $C_{30}H_{24}O_5Na$ [M+Na]: 487.1521, found: 487.1516. Calcd. for $C_{30}H_{25}O_5$ [M+H]: 465.1702, found: 465.1700.

Bis-Allyl Phenol **1.08**

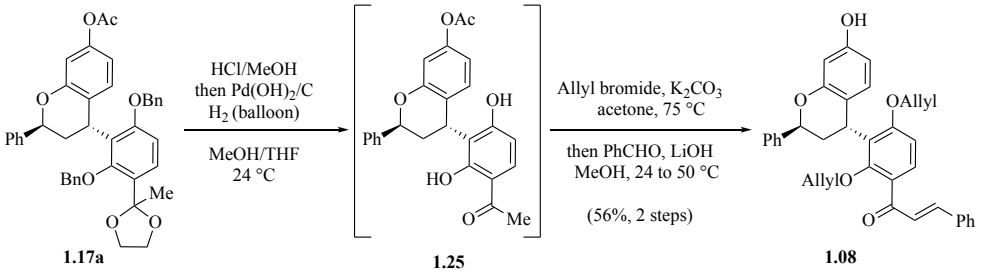

Experimental: In a vial containing a magnetic stir bar with a solution of **1.17a** (41.6 mg,0.065 mmol) in MeOH (3.0 mL) was added 10% aq. HCl (20 μL). The solution stirred at 24 °C for 15 minutes before being sparged with dry argon for 10 minutes, followed by evacuation under vacuum (ca. 15 torr) for 5 minutes. THF (3.0 mL) was then added and the solution then sparged with hydrogen gas for 5 minutes before being placed under a static atmosphere of hydrogen gas. To the resulting solution was added Pearlman's catalyst (30 mg). The resulting suspension was sparged with hydrogen gas for 5 minutes before

being placed under an atmosphere of static hydrogen and stirred for 60 minutes. After the reaction was complete, it was rapidly filtered through a plug of Celite, eluting with ethyl acetate (25 mL). The resulting solution was concentrated under vacuum to give crude bisphenol **1.25**. which was used crude in the next step.

In a 10 mL microwave tube containing a magnetic stir bar with a solution of crude bisphenol **1.25** in acetone (1.5 mL) was added allyl bromide (18.0 μL, 0.21 mmol) and potassium carbonate (37.7 mg, 0.22 mmol). The tube was then sealed and placed under an atmosphere of dry nitrogen before being heated in a microwave at 75 °C for 6 hours. The suspension was then cooled to 24 °C and volatiles removed under vacuum, thoroughly. MeOH (1.5 mL) was then added to the tube and the suspension stirred for 10 minutes before benzaldehyde (19.0 μL, 0.17 mmol) and lithium hydroxide monohydrate (10 mg, 0.24 mmol) were added. The tube was then heated in a microwave at 50 °C for 30 minutes. After being cooled to 24 °C, the suspension was quenched with 10 mL saturated aqueous ammonium chloride. The mixture was then extracted with DCM (5 x 5 mL) and the combined organic phases washed with saturated brine (5 mL), dried over sodium sulfate, filtered, and concentrated. The crude residue was purified by MPLC (12 g gold column, 30 mL/min, 10% to 60% Ethyl acetate/hexanes) to give a Phenol **1.08** as a yellow oil (19.9 mg, 56% yield over two steps). **1.08** exhibited broad ^{1}H resonances in $CDCl_3$, while giving relatively sharp ^{1}H resonances in PhMe-d_8. Variable temperature NMR in PhMe-d_8 suggested the presence of two atropisomers which seemed not to interconvert up at up to 75 ºC. For this reason, **1.08** was carried forward to the next step without rigorous characterization.

p-Quinol **1.07**

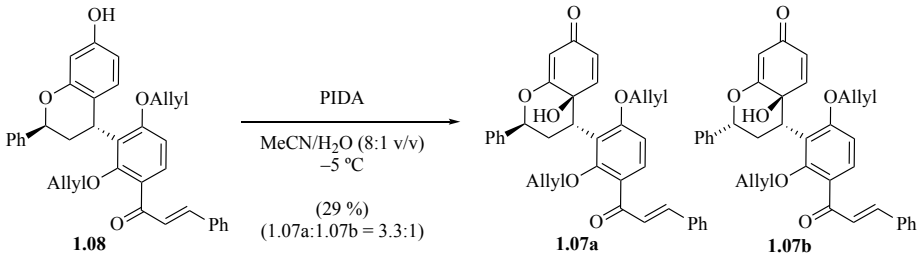

Experimental: In a scintillation vial containing a magnetic stir bar with a stirred solution of crude **1.08** (8.1 mg, 0.015 mmol) in 8:1 (v/v) solution of acetonitrile/water (2.0 mL) at –5 °C was added PIDA (8.6 mg, 0.026 mmol) in one portion. The faint-yellow solution was stirred rapidly for 40 minutes to afford a bright orange solution. After completion, as judged by TLC, the solution was concentrated to ca. 0.3 mL and loaded directly only a 20 cm x 20 cm TLC plate and developed with EtOAc/hexanes (1:1 v/v) to give **1.07a**/**1.07b** (3.3:1) yellow foam (2.4 mg, 29%).

Note: 1.07a was shown to be quite unstable and would oxidize on air over time. Therefore, it was not characterized rigorously.

^{1}H NMR (600 MHz, Chloroform-*d*): δ 7.74 (d, *J* = 15.8 Hz, 1H), 7.65 – 7.58 (m, 3H), 7.49 (d, *J* = 15.7 Hz, 1H), 7.45 (d, *J* = 7.2 Hz, 2H), 7.44 – 7.38 (m, 7H), 7.35 (d, *J* = 7.2 Hz, 1H), 6.73 (d, *J* = 8.8 Hz, 1H), 6.51 (d, *J* = 9.9 Hz, 1H), 6.02 – 5.88 (m, 4H), 5.74 (d, *J* = 1.8 Hz, 1H), 5.52 (dd, *J* = 10.6, 3.7 Hz, 1H), 5.40 – 5.21 (m, 5H), 5.18 (d, J = 10.4 Hz, 1H), 4.48 – 4.45 (m, 2H), 4.44 – 4.42 (m, 3H), 2.99 (ddd, J = 14.5, 10.6, 6.9 Hz, 1H), 2.35 (s, 1H), 2.14 (dt, J = 14.5, 3.8 Hz, 1H) (Note: overlap of the aromatic resonances with impurity accounts for larger integration values). **^{13}C NMR (151 MHz, $CDCl_3$):** δ 191.1, 187.9, 175.8, 160.3, 158.0, 145.5, 143.8, 140.5, 134.8, 132.5, 131.8, 131.3, 130.5, 128.9, 128.6, 128.5, 128.3, 128.1, 126.1, 125.7, 121.7, 119.1, 119.0, 108.3, 106.5, 79.77, 77.5,

68.3, 66.0, 37.9, 34.4. **IR (ATR)**: ν_{max} (cm^{-1}) = 3336 (br), 3030 (w), 2926 (w), 1658 (m), 1592 (s), 1450 (w), 1337 (m), 1275 (m), 1192 (m), 1084 (m), 913 (m), 862 (w), 811 (w), 760 (m), 731 (m), 700 (m), 563 (w). **HRMS (ESI$^+$)** Calcd. for $C_{36}H_{32}O_6Na$. $[M+Na]^+$: 583.2097. Found: 583.2091. **TLC** (EtOAc–hexanes = 1:1), R_f = 0.44.

Caesalpinnone A **1.01**

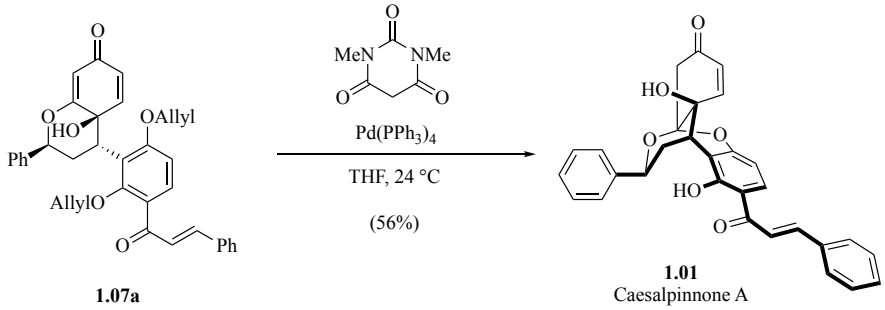

Experimental: In a dry 1.5-dram vial containing a stir bar, **1.07a**/**b** (3.4 mg, 0.0061 mmol, 3.3:1 mixture), 1,3-dimethyl barbituric acid (3.3 mg, 0.0021 mmol, 3.5 equiv), [$Pd(PPh_3)_4$] (0.9 mg, 13 mol %), and a magnetic stir-bar was dry THF (1.5 mL). The bright yellow solution was stirred for 10 minutes before being rapidly filtered through a short plug of silica gel, which was eluted with ethyl acetate (3 mL). The resulting solution as concentrated under vacuum and purified by reverse-phase preparative TLC (4:7 water/acetonitrile). The yellow band was collected affording **1.01** (1.65 mg, 56 %) as a yellow microcrystalline solid.

^{1}H NMR (600 MHz, Acetone-d_6): δ 14.08 (s, 1H), 8.23 (d, J = 8.9 Hz, 1H), 8.07 (d, J = 15.5 Hz, 1H), 7.97 (d, J = 15.4 Hz, 1H), 7.94 – 7.89 (m, 2H), 7.52 – 7.50 (m, 3H), 7.44 (d, J = 7.1 Hz, 2H), 7.35 (t, J = 7.6 Hz, 2H), 7.29 (t, J = 7.3 Hz, 1H), 6.84 (dd, J = 9.9, 1.0 Hz, 1H), 6.48 (d, J = 9.0 Hz, 1H), 5.93 (d, J = 9.9 Hz, 1H), 5.44 (s, 1H), 4.81 (dd, J = 12.2, 3.5

Hz, 1H), 3.74 (t, J = 3.5 Hz, 1H), 3.34 (d, J = 16.8 Hz, 1H), 2.80 (partially overlaps with HDO), 2.76 (d, J = 16.7 Hz), 1.94 (dt, J = 13.3, 3.4 Hz, 1H).**^{13}C NMR (151 MHz, Acetone):** δ 194.6, 192.6, 163.2, 161.6, 148.2, 144.8, 141.3, 134.9, 131.1, 130.8, 130.5, 129.0, 128.9, 128.2, 127.6, 126.2, 120.5, 114.2, 111.4, 106.4, 101.5, 71.5, 64.1, 44.3, 33.7, 32.8. **TLC** (C18 silica: water–acetonitrile = 4:7), R_f = 0.30. **IR (ATR)**: ν_{max} (cm^{-1}) = 3381 (br), 2926 (m), 2853 (w), 1667 (s), 1634 (s), 1594 (s), 1487 (m), 1450 (m), 1421 (m), 1359 (s), 1278 (s), 1223 (s), 1178 (w), 1102 (s), 1009 (s), 994 (s), 885 (w), 854 (w), 788 (m), 699 (m), 570 (w). **HRMS (ESI$^+$)** Calcd. for $C_{30}H_{25}O_5$ [M+H]: 481.1651, found: 481.1644. **TLC** (C_{18} silica: water–acetonitrile = 4:7), R_f = 0.53.

(+)-7-hydroxyflavanone **1.14**

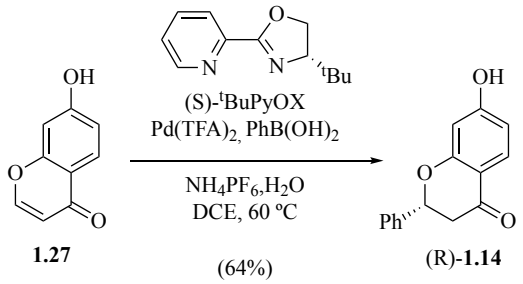

Experimental: In a 50 mL round bottom flask charged with $Pd(TFA)_2$ (84.0 mg, 0.25 mmol), (*S*)-*t*BuPyOX (62.0 mg, 0.30 mmol), ammonium hexafluorophosphate (250.0 mg, 1.5 mmol), and $PhB(OH)_2$ (1.23 g, 10 mmol). The flask was sealed and purged with argon and dry dichloroethane (10 mL) added. The resulting suspension was stirred for 3 minutes at 24 ºC before **1.27** (810 mg, 5 mmol) and water (0.5 mL, 25 mmol) were added. An additional portion of dichloroethane (10 mL) was added and the suspension heated to 60 ºC and stirred vigorously. After 22 h, the reaction cooled to 24 ºC and contents filtered over a pad of silica gel, which was eluted with EtOAc (3 x 50 mL). Silica gel (ca 10 g) was added to the solution and the solvents were removed in vacuo. The free flowing solid was

then chromatographed directly (10% to 40% EtOAc/hexanes) to afford (*R*)-**1.14** (1.83 g, 64%, 96.5:3.5 er, see Appendix A for HPLC trace) yellow microcrystalline solid. The spectral data for (*R*)-**1.14** matched those previously reported.[13]

Optical Rotation: $[\alpha]_D^{24}$: (c = 0.98), +73.2°

(+)-Acetate **1.15**

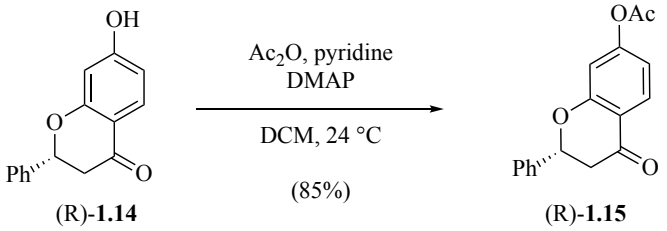

(R)-**1.14** (R)-**1.15**

Experimental: In a 100 mL round bottom flask containing a magnetic stir-bar was charged with (R)-**1.14** (731.5 mg, 3.0 mmol, 1 equiv) and diluted with DCM (32 mL). Successively ,acetic anhydride (0.323 mL, 3.6 mmol, 1.2 equiv), pyridine (0.310 mL, 4.2 mmol, 1.5 equiv), and DMAP (20 mg, 0.16 mmol) were added. The reaction was stirred for 30 minutes before silica gel (ca. 2 g) was added and the volatiles removed in vacuo before being directly loaded in to an empty MPLC cartridge (25 g) and chromatographed (40 g column, 60 mL/min, 10 to 40 % ethyl acetate/hexanes) to give acetate (R)-**1.15** (758 mg, 85%, 96.5:3.5 er, see Appendix A for HPLC trace) as a colorless microcrystalline solid. The spectral data of (R)-**1.15** matched those previously reported.[13]

Optical Rotation: $[\alpha]_D^{24}$: (c = 0.66), +43.0°

(-)-Hydrazone **1.10**

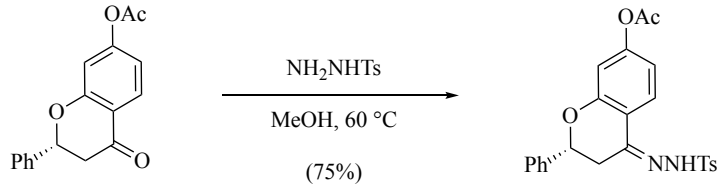

Experimental: In a 100 mL round-bottom flask equipped with a magnetic stir-bar was added (*R*)-**1.15** (645 mg, 2.28 mmol, 1 equiv) and MeOH (28 mL). To the stirred solution was added *p*-tosylhydrazide (797 mg, 4.35 mmol, 1.9 equiv) and the flask then heated to 60 °C under a static atmosphere of nitrogen. After 11 h, the solution slowly cooled to 4 °C over the course of 1 hour. The precipitate was collected in a large Kiriyama filter to yield (*R*)-**1.10** (767 mg, 75%, 95:5 er, see Appendix A for HPLC trace) as a colorless microcrystalline solid. The material was azeotropically-dried from benzene (3 x 10 mL) before being used in the next step. The spectral data for (*R*)-**1.10** matched those for racemic **1.10**.

Optical Rotation: $[\alpha]_D^{24}$: (c = 0.46), –84.4°

Entantioenriched Benzopyran **1.09**

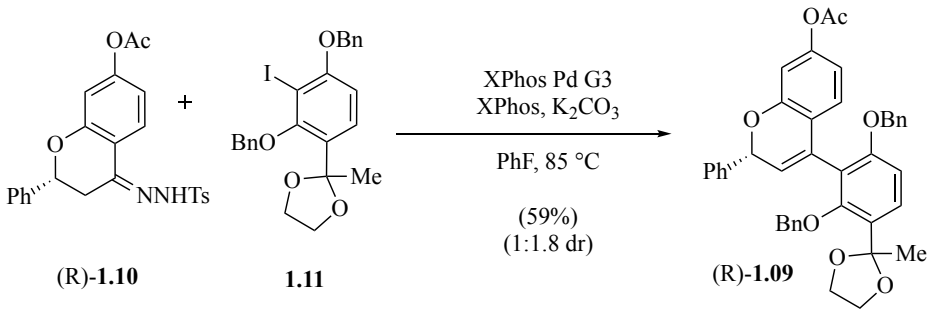

Experimental: A 1.5 dram vial equipped with stir-bar was added **1.10** (80.0 mg, 0.176 mmol, 1.0 equiv) XPhos Pd G3 (27.2 mg, 0.035 mmol, 20 mol %), XPhos (17.2 mg, 0.036

mmol, 20 mol %), followed by dry PhF (1.6 mL). The suspension was stirred under argon for 5 minutes before K_2CO_3 (145.6 mg, 1.05 mmol, 6 equiv) and **1.11** (355.6 g, 0.70 mmol, 4 equiv).The vial was sealed before being left under a static atmosphere of argon and heated to 85 °C for 60 minutes with vigorous stirring. After the reaction was complete, it was cooled to 24 °C and filtered over a pad of silica gel. The silica gel pad was washed with EtOAc (5 x 150 mL) and the washes combined before being concentrated *in vacuo* to give an orange oil. The oil was chromatographed (MPLC, 12 g column, 30 mL/min 0% to 40% EtOAc/hexanes to give **1.09** as a light-yellow foam (63.6 mg, 56%, (Major atropisomer: 93:7 er. Minor atropisomer: 91.5:8.5 er, see Appendix A for HPLC trace). The spectral data for enantioenriched **1.09** were identical to that of racemic **1.09**.

Note: Complete baseline separation of atropisomers was not possible, and therefore an optical rotation is not reported.

(-)-Dihydropyran **1.17a**

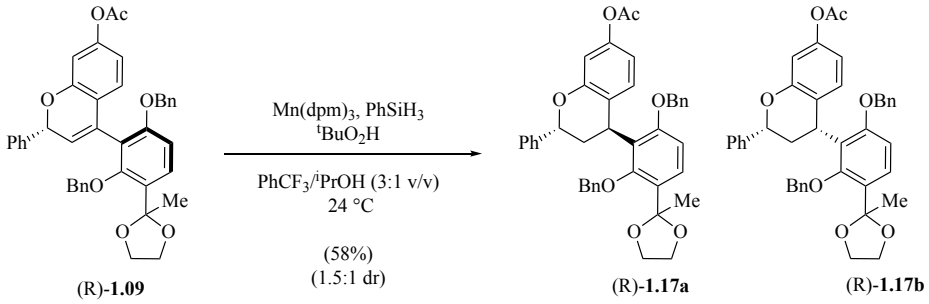

Experimental: In a vial equipped with a magnetic stir-bar was added (*R*)-**1.09** (17 mg, 0.026 mmol, 1 equiv) and then diluted with dry $PhCF_3$/*i*PrOH (1.0 mL, 3:1 v/v). Next, $PhSiH_3$ (7.0 µL, 0.065 mmol, 2.5 equiv) and *t*butyl hydroperoxide (10 µL, 5.5 M in decane, 0.055 mmol, 2.1 equiv) were added. The solution was sparged for 5 minutes with dry argon before $Mn(dpm)_3$ (8.0 mg, 0.013 mmol, 0.5 equiv) was added in one portion. The solution

was then sparged for 10 seconds with dry argon before being left under a static atmosphere of argon and stirred at 24 °C for 40 min. After completion (as judged by ESI-MS), silica gel (ca. 0.5 g) was added and the suspension concentrated to a free-flowing powder, which was chromatographed directly by MPLC (4 g column, 13 mL/min, 10% to 40% EtOAc/hexane) to give **1.17a** and **1.17b** (9.9 mg, 58%) as a 1.5:1 mixture of trans/cis isomers and as a colorless oil. The mixture was separated by, preparative reverse-phase HPLC (21.2 x 100 mm Phenomenex Gemini column (5 μm C_{18} 110 Å, 21.2 x 100 mm), 65% MeCN in H_2O → 100% MeCN over 15 minutes, 20 mL/min) to give **1.17a** (5.8 mg, 89:11 er, colorless microcrystalline solid, see Appendix A for HPLC trace) and **1.17b** (2.1 mg, ca. 92.5:7.5 er, colorless solid, see Appendix A for HPLC trace). The spectral data for enantioenriched **1.17a** and **1.17b** were identical to racemic **1.17a** and **1.17b.**

Optical Rotation: $[\alpha]_D^{24}$ **1.17a** (89:11 er material: $[\alpha]_D^{24}$: (c = 0.29), –5.5°) $[\alpha]_D^{24}$ **1.17b** (ca. 92.5:7.5 er material: $[\alpha]_D^{24}$: (c = 0.12), +23.3°)

(-)-Caesalpinflavan B **1.03**

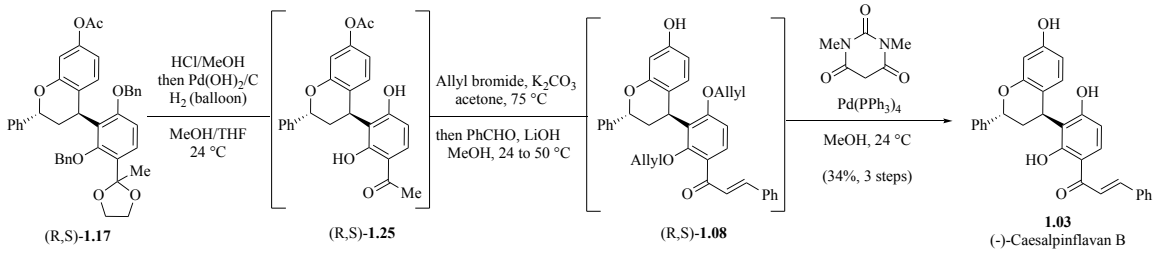

Experimental: In a vial equippied with a magnetic stir-bar was added enantioenriched dihydropyran (–)-**1.17a** (30.0 mg, 0.046 mmol) in MeOH (3.0 mL) and followed by 10% aq. HCl (10.0 μL). The solution stirred at 24 °C for 20 minutes before being sparged with dry argon for 15 minutes, followed by evacuation under vacuum (ca. 15 torr) for 5 minutes. THF (3 mL) was then added and the solution then sparged with hydrogen gas for 5 minutes

before being placed under a static atmosphere of hydrogen gas. To the resulting solution was added Pearlman's catalyst (20.0 mg). The resulting suspension was sparged with hydrogen gas for 5 minutes before being placed under an atmosphere of static hydrogen and stirred vigorously for 50 minutes. After the reaction was complete, it was rapidly filtered through a plug of Celite, eluting with ethyl acetate (5 mL). The resulting solution was concentrated under vacuum to give enantioenriched bisphenol **1.25** (50.7 mg), which was used crude in the next step.

In a 10 mL microwave tube was added a solution of crude enantioenriched bisphenol **1.25** (50.7 mg) in acetone (1.5 mL), followed by bromide (20.0 μL, 0.23 mmol) and potassium carbonate (20.0 mg, 0.144 mmol). The tube was then sealed and placed under an atmosphere of dry nitrogen before being heated in a microwave at 85 °C for 6 hours. The suspension was then cooled to 24 °C and volatiles removed under vacuum, thoroughly. MeOH (1 mL) was then added to the tube and the suspension stirred for 10 minutes before benzaldehyde (40.0 μL, 0.38 mmol) and lithium hydroxide monohydrate (40.0 mg, 0.95 mmol) were added. The tube was then heated in an aluminum heating block at 50 °C for 2 hours. After being cooled to 24 °C, the suspension was quenched with 5 mL saturated aqueous ammonium chloride. The mixture was extracted with ethyl acetate (5 x 5 mL) and the combined organic phases washed with saturated brine (5 mL), dried over sodium sulfate, filtered, and concentrated *in vacuo* (**Note 3**). After drying under high vacuum 6 hours, the crude enantioenriched phenol **1.08** (25.5 mg) was used crude in the next step.

In a dry 20 mL vial containing magnetic stirring was added 1,3-dimethyl barbituric acid (30.0 mg, 0.192 mmol), $[Pd(PPh_3)_4]$ (10.5 mg, 0.0091 mmol), crude phenol **1.08** (25.5

mg) and dry THF (5 mL). The bright yellow solution was stirred for 15 mins before being rapidly filtered through a short plug of silica gel, which was eluted with ethyl acetate (10 mL). The resulting solution was concentrated under vacuum and chromatographed directly by MPLC (4 g column, 13 mL/min, 10% to 60% EtOAC/hexane) to give caesalpinflavan B (8.7 mg, 41% over 3 steps, >99:1 er, see Appendix A for HPLC trace) as a yellow amorphous solid. The analytical data for (–)-**1.03** matched those obtained for racemic **1.03**.

Optical Rotation: $[\alpha]_D^{24}$: (c = 0.20), –38.0°.

1.7 References

[1]Zhang, L.-J.; Bi, D.-W.; Hu, J.; Mu, W.-H.; Li, Y.-P.; Xia, G.-H.; Yang, L.; Li, X.-N.; Liang, X.-S.; Wang, L.-Q. *Org. Lett.* **2017**, *19*, 4315–4318.

[2]Wollenweber, E.; Seigler, D. S. *Phytochem.* **1982**, *21*, 1063–1066.

[3]Tanrisever, N.; Fronczek, F. R.; Fischer, N. H.; Williamson, G. B. *Phytochem.* **1986**, *26*, 175–179.

[4]Pescitelli, G. *Marine Drugs* **2018**, *16*, 388.

[5]Barluenga, J.; Valdés, C. *Angew. Chem., Int. Ed.* **2011**, *50*, 7486–7500.

[6] Bamford, W. R.; Stevens, T. S. 924. *J. Chem.l Soc.* **1952**, 4735.

[7]Pawar, G. G.; Tiwari, V. K.; Jena, H. S.; Kapur, M. *Chem. Eur. J.* **2015**, *21*, 9905

[8]Barton, D. H.; McCombie, S. W. *J. Chem. Soc., Perkin Trans.* **1975**, 16, 1574.

[9]Iwasaki, K.; Wan, K. K.; Oppedisano, A.; Crossley, S. W.; Shenvi, R. *J. Am. Chem. Soc.* **2014**, *136*, 1300–1303.

[10]Pearlman,W. M. *Tetrahedron Lett.* **1967**, 8 , 1663 —1664

[11]Van De Water, R. W.; Hoarau, C.; Pettus, T. R. R. *Tetrahedron Lett.* **2003**, *44*, 5109–5113.

[12]Timmerman, J. C.; Sims, N. J.; Wood, J. L. *J. Am. Chem. Soc.* **2019**, *141*, 10082– 10090

[13]Holder, J. C.; Marziale, A. N.; Gatti, M.; Mao, B.; Stoltz, B. M. *Chem. Eur. J.* **2013**, *19*, 74

[14]Tsuji, J.; Takahashi, H.; Morikawa, M. *Tetrahedron Lett.* **1965**, *6*, 4387–4388.

CHAPTER TWO

Progress Toward the Total Synthesis of (-)-Alterbrassicicene B and Alterbrassicicene C

2.1 Isolation of (-)-Alterbrassicicene B and (+)-Alterbrassicicene C

In 2020, Zhang and coworkers reported the isolation (-)-alterbrassicicene B (**2.01**) and (+)-alterbrassicicene C (**2.02**) along with a number of related congeners from *Alternaria brassicola*.[1] Alterbrassicicene B/C are modified fusicoccane-type diterpenoids that contain unprecedented ring systems for this family (Figure 2.1). Specifically, these congeners possess 5/6/6/5 tetracyclic ring systems which lie in contrast to typical family members that bear a 5/8/5 tricyclic ring system (e.g., (+)-3-ketobrassicicene W (**2.03**)). Additionally, alterbrassicicene C possesses 3 quaternary centers and 2 α,β-unsaturated ketones. In contrast, alterbrassicicene B manifests a single all-carbon quaternary stereocenter which is among an array of 7 contiguous stereocenters. Although alterbrassicicenes B and C showed only modest to no biological activity in a small screen of cancer cell lines, the broader family of fusicoccane natural products has been demonstrated to possess numerous congeners that display incredibly promising and selective biological activities. With these factors in mind, we have sought to synthesize these two natural products with the hope of eventually enabling screening for activity against a wider range of diseases.

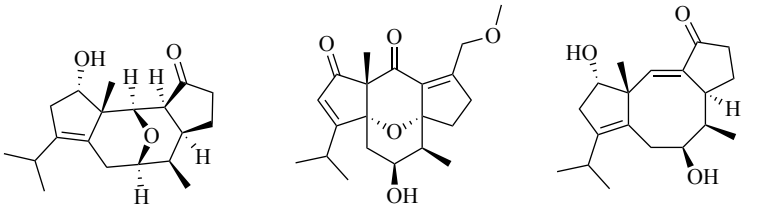

2.01
(-)-alterbrassicicene B

2.02
(+)-alterbrassicicene C

2.03
(+)-3-ketobrassicicene W

Figure 2.1 Fusicoccane natural products

2.2 Divergent Approach to Alterbrassicicene B and C

In planning our route to **2.01** and **2.02**, we wanted to devise a strategy that would provide access to both natural products via a common late-stage intermediate (**2.04**, Scheme 2.1). We believed this to be possible due to their similar fundamental structures and potential ether-type disconnects. Importantly, the stereochemistry is homologous relative to carbon 7", 8" and 11". We believed that an advanced cyclooctadiene, such as **2.04**, would hold considerable promise as an intermediate from which to reach both natural products, due to numerous points of potential functionalization and divergence.

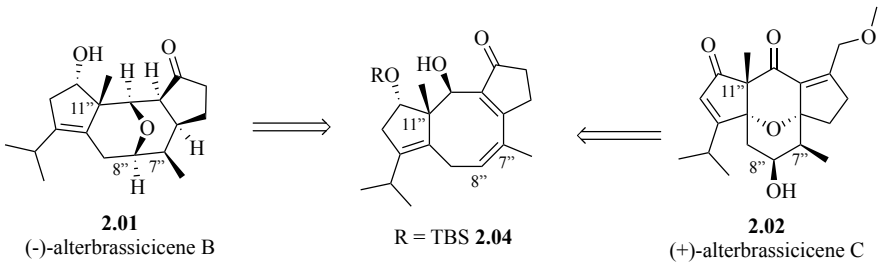

2.01
(-)-alterbrassicicene B

R = TBS **2.04**

2.02
(+)-alterbrassicicene C

Scheme 2.1 Divergent approach to the alterbrassicicenes

After deciding upon this approach, we performed a more in-depth analysis of **2.04**. As illustrated retrosynthetically in Scheme 2.2, we surmised that a ring-closing metathesis (RCM) between the terminal olefin and isopropenyl moieties in intermediate **2.05** would furnish the desired 5/8/5 ring system. Allylic alcohol **2.05** could arise from lithium halogen

exchange with vinyl bromide **2.07** and subsequent nucleophilic addition into neo-pentyl aldehyde **2.06**. The skipped diene (**2.06**) would result from a cross-coupling between allyl stannane and the vinyl triflate derived from ketone **2.08**.[2] The 1,3-dicarbonyl (**2.08**) would be the product of an isomerization/ozonolysis sequence applied to the terminal olefin in **2.09**.

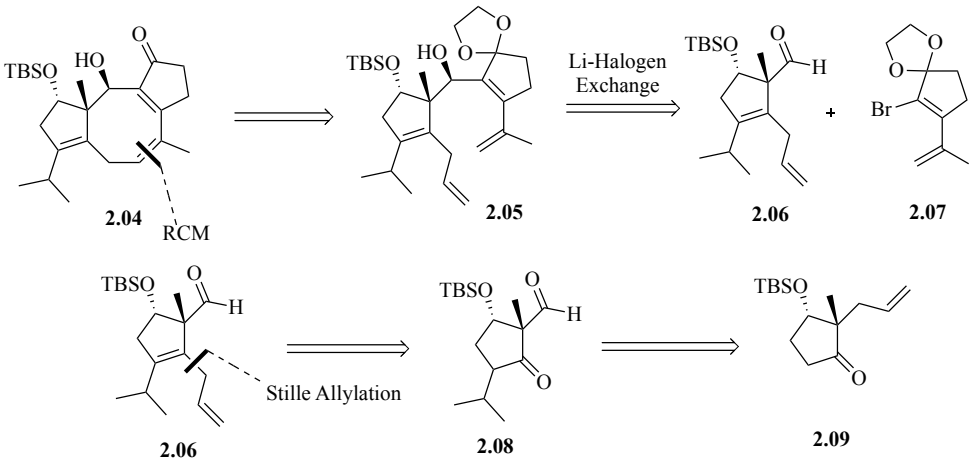

Scheme 2.2 Retrosynthetic analysis of cyclooctadiene

2.3 Route to Cyclooctadiene

2.3.1 Synthesis of Cyclopentanone Fragments

In 1982, Brooks and coworkers reported the use of baker's yeast to reduce 2-Allyl-2-methyl-1,3-cyclopentanedione **2.10** to ketol **2.11** (Scheme 2.3).[3] This enzymatic desymmetrization cleanly sets the stereochemistry with excellent control of both diastereoselectivity and enantioselectivity and establishes the setereogenicity at the all-carbon quaternary center early in the synthesis. This reduction could also be conducted in a racemic series using $NaBH_4$ in glyme.[4] From **2.11**, facile protection of the secondary alcohol with TBSCl gives the silyl ether (**2.12**) in 93% yield.[5] Alkylation to install the

isopropyl group proved to be a challenge. Thus, exposure of **2.12** to various bases under a variety of reaction conditions followed by addition of 2-idopropane was found to typically result in little to no conversion. Modification of conditions described in the literature by using a large excess of both NaH and isopropyl iodide at elevated temperatures resulted in modest yields of an inconsequential mixture of diastereomers.[6] Having accessed sufficient quantities of alkylated cyclopentanone **2.13**, we subjected this material to the Grubbs II catalyst in MeOH to isomerize the terminal olefin to the thermodynamically preferred internal position. The crude isomerization product was then subjected to ozonolysis which provided keto-aldehyde **2.08** in 75% yield over the two-steps. Conversion of **2.08** to the corresponding enol triflate (not shown) was followed, without purification, by Stille cross-coupling with allyltributylstannane to furnish the skipped diene (**2.06**) in 55% yield over the two steps.

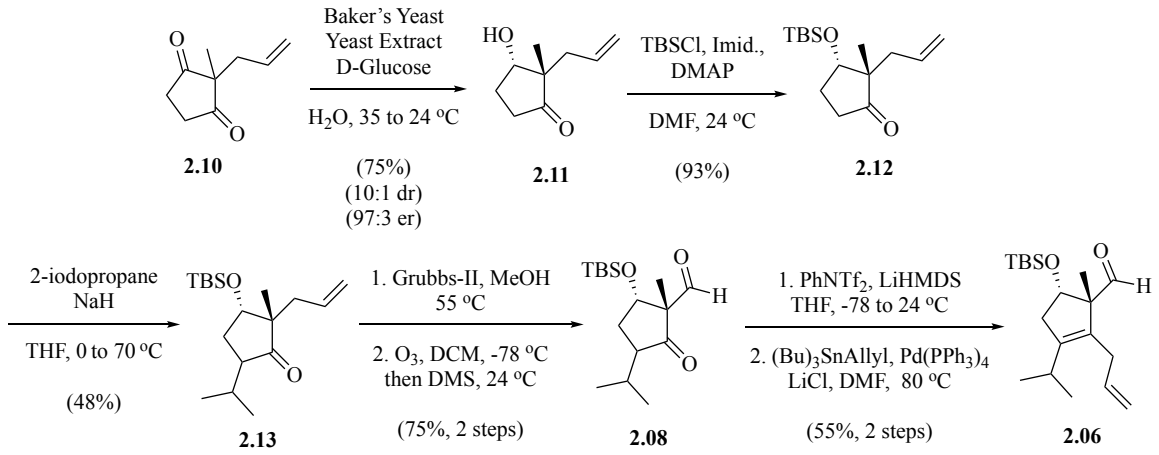

Scheme 2.3 Synthesis of skipped diene

With the skipped diene in hand, we shifted our efforts to constructing vinyl bromide **2.07**. To this end, the readily accessible vinylogous ester **2.14** was subjected to bromination with NBS to yield vinyl bromide **2.15** in 76% yield (Scheme 2.4).[7] Exposure

of **2.15** to isopropenyl magnesium bromide in the presence of cerium trichloride followed by treatment of the derived tertiary alcohol (not shown) with 1M HCl furnished extended enone (**2.16**) as a yellow oil.[8] Finally, protection of the ketone using ethylene glycol and Dean-Stark conditions yields acetal **2.07** in modest yields. This poor yield is due to the instability of the product, which decomposes over time, even when stored in frozen benzene at -20 °C. Notably, Smith and coworkers report similar stability issues with the acetal of bromo-cyclopentenone.[9]

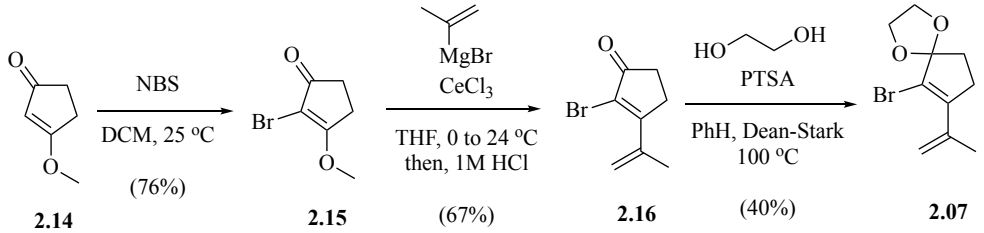

Scheme 2.4 Synthesis of vinyl bromide

2.3.2 Completion of Cyclooctadiene

Upon completion of both cyclopentanone intermediates, we began setting the stage for their coupling by investigating the conditions for lithium halogen exchange of **2.07** and addition of the derived anion to aldehyde **2.06** (Table 2.1). From literature precedents describing reactions of similar vinyl bromides, we first attempted to employ *n*BuLi for the metal halogen exchange.[10] However, *n*BuLi failed to exchange effectively and thus products derived from addition of the butyl anion to **2.06** were typically isolated. Based on these results we shifted focus to the more reactive reagent, *t*BuLi. The well-known rapid rate of metal halogen exchange coupled with the steric hindrance of both the organolithium and aldehyde provided hope that premixing of **2.06** and **2.07** prior to addition of *t*-BuLi would allow for metal halogen exchange followed by immediate

addition. Unfortunately, addition of the BuLi reagent to the aldehyde proved to be much more facile than anticipated. Undeterred, we shifted focus back to pre-forming the vinyl lithium by stirring viny bromide **2.07** with *t*BuLi for 60 minutes to ensure complete metal-halogen exchange. Subsequent addition of **2.06** to the derived vinyl anion resulted in promising yields of the product after warming to 24 °C for 5 hours. Further investigation revealed that improved yields (59%) of **2.05** as a single diastereomer could be achieved by increasing the reaction time and scale.

Table 2.1 Optimization of lithium-halogen exchange

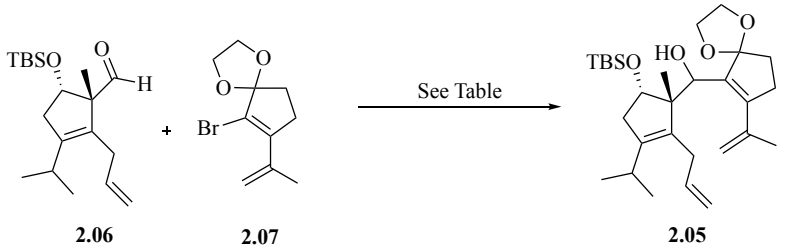

2.06 **2.07** **2.05**

Entry	R-Li (Equiv)	**2.06** (Equiv)	**2.07** (Equiv)	Time for Exchange (Min.)	Nucleophilic Addition (Hours)	Result/Yield of **2.05**
1	*n*BuLi (1.05)	1.0	1.05	15	1	*n*BuLi addition into **2.06**
2[a]	*t*BuLi (3.00)	1.0	1.50	0	1	*t*BuLi addition into **2.06**
3	*t*BuLi (2.10)	1.0	1.05	60	5	52%
4[b]	*t*BuLi (2.10)	1.0	1.05	60	6	59%

[a]**2.06** and **2.07** were pre-mixed. [b]About 500 mg scale.

Having successfully conjoined the cyclopentanone fragments, we next explored construction of the central eight-membered ring via ring closing metathesis (RCM) (Scheme 2.5). To this end we took inspiration from Nakada's synthetic efforts toward Ophiobolin A wherein a similar RCM was employed.[11] In the event, we were pleased to find that application of Nagata's conditions to **2.05**, which involved the use of 1,4-benzoquinone as an additive to prevent isomerization, led to formation of cyclooctadiene

2.04 in good yield. We eventually found that advancing the crude product from the nucleophilic addition to the RCM worked well and avoided issues encountered upon isolation of **2.05** that were due to the instability of the acetal on silica gel. Additionally, upon completion of the RCM, an acidic work-up was found to readily cleave the acetal to cleanly afford the extended enone in 54% yield over two-steps. Gratifyingly, the RCM product (**2.04**) was a crystalline solid and provided crystals suitable for X-ray analysis. The latter, not only confirmed overall connectivity of **2.04** but also allowed the unambiguous assignment of stereochemistry at the stereogenic allylic secondary alcohol formed upon the coupling of **2.06** and **2.07** (Scheme 2.5).

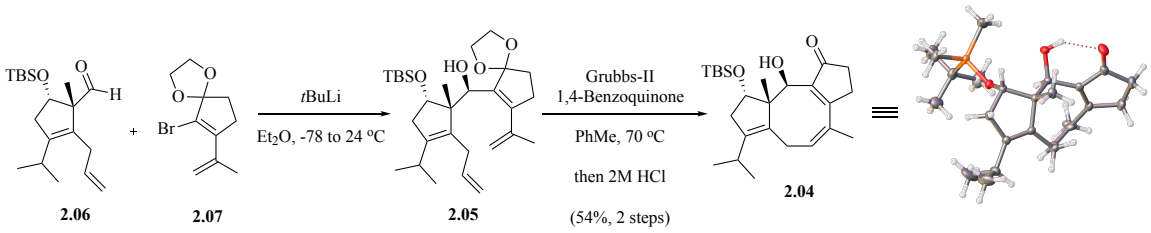

Scheme 2.5 Ring closing metathesis to cyclooctadiene

2.4 Initial Attempts at Alterbrassicicene B

2.4.1 Direct approach of Alterbrassicicene B

Having successfully accessed the entire carbon skeleton in the form of cyclooctadiene **2.04**, we next turned toward completing the synthesis of alterbrassicicene B. As illustrated in Scheme 2.6 this would involve a late-stage reduction and deprotection of ether **2.17** which would, in turn, derive from a trans-annular etherification via 1,6-oxa-Michael addition into the extended enone of **2.04**.

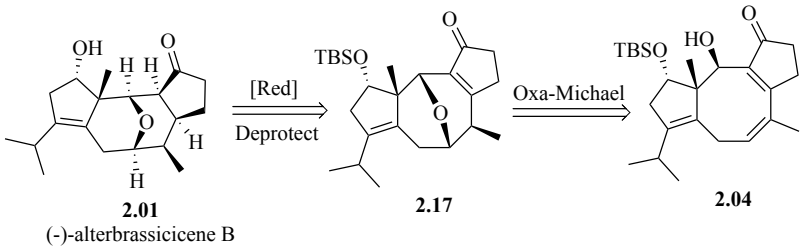

Scheme 2.6 Direct retrosynthetic approach to Alterbrassicicene B

In efforts to implement the planned oxa-Michael, we initially investigated a variety of bases (Scheme 2.7). For example, the allylic alcohol **2.04** was exposed to both thermodynamic bases (DBU) or kinetic bases (NaH, LDA), however, none of the attempted conditions were found to promote the oxa-Michael addition and in most cases returned starting material. Since increasing the nucleophilicity of the alcohol was not providing satisfactory results, we shifted our focus to increasing the electrophilicity of the enone. Unfortunately, treatment of **2.04** with Lewis acids such as BF_3-OEt_2 and TMSOTf was also found to be ineffective in promoting the oxa-Michael and, in the case of TMSOTf, only resulted in silylation of the secondary alcohol. Inspection of simple hand-held models of **2.04** led us to attribute the unsuccessful oxa-Michael reactions to the rigidity of the 8-member ring and inability of the substrate to adopt a conformation suitable for ring closure.

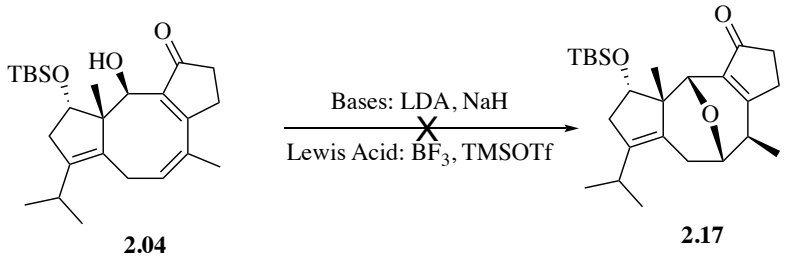

Scheme 2.7 Forward attempts to oxa-Michael

To overcome the issue of additions to the extended enone, we opted to modify the substrate and thus investigated selective 1,4-reductions of dienone **2.04** in hope of

generating the isolated tri-substituted olefin **2.18a** (Scheme 2.8, bottom). Initial studies using 1,4-selective reduction conditions, like copper hydrides, returned starting material and subsequent attempts with homo- and heterogenous hydrogenations led to mixtures of products, typically resembling only reduction of the trisubstituted olefin (i.e., **2.18b**). Turning next to dissolving metal reactions, we found that conditions such as the Birch reduction cleanly reduced cyclooctadiene **2.04** in a 1,6-fashion to produce **2.18b**, as evidenced by crude ^{1}H NMR.

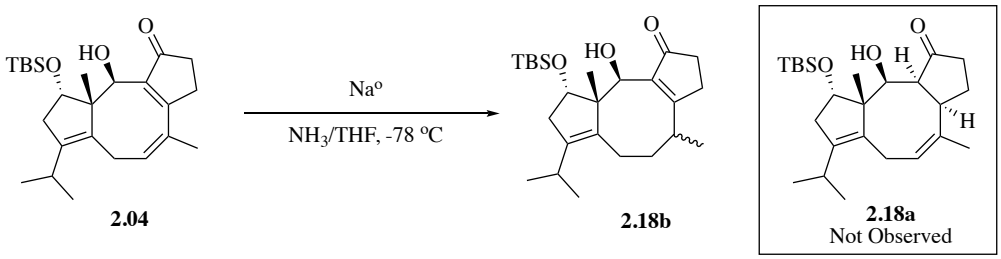

Scheme 2.8 Birch reduction of cyclooctadiene

In light of the failed reduction chemistry, we turned to alternative methods for introducing the trans-annular ether bridge from alcohol **2.04**. Since, direct trans-annular additions to the olefin had suggested that a conformational change was needed and efforts to address this need via reduction had failed, we began to consider a halo-etherification approach. Although this approach would require a subsequent dehalogenation step, the intermediacy of a halonium ion, which would induce an associated conformational change, was seen as an intriguing potential benefit. In addition to halo-etherification, selective epoxidation of the trisubstituted olefin followed by subsequent transannular epoxide opening also held potential. Given the likely ability to isolate the intermediate epoxide and confirm the subsequent course of the reaction we opted to first attempt this latter option.

Unfortunately, these efforts along with a brief foray into hydroboration/oxidation of the trisubstituted olefin proved unsuccessful. Finally, we turned to halo-etherification and in initial attempts, using elemental iodine or bromine, were again met with failure. Fortunately, we eventually turned to NBS, which gave what appeared to be a halo-ether product that had also undergone concomitant desilylation of the TBS group. Excited by this result, we attempted to elucidate the structure and discovered that this reaction had actually resulted in the formation of the 5/5/7/5 ring system (**2.19**, Scheme 2.9). This was most likely due to the stabilization of the, developing tertiary allylic carbocation coupled with the kinetically preferred closure of the 5- vs. 6-membered ring. With the hope of advancing **2.19**, we turned to known conditions wherein treatment of halo-ethers with silver salts can induce migration of the C-O bond.[13] Accordingly, under conditions that were slightly modified from those found in the literature, we found that Ag(TFA) in nitromethane did indeed effect migration of the newly form C-O bond. However, to our surprise, this migration was accompanied by further reaction of the secondary alcohol by nucleophile to attack onto the incipient allylic oxiranium ion **2.19a**. Thus, the product, isolated in an excellent 88% yield, possessed a 5/5/6/6/5 caged ring system (i.e., **2.20**). As illustrated the latter structure was eventually confirmed via single crystal X-ray analysis.

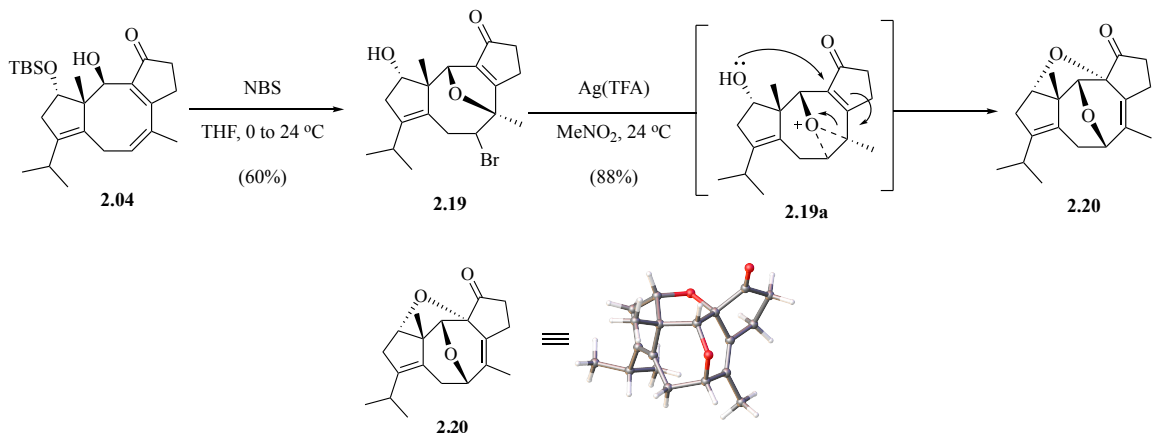

Scheme 2.9 Silver induced ether migration and X-ray image

2.4.2 Utilization of Novel Caged Dihydropyran

Although the novel caged intermediate **2.20** was not desired, the overall atom connectivity was quite promising in terms of accessing alterbrassicicene B. To this end, we recognized that cleavage of the ether bond alpha to the ketone would deliver the desired advanced intermediate **2.17** sans the TBS silyl ether (*vide supra*, Scheme 2.6). Accordingly, we treated **2.20** with standard Birch conditions (Scheme 2.10A) and indeed observed the production of a product arising from cleavage of the desired ether bond. Unfortunately, this transformation furnished **2.21a** as a single diastereomer having the incorrect methyl stereochemistry. The latter was confirmed as the illustrated β-isomer by low-quality SCXRD. In attempts to effect epimerization to the desired diastereomer **2.21b** via an intermediate extended enolate or enol we exposed **2.21a** to a variety of conditions, including: DBU, pyrrolidine, TMSOTf, and LiMHDS. Unfortunately, under all the attempted conditions the result was either recovery of starting material or decomposition. The latter was particularly acute when the reaction was exposed to atmospheric oxygen. In order to circumvent the formation of the incorrect methyl stereochemistry we attempted to selectively reduce the Eastern tetrasubstituted olefin prior to reductive cleavage of the

ether bond. Unfortunately, attempts at hydrogenation of **2.20** with Pd/C returned starting material, while stronger catalysts such as PtO_2 reduced the ketone (Scheme 2.10B). Employing Shenvi's HAT chemistry resulted in complex mixtures of products.

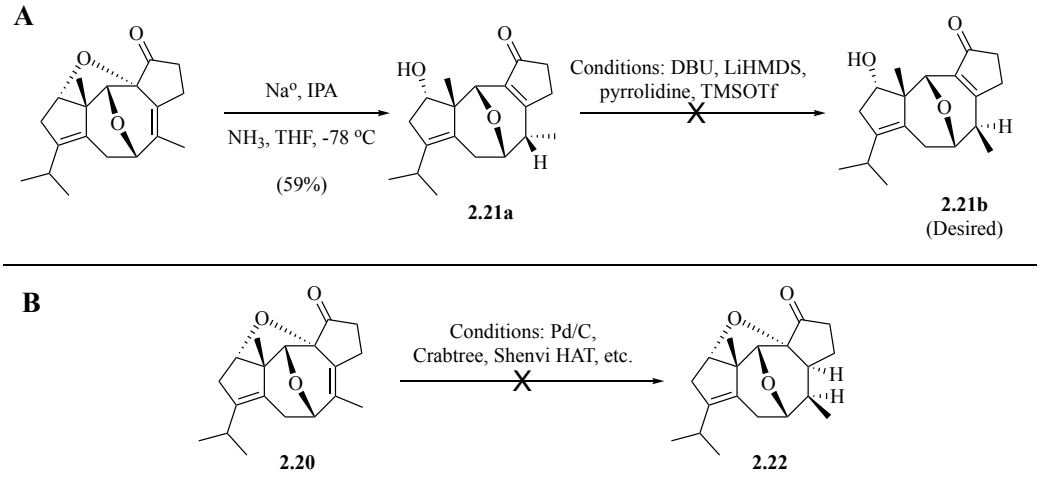

Scheme 2.10 Direct attempts at reduction

To overcome the challenges in directly reducing the requisite tetrasubstituted olefin, we turned to multistep approaches. In this regard, we recognized the Schenk-ene reaction as having potential to deliver a product that could be further manipulated to alterbrassicicene B.[15] After several trials with various photosensitizers and solvents, the only promising result was observed with methylene blue in MeCN, which delivered a low yield of allylic alcohol **2.23** (Scheme 2.11), where singlet oxygen approaches from the convex face – this was supported by fast-scan X-ray data (See appendix E). Despite the poor yield, we moved **2.23** forward by employing Shenvi's HAT conditions. The latter resulted in reduction of the trisubstituted olefin in 40% yield as a single diastereomer. Although unconfirmed, it was hypothesized that thermodynamic preference for the cyclopentanone would be syn-fused as illustrated in **2.24**. Excited with the potential of this

approach, we screened a multitude of conditions to effect conversion of **2.24** to a xanthate ester thereby enabling de-oxygenation of the tertiary alcohol. However, all attempts to acylated **2.24** resulted in returned starting material or elimination back to **2.20**. Attempts to treat alcohol **2.24** with Birch conditions, in hope of cleaving the alpha-ether bond, only gave **2.21a** by crude ^{1}H NMR. Based on this observation it was clear that the alpha-ether cleavage was successful, however, this was accompanies by the unwanted elimination of the tertiary alcohol and isomerization to the enone, either in the reaction or during work-up. Considering these latter results and our inability to obtain only modest to low yields in several of the reactions, we thought it best to halt further exploration of this route.

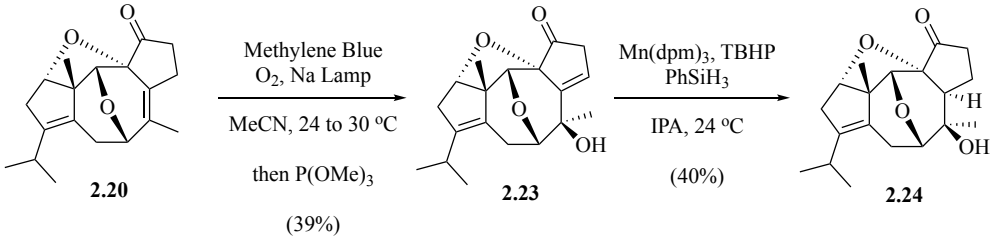

Scheme 2.11 Schenk-ene route to net reduction

2.5 Approach to Alterbrassicicene C

2.5.1 Retrosynthetic Strategy for Alterbrassicicene C

As discussed in section 2.2, we were targeting cyclooctadiene **2.04** as the point of divergence in accessing alterbrassicicenes B and C. As illustrated retrosynthetically in Scheme 2.12, advancing **2.04** to **2.02** would involve late-stage introduction of the methoxymethyl unit via Stille coupling on an intermediate enol triflate derived from 1,3-diketone **2.25**. Exposure of the product derived from the Stille reaction to olefin hydration conditions would then deliver the natural product. The 5/6/6/5 tetracycle **2.25** was

envisioned as arising from **2.26** via a transannular oxa-Michael addition. A series of oxidations would provide the desired oxa-Michael precursor (**2.26**) from cyclooctadiene **2.04**.

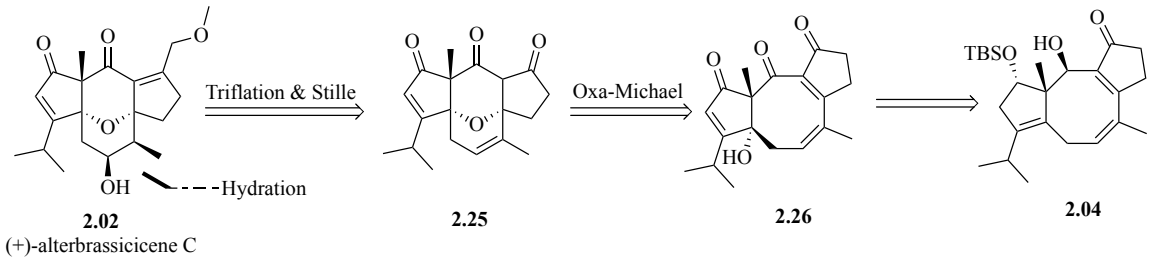

Scheme 2.12 Retrosynthetic approach to alterbrassicicene C

2.5.2 Early Attempts Toward Alterbrassicicene C

In advancing **2.04** to **2.26** we had to first remove the TBS silyl ether (Scheme 2.13). Initial attempts using TBAF yielded poor results and furnished only small quantities of free secondary alcohol **2.27**. Eventually it was found that exposure of **2.04** to HF in pyridine provides alcohol **2.27** cleanly enough to be advanced without purification. In advancing **2.27** we hoped the Henbest effect, alcohol directed epoxidation, would work to our advantage in controlling the diastereoface selectivity. To maximize the likelihood of stereo-controlled epoxidation we employed a non-coordinating solvent, benzene, and a single equivalent of mCPBA. To our delight these conditions led to the regio- and stereoselective epoxidation of the desired olefin to deliver **2.28**. Finally, exposure of **2.28** to an excess of DMP resulted in oxidation of both alcohols to provide triketone **2.29**.

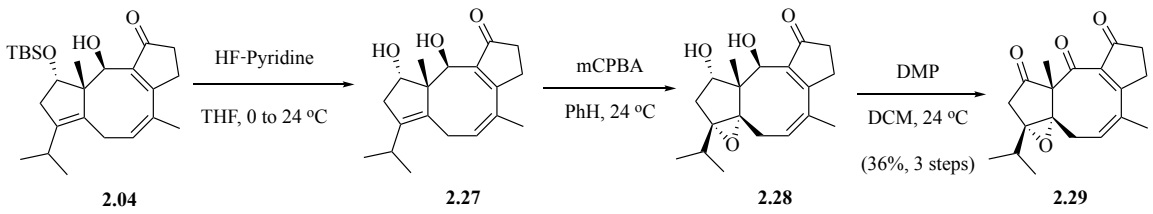

Scheme 2.13 Epoxidation approach for elimination

Having advanced **2.04** to an oxidation level consistent with that found in **2.25** we began exploring conditions to effect a cascade sequence for the **2.29** to **2.25** interconversion. To this end, in initial studies exposure of **2.29** to triethylamine was found to induce an E1cB elimination/epoxide-opening which provides the tertiary allylic alcohol precursor to the oxa-Michael. In a brief optimization effort, we found that treatment of **2.29** with super-stoichiometric amounts of triethylamine in DCM overnight gave quantitative amounts of allylic alcohol **2.26** (Scheme 2.14).

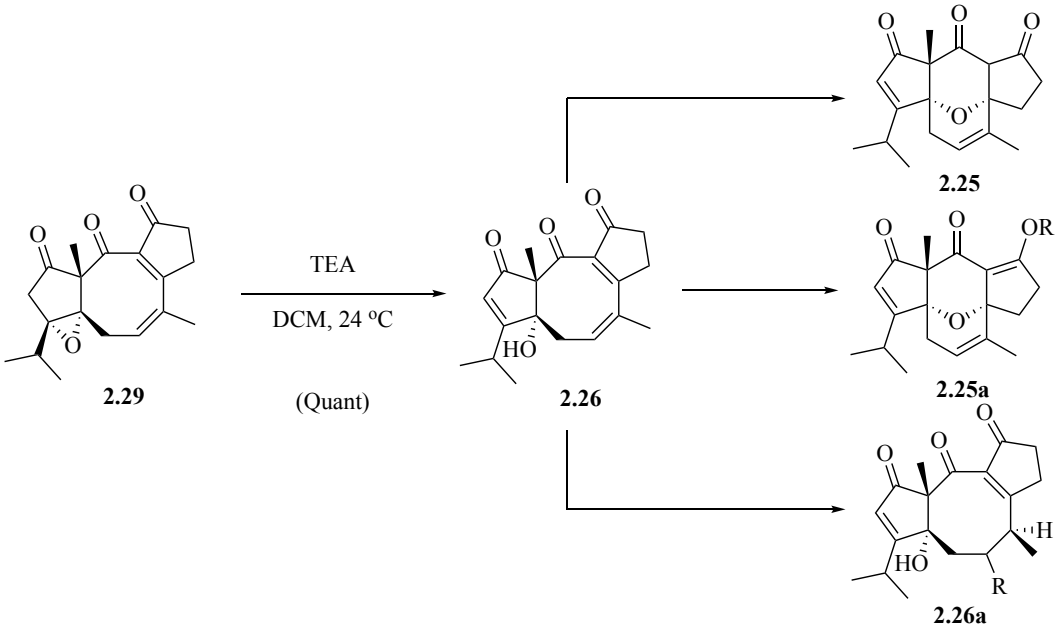

Scheme 2.14 Attempts to promote oxa-Michael

Following the highly effective formation of alcohol **2.26**, we sought to induce the transannular oxa-Michael to form diketone **2.25**. Initial screening included bases such as DBU and K_2CO_3 and also included the exploration of various temperatures and solvents. Much to our surprise, none of these conditions were found to result in oxa-Michael addition into the doubly electron withdrawn electrophile (i.e., diendione). In light of these failures, we shifted our focus to kinetic bases such as LiHMDS, NaH, and LDA. Unfortunately, exposure of **2.26** to these stronger bases also resulted only in returned starting material. We speculated that perhaps ring-strain was leading to an unfavorable equilibrium favoring the retro-oxa-Michael product. To explore and perhaps overcome this potential liability, we attempted to trap the intermediate as the corresponding vinylogous ester by co-addition of various electrophiles. For example, we explored the use of TMSOTf (**2.25a**, R = TMS) which was expected to not only promote the oxa-Michael in its capacity as a Lewis acid but also trap the resultant alkoxide to deliver the vinylogous silyl ester. Unfortunately, this reagent only led to decomposition and recovery of trace starting material. With an eye toward the planned Stille chemistry (Scheme 2.12) we also attempted to trap the intermediate enolate as the corresponding enol triflate by running the oxa-Michael in the presence of Tf_2O (**2.25a**, R = Tf). This only resulted in starting material.

The multitude of failures encountered in efforts to achieve the transannular oxa-Michael addition were reminiscent of similar failures we faced during attempted transannular etherification reactions in our efforts towards alterbrassicicene B. As with the latter, we again conjectured that the lack of desired reactivity might be due to conformational constraints decreasing propinquity of the alcohol and olefin moieties; not an unreasonable notion given that 5 of the 8 carbons in the central ring are sp^2 hybridized.

To increase the flexibility of the central ring, we opted to change the sequence of events by hydrating the trisubstituted olefin prior to oxa-Michal addition (See **2.26a** R = OH in Scheme 2.14). Toward this latter end, attempted hydroboration/oxidation of **2.26** utilizing BH_3 was found to result in various ketone reductions, with no evidence of hydration following the standard oxidative workup. In an attempt to chemoselectively engage the most electron rich (tri-substituted) olefin, we subjected **2.26** to Sharpless dihydroxylation conditions.[17] To our surprise, no reaction occurred and only starting material was recovered. Other attempts were made to advance **2.26**, including epoxidation of the trisubstituted olefin, but nothing promising ever resulted.

2.5.3 Reimagining the Transannular Oxa-Michael

The failure of the oxa-Michael accompanied by those encountered in attempts to alter the starting diendione (**2.26**) led us to reconsider approaches that could be applied to the caged bis-ether that we had prepared in our work towards alterbrassicicene B (See **2.20**, Scheme 2.9). In order to utilize this latter intermediate, we would again need to fragment the tetrahydrofuran ring by rupturing the ether bond alpha to the ketone. Previously, we had successfully employed Birch conditions to effect this fragmentation. However, that approach eventually failed due to the resultant, incorrect, stereochemistry of the methyl group. As an alternative to reduction, in this current effort we explored the effect of various Lewis acids on **2.20** (Scheme 2.15). Initial attempts with super-stoichiometric amounts of $SnCl_4$ resulted only in the recovery of starting material, even upon prolonged exposure. Eventually, we turned to BCl_3, a more reactive Lewis acid, and to our delight saw very clean formation of chloride **2.30**, as a single diastereomer. Although initially uncertain as to the stereochemical outcome of this transformation it was eventually confirmed to be as

illustrate by SCXRD on a subsequent intermediate (*vide infra*). Thus, the derived material clearly arises by capture of the chloride anion from the convex face of the transient allylic cation **2.20a**. Having successfully opened the tetrahydrofuran, we next performed a hydroxy-directed epoxidation with mCPBA to stereoselectively deliver epoxy alcohol **2.31**. Finally, oxidation of the sole alcohol in **2.31** with DMP gave keto-epoxide **2.32** in 70% yield over three-steps.

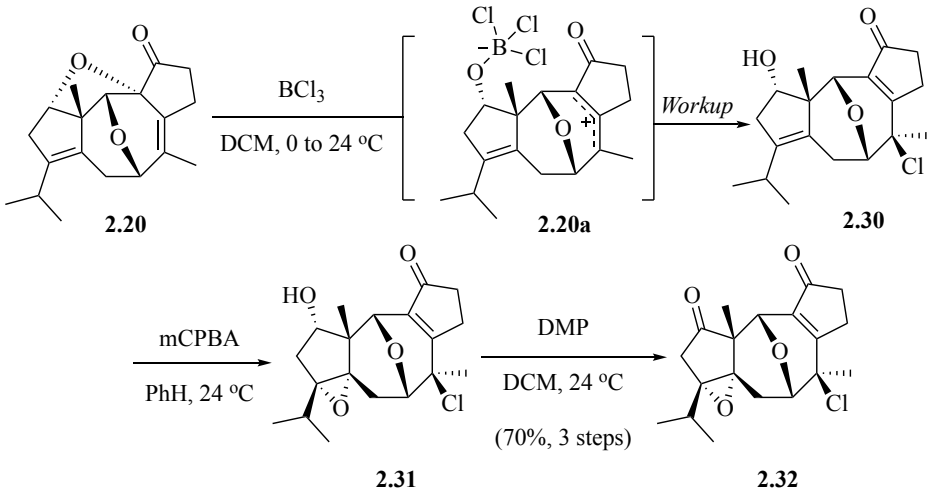

Scheme 2.15 Formation of modified keto-epoxide

The synthesis of the aforementioned keto-epoxide (**2.32**) set the stage for an E_1cB elimination/epoxide opening to deliver the tertiary alcohol needed for the oxa-Michael. Following our own precedent (*vide supra*), we first tried triethylamine/DCM, however under these conditions no reaction was observed (Table 2.2). To our delight, we found that increasing the strength of the base to DBU in DCM not only promoted the E_1cB but also resulted in a spontaneous oxa-Michael addition to form **2.33**! Careful examination of these initial reaction mixtures revealed minor product in the crude ^1H NMR, which, upon isolation and further characterization was found to be enone **2.34**. In this remarkable

cascade reaction, the epoxide is eliminated open, the resultant tertiary alkoxide spontaneously undergoes transannular oxa-Michael addition to the pendant enone, and the resultant enolate induces a retro-oxa-Michael of the bis-oxa-adamantane to form the corresponding enone of **2.34**. Excited by this result, as **2.34** is structurally quite similar to the natural product, our efforts turned to optimizing the conditions in hope of delivering the retro-oxa-Michael product (**2.34**) exclusively. To this end, we eventually found that switching the solvent and increasing the concentration of the reaction led to complete conversion of **2.32** to enone **2.34** (68% yield). Notably, this intermediate contains the complete oxa-tetracyclic skeleton found in alterbrassicicene C.

Table 2.2 Optimization of oxa-Michael sequence

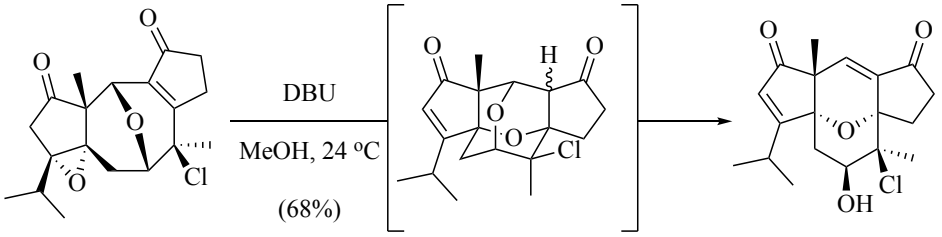

2.32 **2.33** **2.34**

Entry	Base	Solvent	**2.33/2.34**	Yield (%)
1	TEA	DCM	-	S.M.
2	DBU	DCM	3/1	-
3	DBU	MeOH [0.05 M]	0/1	61
4	DBU	MeOH [0.2 M]	0/1	68

2.5.4 Enone Functionalization and Oxidation

Upon completion of the oxygen-carbon skeleton, only three main transformations remain to complete alterbrassicicene C. As illustrated retrosynthetically in Scheme 2.16, these challenges include, adjusting the oxidation at position C-1”, installing the methoxy methyl moiety at C-3”, and de-chlorination at C-7”.

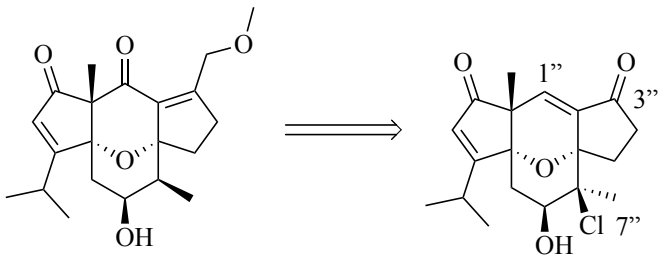

2.02
(+)-alterbrassicicene C

2.34

Scheme 2.16 Final disconnections for alterbrassicicene C

In exploring these remaining transformations, we turned first toward adjusting the oxidation level at C-1”. To our knowledge, there are no robust ways for direct oxidation of an enone to a 1,3-diketone. Thus, our initial efforts focused on formation of a β-hydroxyketone which would then be oxidized to the corresponding dicarbonyl. Attempts at treating enone **2.34** with borane led to reduction products. Products of olefin hydroboration/oxidation were never observed, even when using excess borane (Scheme 2.17). Likewise, nucleophilic addition of $NaOH/H_2O$ also gave none of the desired hydroxyketone **2.35**. Inspired by a recent report from Guangbin Dong, wherein a conjugate borylation/oxidation sequence was employed en route to the penicibiliaenes, we exposed **2.34** to B_2pin_2 in the presence of catalytic CuCl.[18] Unfortunately, in our system no borylation products were observed, only decomposition of the starting material.

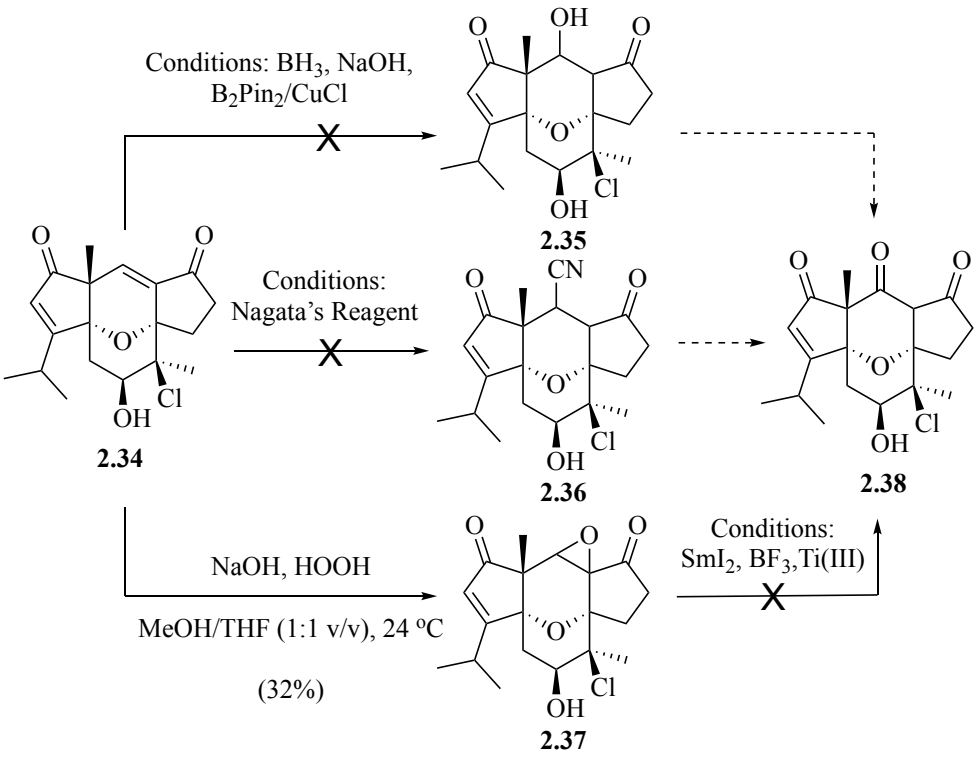

Scheme 2.17 Approaches to prepare a 1,3-diketone

Undeterred by our failure to effect a direct hydroxylation of the enone, we turned to conjugate nitrile addition in hope of subsequently converting of derived nitrile (**2.36**) to the corresponding cyanohydrin (not shown) which, upon exposure to acid would furnish the desired ketone (**2.38**). To this end, we treated **2.34** with Nagata's reagent (i.e., diethylaluminium cyanide), which has proven very effective in numerous cyano-Michael reactions.[19] Regrettably, this reaction only returned starting material. At this point, we decided to go through a potentially longer approach by oxidizing the enone to the epoxyketone **2.37**. This would be an effective intermediate that one could envision advancing via multiple approaches to the diketone. To epoxidize, we attempted many conditions including DBU/TBHP, mCPBA/$NaHCO_3$, DMDO, and even NaOH/HOOH. Most of these conditions only resulted in starting material, with the latter giving only trace

products, even after multiple days. Eventually, we found that prolonged treatment (48h) of enone **2.34** with 10 equiv of HOOH in a co-solvent system of MeOH/THF gave modest yields of **2.37** as a single inconsequential diastereomer. Excited with this result we next attempted conversion of **2.37** to diketone **2.38**. Overall, this transformation was seen as proceeding via reductive opening of the epoxide followed by oxidation of the derived secondary alcohol. For the reductive epoxide opening, we initially explored SmI_2 and in a subsequent attempt turned to Ti(III). Unfortunately these latter conditions only led to either the recovery of starting material or decomposition, respectively.[19] Recognizing that the desired transformation could possibly be achieved in a single step via the Meinwald rearrangement we exposed epoxyketone **2.37** to BF_3•OEt_2. Unfortunately, recovery of starting material was once again the only result. Having experienced only limited success in our efforts to advance **2.34** we opted to again change the order of events focused our attention on installing the methoxy methyl moiety.

2.5.5 Studies Towards Installing Methoxy Methyl Moiety

To install the methoxy methyl moiety, we initially explored the lithium-tin exchange of **2.40** followed by addition of **2.34** (Scheme 2.18, top). Our expectation was that 1,2-addition of the anion derived from **2.40** to the least sterically encumbered Eastern enone in **2.34** would deliver an intermediate tertiary alcohol that could be readily advanced. Alas, we were unable to effect regioselective addition to the desired ketone relative to the neopentyl ketone, which we presumed would be more hindered. Seeking yet another alternative route we investigated advancing epoxyketone (**2.37**). To this end, treatment of **2.37** with excess KHMDS (2.2 equiv), followed by Comin's reagent, afforded vinyl triflate **2.39** in 50% yield.

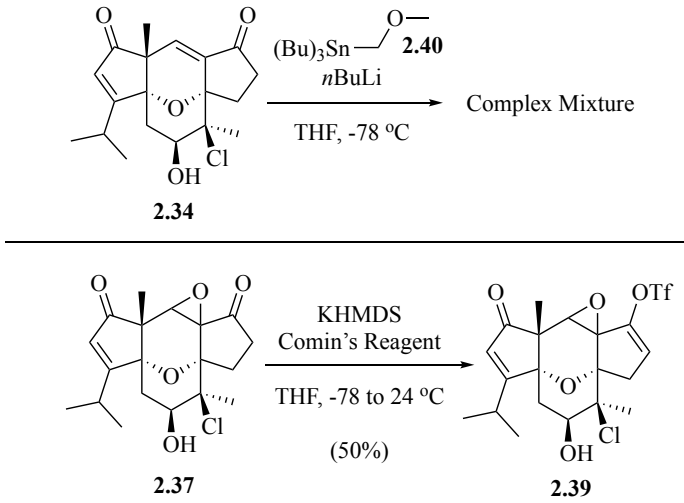

Scheme 2.18 Triflation of the epoxy-ketone

2.5 Future Work to Alterbrassicicene C

To complete the synthesis of alterbrassicicene C from what is currently our most advanced intermediate (**2.39**), we propose the following. The vinyl triflate (**2.39**) will be advanced via S_N2' reduction/epoxide opening which will result in olefin transposition to afford allylic alcohol **2.41** (Scheme 2.19). Subsequent oxidation of **2.41** will convert the allylic alcohol to the requisite enone **2.43**. A Stille cross-coupling of **2.43** with the methoxy methyl stannane will introduce the remaining carbon oxygen atoms. Finally, a radical dehalogenation of the tertiary chloride will furnish the natural product, alterbrassicicene C.

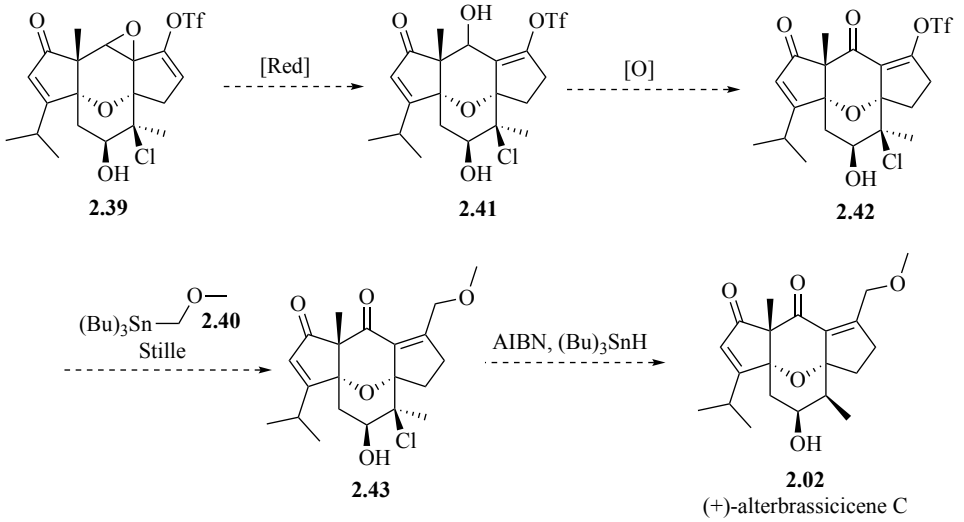

Scheme 2.19 Projected end-game of alterbrassicicene C

2.6 Experimental

Silyl Ether **2.12**

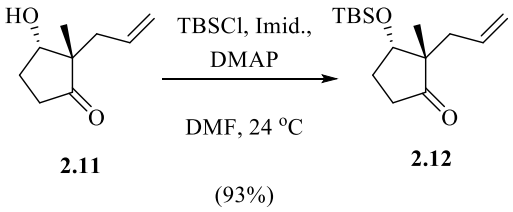

Experimental: In a 500 mL flame dried round bottom flask, under argon and equipped with magnetic stirring, was added **2.11** (32.0 g, 207.8 mmol, 1 equiv) followed by dry DMF (170 mL). Imidazole (35.3 g, 519.1 mmol, 2.5 equiv) and DMAP (1.3 g, 10.7 mmol, 0.05 equiv) were then sequentially added to the stirred solution. Finally, to the reactor was added TBSCl (39.4 g, 260.9 mmol, 1.3 equiv) at 23 °C. After 5 hours, TLC showed consumption of starting material. The reaction was diluted with water (150 mL) and extracted with hexanes (3 x 200 mL). The combined organics were washed with water (100 mL), brine (100 mL), dried over Na_2SO_4, and then concentrated under vacuum. The crude yellow oil

was purified by flash column (7.5% EtOAc/Hexanes) to yield 52.0 g (93%) of **2.12** as an off-clear oil.

^{1}H NMR (600 MHz, $CDCl_3$) δ 5.81-7.73 (m, 1H), 5.07-5.04 (m, 1H), 5.03 (t, J = 1.2 Hz, 1H) 4.03 (t, J = 5.6 Hz, 1H), 2.40 (ddd, J = 18.0, 9.6, 2.6 Hz, 1H), 2.31-2.28 (m, 1H), 2.25-2.16 (m, 2H), 2.14-2.09 (m, 1H), 1.94-1.88 (m, 1H), 0.94 (s, 3H), 0.89 (s, 9H), 0.10 (s, 3H), 0.08 (s, 3H. **^{13}C NMR (151 MHz, $CDCl_3$)** δ 220.6, 134.4, 117.8, 78.2, 53.6, 35.5, 34.4, 28.4, 25.9, 19.7, 18.1, -4.1, -4.8. **IR (ATR):** ν_{max} (cm^{-1}) = 2955 (m), 2929 (m), 2857 (m), 1731 (m), 834 (s), 773 (s). **HRMS (ESI^+)** Calcd. for $C_{15}H_{28}O_2SiNa$. $[M+Na]^+$: 291.1756 found: 291.1756. **Optical Rotation** $[\alpha]_D^{25}$= +36.8 (c = 0.076, MeOH). **TLC** (EtOAc/hexanes = 10%, $KMnO_4$): R_f = 0.42.

Isopropyl **2.13**

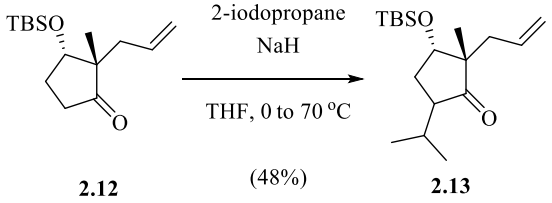

2.12 **2.13**

Experimental: In a 500 mL flame dried round bottom flask, under argon and equipped with magnetic stirring and a reflux condenser, was added 60% sodium hydride (10.1 g, 252.5 mmol, 5 equiv) followed by dry THF (125 mL). The reactor was cooled to 0 °C and **2.12** (13.5 g, 50.4 mmol, 1 equiv) in dry THF (70 mL) was added dropwise to the grey suspension, followed by 2-Iodopropane (56.9 mL, 569 mmol, 11 equiv). Upon completion of the addition, the reaction was heated to 70 °C and stirred vigorously. The grey suspension turned to a thick tan mixture after 2 hours into the heating process. The reaction

was monitored TLC and showed consumption after 15 hours. The reaction was cooled to 0 °C and water (25 mL) was added to quench the reaction, followed by 2M HCl (75 mL). The biphasic mixture was allowed to stir for 1 hour at 23 °C, at which time the layers were separated and the aqueous layer was extracted with ether (2 x 100 mL). The combined organics were washed with sat. $Na_2S_2O_5$ (2 x 200 mL), water (100 mL), brine (100 mL), and dried over Na_2SO_4, and then concentrated under vacuum. The crude oil was purified by flash column (25% DCM/Hexanes) to yield 7.5 g (48%) of an inconsequential mixture of diastereomers **2.13** as a yellow oil.

Note: Only the major diastereomer was isolatable as pure material.

Data for major diastereomer:

^{1}H NMR (600 MHz, $CDCl_3$) δ 5.82-5.75 (m, 1H), 5.03-4.97 (m, 2H), 3.95 (dd, *J* = 9.6, 5.7 Hz, 1H), 2.23-2.05 (m, 5H), 1.76-1.69 (m, 1H), 1.01 (s, 3H), 0.99 (d, *J* = 7.0 Hz, 3H), 0.92 (s, 9H), 0.84 (d, *J* = 7.0 Hz, 3H), 0.10 (s, 3H), 0.09 (s, 3H). **^{13}C NMR (151 MHz, $CDCl_3$)** δ 220.2, 134.4, 117.7, 77.6, 53.4, 53.0, 34.8, 30.6, 27.6, 26.0, 21.4, 20.8, 19.1, 18.2, -4.1,-4.7. **IR (ATR):** ν_{max} (cm^{-1}) = 2956 (m), 2929 (m), 2857 (m), 1734 (m), 1112 (m), 834 (s), 774 (s). **HRMS (ESI$^+$)** Calcd. for $C_{18}H_{34}O_2SiNa$. $[M+Na]^+$: 333.2223, found: 333.2226. **Optical Rotation** $[\alpha]_D^{23}$= -38.6 (c = 0.56, MeOH). **TLC** (EtOAc/hexanes = 10%, $KMnO_4$): R_f = 0.81.

Keto-Aldehyde **2.08**

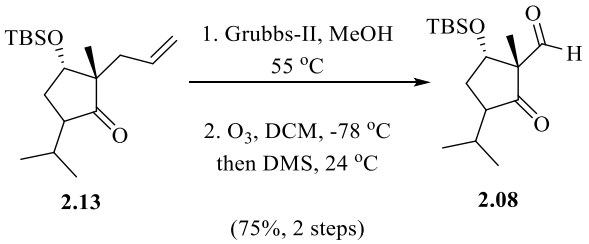

2.13 **2.08**

(75%, 2 steps)

Experimental: In a 1 L round bottom flask, purged with argon and equipped with magnetic stirring, was added the diastereomeric mixture of **2.13** (7.0 g, 22.5 mmol, 1 equiv), followed by MeOH (dried over 3 Å molecular sieves, 300 mL). The brown-yellow solution was sparged with argon for 5 minutes while stirring. Grubb's 2nd generation catalyst (1.87 g, 2.2 mmol, 0.1 equiv) was added in a singular portion. The brown solution was then heated to 55 ^{o}C for 14 hours. The reaction can be monitored by NMR aliquots. Upon waiting the 14 hours, the reaction was cooled and concentrated directly on a rotary evaporator. The concentrated residue was then flushed through a silica plug with DCM to remove residual catalyst. The material was then re-concentrated and the crude isomerized olefin was transferred to 250 mL round bottom flask and diluted with DCM (110 mL). The flask was left open to the atmosphere and cooled to -78 ^{o}C in a dry-ice/acetone bath. O_3 was then bubbled through the solution for 35 minutes, indicated by TLC that it was complete. O_2 was then used to sparge the solution for 30 minutes, at which time dimethyl sulfide (5 mL) was added at -78 ^{o}C and allowed to warm to room temperature naturally. After 4 hours, the solution was concentrated and purified directly by flash column (10% to15% EtOAc/Hexanes) to yield 5.05 g (75%, 2 steps) of **2.08**, a light brown oil.

Note: Only the major diastereomer was isolatable as pure material.

Data for major diastereomer:

^{1}H NMR (600 MHz, $CDCl_3$) δ 9.59 (s, 1H), 4.17 (dd, *J* = 9.6, 6.3 Hz, 1H), 2.33 (ddd, *J* = 12.5, 8.2, 6.3 Hz, 1H) 2.28-2.18 (m, 2H), 2.02 (td, *J* = 12.3, 9.6 Hz, 1H), 1.29 (s, 3H), 1.02 (d, *J* = 6.8 Hz, 3H), 0.91 (d, *J* = 6.8 Hz, 3H), 0.88 (s, 9H), 0.11 (s, 3H), 0.09 (s, 3H). **^{13}C NMR (151 MHz, $CDCl_3$)** δ 213.9, 198.5, 78.5, 66.9, 54.6, 32.6, 27.8, 25.8, 21.4, 19.4, 18.1, 16.2, -4.3, -4.9. **IR (ATR):** ν_{max} (cm^{-1}) = 2956 (m), 2930 (m), 2858 (w), 1749 (m),

1712 (m), 1108 (s), 835 (s), 777 (m). **HRMS (ESI$^+$)** Calcd. for $C_{16}H_{30}O_3BrNa$. $[M+Na]^+$: 321.1858, found: 321.1862. **Optical Rotation** $[\alpha]_D^{22}$= -16.1 (c = 2.73, MeOH). **TLC** (EtOAc/hexanes = 7.5%, $KMnO_4$): R_f = 0.33.

Skip Diene **2.06**

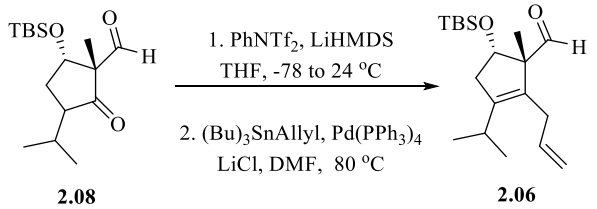

2.08 **2.06**

(55%, 2 steps)

Experimental: In a 100 mL round bottom flask which was flame dried under vacuum, equipped with magnetic stirring, and purged with argon, was added **2.08** (2.0 g, 6.71 mmol, 1 equiv) as a mixture of diastereomers. To the flask was added dry THF (40 mL) and subsequentially cooled to -78 °C in a dry-ice/acetone bath under argon. To this solution was added 1.0M LiHMDS in THF (8.72 mL, 8.72 mmol, 1.3 equiv) dropwise and the resulting yellow solution was stirred for 1 hour. Still at -78 °C, a solution of $PhNTf_2$ (3.11 g, 8.71 mmol, 1.3 equiv) in dry THF (20 mL) was cannula transferred into the reactor. The green-yellow solution was stirred overnight, allowing to warm to 24 °C, naturally. After 18h in total, the resulting solution was quenched with brine (50 mL), and then extracted with ethyl acetate (3 x 50 mL). The combined organics were washed with water (100 mL) and brine (50 mL), followed by drying with Na_2SO_4 and subsequent concentration with a rotary evaporator. This semi-solid material was then used as is in the following reaction.

Crude triflate (2.9 g) was loaded into a 100 mL flask, purged with vacuum/argon (3x), and equipped with magnetic stirring. Dry DMF (40 mL) was added to the flask and then sparged with argon for 5 minutes, before being put under a static argon atmosphere.

To the solution was added anhydrous LiCl (1.69 g, 40.23 mmol, 6 equiv), $Pd(PPh_3)_4$ (774 mg, 0.67 mmol, 0.1 equiv), and finally $(Bu)_3SnAllyl$ (4.43 mL, 14.32 mmol, 2 equiv). The reaction was then heated to 80 °C. After 8 hours, TLC showed consumption of the starting material and the reactor was cooled to 23 °C. The reaction was transferred to a separatory funnel and diluted with diethyl ether (250 mL). The organic layer was washed with water (2 x 20 mL). The combined water washes were then back extracted with diethyl ether (100 mL) and the combined organics were washed with water (50 mL) and then brine (50 mL). The organics were concentrated and then redissolved in a mixture of hexanes (20 mL) and acetonitrile (20 mL). The layers were separated, and the hexanes layer was washed with more acetonitrile (3 x 20 mL). The combined acetonitrile layers were dried with Na_2SO_4 and concentrated a final time. The resulting residue was purified by flash column (3% triethylamine/hexanes) to afford 1.2 g (55%, 2 steps) of **2.06**.

^{1}H NMR (600 MHz, $CDCl_3$) δ 9.57 (s, 1H), 5.62-5.55 (m, 1H), 4.99-4.92 (m, 2H), 4.21 (t, *J* = 6.8 Hz, 1H), 2.78 (sept, *J* = 6.8 Hz, 1H), 2.69 (dd, *J* = 15.5, 6.5 Hz, 1H), 2.63-2.58 (m, 2H), 2.47 (dd, *J* = 15.8, 8.1 Hz, 1H), 1.13 (s, 3H), 1.03-1.01 (m, 6H), 0.85 (s, 9H), 0.04 (s, 3H), 0.03 (s, 3H). **^{13}C NMR (151 MHz, $CDCl_3$)** δ 202.2, 147.4, 136.0, 129.3, 115.8, 82.1, 65.7, 37.8, 29.9, 27.4, 25.8, 21.6, 21.0, 18.1, 16.4. **IR (ATR):** ν_{max} (cm^{-1}) = 2958 (m), 2929 (m), 2857 (m), 1723 (m), 834 (s), 775 (s). **HRMS (ESI^+)** Calcd. for $C_{16}H_{30}O_2SiNa$. $[M+Na]^+$: 345.2226, found: 345.2224. **Optical Rotation** $[\alpha]_D^{23}$= -205.9 (c = 1.5, MeOH). **TLC** (EtOAc/hexanes = 10%, $KMnO_4$): R_f = 0.52.

Vinyl Bromide **2.16**

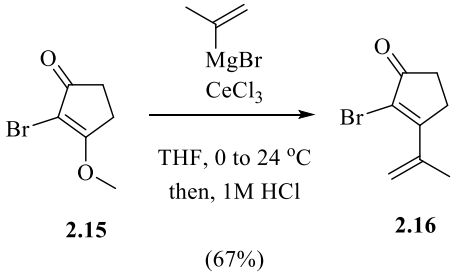

Experimental: In a 1 L round bottom flask which was flame dried under vacuum, equipped with magnetic stirring, and purged with argon, was added $CeCl_3 \cdot H_2O$ (19.7 g, 79.7 mmol, 1.5 equiv) which was dried at 140 °C for 2 hours under vacuum. The reactor was then cooled to room temperature (24 °C), and backfilled 3x with argon. Dry THF (350 mL) is then added and the mixture is stirred vigorously for 2 hours, at which time **2.15** (10.15 g, 53.1 mmol, 1 equiv) was added as solution in THF (180 mL). This mixture was stirred for 1 hour and then cooled to 0 °C. Isopropenyl magnesium bromide (160 mL, 0.5M, 1.5 equiv) was then added slowly and the milky-yellow reaction was stirred for 1 hour and 0 °C. After which time, sat. NH_4Cl (150 ml) and 1M HCl (150 mL) were added in that order. The layers were separated and the aqueous was extracted with ethyl acetate (3 x 300 mL). The combined organics were washed with brine, dried over Na_2SO_4, and then concentrated under vacuum. The crude material was purified by flash column (20% to 30% EtOAc/hexanes) to afford 7.1 g (67%) of clear oil **2.16**.

^{1}H NMR (600 MHz, $CDCl_3$) δ 5.68 (s, 1H), 5.46 (s, 1H), 2.82-2.80 (m, 2H), 2.58-2.56 (m, 2H), 2.20 (s, 3H) . **^{13}C NMR (151 MHz, $CDCl_3$)** δ 202.0, 168.7, 140.9, 139.6, 121.8, 121.6, 32.3, 30.1, 21.8. **IR (ATR)**: ν_{max} (cm^{-1}) = 3008 (w), 2949 (w), 1707 (s), 1200 (m), 927 (s), 574 (m). **HRMS (ESI^+)** Calcd. for C_8H_9BrNa. $[M+Na]^+$: 222.9734, found: 222.9733. **TLC** (EtOAc/hexanes = 33%, UV, $KMnO_4$): R_f = 0.34.

Acetal **2.07**

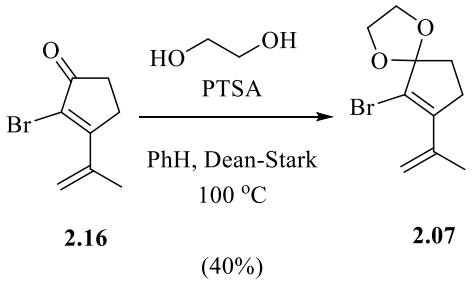

2.16 **2.07**

(40%)

Synthesis of Acetal S11: In a 500 mL round bottom flask equipped with a Dean-Stark apparatus, Vigreux column, and magnetic stirring was flame dried and backfilled with argon. The flask was charged with **2.16** (7.2 g, 35.8 mmol, 1 equiv), PhH (250 mL), ethylene glycol (10.0 mL, 179.1 mmol, 5 equiv), and PTSA (308 mg, 1.8 mmol, 0.05 equiv). The reaction was placed into a heating mantle, wrapped in foil, and heated to 100 °C for 11 hours. Reaction was cooled to 24 °C and the reaction was quenched with sat. $NaHCO_3$ (100 mL). The layers were separated and the aqueous was extracted with ethyl acetate (3 x 100 mL). The combined organics were washed with brine, dried over Na_2SO_4, and then concentrated under vacuum. The crude material was purified by flash column (20% to 40% EtOAc/hexanes) to afford 3.4 g (40%) of a yellow-orange oil **2.07** and 3.0 g of **2.16**.

^{1}H NMR (400 MHz, $CDCl_3$) δ 5.24-5.23 (m, 1H), 5.17 (p, J = 1.5 Hz, 1H), 4.25-4.17 (m, 2H), 4.04-3.96 (m, 2H), 2.54-2.51 (m, 2H), 2.18-2.14 (m, 2H), 2.05-2.04 (m, 3H). **^{13}C NMR (101 MHz, $CDCl_3$)** δ 145.1, 139.6, 119.1, 118.7, 117.9, 66.1, 33.7, 31.5, 21.9. **IR (ATR):** ν_{max} (cm^{-1}) = 2974 (w), 2887 (w), 1623 (w), 1151 (s), 1032 (s), 890 (s). **HRMS (ESI$^+$)** Calcd. for $C_{10}H_{14}BrO_2$. $[M+H]^+$: 245.0177, found: 245.0175. **TLC** (EtOAc/hexanes = 33%, $KMnO_4$): R_f = 0.47.

Cyclooctadiene **2.04**

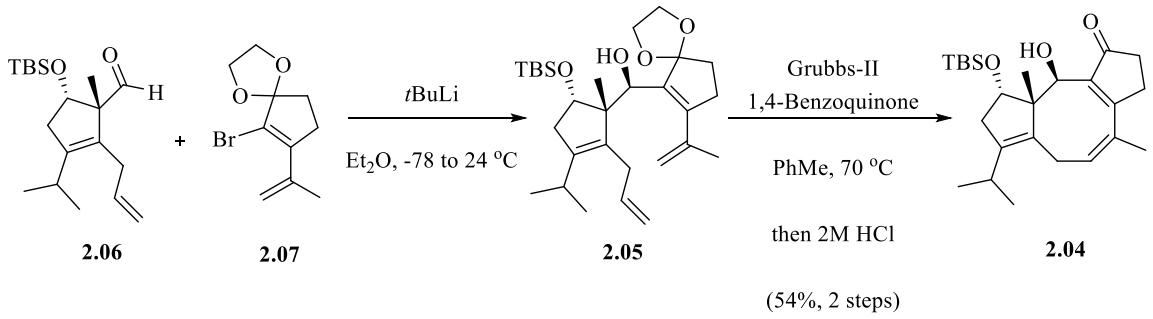

Experimental: In a 100 mL round bottom flask which was flame dried under vacuum, equipped with magnetic stirring, and purged with argon, was added azeotroped (benzene 2 x 10 mL) **2.07** (842 mg, 3.66 mmol, 1.1 equiv) followed by dry diethyl ether (25 mL). The reactor was cooled to -78 °C under argon. tBuLi (4.36 mL, 1.7 M, 6.97 mmol, 2.1 equiv) was added dropwise, carefully. The green-yellow mixture was then allowed to stir for 1h. **2.06** (1.07 g, 3.32 mmol, 1.0 equiv) in dry diethyl ether (10 mL) was then cannulated into the reactor at -78 °C. The reaction stirred for 1 hour at that temperature and then the dry ice-acetone bath was removed. After an additional 1.5 hours, the reaction was quenched at 24 °C with half-sat. NH_4Cl (20 mL). The layers were separated and the aqueous was extracted with ethyl acetate (3 x 20 mL). The combined organics were washed with brine, dried over Na_2SO_4, and then concentrated under vacuum. The crude material was carried forward as an orange-yellow oil (1.1g). Crude oil **2.05** (1.1 g, 2.2 mmol, 1 equiv) was loaded into a 1 L round bottom flask equipped with magnetic stirring and under an argon atmosphere. The starting material was diluted with dry toluene (300 mL, ~0.0075 M) and sparged with an argon balloon to remove oxygen. Grubb's II (186 mg, 0.22 mmol, 0.1 equiv) and 1,4-benzoquinone (24 mg, 0.22 mmol, 0.1 equiv) were added sequentially to the reactor. The reaction was heated to 70 °C in a heating mantle for 1 hour. Upon completion of the ring-closing metathesis, the reactor was cooled to 24 °C and 2 M HCl

(150 mL) was added and the bi-phasic reaction was stirred vigorously for 2 hours. The reaction was transferred to a separatory funnel. The layers were separated and the aqueous was extracted with ethyl acetate (3 x 100 mL). The combined organics were washed with water, brine, dried over Na_2SO_4, and then concentrated under vacuum. The crude material was purified by flash column (15% EtOAc/hexanes) to afford 753 mg (54%, 2 steps) of a clear crystalline solid **2.04**.

Melting Point 141-145 °C. **^{1}H NMR (400 MHz, $CDCl_3$)** δ 5.57 (ddt, *J* = 9.0, 7.5, 1.4 Hz, 1H), 4.80 (d, *J* = 9.2 Hz, 1H), 4.59 (d, *J* = 9.2 Hz, 1H), 4.08 (d, *J* = 4.0 Hz, 1H), 2.84-2.79 (m, 2H), 2.72 (sept, *J* = 7.10 Hz, 1H), 2.57-2.49 (m, 5H), 2.14 (d, *J* = 15.5 Hz, 1H), 1.98 (m, 1H), 1.85 (s, 3H), 1.03 (d, *J* = 7.1 Hz, 3H), 0.91 (d, *J* = 7.1 Hz, 3H), 0.83 (m, 12H), 0.06 (s, 6H). **^{13}C NMR (151 MHz, $CDCl_3$)** δ 211.8, 172.9, 140.4, 140.1, 132.6, 132.2, 128.7, 77.4, 71.5, 56.6, 38.3, 35.5, 28.0, 26.8, 26.0, 25.5, 22.3, 21.0, 19.7, 18.2, 15.9, -4.3, -4.8. **IR** (ATR): ν_{max} (cm^{-1}) = 3437 (w), 2955 (w), 2927 (m), 2856 (w), 1673 (m), 831 (s), 774 (s). **HRMS (ESI$^+$)** Calcd. for $C_{25}H_{40}O_3SiNa$. $[M+Na]^+$: 439.2644, found: 439.2641. **Optical Rotation** $[\alpha]_D^{24}$= 757.9 (c = 0.19, MeOH). **TLC** (EtOAc/hexanes = 33%, UV): R_f = 0.60.

Trans-Annular Ether **2.19**

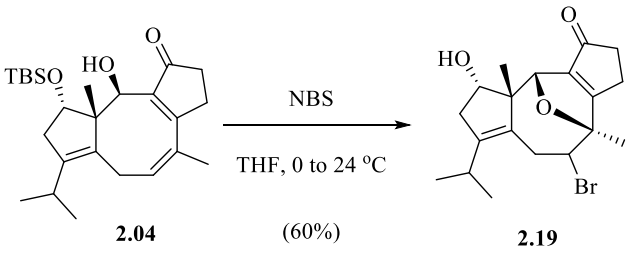

2.04 **2.19**

Experimental: In a 50 mL round bottom flask which was flame dried under vacuum, equipped with magnetic stirring, and purged with argon, was added **2.04** (250 mg, 0.60 mmol, 1 equiv). Dry THF (12 mL) was then added. NBS (374 mg, 2.10 mmol, 3.5 equiv) was added at room temperature in one portion and the yellow solution was stirred rapidly for 6 hours. The reaction was quenched with sat. $Na_2S_2O_3$ (5 mL) and sat. $NaHCO_3$ (5 mL) and stirred for 10 minutes. The layers were separated and the aqueous was extracted with diethyl ether (3 x 10 mL). The combined organics were washed with brine, dried over Na_2SO_4, and then concentrated under vacuum. The crude material was purified by flash column (25% EtOAc/hexanes) to afford 137 mg (60%) of a syrup like solid **2.19**.

^{1}H NMR (400 MHz, $CDCl_3$) δ 4.75 (dd, *J* = 2.3, 1.2 Hz, 1H), 4.41 (d, *J* = 12.1 Hz, 1H), 4.28 (dd, *J* = 6.6, 1.7 Hz, 1H), 4.06 (dt, *J* = 12.1, 9.0 Hz, 1H) 3.18-3.10 (m, 1H) 3.00-2.84 (m, 5H), 2.78-2.69 (m, 1H), 2.55 (ddd, *J* = 16.8, 9.2, 1.5 Hz, 1H), 1.76 (q, *J* = 8.8 Hz, 1H), 1.56 (s, 3H), 1.35 (s, 3H), 0.93-0.91 (m, 6H). **^{13}C NMR (101 MHz, $CDCl_3$)** δ 204.1, 190.2, 148.4, 147.3, 128.4, 87.2, 83.6, 79.5, 59.3, 55.8, 42.0, 36.3, 32.1, 27.3, 27.1, 24.5, 24.2, 21.6, 21.2. **IR (ATR):** ν_{max} (cm^{-1}) = 3403 (w), 2958 (w), 2927 (m), 2666 (w), 1680 (s), 1635 (m). **HRMS (ESI$^+$)** Calcd. for $C_{19}H_{25}BrNaO_2$. $[M+Na]^+$: 403.0881, found: 403.0885. **Optical Rotation** $[\alpha]_D^{23}$= 63.0 (c = 0.87, MeOH). **TLC** (EtOAc/hexanes = 20%, UV): R_f = 0.63.

Bis-Ethereal Cage **2.20**

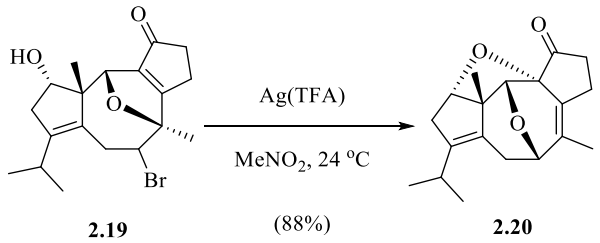

2.19 **2.20**

Experimental: In a 20 mL vial which equipped with magnetic stirring, and purged with argon, was added **S14** (242 mg, 0.63 mmol, 1.0 equiv). At 24 ºC, dry $MeNO_2$ (6.3 mL, dried over 3 angstrom molecular sieves) was added under argon. In one single portion, Ag(TFA) (404 mg, 1.56 mmol, 2.5 equiv) was added and the grey yellow solution was stirred for 2 hours. The yellow solution became a grey suspension over time. After the 2 hours, the solution was concentrated directly and loaded onto a flash column (15% EtOAc/hexanes) to afford 167 mg (88%) of a white crystalline solid **S15**.

Melting Point 147-149 ºC. **^{1}H NMR (400 MHz, $CDCl_3$)** δ 4.51 (s, 1H), 4.15 (d, *J* = 4.5 Hz, 1H), 4.11 (d, *J* = 2.6 Hz, 1H), 2.65-2.39 (m, 6H), 2.28-2.08 (m, 3H), 1.68 (d, *J* = 1.29 Hz, 3H), 1.24 (s, 3H), 0.95 (d, *J* = 6.8 Hz, 3H), 0.85 (d *J* = 6.8 Hz, 3H). **^{13}C NMR (101 MHz, $CDCl_3$)** δ 212.5, 141.6, 136.2, 132.4, 129.3, 85.8, 80.1, 77.4, 73.5, 55.7, 36.4, 35.7, 26.3, 25.3, 22.3, 21.0, 20.7, 16.9, 16.3. **IR (ATR)**: ν_{max} (cm^{-1}) = 3403 (w), 2958 (m), 2927 (m), 2866 (w), 1680 (s), 1635 (m), 1433 (m), 1068 (m), 730 (m). **HRMS (ESI^+)** Calcd. for $C_{19}H_{24}NaO_3$. $[M+Na]^+$: 323.1623, found: 323.1618. **Optical Rotation** $[\alpha]_D^{22}$= -69.7 (c = 0.39, MeOH). **TLC** (EtOAc/hexanes = 50%, PMA): R_f = 0.76.

Enone **2.21a**

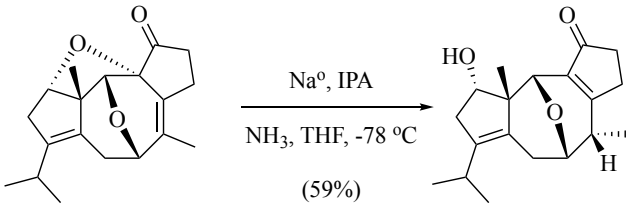

2.20 **2.21a**

Experimental: In a 25 mL 3-neck round bottom flask equipped with a cold-finger, magnetic stir-bar, and an adapter for an ammonia line was condensed NH_3 (5-10 mL) at -78 °C (bath and cold-finger) under an argon atmosphere. Upon completion of condensation, sodium metal (26 mg, 1.13 mmol, 10 equiv) was added and the solution became deep blue. After 10 minutes at -78 °C, a solution of **2.20** (34 mg, 0.113 mmol, 1.0 equiv), 2-propanol (25 µL, 0.227 mmol, 2.0 equiv) in THF (2 mL) was added over 1 minute. After 10 minutes, solid NH_4Cl (~250 mg) was added and the bath and cold-finger were removed. The reaction was kept under argon and Et_2O (5 mL) was added. Upon reaching 24 °C, water (5 mL) was added and the mixture was transferred to a separatory funnel. The layers were separated and the aqueous layer was extracted with Et_2O (3 x 5 mL). The combined organics were washed with brine, dried over Na_2SO_4, and then concentrated under vacuum. The crude material was purified by flash column (40% EtOAc/hexanes) to afford 20 mg (59%) of a semi-solid **2.21a**.

^{1}H NMR (600 MHz, $CDCl_3$) δ 4.65 (d, *J* = 12.6 Hz, 1H), 4.44 (s, 1H), 4.22 (t, *J* = 6.5 Hz, 1H) 4.05 (ddd, *J* = 12.6, 9.6, 8.5 Hz, 1H), 2.93 (p, *J* = 7.5 Hz, 1H), 2.70-2.60 (m, 2H), 2.53-2.40 (m, 6H), 1.50 (s, 3H), 1.35-1.30 (m, 1H), 1.14 (d, *J* = 7.7 Hz, 3H), 0.94 (d, *J* = 6.9 Hz, 3H), 0.81 (d, *J* = 6.9 Hz, 3H). **^{13}C NMR (151 MHz, $CDCl_3$)** δ 209.8, 180.9, 139.6, 138.4, 129.0, 80.0, 73.4, 72.6, 55.0, 37.5, 37.4, 34.9, 28.1, 26.8, 24.0, 23.8, 22.0, 20.9, 13.1. **IR (ATR)**: ν_{max} (cm^{-1}) = 3378 (br), 2959 (m), 2923 (m), 1673 (s), 1627 (s), 1436 (w), 1078

(w), 1052 (w) . **HRMS (ESI$^+$)** Calcd. for $C_{19}H_{26}NaO_3$. $[M+Na]^+$: 325.1780, found: 325.1776. **TLC** (EtOAc/hexanes = 50%, UV/PMA): R_f = 0.36.

Allylic Alcohol **2.23**

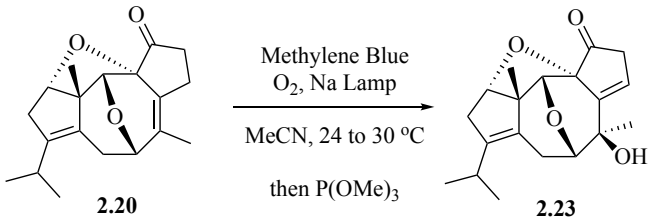

2.20 **2.23**

Experimental: In a 6 dr vial equipped with a magnetic stir bar was charged with **2.20** (25 mg, 0.083 mmol, 1.0 equiv), methylene blue (1 mg), and then diluted with MeCN (2 mL) under atmosphere. The blue reaction was then sparged with O_2 for 2 minutes and then kept under an O_2 atmosphere for the remainder of the reaction. The reactor was placed into a photo-box equipped with a high pressure sodium lamp and a fan. After 5 hours, the reaction was removed from the light source and was sparged with argon for 5 minutes. To the flask was then added $P(OMe)_3$ (205 µL, 1.67 mmol, 20 equiv) at 24 °C. After 1 hour, the reaction was concentrated directly. The concentrate was purified by flash column (33% EtOAc/hexanes) to afford 7.5 mg (29%) of an oil (**2.23**)**.**

^{1}H NMR (600 MHz, $CDCl_3$) δ 6.60 (dd, *J* = 3.1, 1.7 Hz, 1H), 4.49 (s, 1H), 4.20 (d, *J* = 2.5 Hz, 1H), 4.08 (dd, *J* = 5.5, 1.7 Hz, 1H), 3.20 (dd, *J* = 21.9, 1.7 Hz, 1H), 2.74-2.61 (m, 3H), 2.50-2.42 (m, 2H), 2.29 (d, *J* = 15.6 Hz, 1H), 2.17 (s, 1H), 1.37 (s, 3H), 1.19 (s, 3H), 1.00 (d, *J* = 6.7 Hz, 3H), 0.97 (d, *J* = 6.7 Hz, 3H). **^{13}C NMR (151 MHz, $CDCl_3$)** δ 212.2, 148.8, 139.3, 130.6, 129.4, 86.6, 83.00, 82.4, 81.8, 73.9, 55.8, 39.5, 34.5, 27.0, 26.5, 24.9, 23.0, 20.0, 17.5. **IR (ATR)**: ν_{max} (cm^{-1}) =3435 (br), 2959 (s), 2931 (m), 1754 (s), 1362

(m), 1075 (m), 1005 (s), 829 (m). **HRMS (ESI$^+$)** Calcd. for $C_{19}H_{24}NaO_4$. $[M+Na]^+$: 339.1572, found: 339.1575. **TLC** (EtOAc/hexanes = 30%, PMA): R_f = 0.41.

Aliphatic Acohol **2.24**

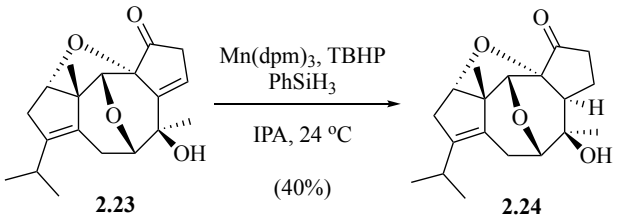

2.23 **2.24**

Experimental: In a 2 dr vial equipped with a magnetic stir-bar was charged with **2.23** (7.0 mg, 0.022 mmol, 1.0 equiv) and then diluted with dry IPA (dried over 3 Å molecular sieves, 500 μL) at 24 °C, under an argon atmosphere. To the clear solution was added $PhSiH_3$ (5 μL, 0.044 mmol, 2.0 equiv), TBHP (5.5M in nonane, 6 μL, 0.033, 1.5 equiv), and $Mn(dpm)_3$ (3 mg, 0.006 mmol, 0.25 equiv). The mixture was then sparged with argon for 1 minute and the brown solution was stirred for 10 minutes. The reaction was immediately concentrated under vacuum. The concentrate was purified by flash column (50% EtOAc/hexanes) to afford 3 mg (40%) of a semi-pure oil (**2.24**).

Note: The purification of **2.24** proved to be a challenge due to a co-eluting byproduct (see appendix B). The material was used as the semi-pure product. The tabulated data below reflects as such:

^{1}H NMR (600 MHz, $CDCl_3$) δ 4.55 (d, *J* = 12.6 Hz, 1H), 4.42 (d, *J* = 2.4 Hz, 1H), 4.09-4.01 (m, 2H), 2.87 (ddt, *J* = 19.0, 7.4, 1.8 Hz, 1H), 2.63-2.52 (m, 6H), 2.48-2.41 (m, 4H), 1.50 (m, 3H), 1.39 (ddd, *J* = 15.9, 9.5, 3.1 Hz, 1H), 1.32 (s, 3H), 0.93 (d, *J* = 6.7 Hz, 3H), 0.79 (d, *J* = 6.7 Hz, 3H). **^{13}C NMR (151 MHz, $CDCl_3$)** δ 210.8, 177.7, 139.6, 138.6, 127.8, 79.9, 79.1, 73.9, 69.3, 54.4, 36.9, 35.0, 31.1, 26.8, 24.8, 24.8, 24.7, 23.4, 21.9, 21.0, 19.7.

IR (ATR): ν_{max} (cm^{-1}) = 3435 (br), 2959 (m), 2931 (m), 1754 (s), 1454 (w), 1362 (m), 1075 (m), 1005 (s). **HRMS (ESI$^+$)** Calcd. for $C_{19}H_{26}NaO_4$. $[M+Na]^+$: 341.1729, found: 341.1727. **TLC** (EtOAc/hexanes = 50%, PMA): R_f = 0.28.

Triketone **2.29**

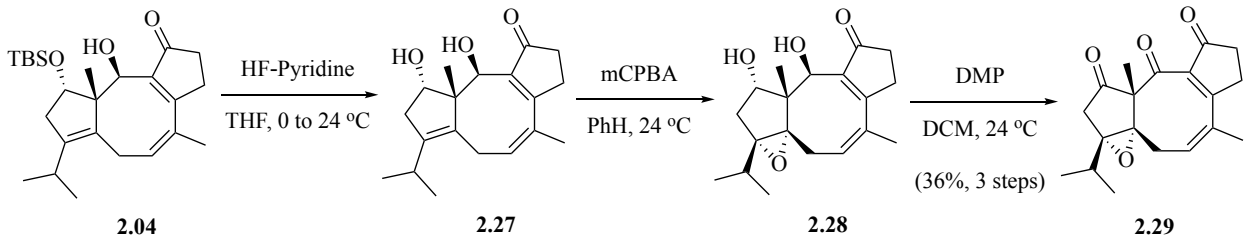

2.04 **2.27** **2.28** **2.29**

Experimental: In a 20 mL HDPE vial equipped with magnetic stirring, and purged with argon, was added **2.04** (90 mg, 0.216 mmol, 1.0 equiv). At 0 °C, dry THF (4 mL) was added under argon. Dropwise, HF-Pyridine (70% HF, 1 mL) was added and yellow solution was stirred for 2 hours, warming to 24 °C. Upon completion (indicated by an aliquot on low-resolution mass spec), the solution was carefully dumped into a 250 mL beaker that contained ice-cold sat. $NaHCO_3$ (20 mL), ethyl acetate (20 mL), and $CaCl_2$ (500 mg). After 10 minutes, the solution was transferred to a separatory funnel. The layers were separated and the aqueous layer was extracted with ethyl acetate (2 x 10 mL). The combined organic were washed with water and brine. The organics were dried and concentrated. The crude yellow material (**2.27**) was taken forward as is.

In a 20 mL scintillation vial equipped with magnetic stirring, crude diol **2.27** (~90 mg) was added, and then subsequently diluted with dry benzene (3 mL) under argon atmosphere. In a single portion, mCPBA (77%, 67 mg, 0.298 mmol, 1.3 equiv) was added at 24 °C. After 20 minutes (by TLC), the reaction was complete. To the reaction was added sat. $NaHCO_3$ (5 mL) and sat. $Na_2S_2O_3$ (5 mL). After 5 additional minutes, the mixture was

transferred to a separatory funnel, where the aqueous layer was extracted with ethyl acetate (2 x 5 mL) and the combined organics were washed with water and then brine. The organics were dried and concentrated. The crude oil was taken directly into subsequent oxidation.

In a 20 mL scintillation vial equipped with magnetic stirring, crude epoxide **2.28** (~100 mg) was added. The starting material was diluted with DCM (5 mL) under atmosphere, and then at 24 °C, DMP (380 mg, 0.894 mmol, 4.1 equiv) was added. The cloudy suspension was stirred for 20 minutes, at which sat. $NaHCO_3$ (5 mL) and sat. $Na_2S_2O_3$ (5 mL) were added. After 10 minutes, the mixture was transferred to a separatory funnel, where the aqueous layer was extracted with DCM (2 x 5 mL) and the combined organics were washed with water and then brine. The organics were dried and concentrated. The crude oil was chromatographed directly by MPLC (10 g column, 30% to 40% EtOAc/hexanes) to give **2.29** (34 mg, 36%, 3 steps).

^{1}H NMR (600 MHz, $CDCl_3$) δ 5.60 (ddd, J = 7.0, 3.3, 1.6 Hz, 1H), 2.91 (dd, J = 18.4, 7.0 Hz, 1H), 2.82-2.74 (m, 1H), 2.68-2.58 (m, 3H), 2.55-2.45 (m, 2H), 2.41 (dt, J = 18.4, 2.8 Hz, 1H), 1.96-1.91 (m, 3H), 1.81 (p, J = 6.9 Hz, 1H), 1.35 (s, 3H), 1.08 (d, J = 6.9 Hz, 3H), 1.04 (d, J = 6.9 Hz, 3H). **^{13}C NMR (151 MHz, $CDCl_3$)** δ 203.5, 202.8, 198.4, 168.2, 142.7, 134.0, 123.5, 71.2, 71.2, 70.4, 36.9, 35.0, 28.9, 28.5, 23.2, 18.8, 18.6, 17.8. **IR (ATR):** ν_{max} (cm^{-1}) = 2967 (m), 2933 (m), 1760 (s), 1688 (s), 1641 (m), 1289 (m), 1240 (m), 1023 (m). **HRMS (ESI$^+$)** Calcd. For $C_{19}H_{22}NaO_4$. $[M+Na]^+$: 337.1416, found: 337.1405. **TLC** (EtOAc/hexanes = 50%, UV): R_f = 0.16

Hydroxy Enone **2.26**

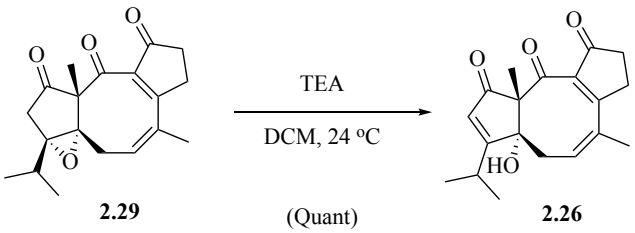

2.29 **2.26**

Experimental: In a 20 mL scintillation vial equipped with a magnetic stir-bar was charged with **2.29** (5 mg, 0.016 mmol, 1.0 equiv). The reactor was then diluted with dry DCM (1 mL) and at 24 °C, under argon, was added triethylamine (4.5 µL, 0.032 mmol, 2.0 equiv). The yellow solution was then stirred for 18 hours. Upon completion (monitored by TLC), the reaction was concentrated directly. The concentrate was purified by flash column (50% EtOAc/hexanes) to afford alcohol **2.26** (5 mg, quant.).

^{1}H NMR (600 MHz, $CDCl_3$) δ 6.03 (d, *J* = 1.0 Hz, 1H), 5.74 (dt, *J* = 6.0, 1.8 Hz, 1H), 3.26 (s, 1H), 2.84-2.76 (m, 2H), 2.57-2.52 (m, 1H), 2.42 (ddd, *J* = 9.5, 1.6, 0.7 Hz, 1H), 2.23-2.06 (m, 3H), 1.74-1.72 (m, 3H), 1.26 (s, 3H), 1.25 (d, *J* = 6.8 Hz, 3H), 1.19 (d, *J* = 6.8 Hz, 3H). **^{13}C NMR (151 MHz, $CDCl_3$)** δ 205.5, 199.4, 196.8, 183.7, 134.2, 127.0, 121.4, 85.3, 83.6, 65.9, 62.0, 35.6, 29.8, 28.1, 26.9, 23.0, 22.6, 22.3, 18.7. **IR (ATR):** ν_{max} (cm^{-1}) = 3331 (br, s), 2919 (s), 2851 (m), 1759 (m), 1624 (m), 1461 (m), 1104 (m), 1035 (s). **HRMS (ESI^+)** Calcd. for $C_{19}H_{22}NaO_4$. $[M+Na]^+$: 337.1416, found: 337.1407. **TLC** (EtOAc/hexanes = 50%, $KMnO_4$): R_f = 0.13

Keto-Aldehyde **2.32**

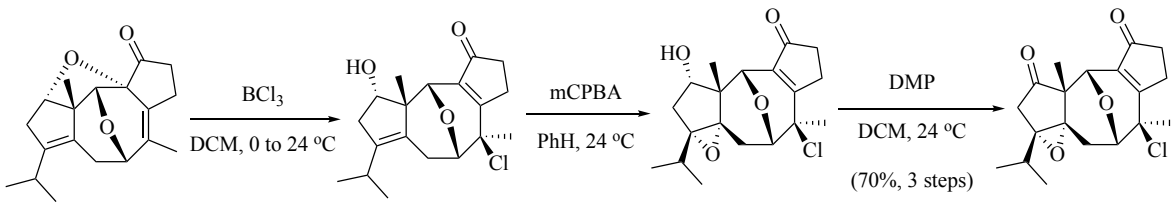

2.20 **2.30** **2.31** **2.32**

Experimental: In a 6 dr vial equipped with a magnetic stir-bar was charged with **2.20** (160 mg, 0.53 mmol, 1 equiv) under an argon atmosphere. At 24 °C, dry DCM (10.6 mL) was added in a single portion. Finally, BCl_3 (1.0 M in DCM, 1.6 mL, 1.60 mmol, 3.0 equiv) was added dropwise to the reactor at 0 °C. The yellow solution was stirred for 2.5 hours (monitored by low-res mass spec.) and upon completion, the reaction was quenched with ice-cold $NaHCO_3$ and diluted with DCM (5 mL). The layers were separated and the aqueous was extracted with DCM (3 x 5 mL). The combined organics were washed with water, brine, dried over Na_2SO_4, and then concentrated under vacuum. The material (**2.30**) was quickly taken forward crude.

In a 20 mL scintillation vial, equipped with magnetic stirring, was added crude **2.30** (180 mg), followed by benzene (5 mL) under argon. At 24 °C, mCPBA (77%, 143 mg, 0.64 mmol, 1.2 equiv) was added in one portion and stirred for 15 minutes. To the reaction was added sat. $NaHCO_3$ (5 mL) and sat. $Na_2S_2O_3$ (5 mL). After 5 additional minutes, the mixture was transferred to a separatory funnel, where the aqueous layer was extracted with ethyl acetate (2 x 5 mL) and the combined organics were washed with water and then brine. The organics were dried and concentrated. The crude oil (**2.31**) was taken directly into subsequent oxidation.

In a 6 dr vial equipped with magnetic stirring, crude epoxide **2.31** (185 mg) was added. The starting material was diluted with DCM (5 mL) under atmosphere, and then at 24 °C, DMP (254 mg, 0.6 mmol, 1.2 equiv) was added. The cloudy suspension was stirred for 45 minutes, at which sat. $NaHCO_3$ (5 mL) and sat. $Na_2S_2O_3$ (5 mL) were added. After 10 minutes, the mixture was transferred to a separatory funnel, where the aqueous layer was extracted with DCM (2 x 5 mL) and the combined organics were washed with water

and brine. The organics were dried and concentrated. The crude oil was chromatographed directly (35% to 45% EtOAc/hexanes) to give white semi-solid **2.32** (130 mg, 70%, 3 steps).

^{1}H NMR (600 MHz, $CDCl_3$) δ 4.83 (br s, 1H), 4.68 (d, *J* = 6.7 Hz, 1H), 2.87-2.76 (m, 1H), 2.71-2.60 (m, 2H), 2.56 (d, *J* = 18.0 Hz, 1H), 2.46 (t, 4.9 Hz, 2H), 2.18 (d, *J* = 18.0 Hz, 1H), 1.90 (d, *J* = 14.8 Hz, 1H), 1.82 (s, 3H), 1.68 (sept, *J* = 7.0 Hz, 1H), 1.47 (s, 3H), 1.03 (m, 6H). **^{13}C NMR (151 MHz, $CDCl_3$)** δ 207.4, 204.3, 169.0, 137.1, 78.1, 69.9, 68.7, 68.0, 53.8, 37.5, 34.4, 29.9, 28.1, 25.8, 25.2, 24.6, 20.6, 19.5, 18.4. **IR (ATR):** ν_{max} (cm^{-1}) = 2961 (m), 2618 (m), 1756 (s), 1709 (s), 1651 (w), 1373 (w), 1233 (m), 1056 (m), 1304 (m). **HRMS (ESI$^+$)** Calcd. for $C_{19}H_{23}ClNaO_4$. $[M+Na]^+$: 373.1183, found: 373.1175. **TLC** (EtOAc/hexanes = 50%, UV): R_f = 0.30.

Secondary Alcohol **2.34**

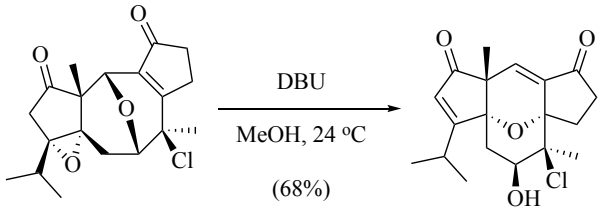

2.32 **2.34**

Experimental: In a 2 dr vial equipped with a magnetic stir bar was added **2.32** (130 mg, 0.37 mmol, 1.0 equiv) followed by HPLC MeOH (1.85 mL). The clear solution was then added DBU (122 mg, 0.74 mmol, 2.0 equiv) at 24 °C and the reaction quickly turned dark yellow. After 90 minutes (monitored by TLC), the reaction was concentrated directly. The crude oil mixture was chromatographed directly (33% EtOAc/hexanes) to give **2.34** (89 mg, 68%).

^{1}H NMR (600 MHz, $CDCl_3$) δ 6.83 (s, 1H), 5.90 (d, *J* = 1.1 Hz, 1H), 4.07-4.05 (m, 1H), 2.75-2.64 (m, 2H), 2.59 (br s, 1H), 2.57-2.47 (m, 2H), 2.38 (ddd, *J* = 18.9, 11.1, 1.5 Hz, 1H), 2.26 (dd, *J* = 14.6, 2.4 Hz, 1H), 1.88 (s, 3H), 1.77 (dt, *J* = 13.9, 11.0 Hz, 1H), 1.46 (s, 3H), 1.26 (d, *J* = 6.8 Hz, 3H), 1.20 (d, *J* = 6.8 Hz, 3H). **^{13}C NMR (151 MHz, $CDCl_3$)** δ 207.0, 202.6, 181.0, 142.2, 135.9, 125.5, 84.5, 81.4, 76.6, 74.1, 54.2, 37.3, 31.0, 29.1, 27.8, 25.4, 22.7, 22.7, 22.5. **IR (ATR):** ν_{max} (cm^{-1}) = 3425 (br), 2918 (m), 2849 (m), 1713 (s), 1654 (m), 1458 (w), 1214 (w), 1038 (w) . **HRMS (ESI$^+$)** Calcd. for $C_{19}H_{23}ClNaO_4$. $[M+Na]^+$: 373.1183, found: 373.1178. **TLC** (EtOAc/hexanes = 50%, UV/$KMnO_4$): R_f = 0.52.

Epoxy-Ketone **2.37**

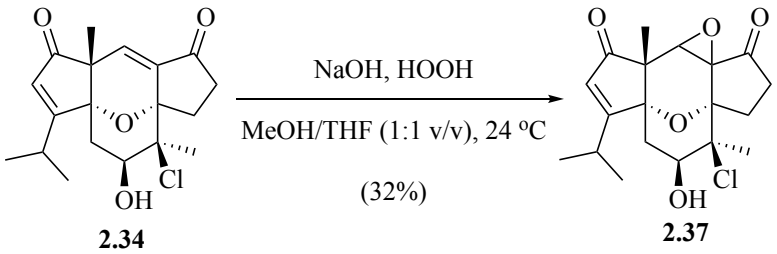

2.34 **2.37**

Experimental: In a 50 mL round bottom flask equipped with a magnetic stir bar was charged with **2.34** (100 mg, 0.286 mmol, 1.0 equiv) under an argon atmosphere. The reaction was then diluted with THF (2.86 mL) and MeOH (2.86 mL). HOOH (30% in water, 324 µL, 2.86 mmol, 10.0 equiv) was added, followed by NaOH (5% in water, 229 µL, 0.286 mmol, 1.0 equiv). The slightly cloudy reaction was stirred vigorously at 24 °C for 36 hours. At which time the reaction was quenched with ice-cold sat. $Na_2S_2O_3$ (5 mL) and diluted with ethyl acetate (5 mL). The mixture was transferred to a separatory funnel and the aqueous layer was washed with ethyl acetate (5 x 2 mL) upon separation. The combined organics were washed with water, brine, and dried over Na_2SO_4 and then

concentrated. The crude oil was chromatographed (33% EtOAc/hexanes) to give **2.37** (32 mg, 32%).

^{1}H NMR (600 MHz, $CDCl_3$) δ 6.01 (d, *J* = 1.0 Hz, 1H), 5.34 (d, *J* = 11.5 Hz, 1H), 3.94 (ddd, *J* = 11.5, 5.4, 1.8 Hz, 1H), 3.87 (s, 1H), 2.86-2.81 (m, 1H), 2.69 (sept, *J* = 6.4 Hz, 1H), 2.60-2.52 (m, 3H), 2.16-2.10 (m, 2H), 1.86 (s, 3H), 1.43 (s, 3H), 1.25 (d, *J* = 6.4 Hz, 3H), 1.20 (d, *J* = 6.4 Hz, 3H). **^{13}C NMR (151 MHz, $CDCl_3$)** δ 207.2, 205.8, 183.0, 126.2, 82.5, 82.4, 71.3, 71.0, 66.5, 64.3, 50.4, 34.3, 30.9, 30.9, 28.0, 26.2, 22.8, 22.8, 21.2. **IR (ATR):** ν_{max} (cm^{-1}) = 3430 (w), 2968 (w), 1757 (s), 1714 (s), 1454 (w), 1117 (m), 1023 (m). **HRMS (ESI$^+$)** Calcd. for $C_{19}H_{23}ClNaO_5$. $[M+Na]^+$: 389.1132, found: 389.1130. **TLC** (EtOAc/hexanes = 50%, $KMnO_4$): R_f = 0.48

Triflate **2.39**

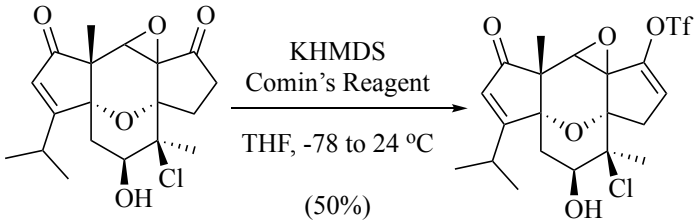

2.37 **2.39**

Experimental: In a vial containing a magnetic stir-bar and **2.37** (12 mg, 0.033 mmol, 1.0 equiv) was diluted with dry THF (3.3 mL) under an argon atmosphere. The reactor was cooled to -78 °C and KHMDS (1.0 M in THF, 144 µL, 0.072 mmol, 2.2 equiv) was added over 1 minute to form a deep yellow solution. After 30 minutes, Comin's reagent (15 mg, 0.039 mmol, 1.2 equiv) was added quickly as a solid. The reaction was kept at 30 minutes more and then allowed to warm to 24 °C. After 4 hours, TLC showed disappearance of starting material and the reaction was quenched with sat. NH_4Cl (2 mL) and diluted with ethyl acetate (2 mL). The organic was pipetted from the vial and ethyl acetate (3 x 2 mL)

was used to extract remaining organics. The combined organics were washed with water, brine, and dried over Na_2SO_4 and then concentrated. The crude oil was subjected to a silica plug (25 % to 35 % EtOAc/hexanes) to give **2.39** (6 mg, 50%) as a semi-pure oil and was not rigorously characterized as such.

^{1}H NMR (600 MHz, $CDCl_3$) δ 6.03 (t, *J* = 2.7 Hz, 1H), 6.01 (br s, 1H), 5.58-5.52 (m, 1H), 3.96-3.91 (m, 1H), 3.88 (s, 1H), 3.24 (dd, *J* = 14.8, 3.0 Hz, 1H), 2.66 (sept, *J* = 6.5 Hz, 1H), 2.54-2.46 (m, 2H), 2.10 (dd, *J* = 15.3, 3.0 Hz, 1H), 1.83 (s, 3H), 1.44 (s, 3H), 1.24-1.16 (m, 6H).

2.7 References

[1]Li, F.; Lin, S.; Zhang, S.; Pan, L.; Chai, C.; Su, J.-C.; Yang, B.; Liu, J.; Wang, J.; Hu, Z.; Zhang, Y. *J. Nat. Prod.* **2020**, *83*, 1931–1938.

[2]Cordovilla, C.; Bartolomé, C.; Martínez-Ilarduya, J. M.; Espinet, P. *ACS Catal.* **2015**, *5*, 3040–3053.

[3]Brooks, D. W.; Grothaus, P. G.; Irwin, W. L. *J. Org. Chem.* **1982**, *47*, 2820–2821.

[4]Carr, J. M.; Snowden, T. S. *Tetrahedron* **2008**, *64*, 2897–2905.

[5]Liu, L. L.; Chiu, P. *Chem. Comm.* **2011**, *47* (12), 3416.

[6]Wu, G.-J.; Zhang, Y.-H.; Tan, D.-X.; He, L.; Cao, B.-C.; He, Y.-P.; Han, F.-S. *J. Org. Chem.* **2019**, *84*, 3223–3238.

[7]Krueger, A. C.; Warren, K. M.; Carroll, W. M.; Pratt, J. K.; Hutchins, D. K. WO2012083170A1, 2012.

[8]He, F.; Bo, Y.; Altom, J. D.; Corey, E. J. *J. Am. Chem. Soc.* **1999**, *121*, 6771–6772.

[9]Smith, A. B.; Branca, S. J.; Pilla, N. N.; Guaciaro, M. A. *J. Org. Chem.* **1982**, *47*, 1855–1869.

[10]Bader, S. J.; Snapper, M. L. *J. Am. Chem. Soc.* **2005**, *127*, 1201–1205.

[11]Tsuna, K.; Noguchi, N.; Nakada, M. *Chem. Eur. J.* **2013**, *19*, 5476–5486.

[12]Paquette, L. A.; Romine, J. L.; Lin, H.-S. *Tetrahedron Lett.* **1987**, *28*, 31–34.

[13]Bartlett, P. A.; Mori, I.; Bose, J. A. *J. Org. Chem.* **1989**, *54*, 3236–3239.

[14]Mander, L. N. *Comp. Org. Syn.* **1991**, 489–521.

[15]Stork, G.; Sher, P. M.; Chen, H. L. *J. Am. Chem. Soc.* **1986**, *108*, 6384–6385.

[16]Hoveyda, A. H.; Evans, D. A.; Fu, G. C. *Chem. Rev.* **1993**, *93*, 1307–1370.

[17]Kolb, H. C.; VanNieuwenhze, M. S.; Sharpless, K. B. *Chem. Rev.* **1994**, *94*, 2483–2547.

[18]Xue, Y.; Dong, G. *J. Am. Chem. Soc.* **2021**, *143* (22), 8272–8277.

[19]Nagata, W.; Yoshioka, M. *Tetrahedron Lett.* **1966**, *7*, 1913–1918.

[20]Hafeman, N. J.; Loskot, S. A.; Reimann, C. E.; Pritchett, B. P.; Virgil, S. C.; Stoltz, B. M. *J. Am. Chem. Soc.* **2020**, *142*, 8585–8590.

APPENDICES

APPENDIX A

Spectral Data for Chapter One

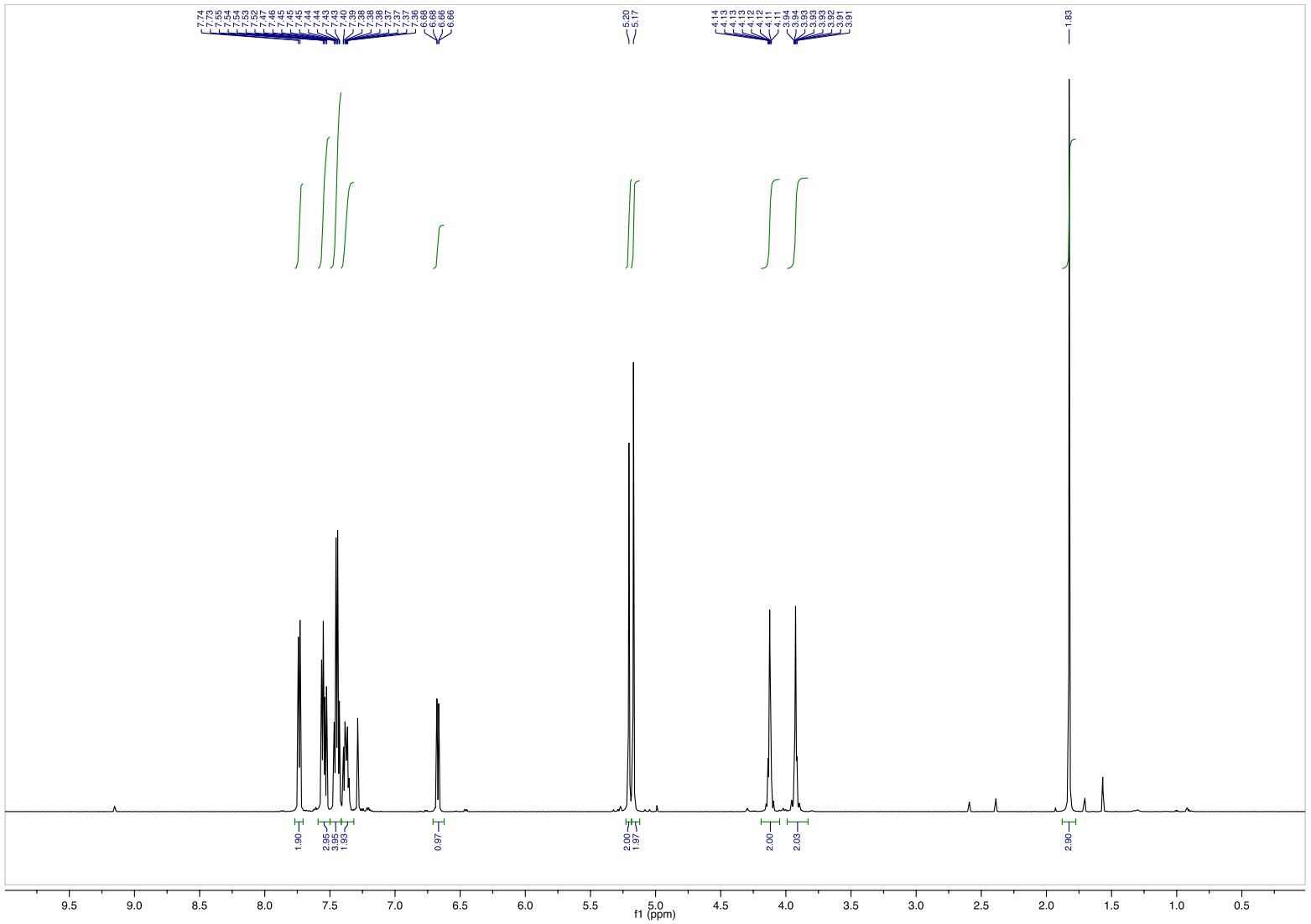

Figure A.1. ^{1}H NMR (600 MHz, $CDCl_3$), **1.11**

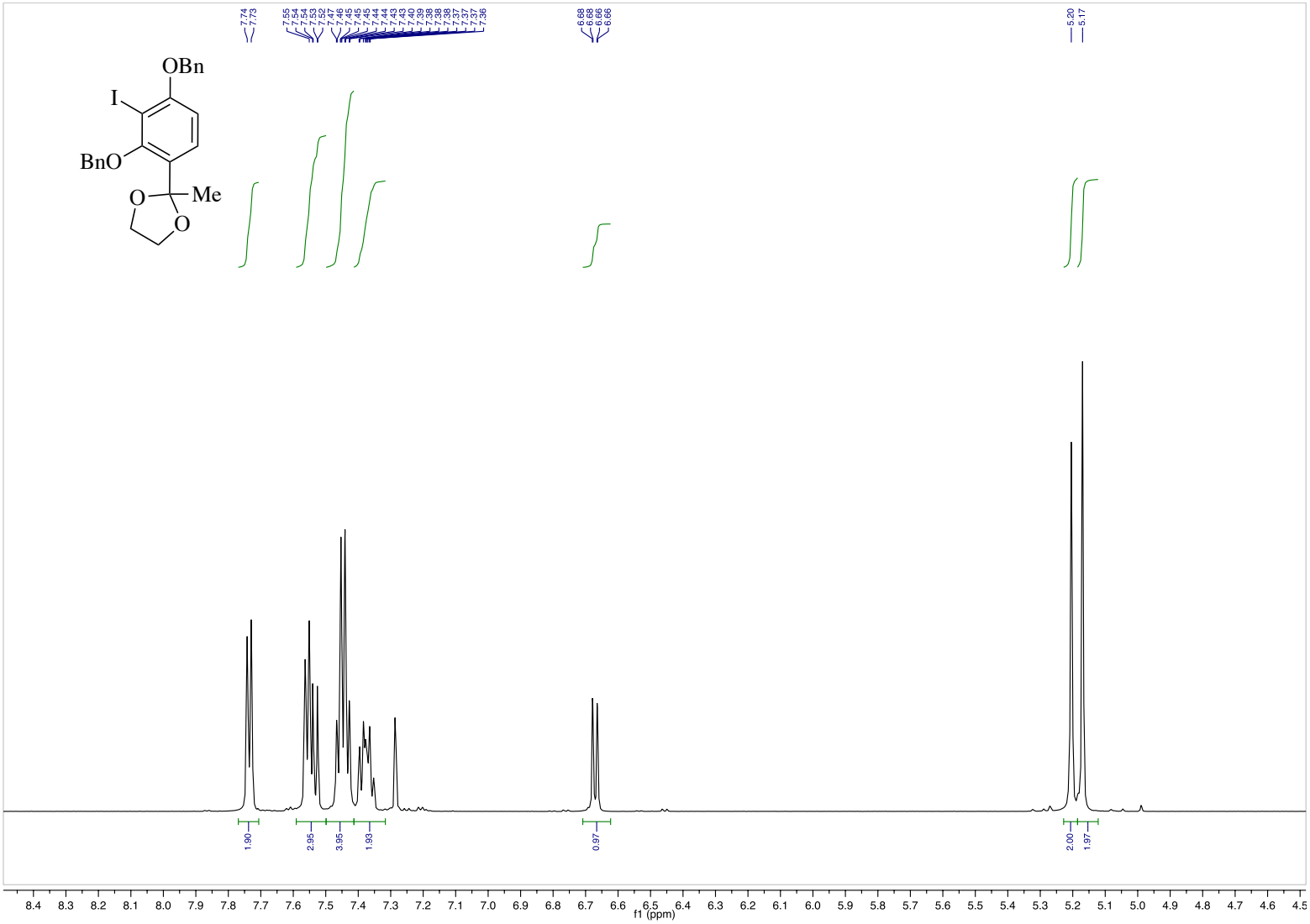

Figure A.2. ^{1}H NMR (600 MHz, $CDCl_3$), **1.11** (inset)

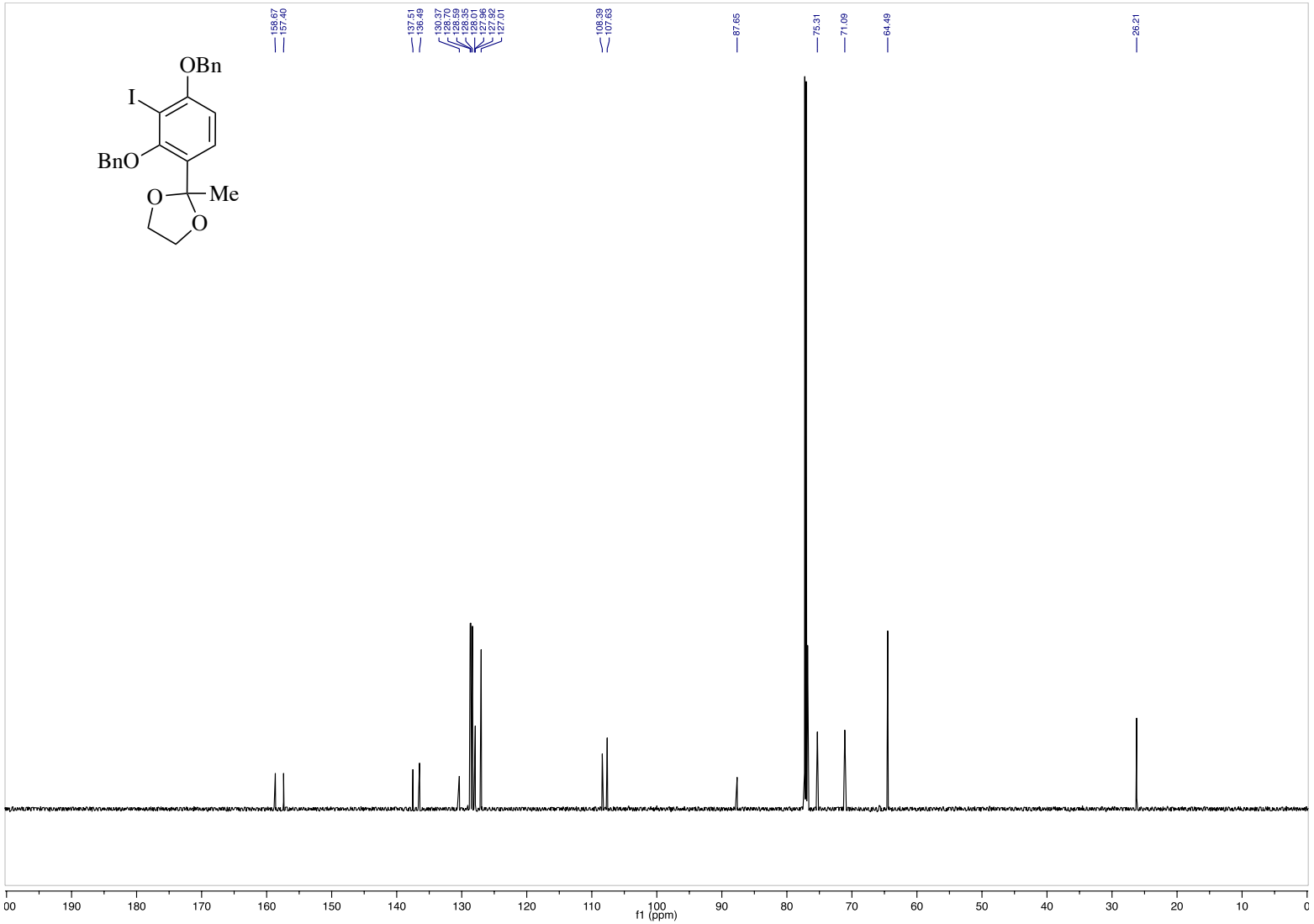

Figure A.3. ^{13}C NMR (151 MHz, $CDCl_3$), **1.11**

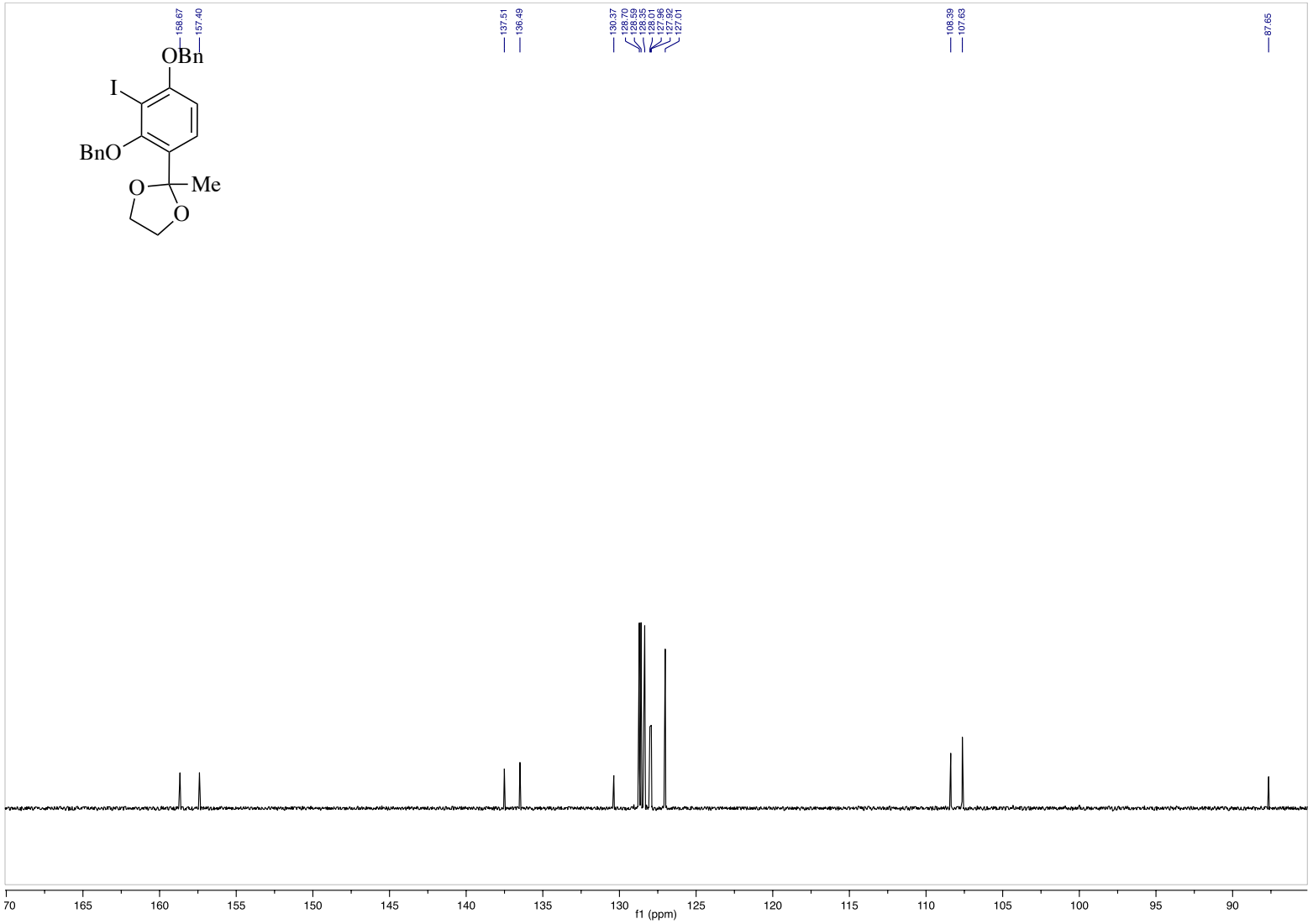

Figure A.4. ^{13}C NMR (151 MHz, $CDCl_3$), **1.11** (inset)

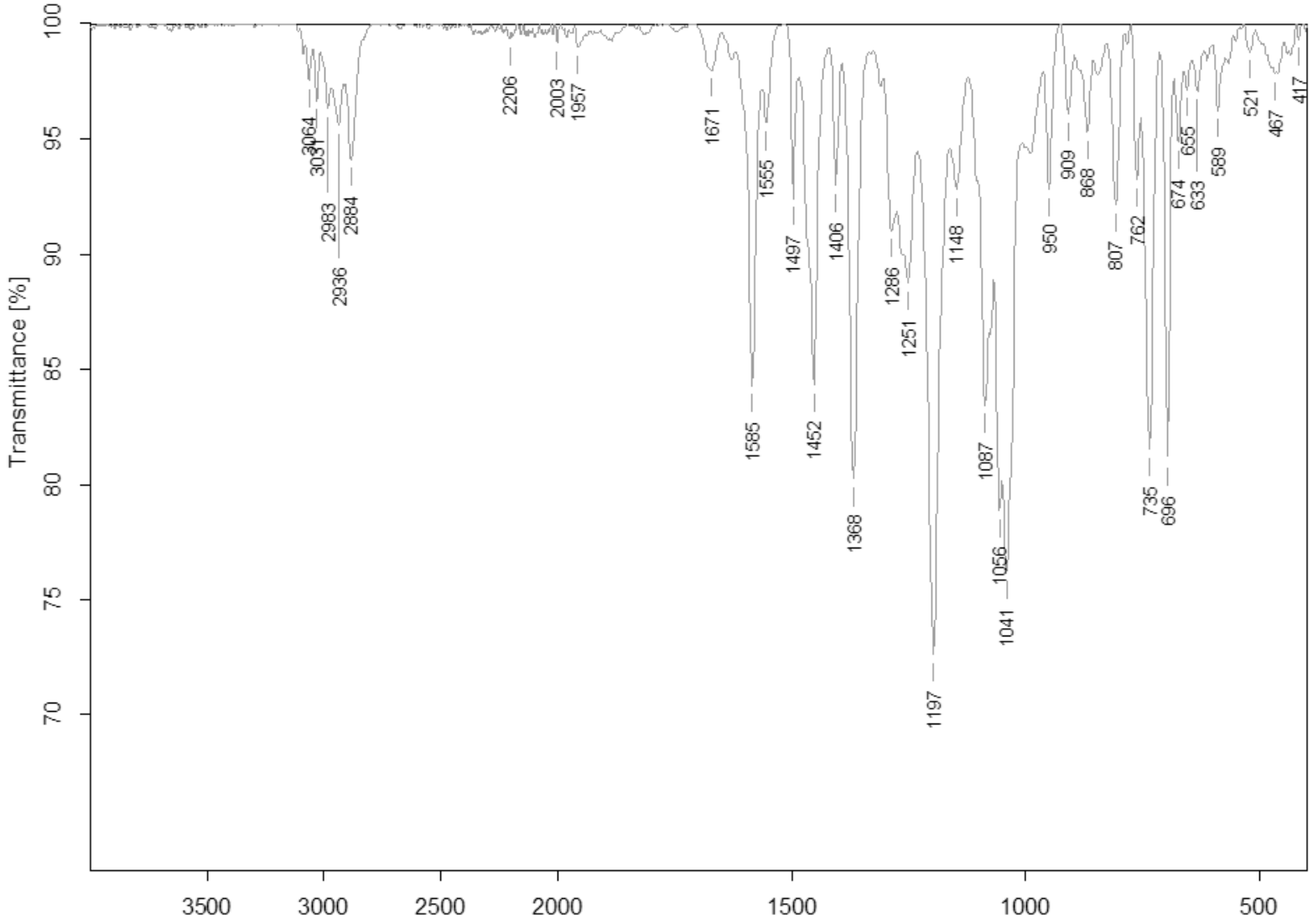

Figure A.5. IR (ATR), **1.11**

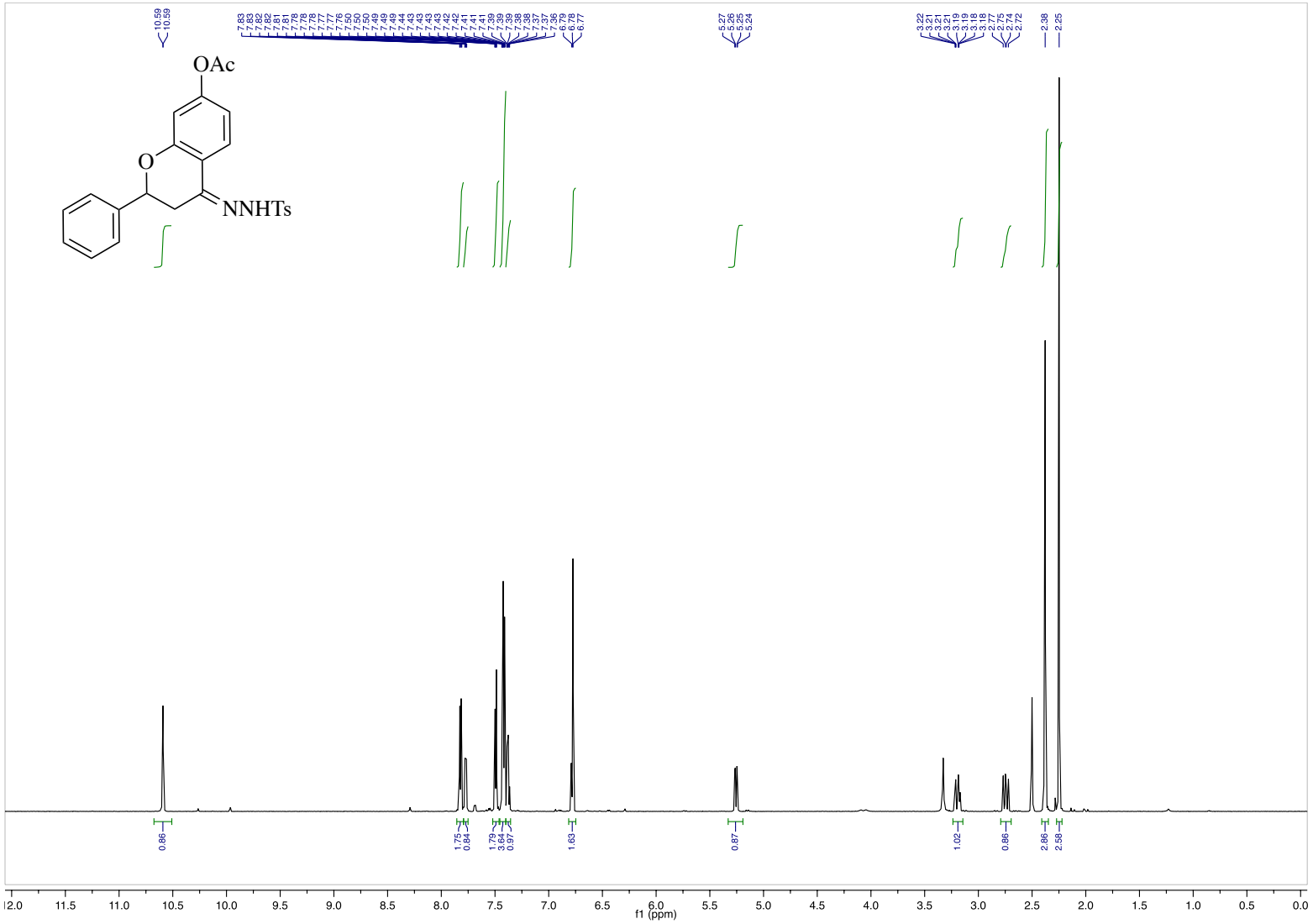

Figure A.6. ^{1}H NMR (600 MHz, DMSO-d_6), **1.10**

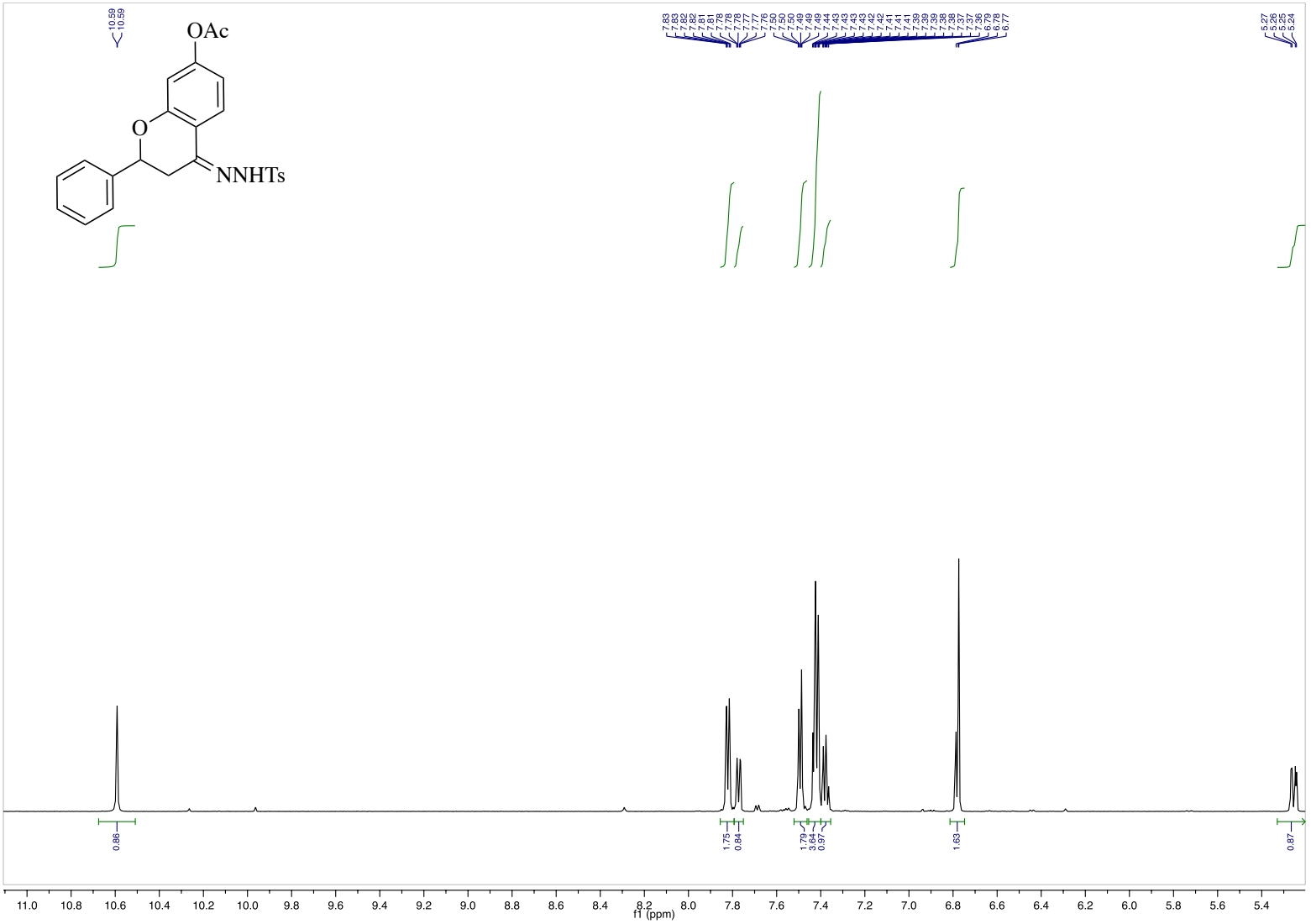

Figure A.7. ^{1}H NMR (600 MHz, DMSO-d_6), **1.10** (inset)

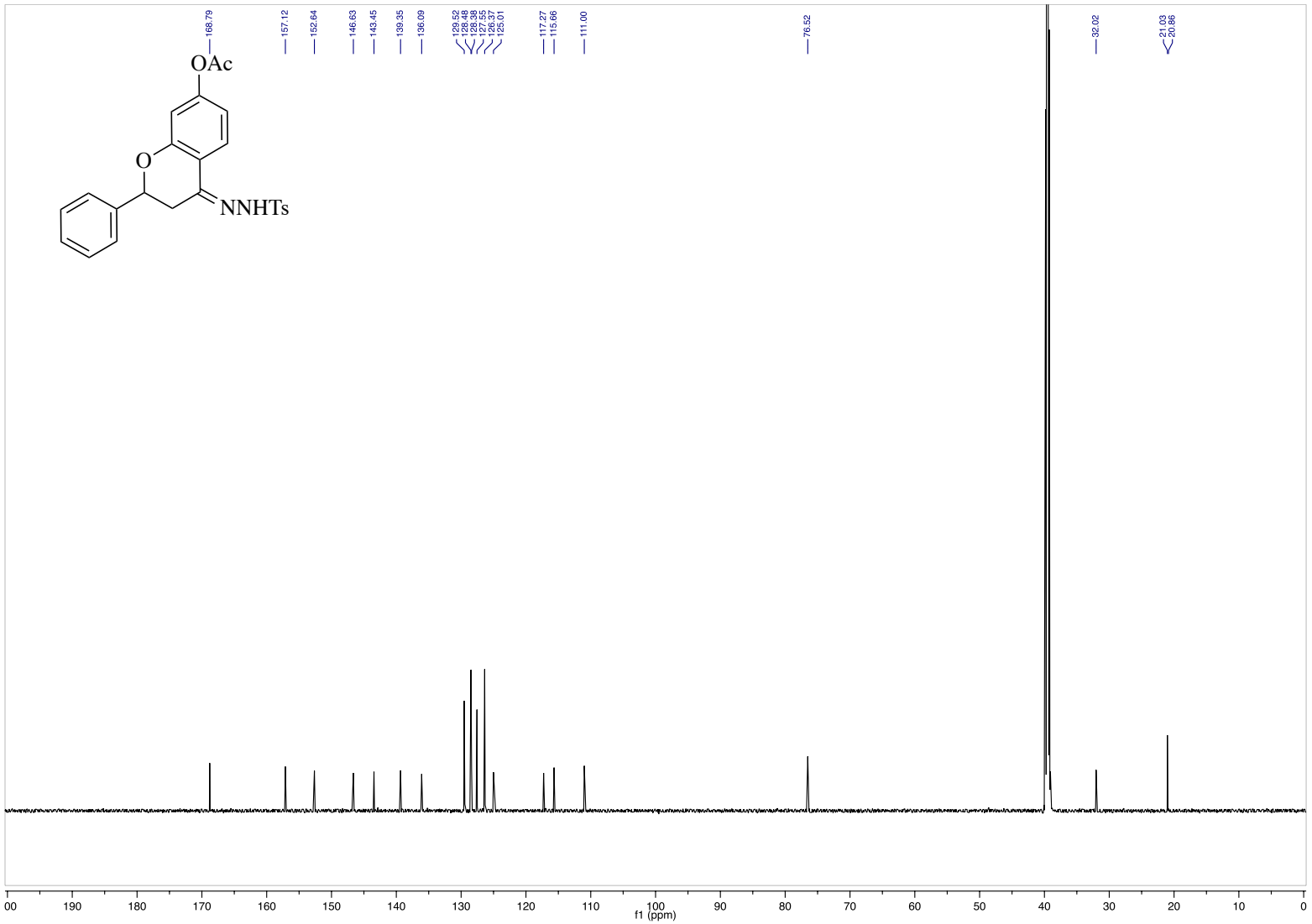

Figure A.8. ^{13}C NMR (151 MHz, DMSO-d_6), **1.10**

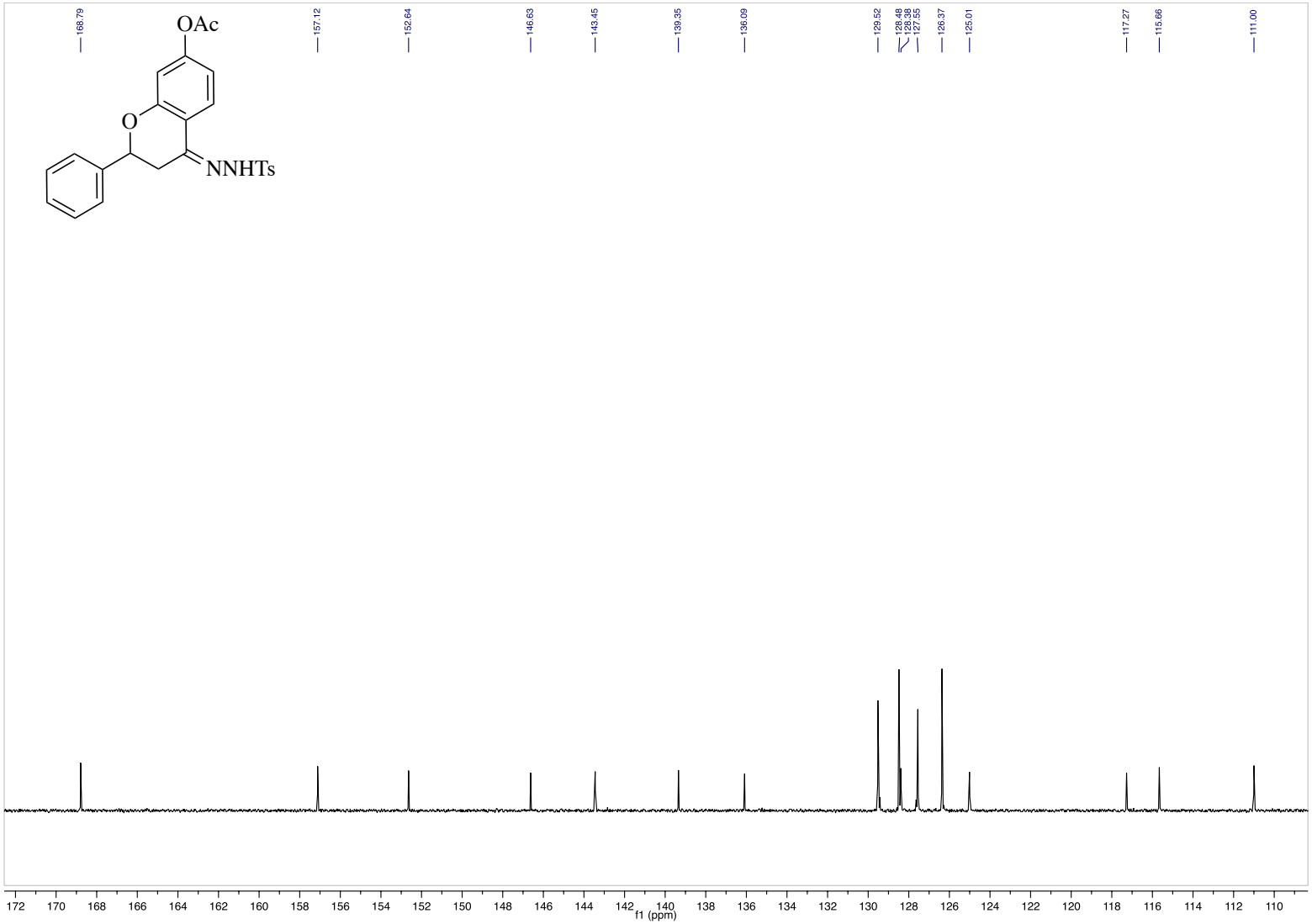

Figure A.9. ^{13}C NMR (151 MHz, DMSO-d_6), **1.10** (inset)

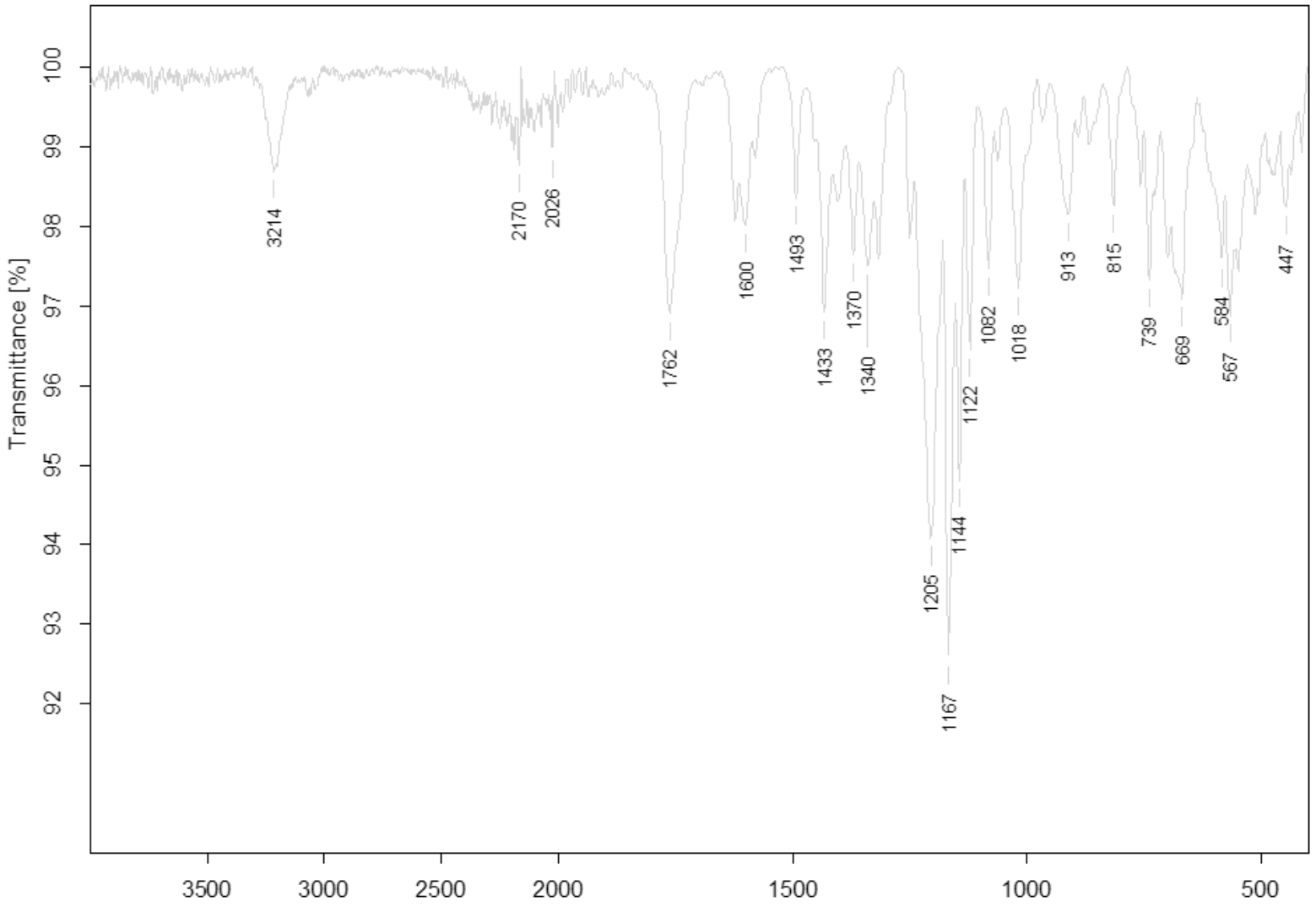

Figure A.10. IR (ATR), **1.10**

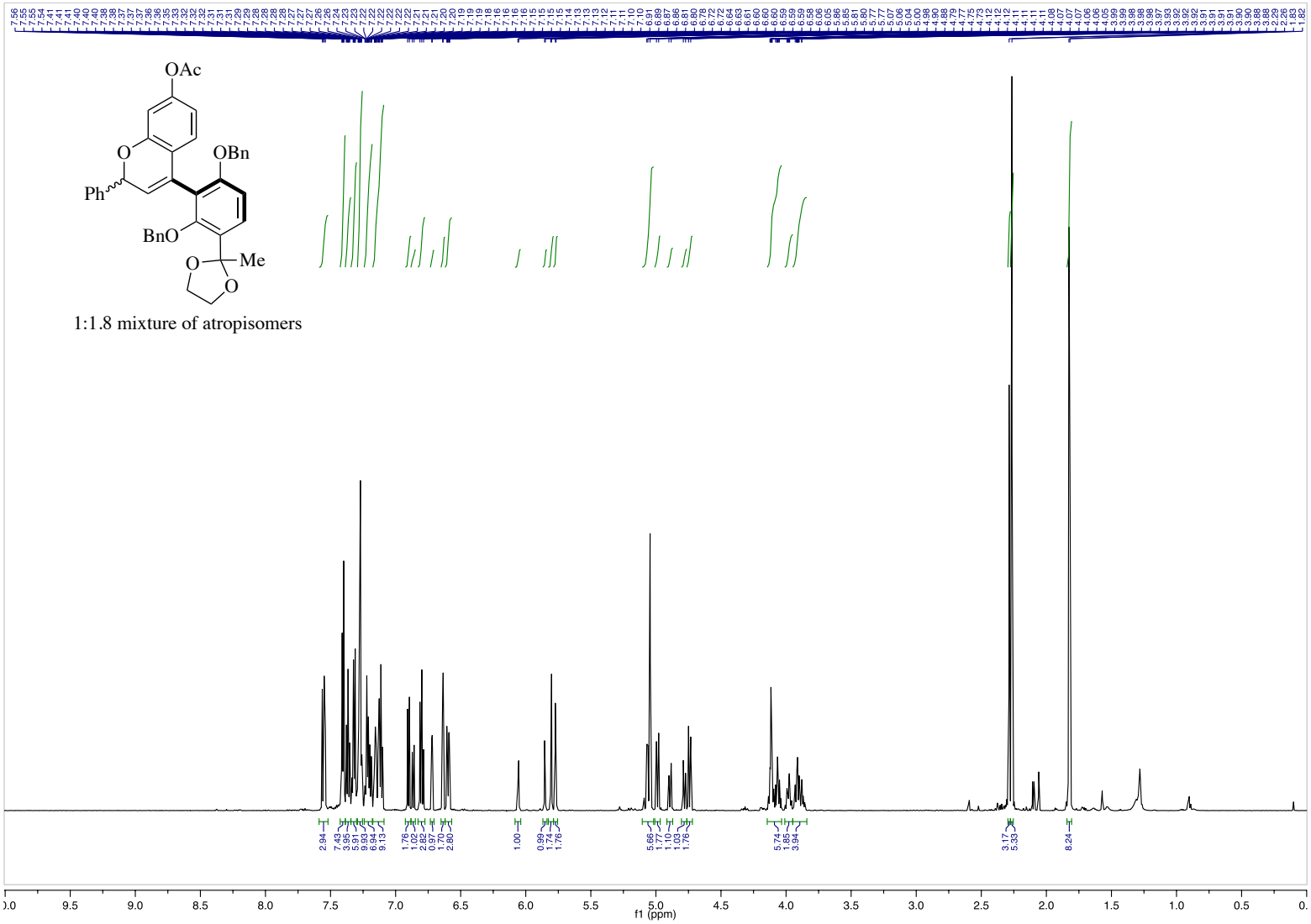

Figure A.11. ^{1}H NMR (600 MHz, $CDCl_3$), **1.09**

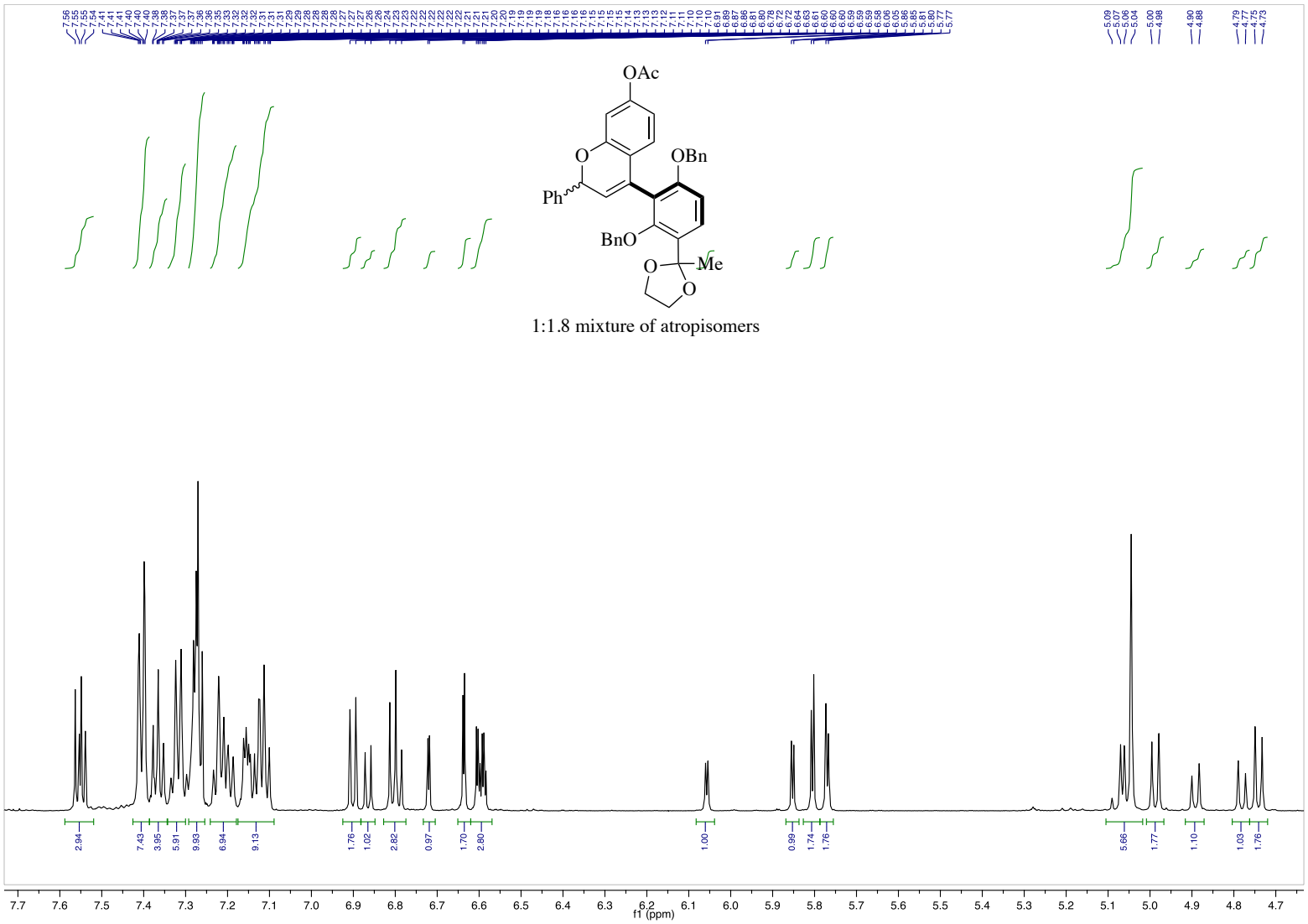

Figure A.12. ^{1}H NMR (600 MHz, $CDCl_3$), **1.09** (inset)

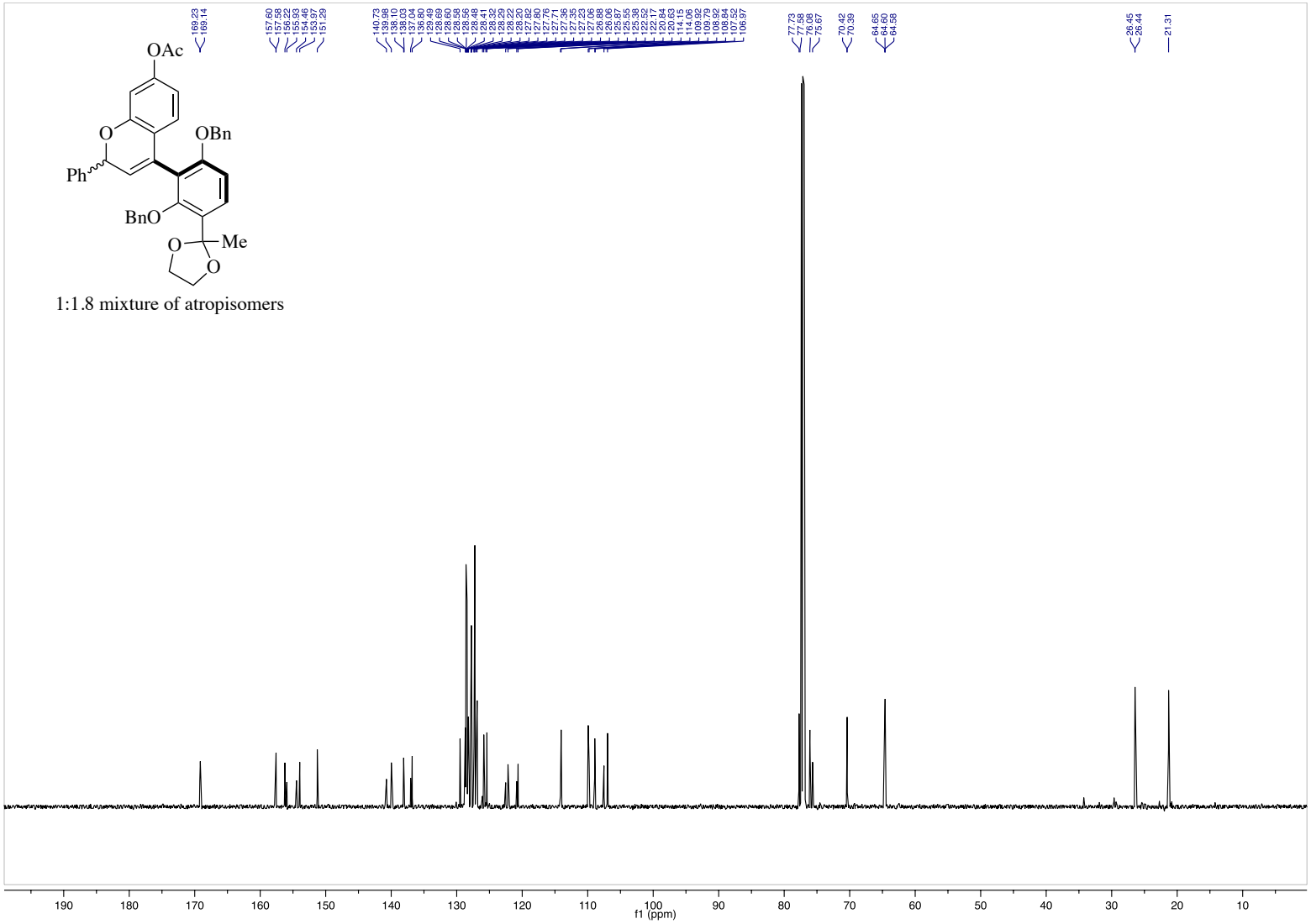

Figure A.13. ^{13}C NMR (151 MHz, $CDCl_3$), **1.09**

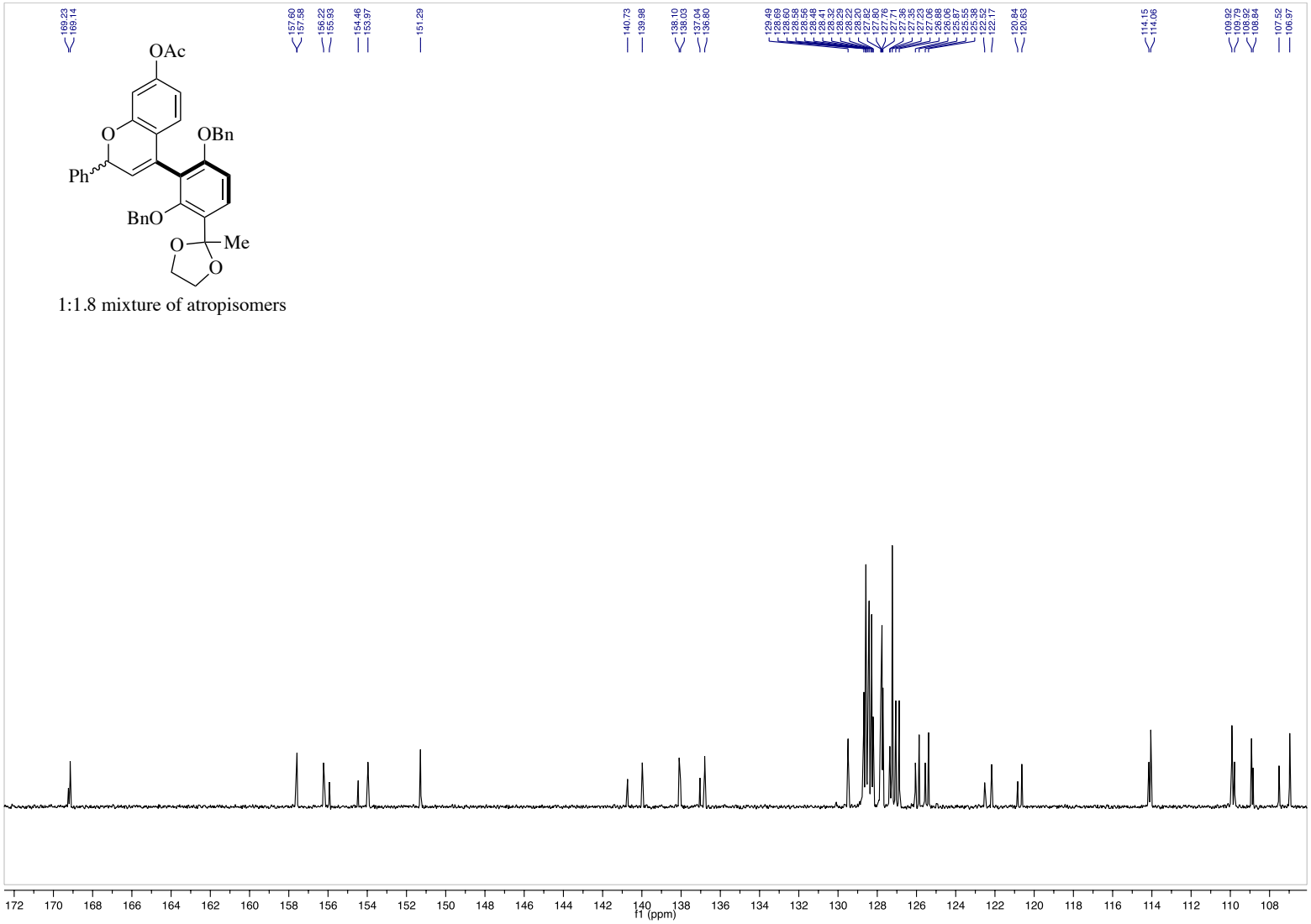

Figure A.14. ^{13}C NMR (151 MHz, $CDCl_3$), **1.09** (inset)

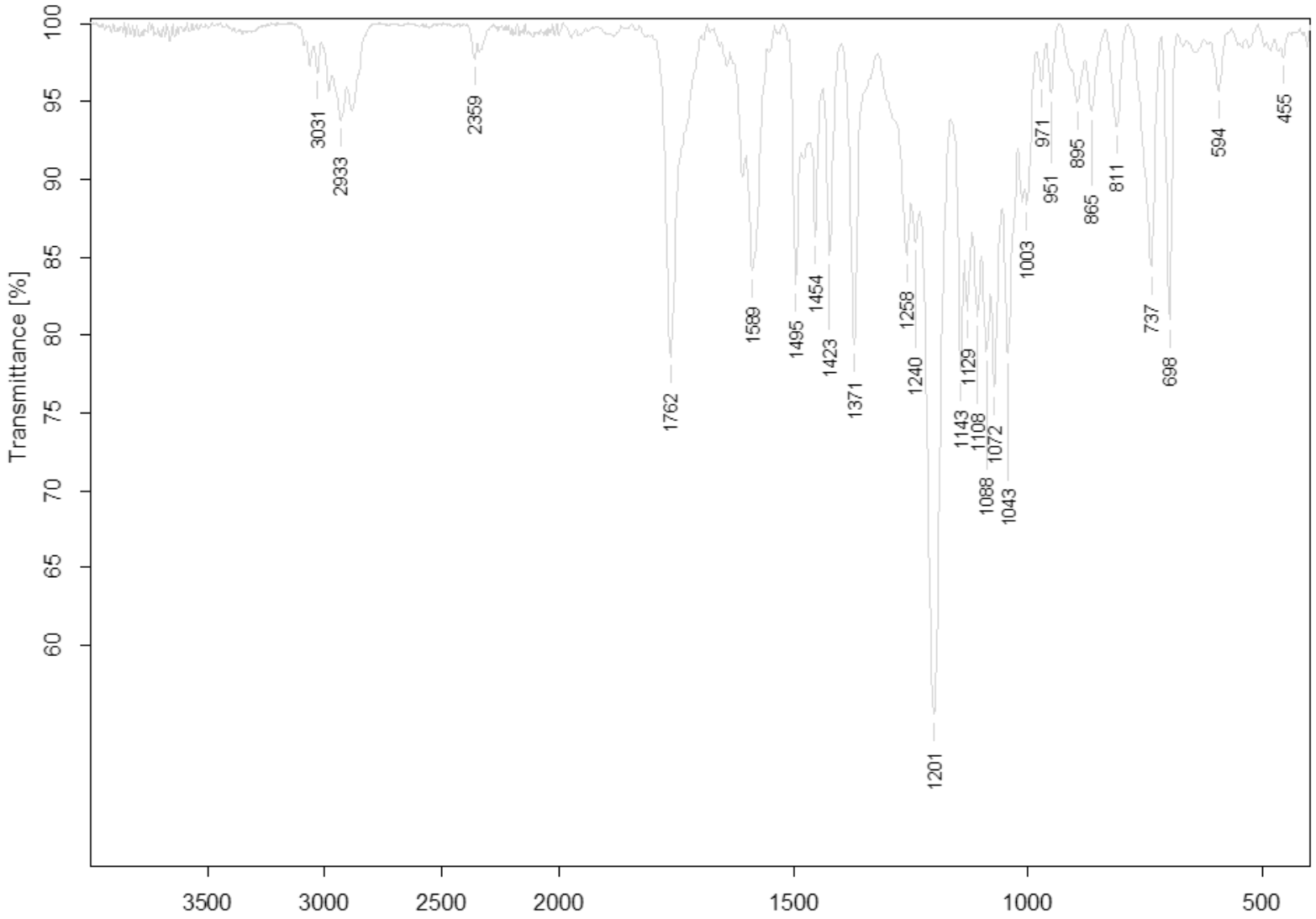

Figure A.15. IR (ATR), **1.09**

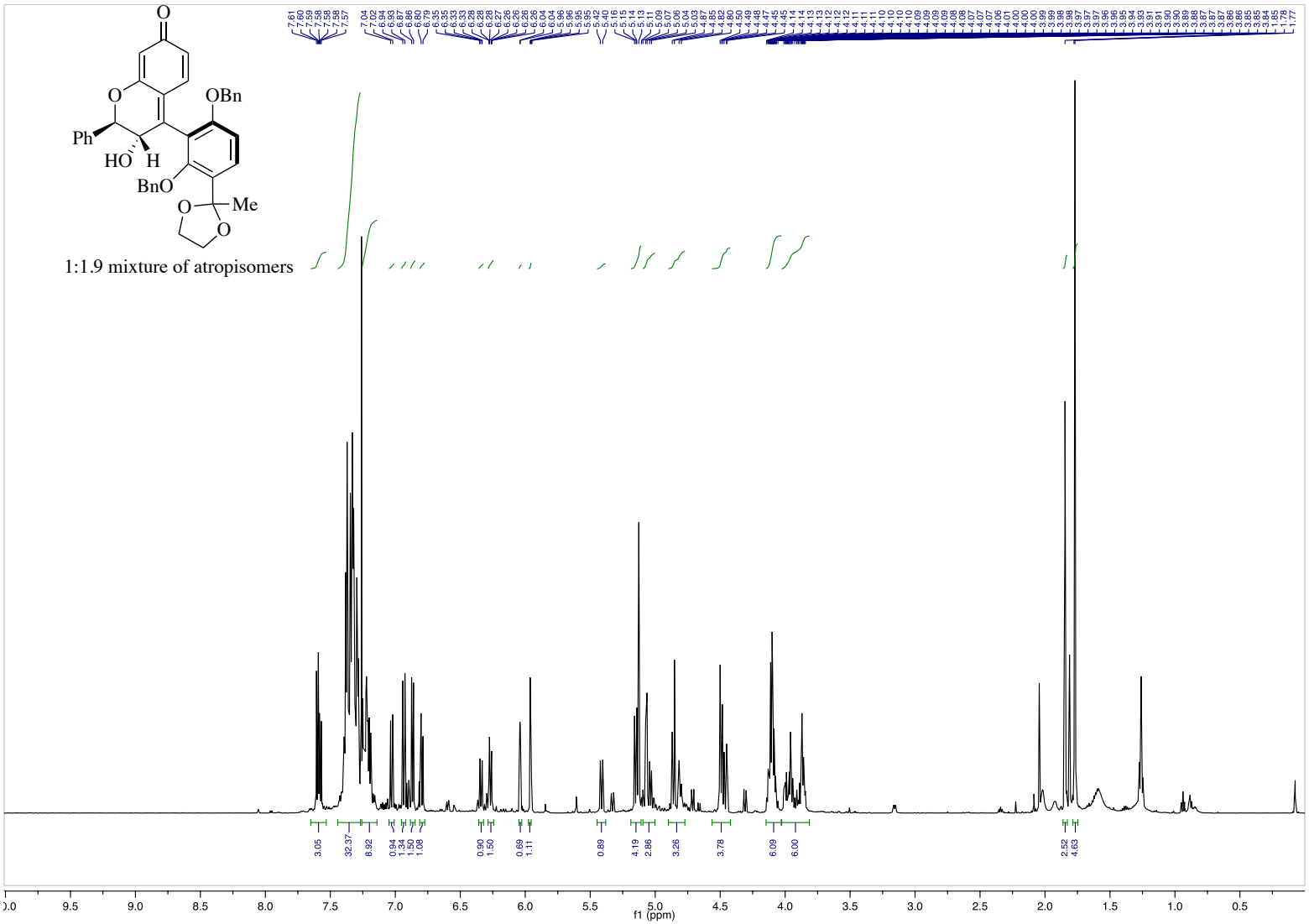

Figure A.16. ^{1}H NMR (600 MHz, $CDCl_3$), **1.19**

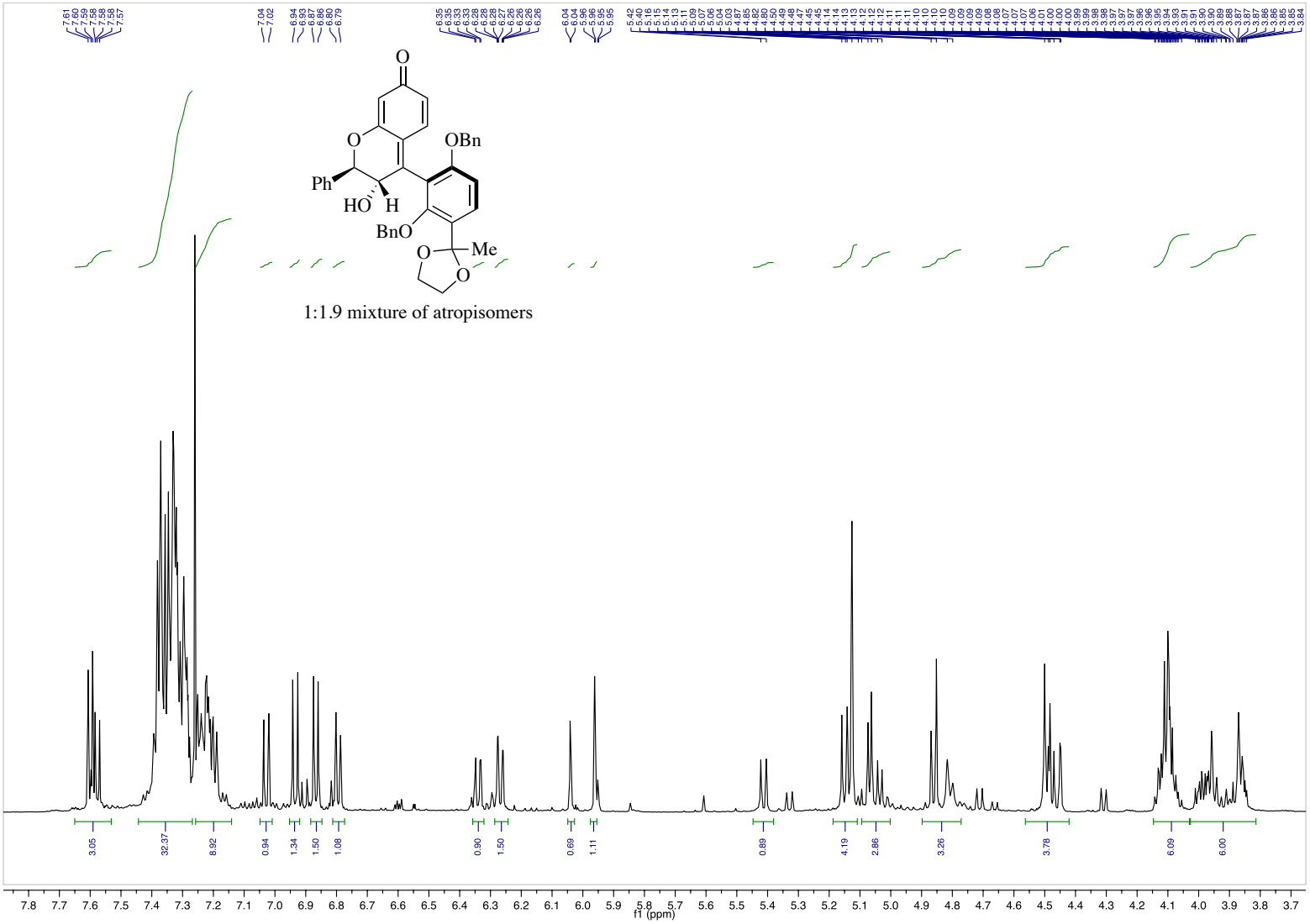

Figure A.17. ^{1}H NMR (600 MHz, $CDCl_3$), **1.19** (inset)

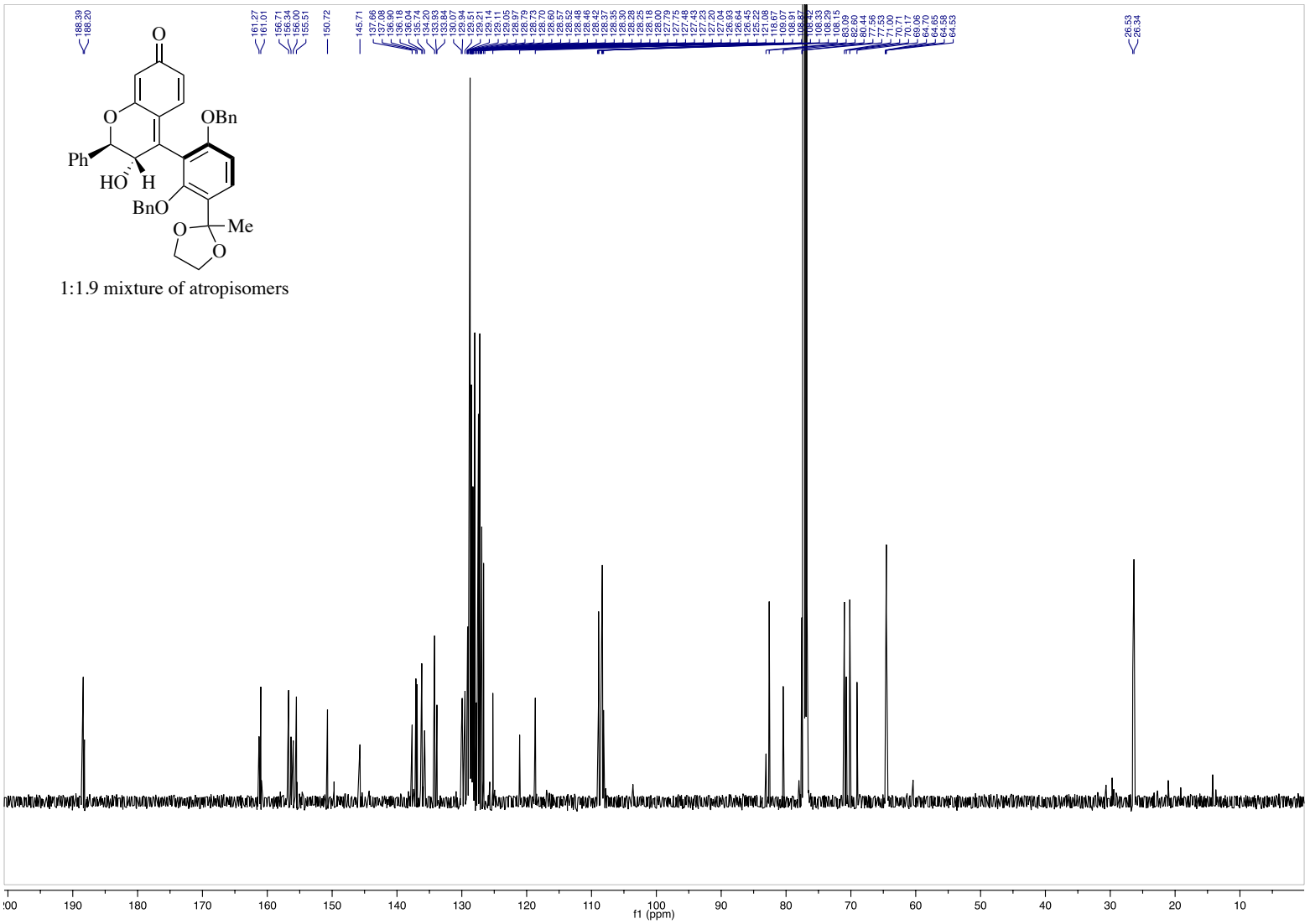

Figure A.18. ^{13}C NMR (151 MHz, $CDCl_3$), **1.19**

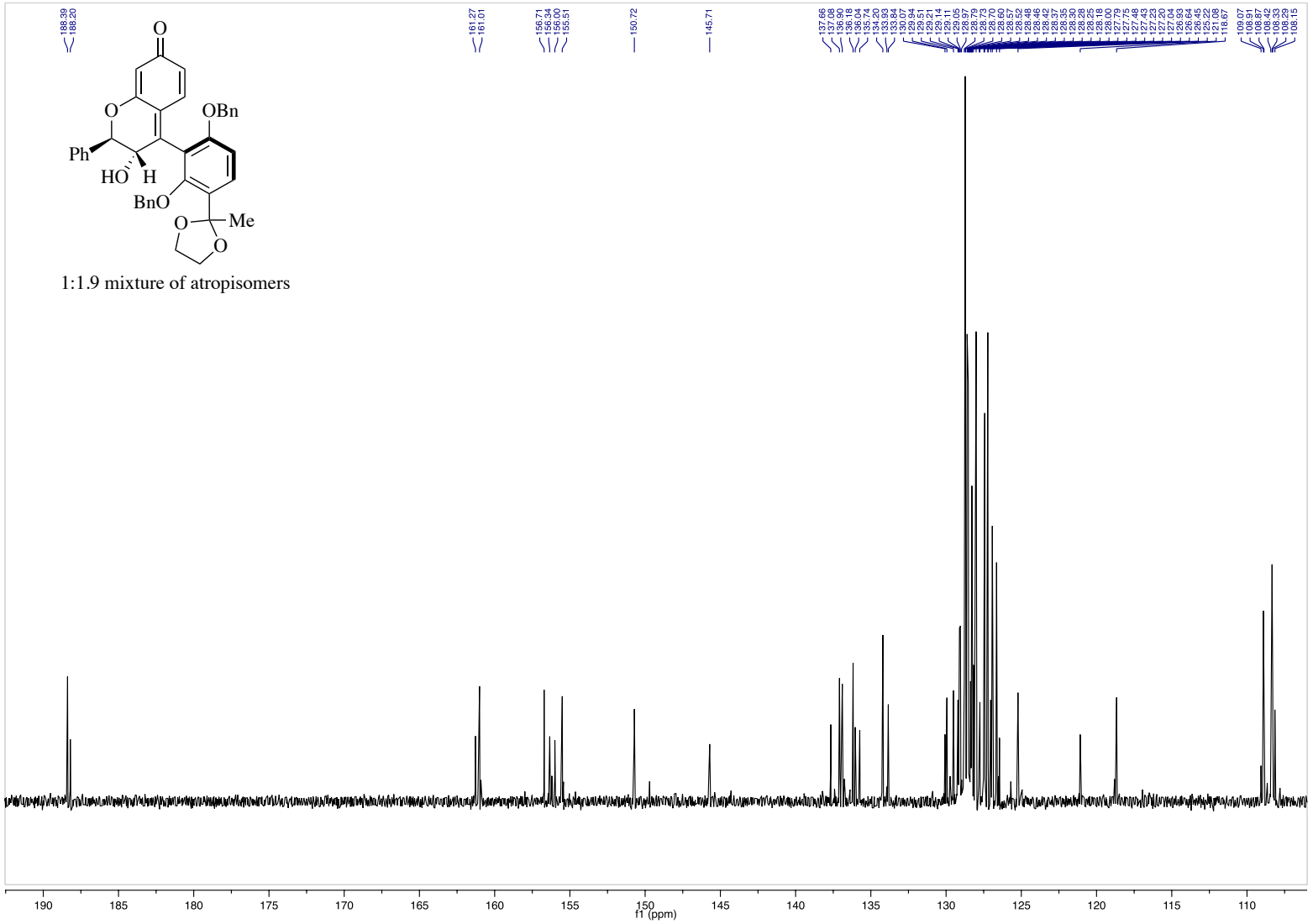

Figure A.19. ^{13}C NMR (151 MHz, $CDCl_3$), **1.19** (inset)

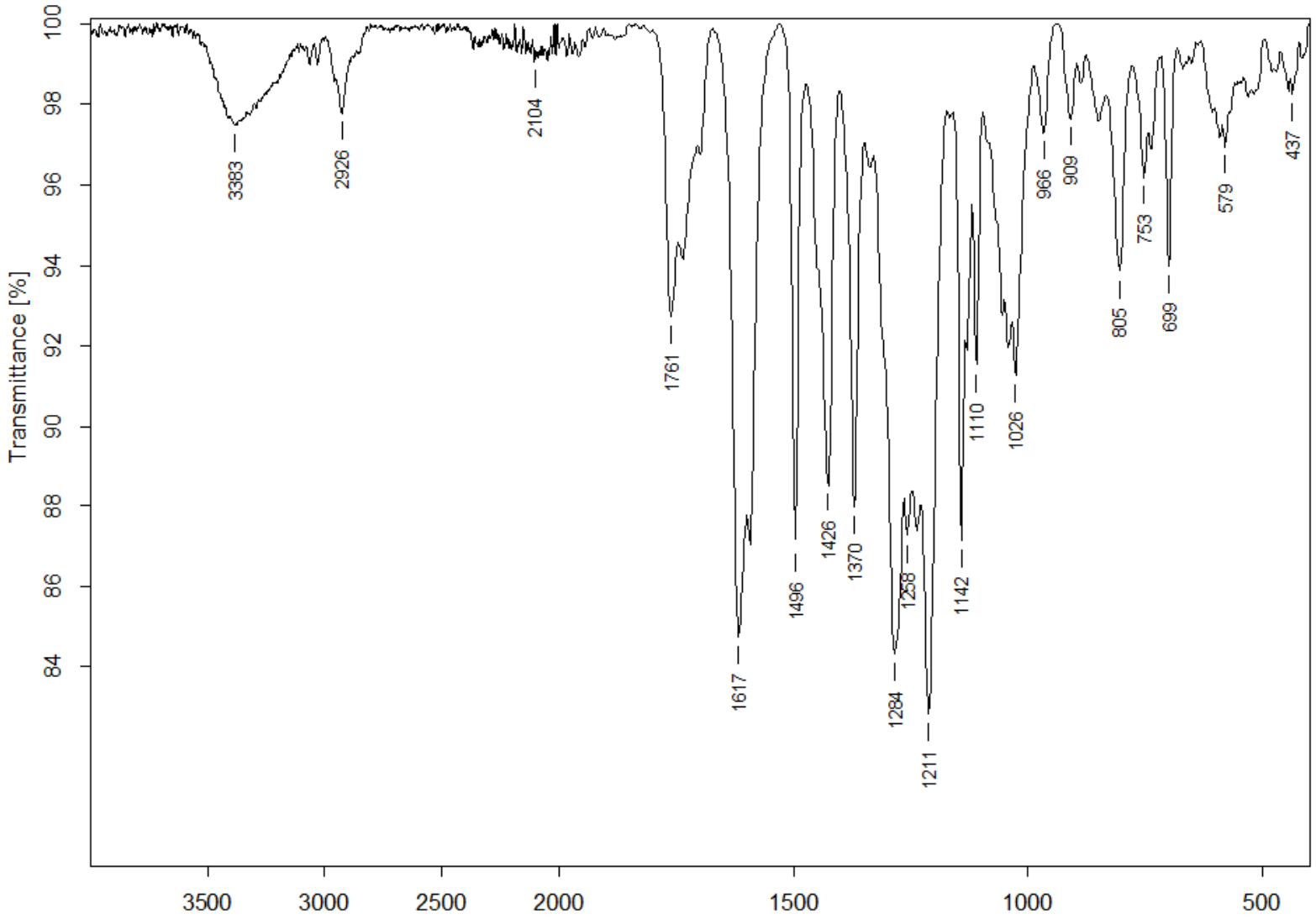

Figure A.20. IR (ATR), **1.19**

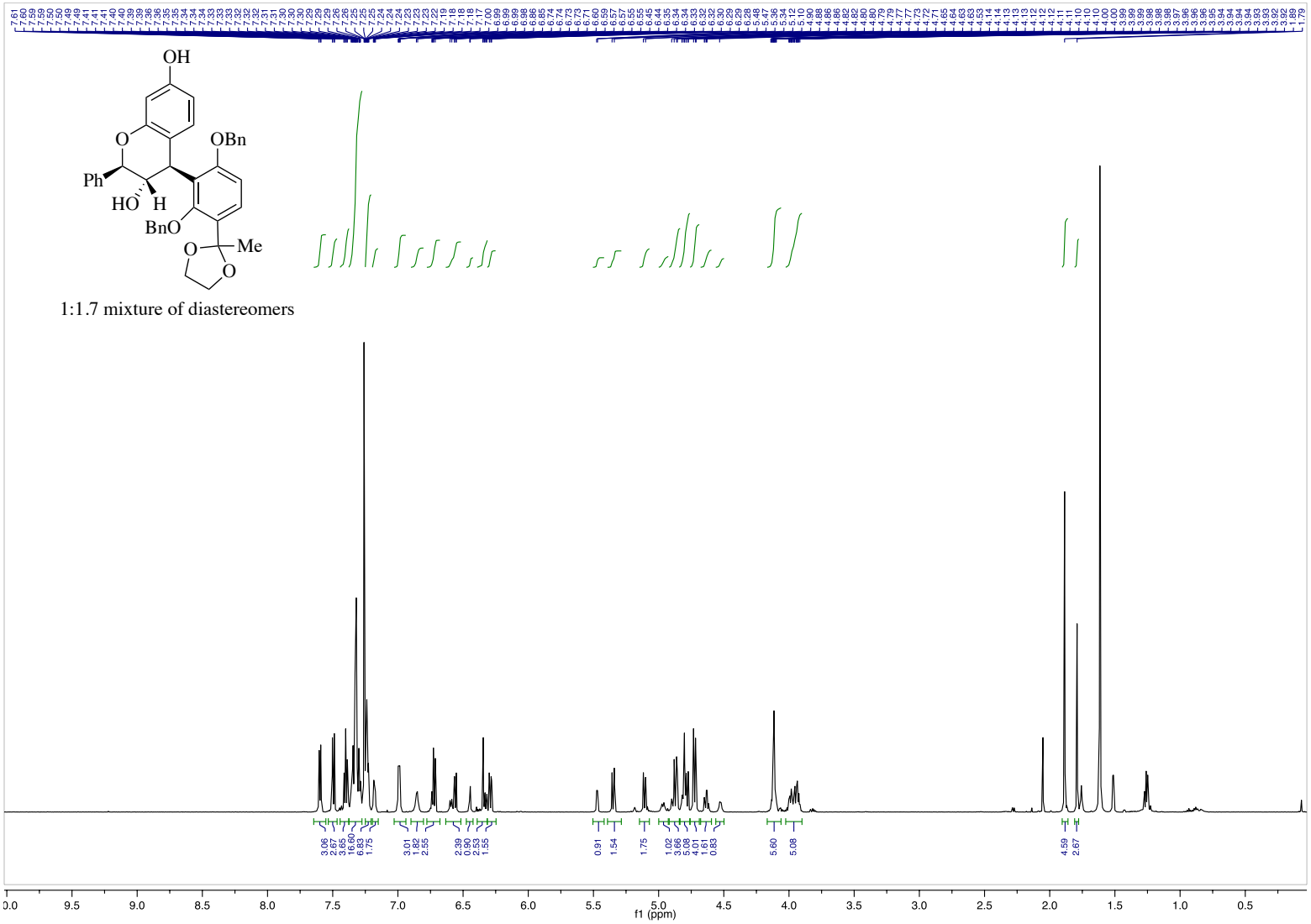

Figure A.21. ^{1}H NMR (600 MHz, $CDCl_3$), **1.20**

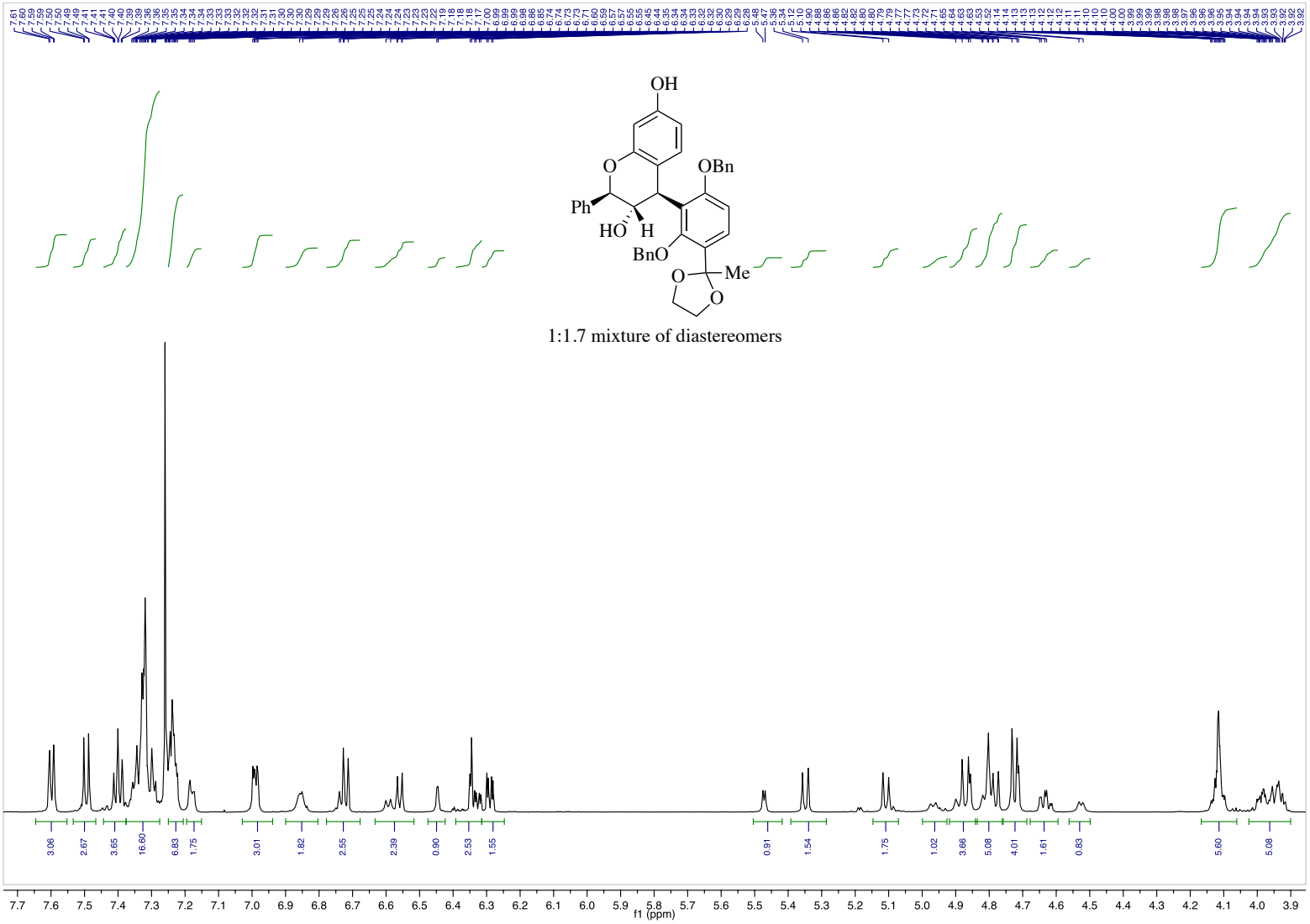

Figure A.22. ^{1}H NMR (600 MHz, $CDCl_3$), **1.20** (inset)

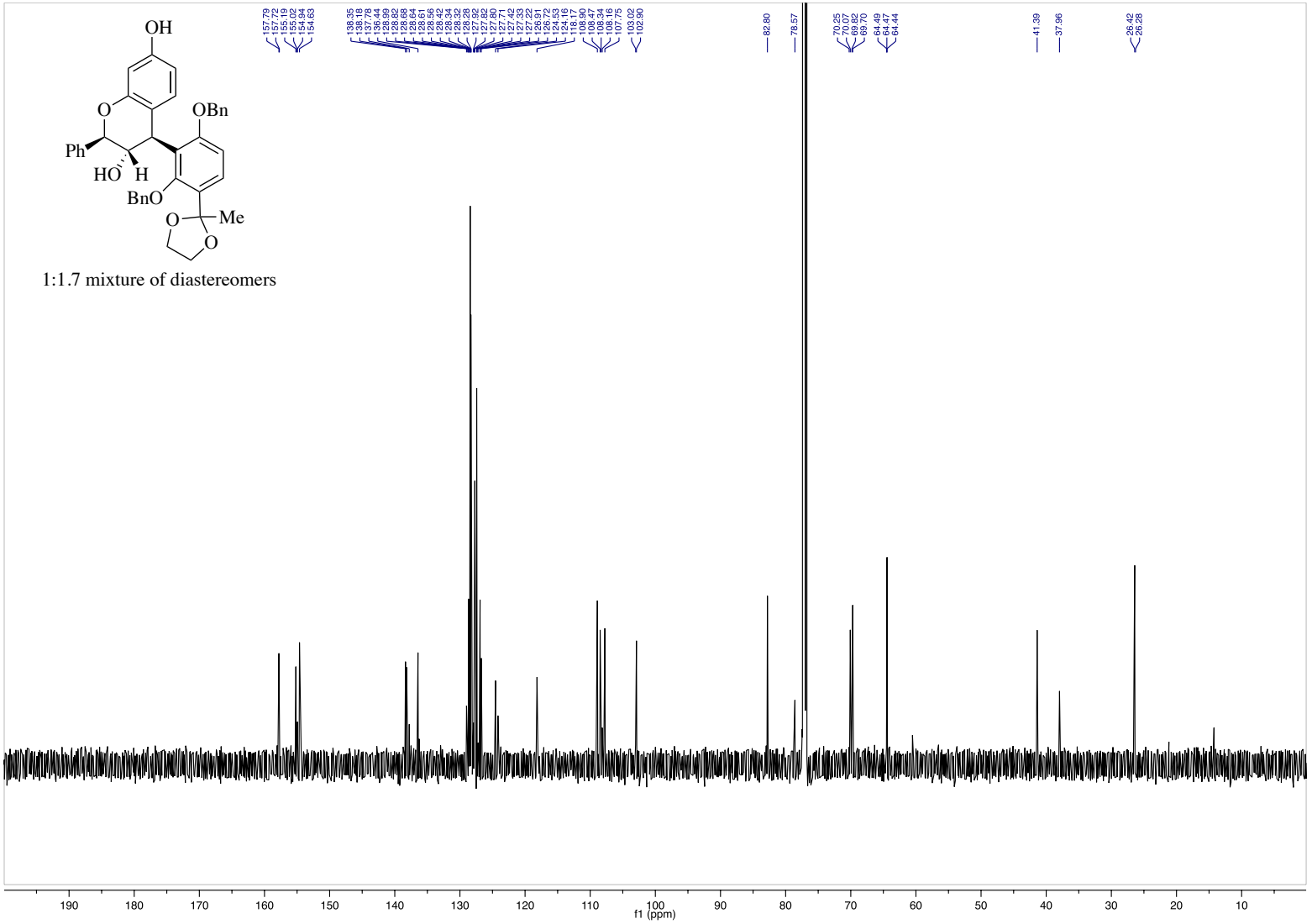

Figure A.23. ^{13}C NMR (151 MHz, $CDCl_3$), **1.20**

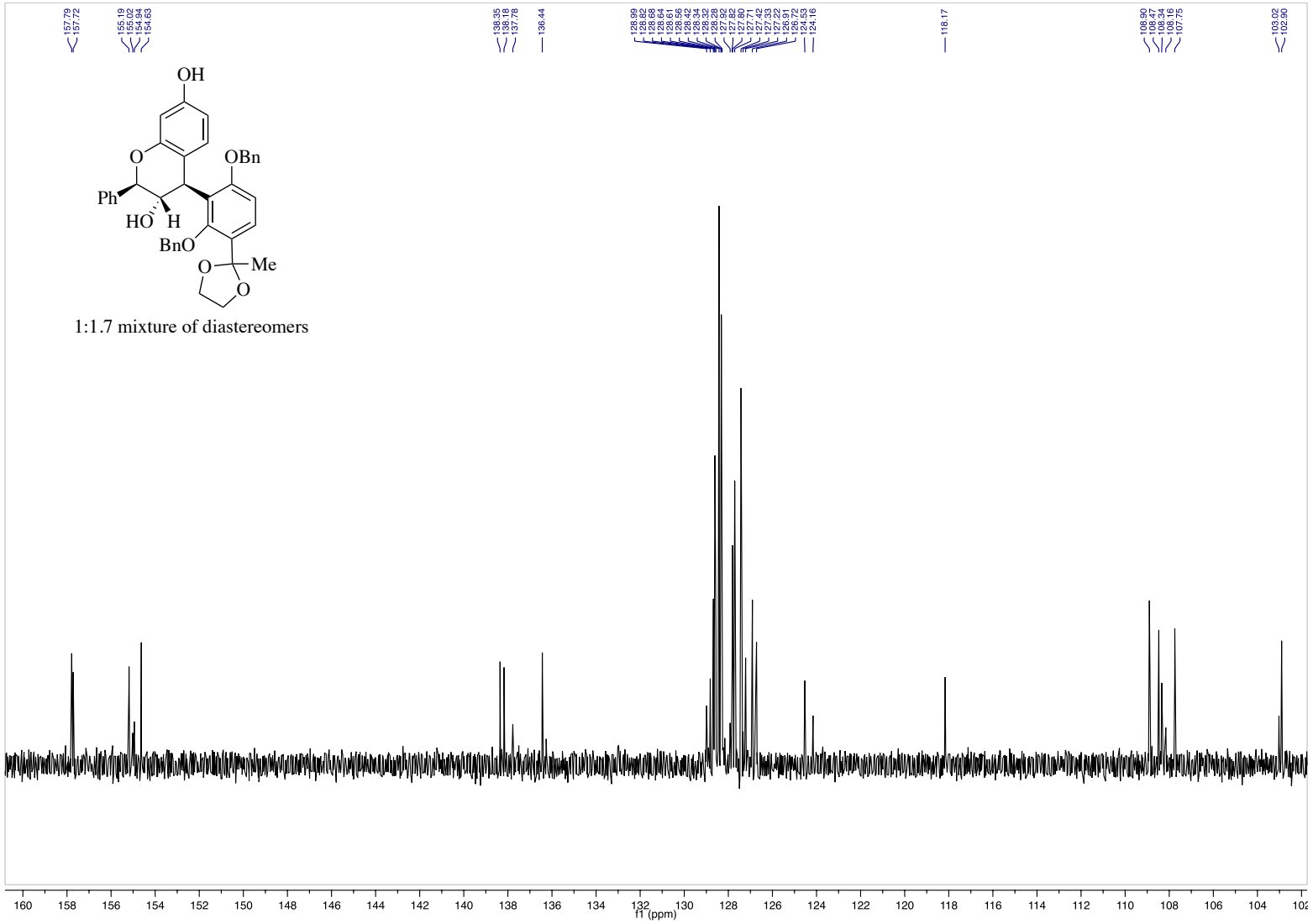

Figure A.24. ^{13}C NMR (151 MHz, $CDCl_3$), **1.20** (inset)

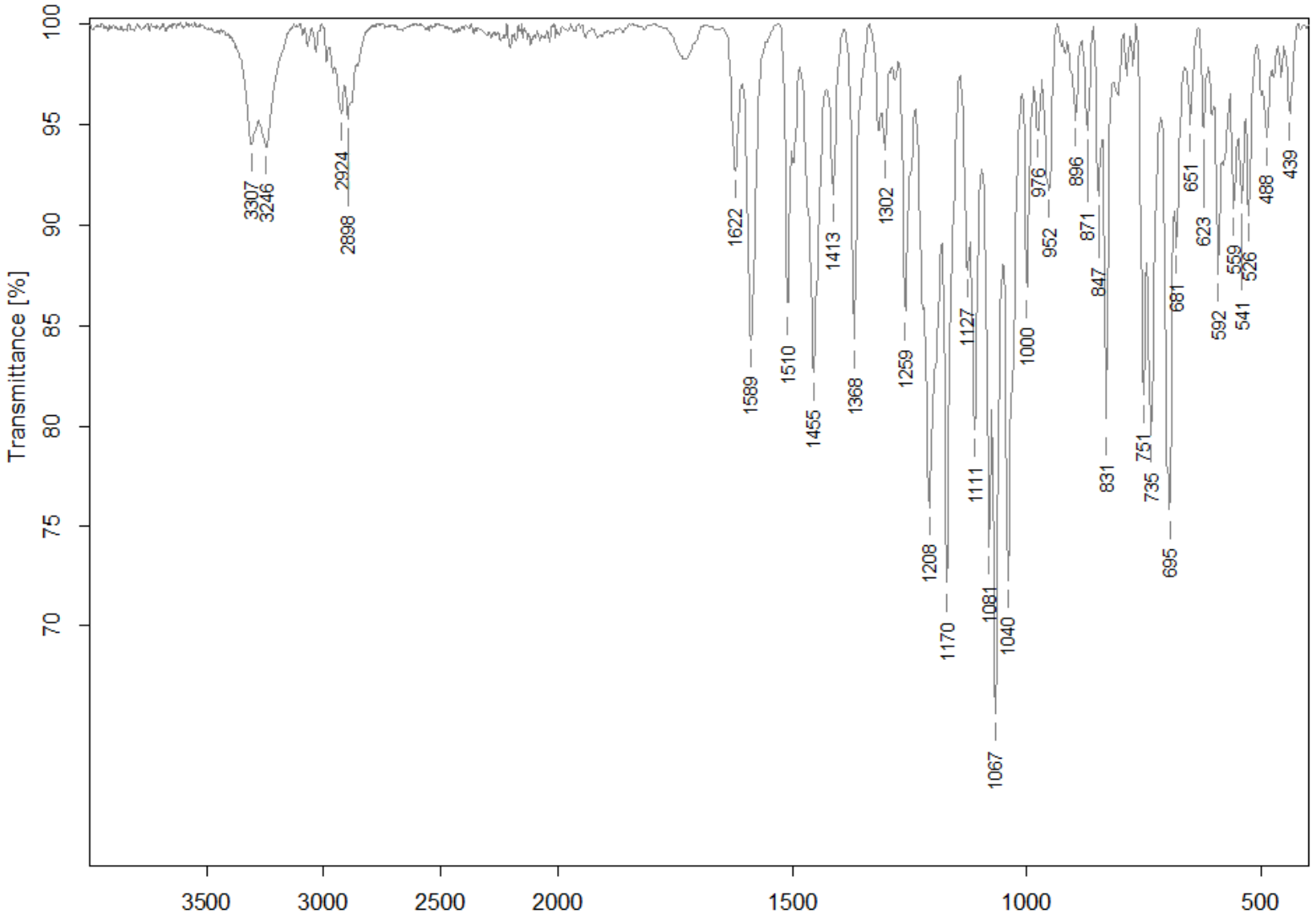

Figure A.25. IR (ATR), **1.19**

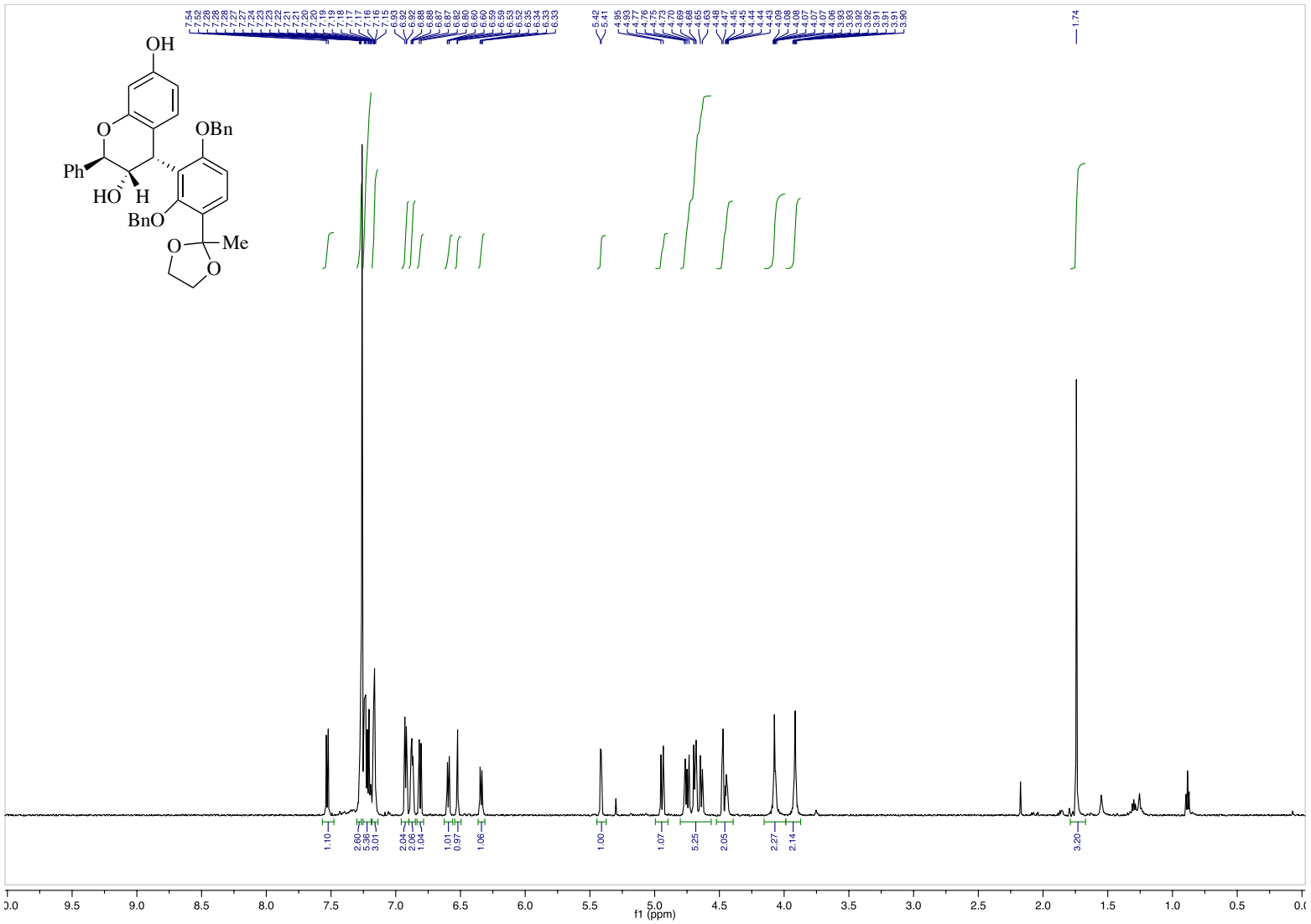

Figure A.26. ^{1}H NMR (600 MHz, $CDCl_3$), **1.23**

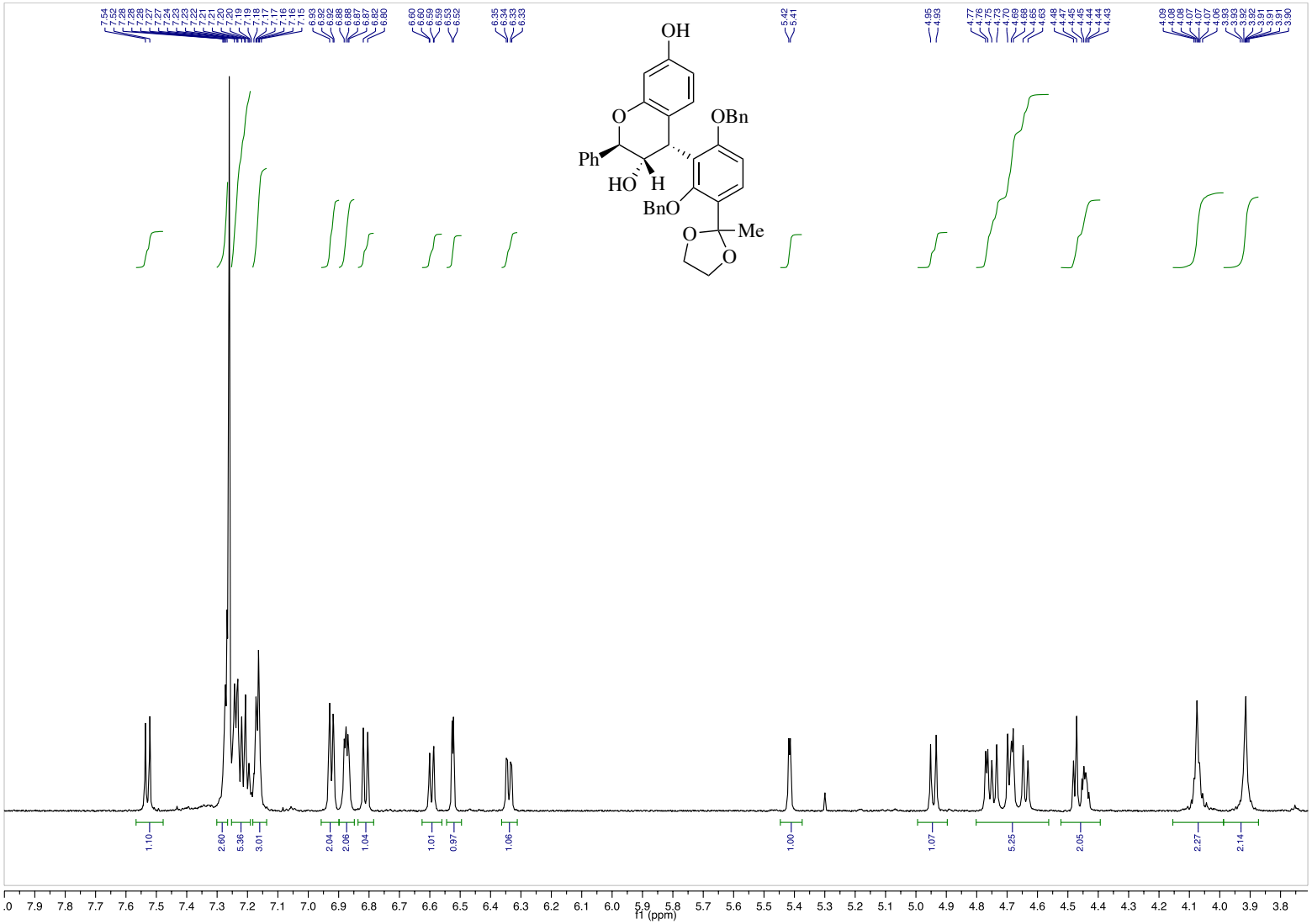

Figure A.27. ^{1}H NMR (600 MHz, $CDCl_3$), **1.23** (inset)

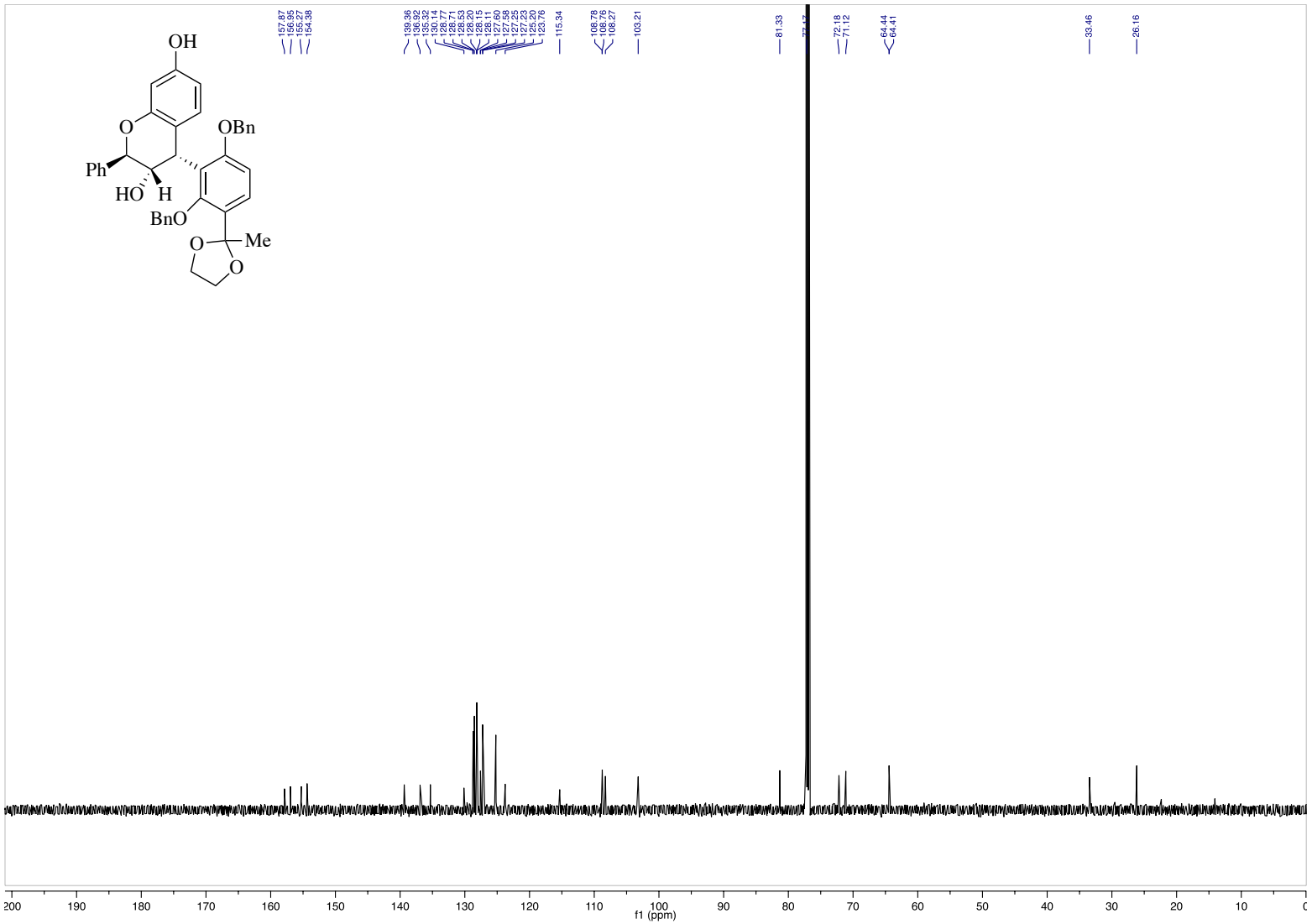

Figure A.28. ^{13}C NMR (151 MHz, $CDCl_3$), **1.23**

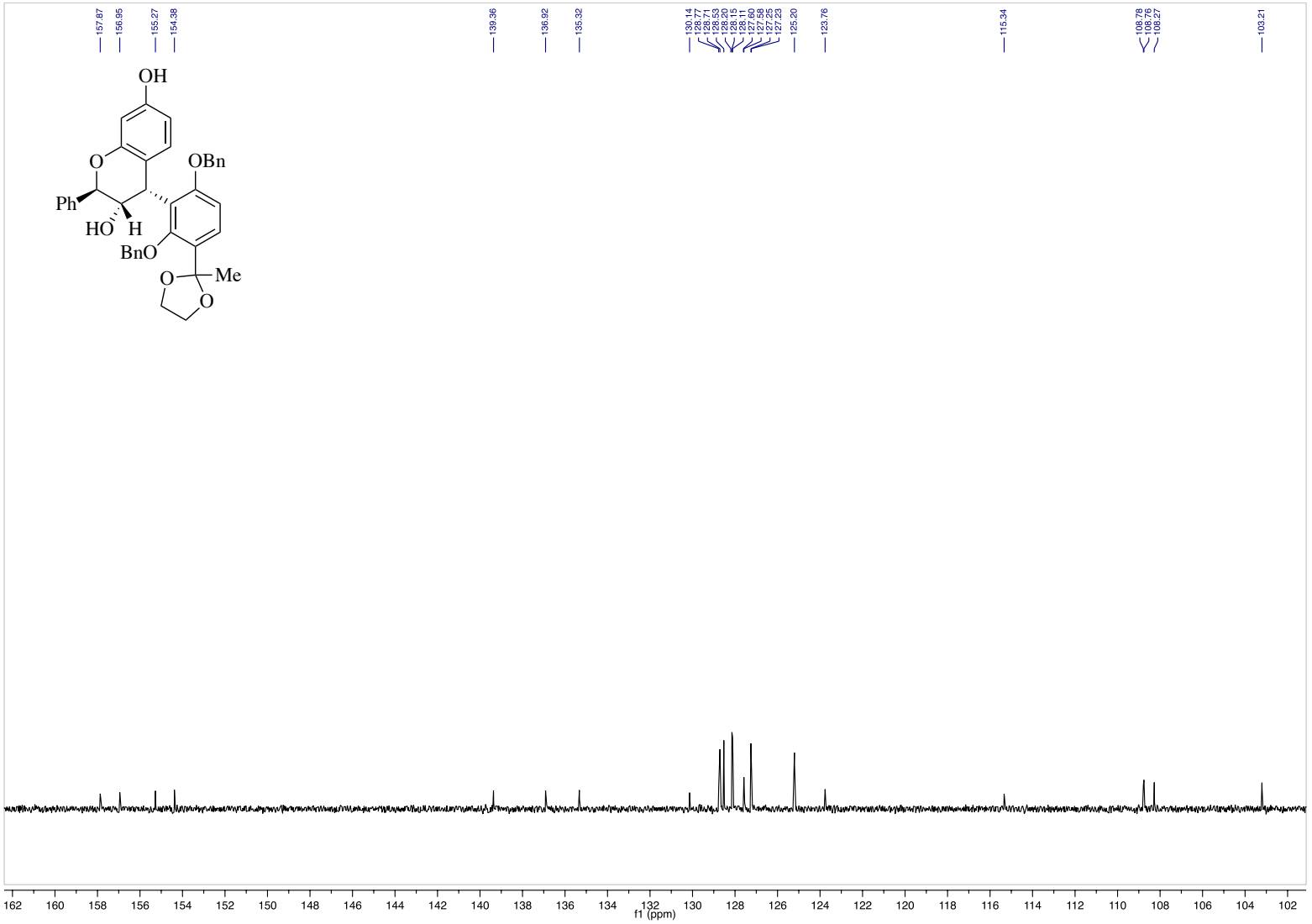

Figure A.29. ^{13}C NMR (151 MHz, $CDCl_3$), **1.23** (inset)

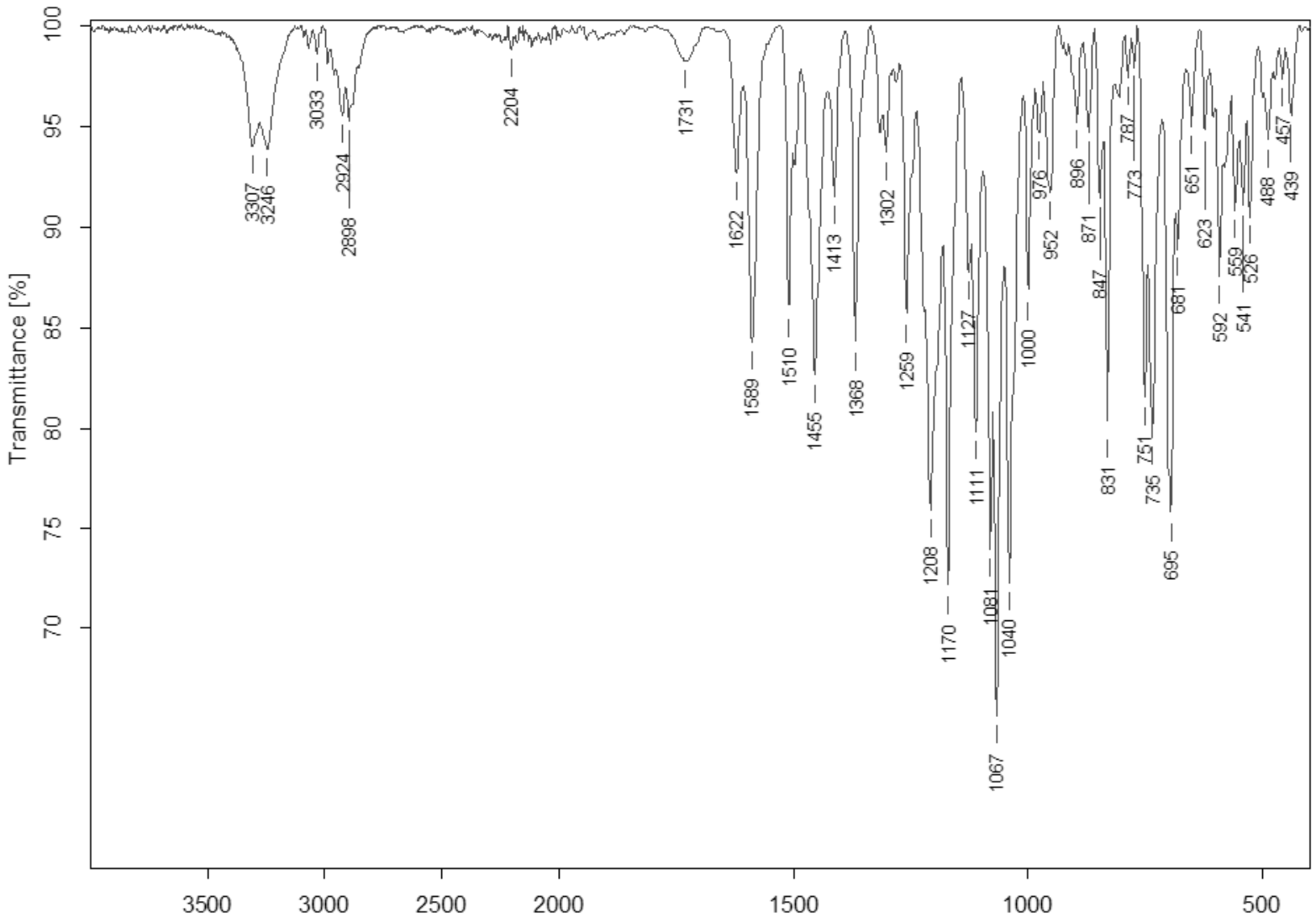

Figure A.30. IR (ATR), **1.23**

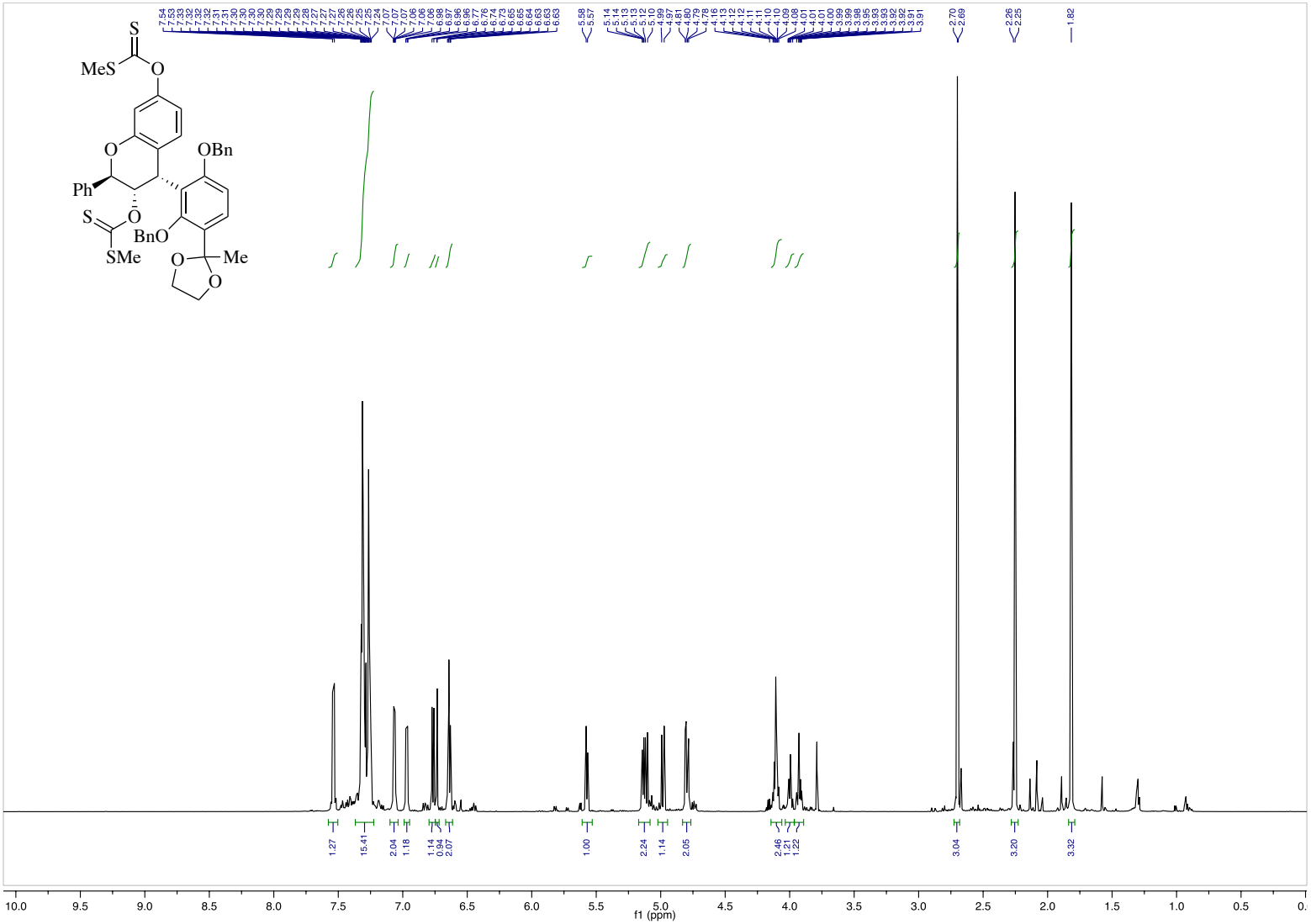

Figure A.31. ^{1}H NMR (600 MHz, $CDCl_3$), **1.24**

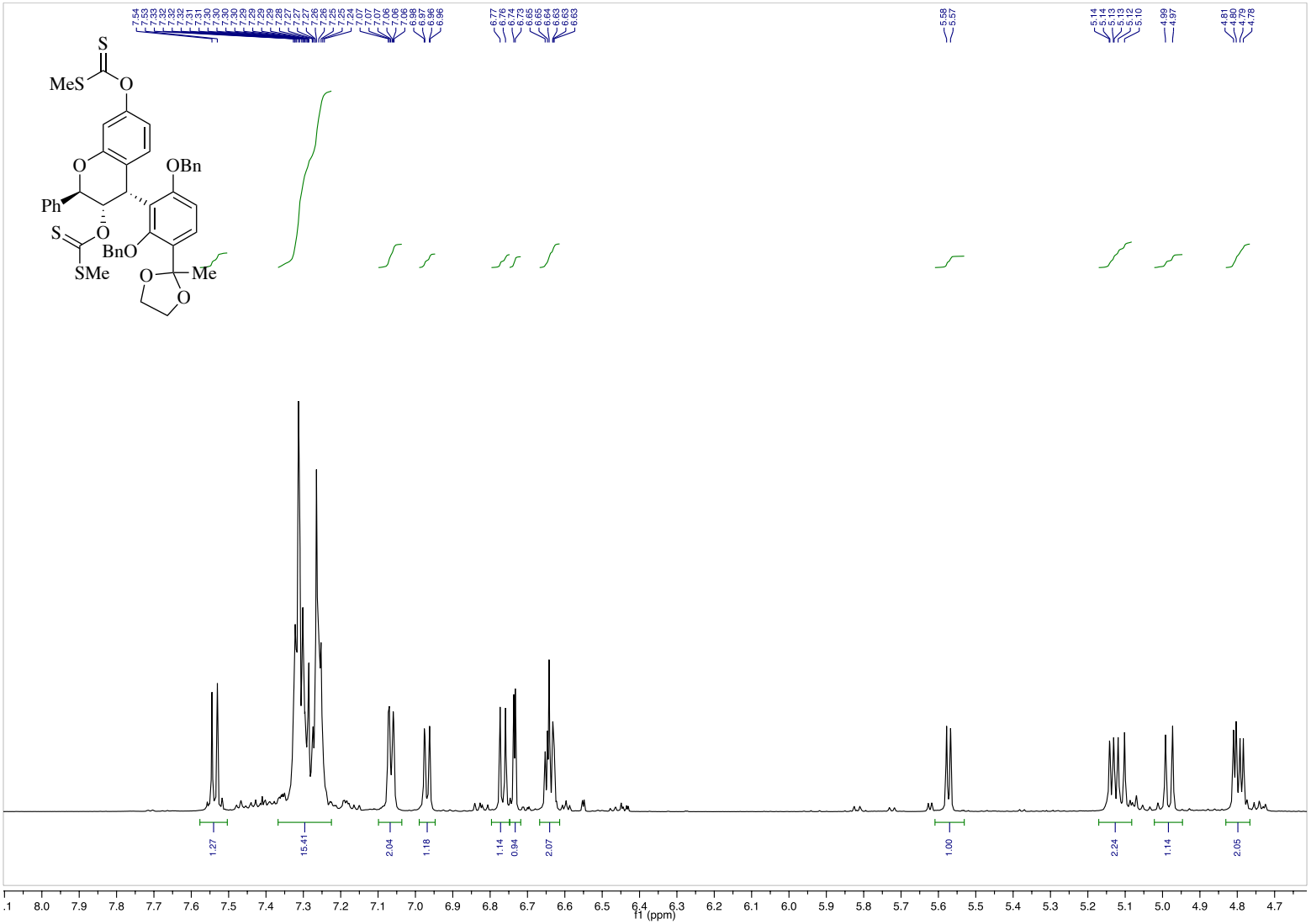

Figure A.32. ^{1}H NMR (600 MHz, $CDCl_3$), **1.24** (inset)

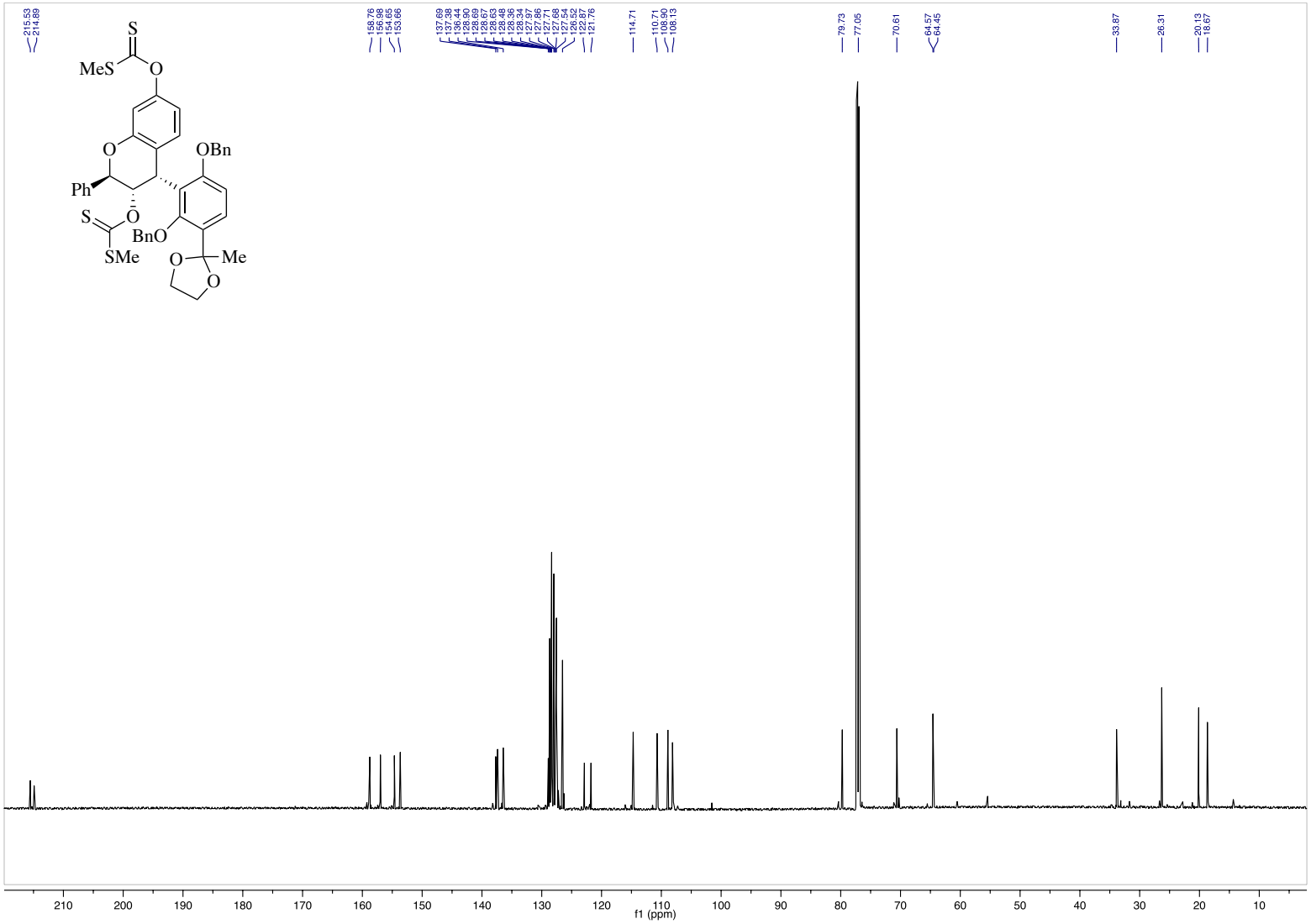

Figure A.33. ^{13}C NMR (151 MHz, $CDCl_3$), **1.24**

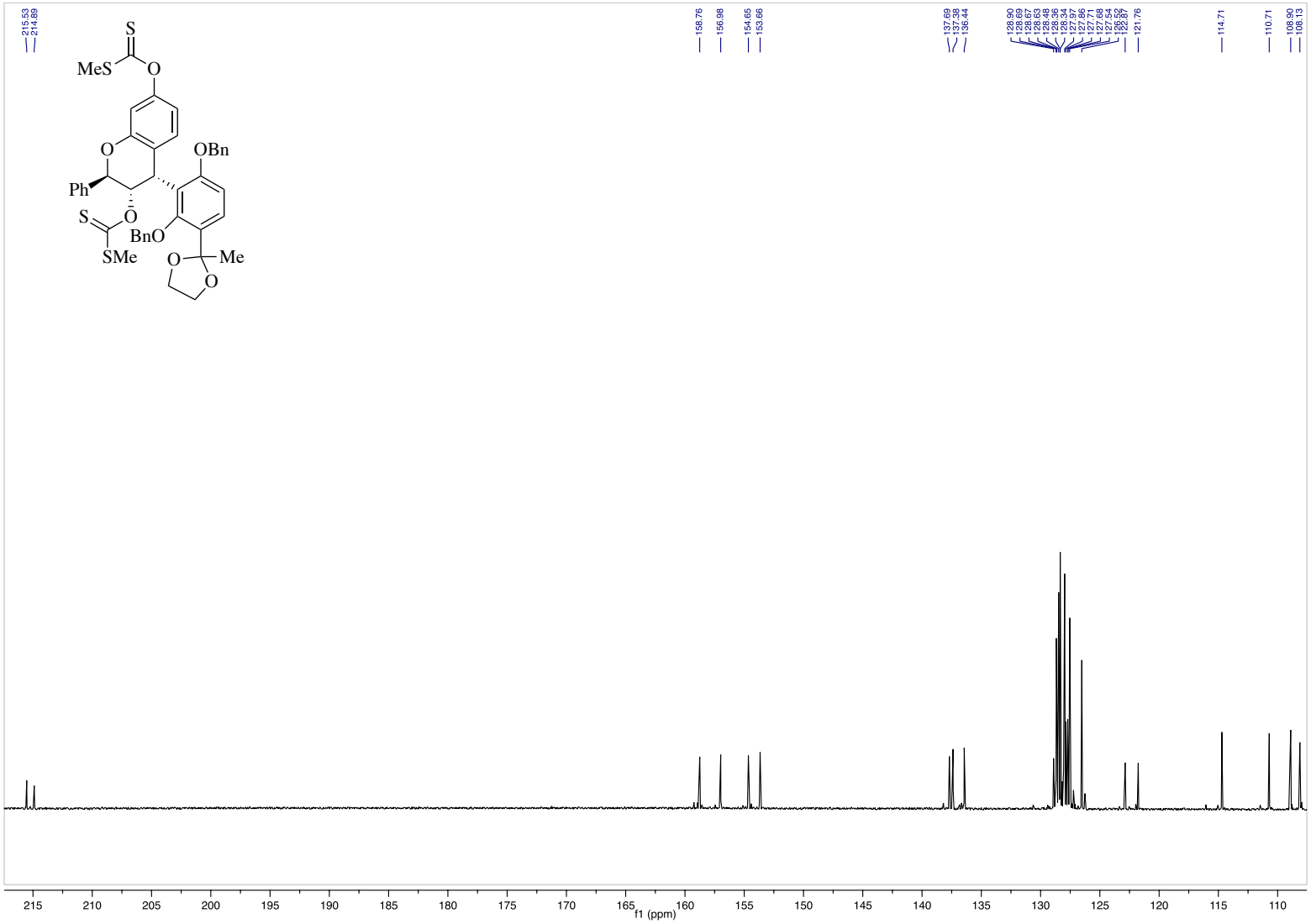

Figure A.34. ^{13}C NMR (151 MHz, $CDCl_3$), **1.24** (inset)

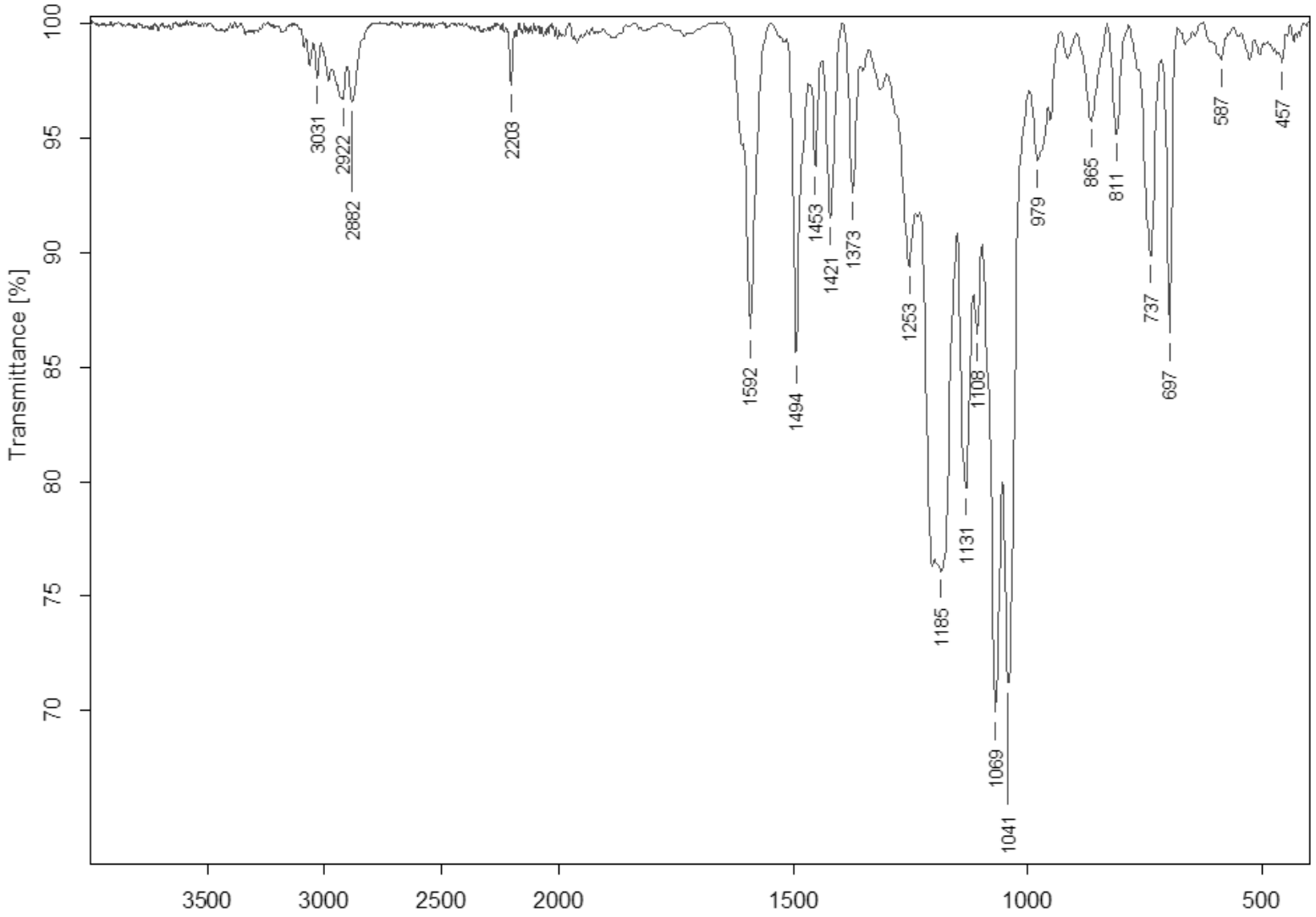

Figure A.35. IR (ATR), **1.24**

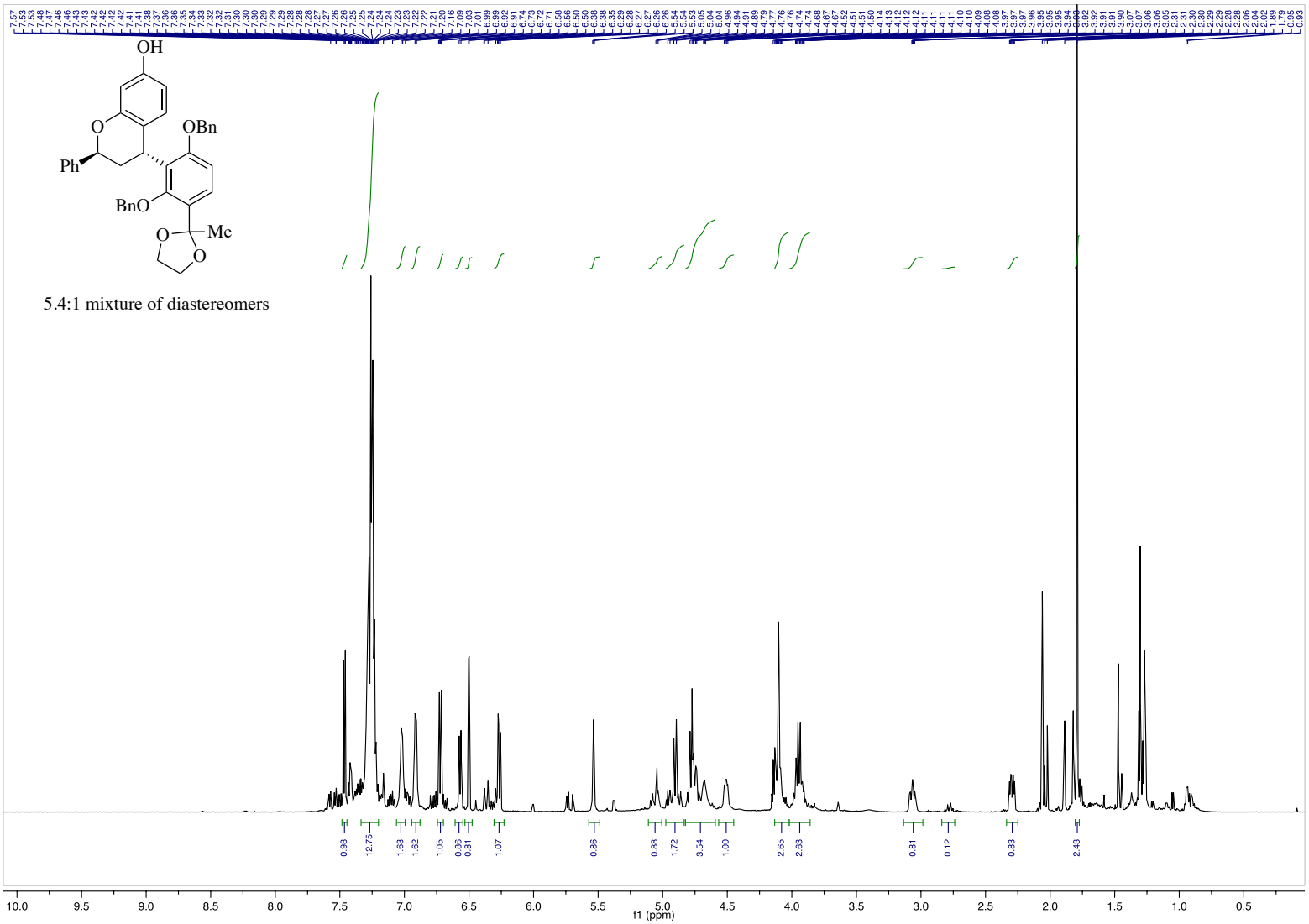

Figure A.36. ^{1}H NMR (600 MHz, $CDCl_3$), **1.17**

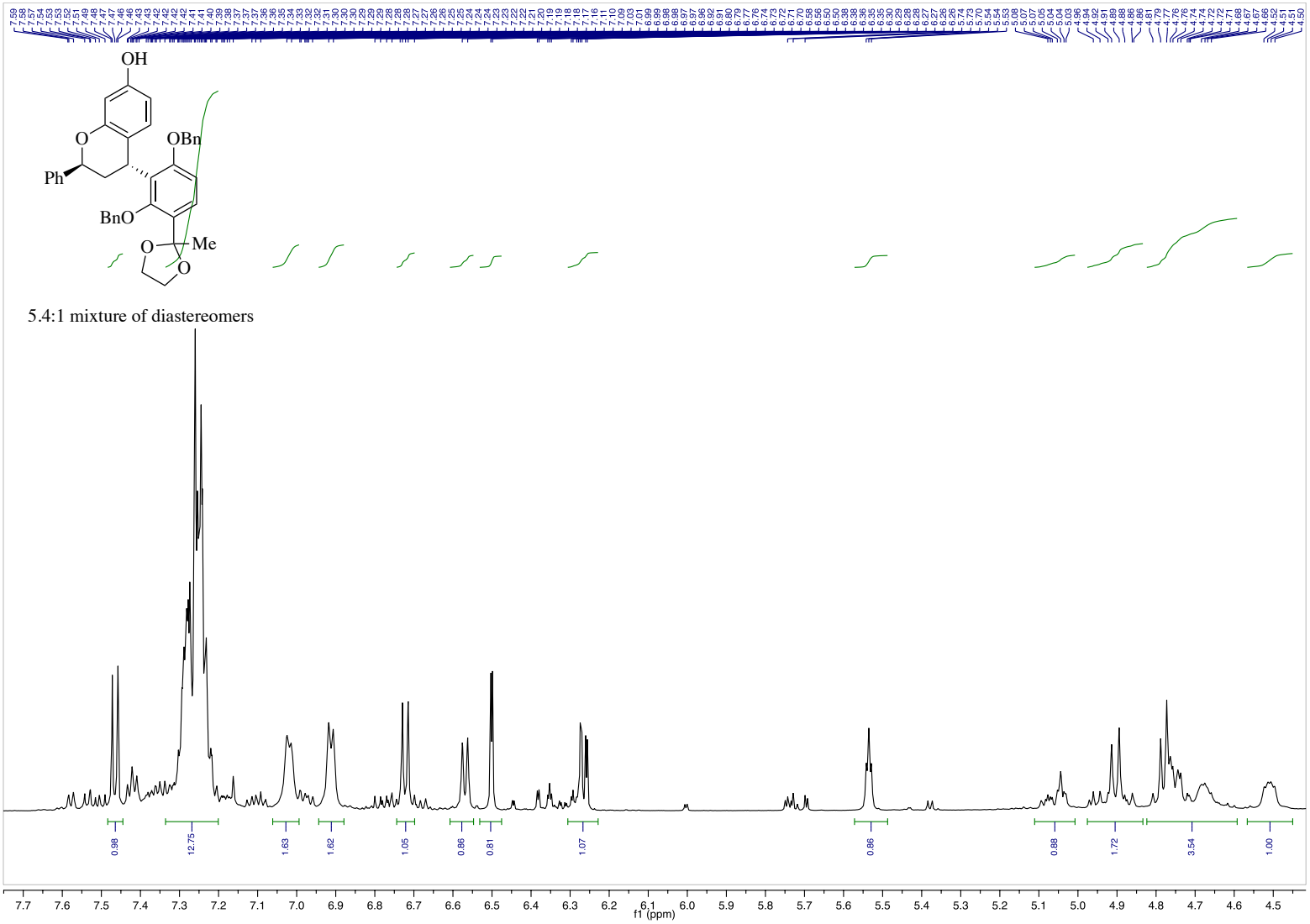

Figure A.37. ^{1}H NMR (600 MHz, $CDCl_3$), **1.17** (inset)

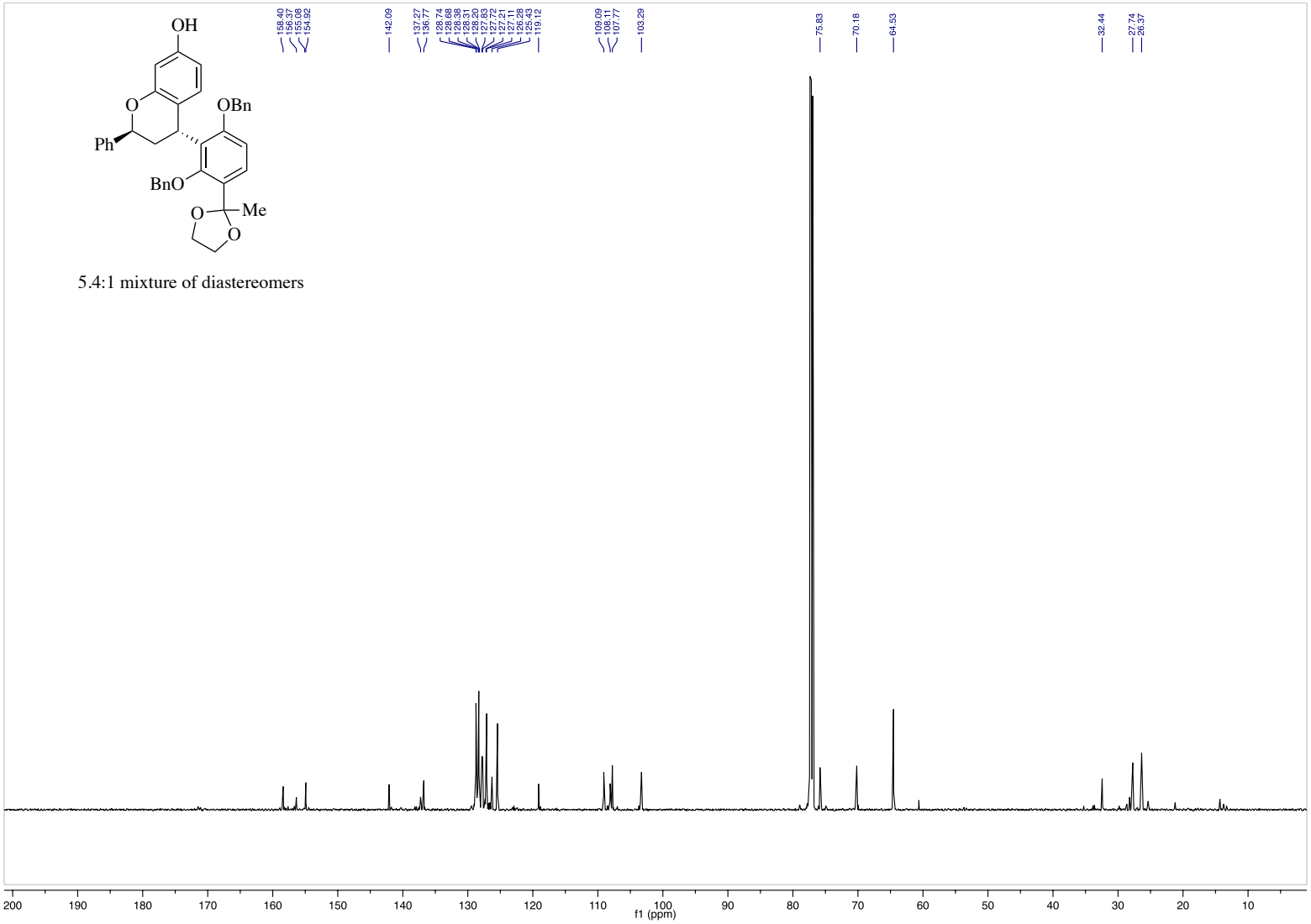

5.4:1 mixture of diastereomers

Figure A.38. ^{13}C NMR (151 MHz, $CDCl_3$), **1.17**

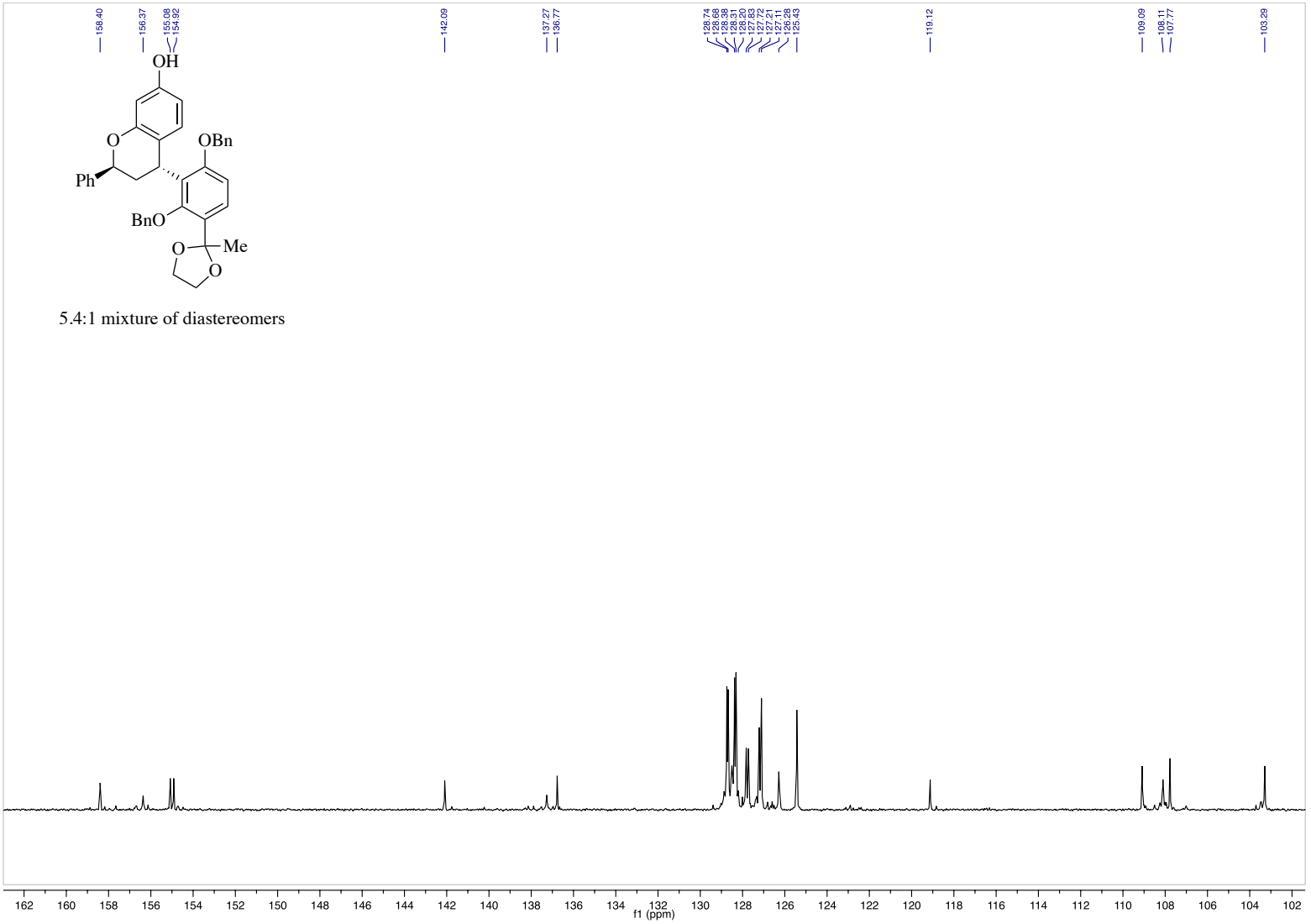

Figure A.39. ^{13}C NMR (151 MHz, $CDCl_3$), **1.17** (inset)

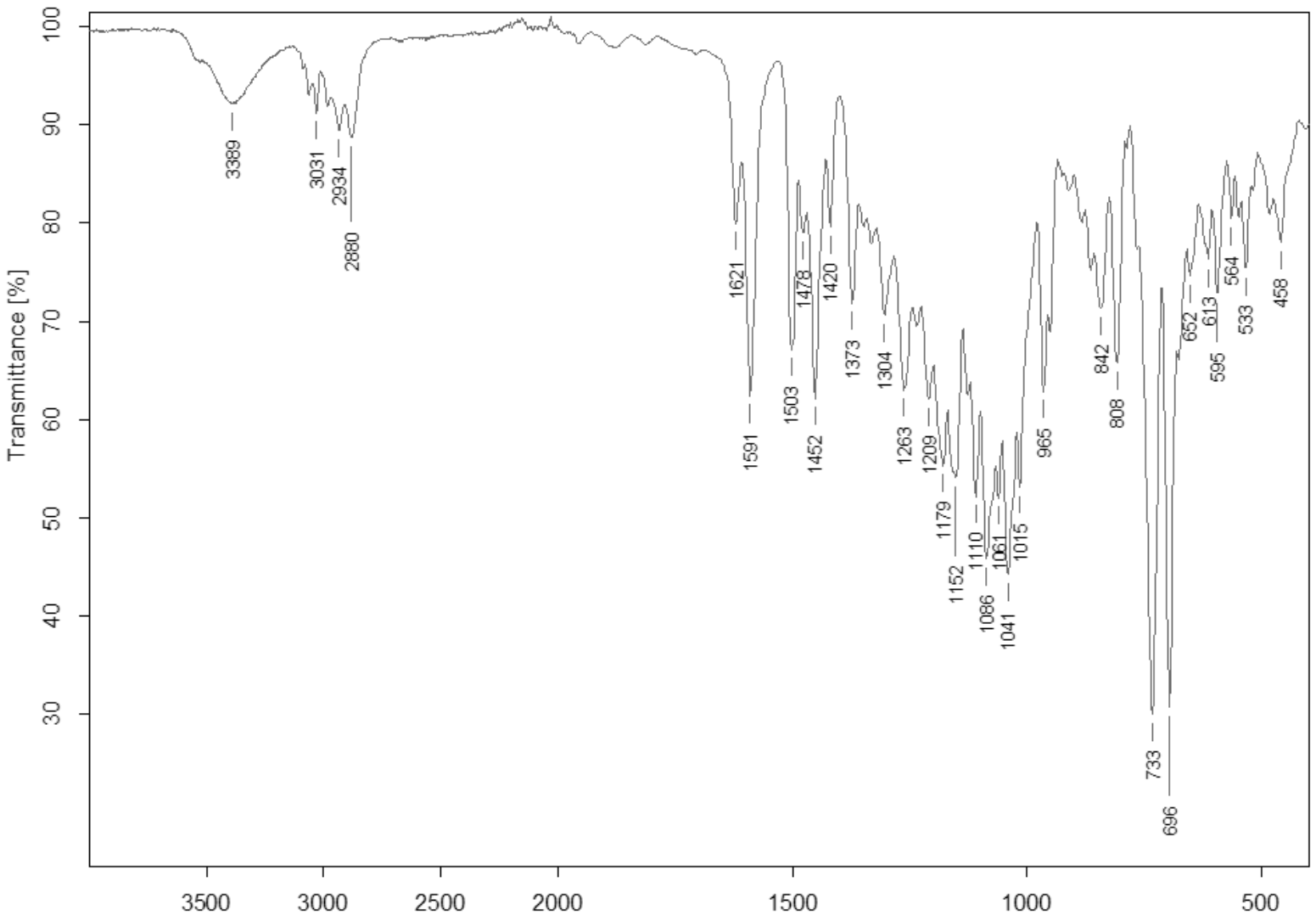

Figure A.40. IR (ATR), **1.17**

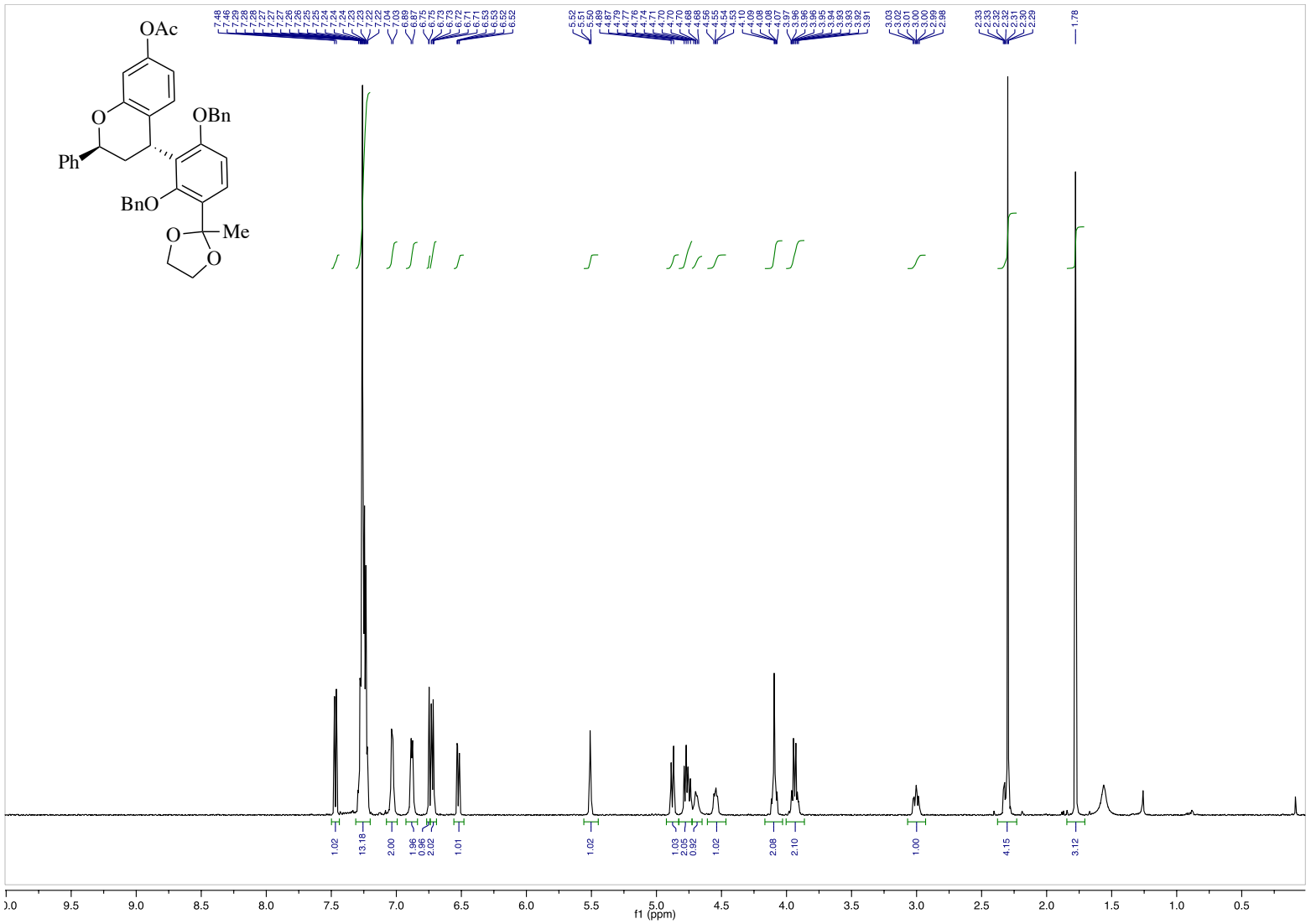

Figure A.41. ^{1}H NMR (600 MHz, $CDCl_3$), **1.17a**

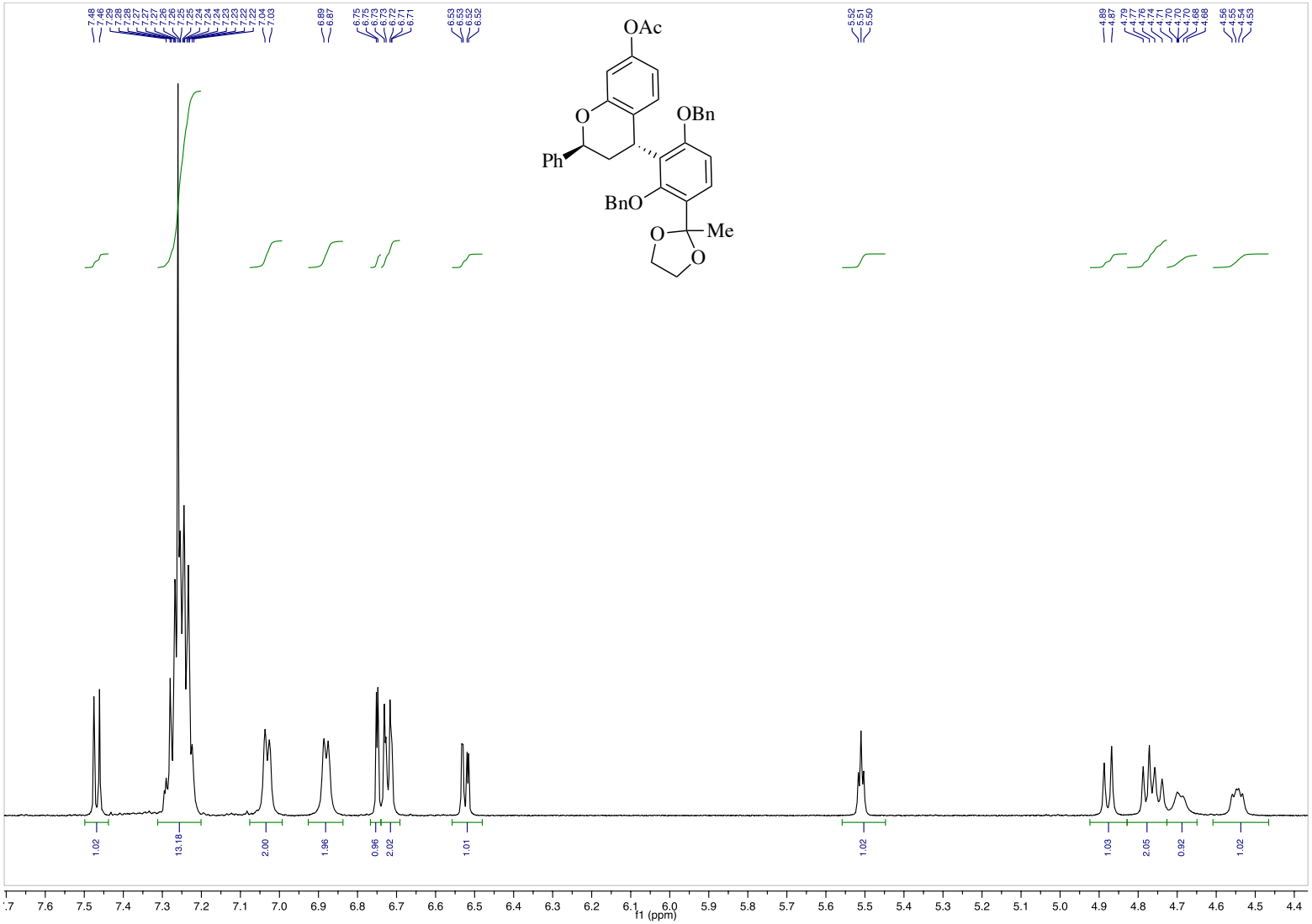

Figure A.42. ^{1}H NMR (600 MHz, $CDCl_3$), **1.17a** (inset)

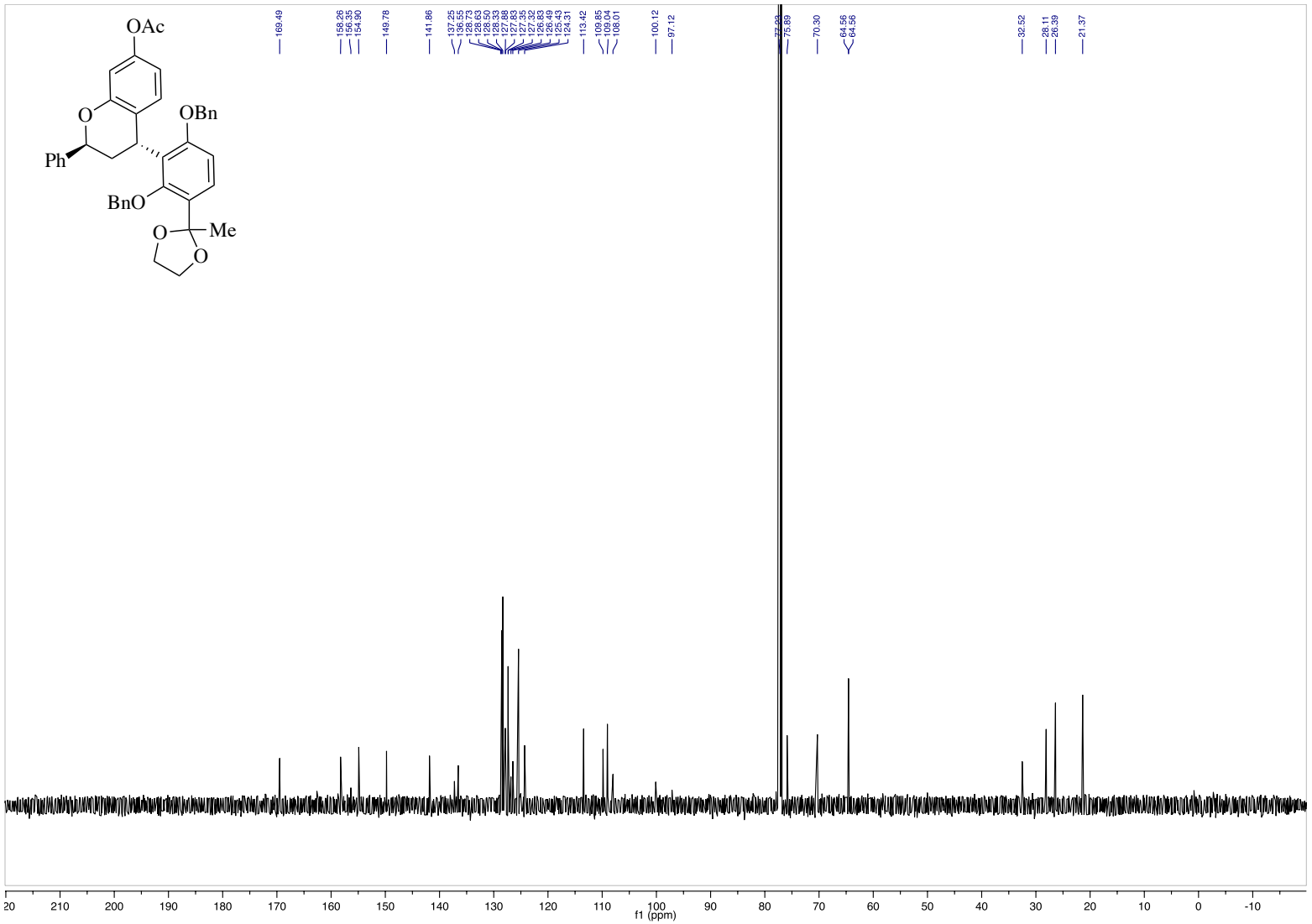

Figure A.43. ^{13}C NMR (151 MHz, $CDCl_3$), **1.17a**

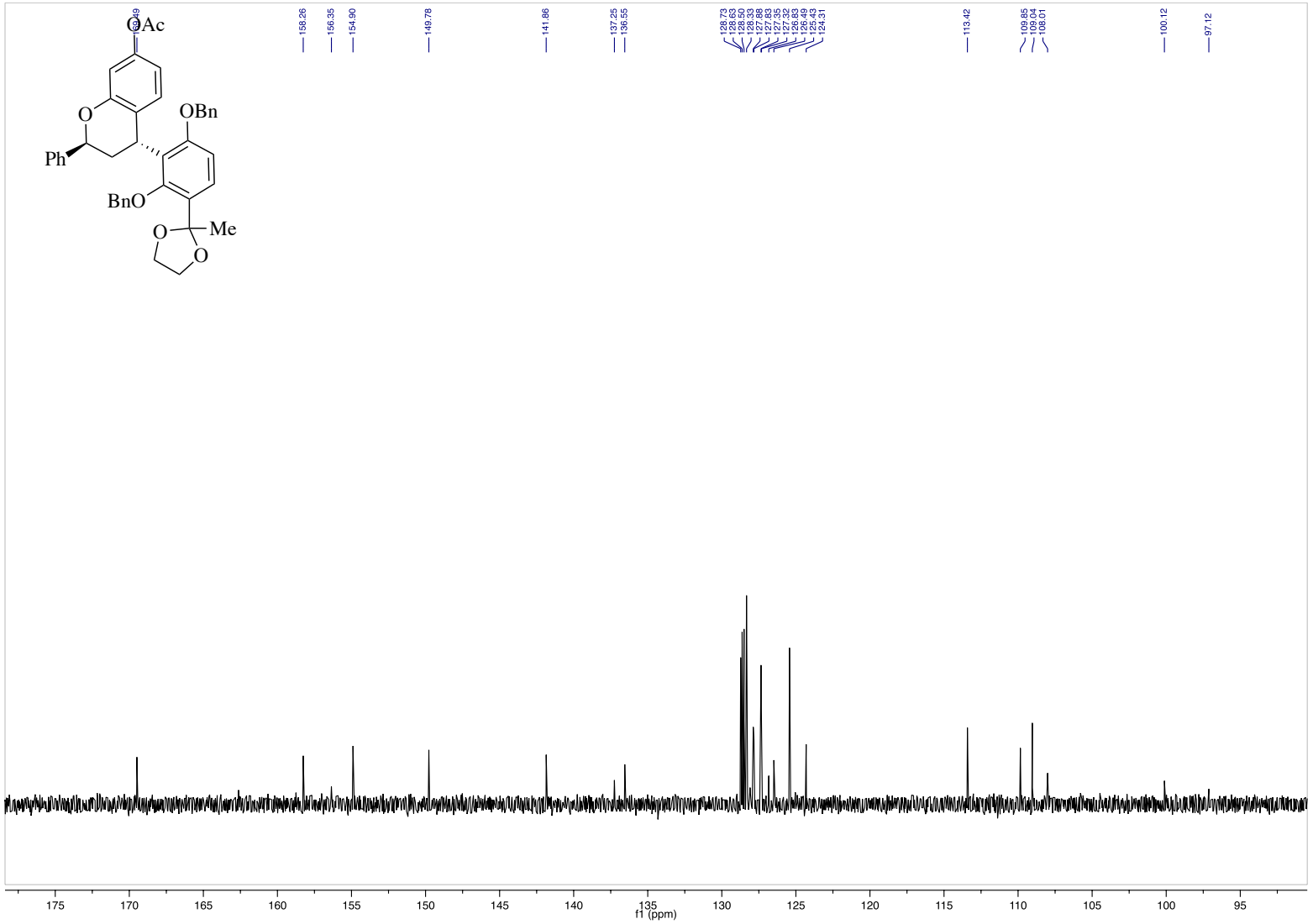

Figure A.44. ^{13}C NMR (151 MHz, $CDCl_3$), **1.17a** (inset)

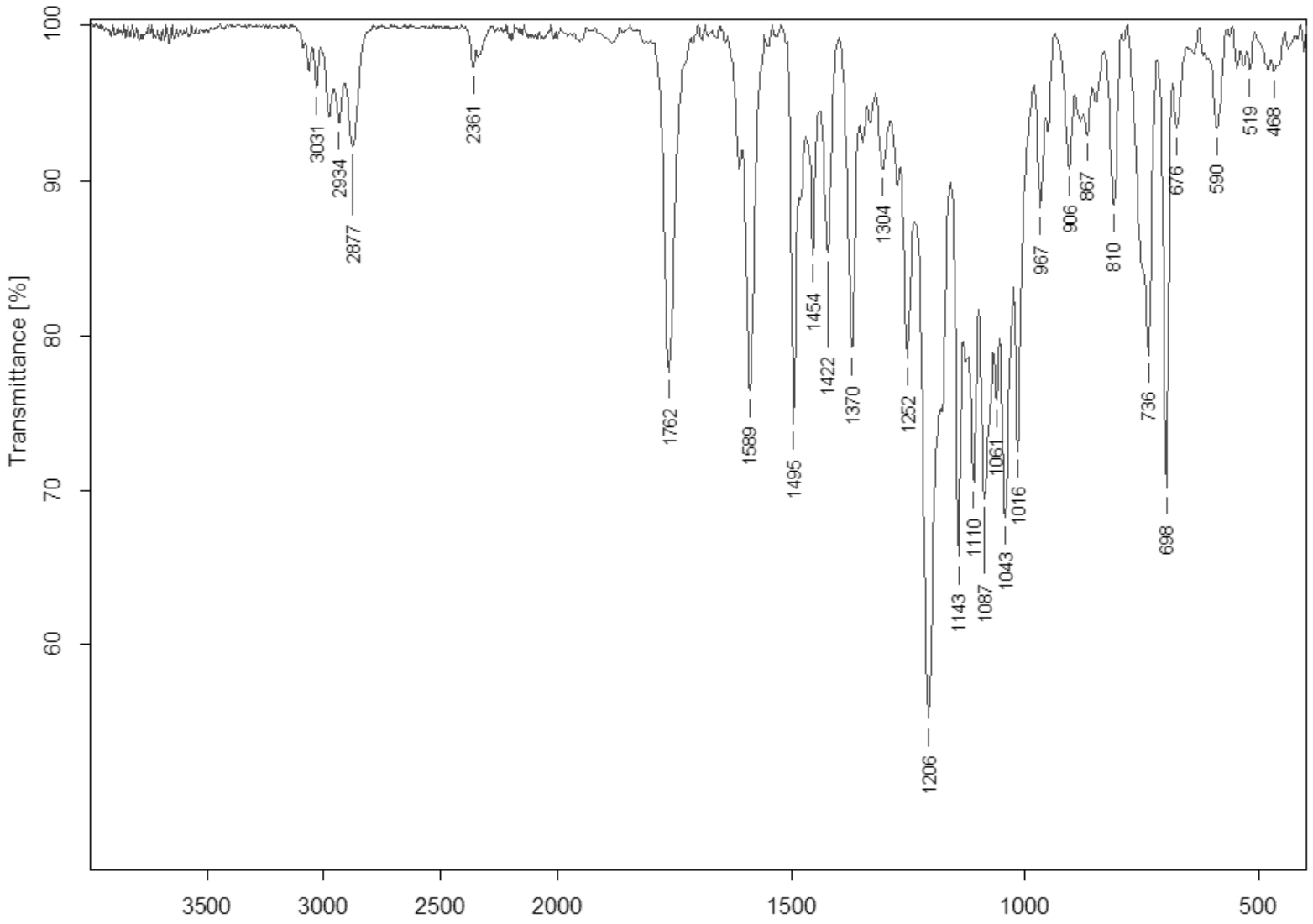

Figure A.45. IR (ATR), **1.17a**

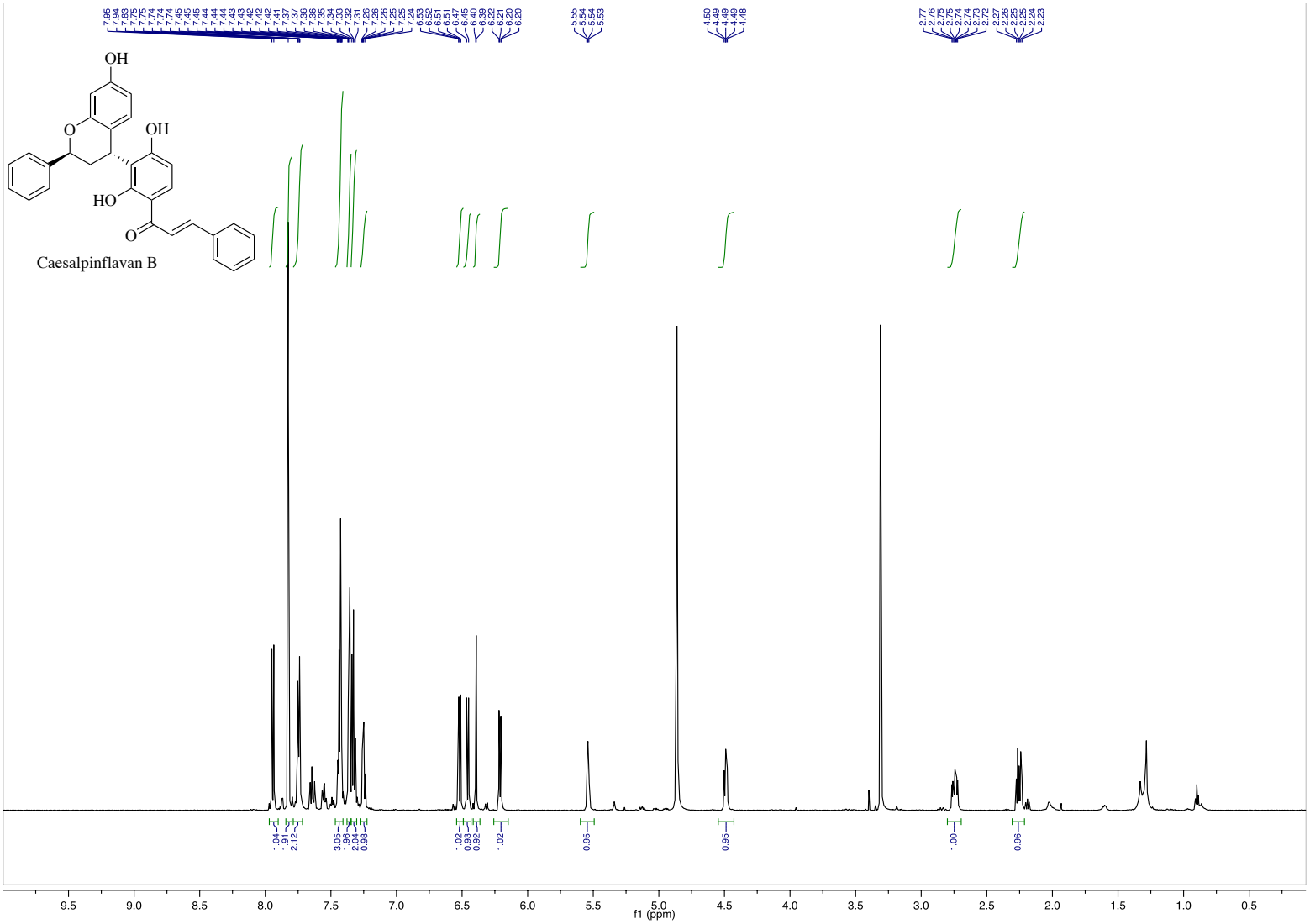

Figure A.46. ^{1}H NMR (600 MHz, $CDCl_3$), **1.03**

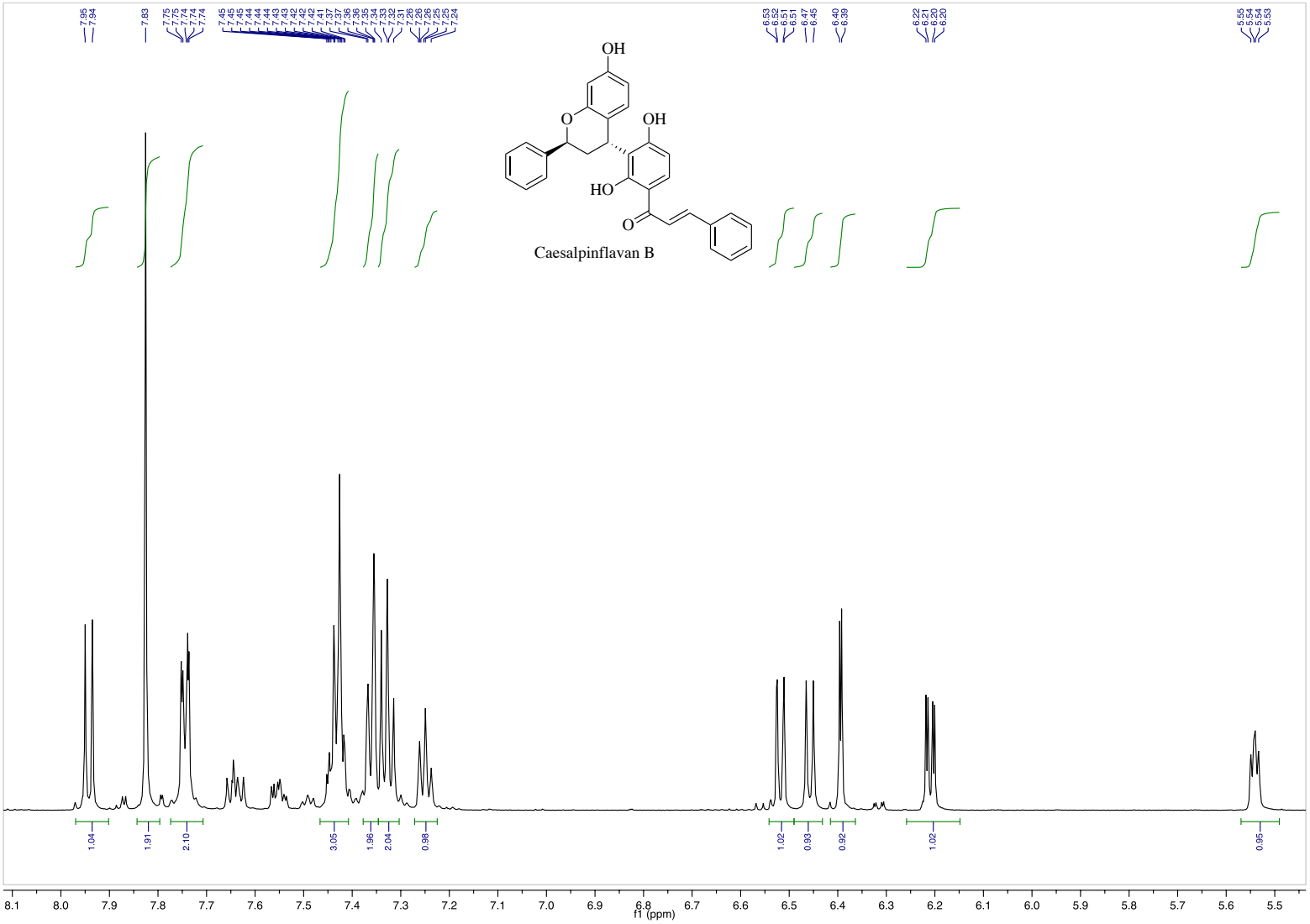

Figure A.47. ^{1}H NMR (600 MHz, $CDCl_3$), **1.03** (inset)

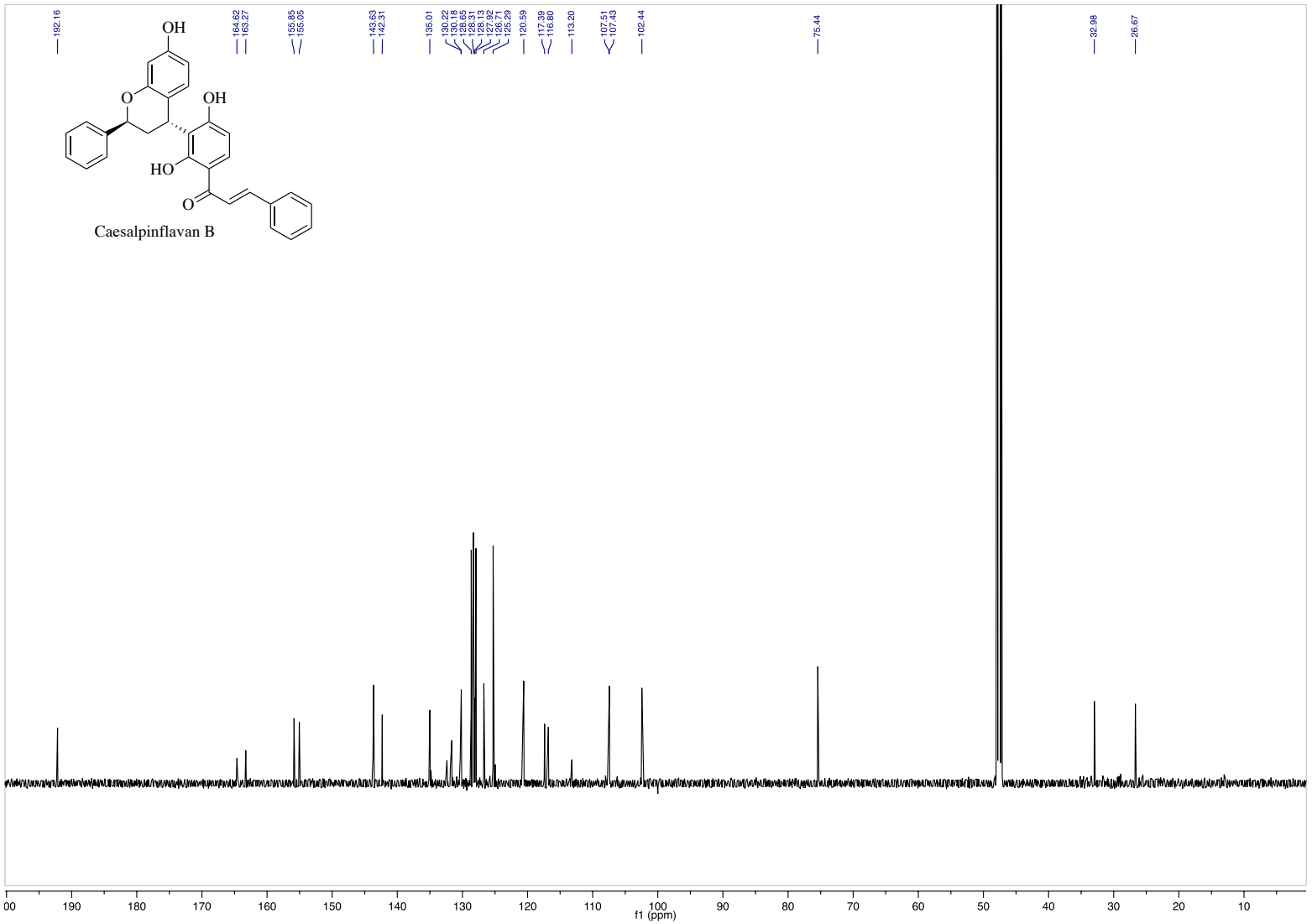

Figure A.48. ^{13}C NMR (151 MHz, $CDCl_3$), **1.03**

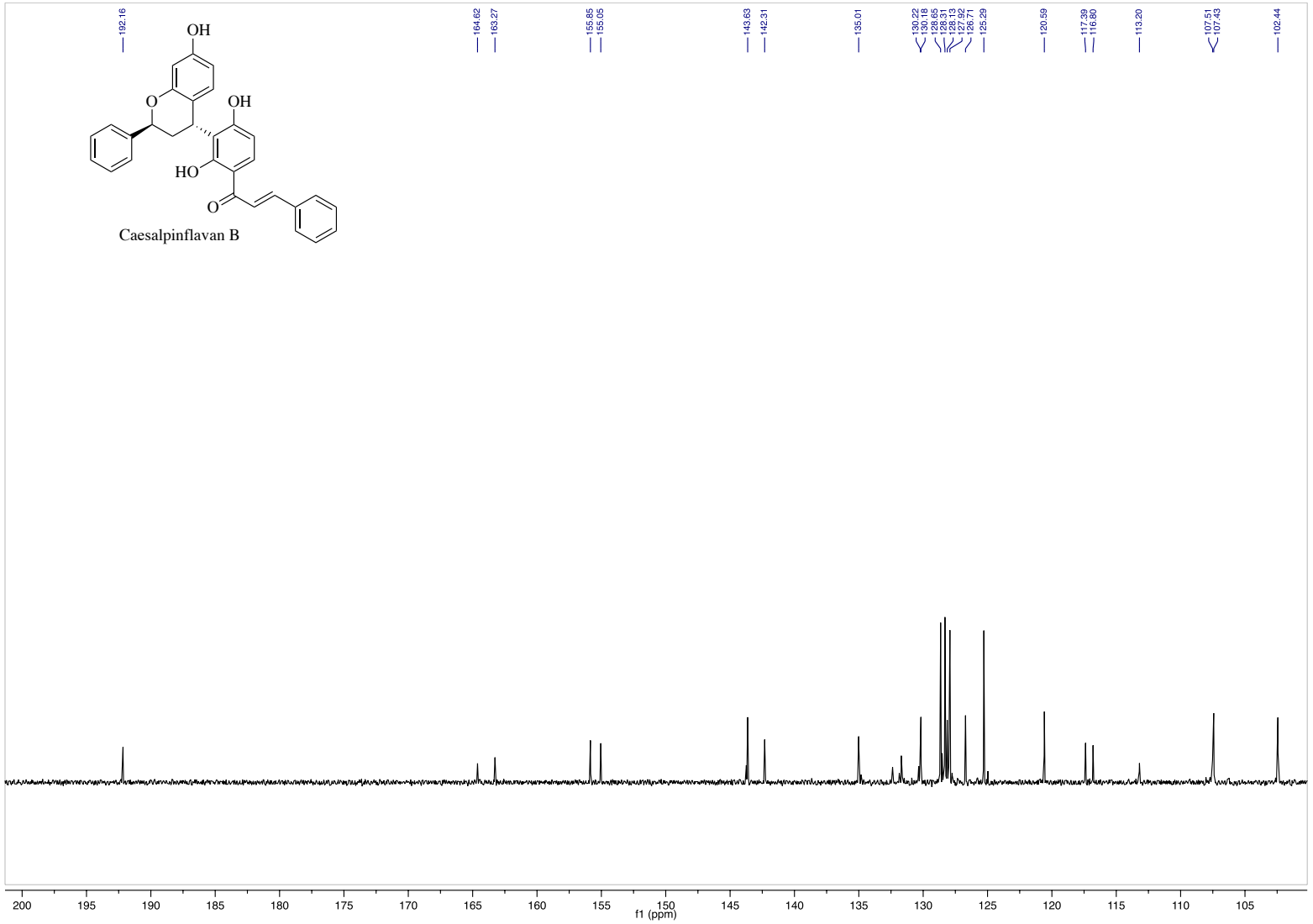

Figure A.49. ^{13}C NMR (151 MHz, $CDCl_3$), **1.03** (inset)

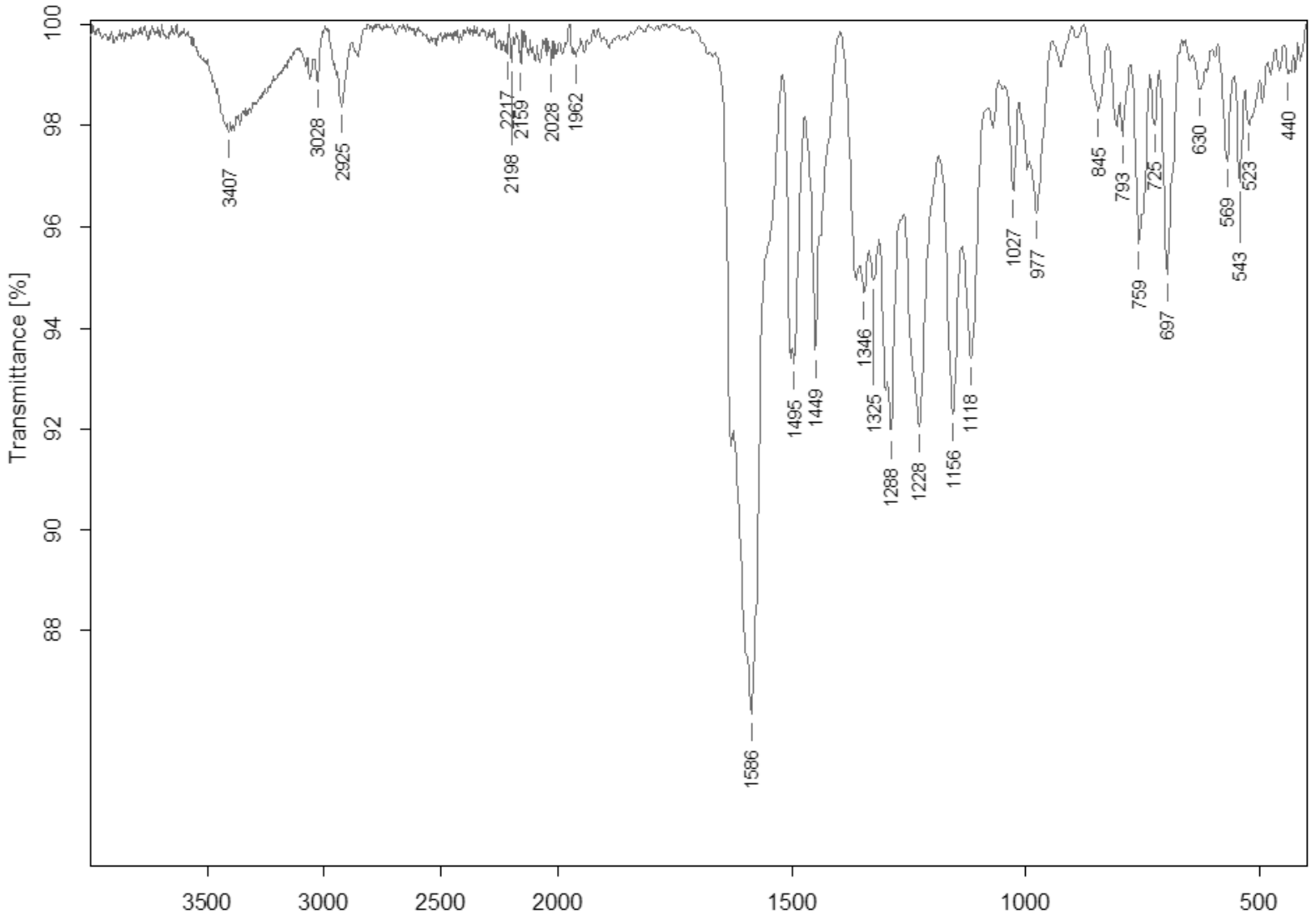

Figure A.50. IR (ATR), **1.03**

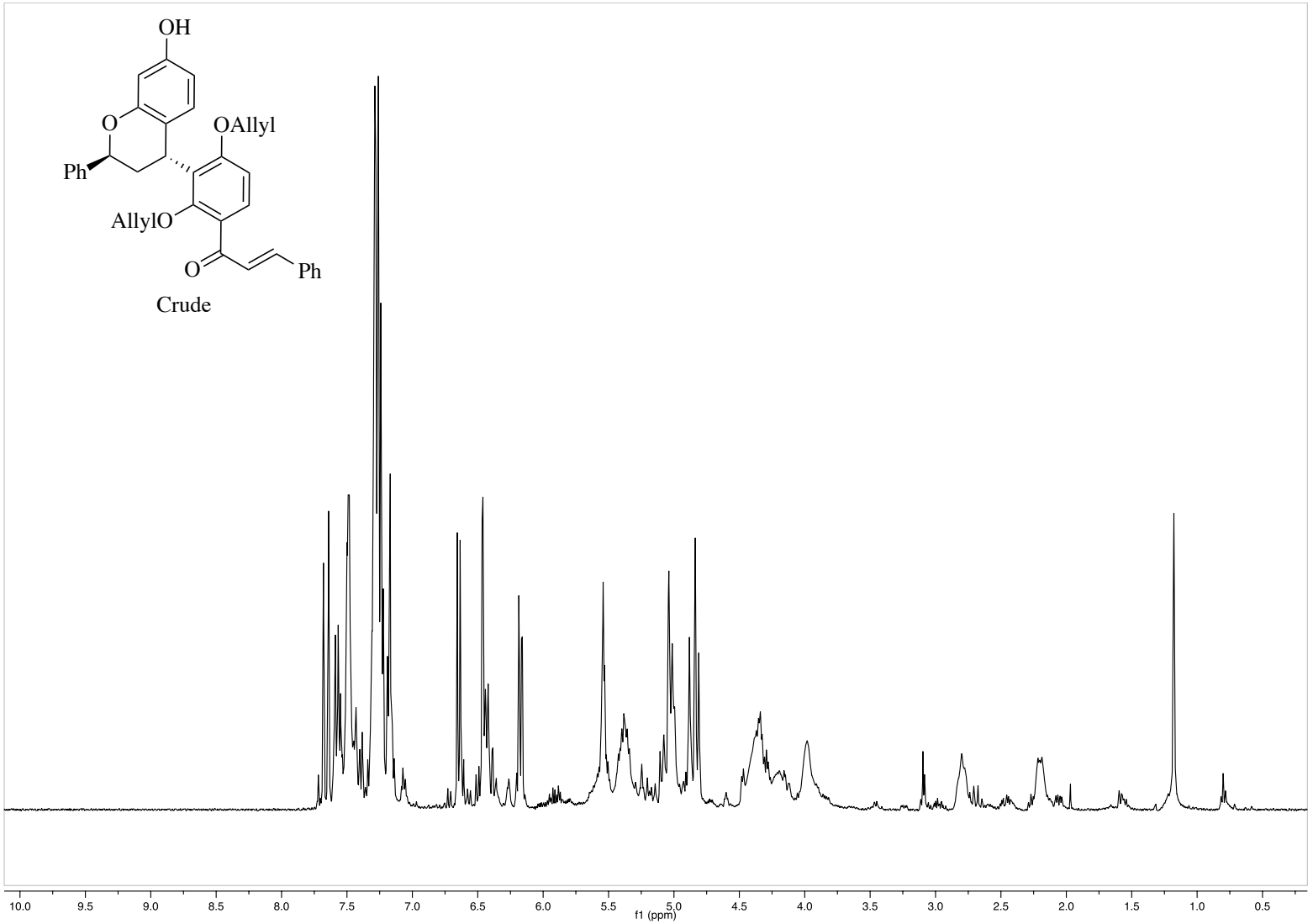

Figure A.51. ^{1}H NMR (600 MHz, $CDCl_3$), **1.08**

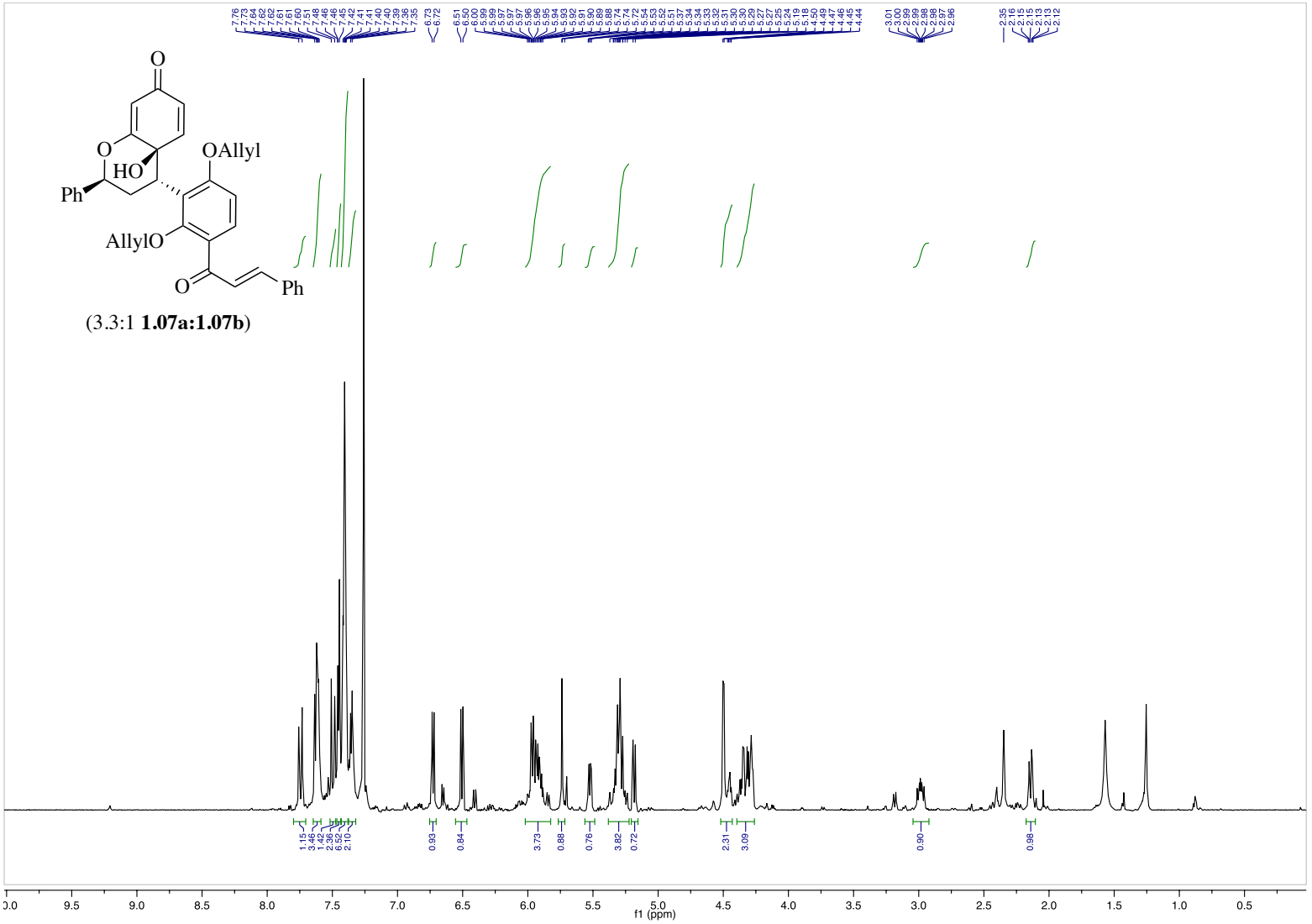

Figure A.52. ^{1}H NMR (600 MHz, $CDCl_3$), **1.07a**

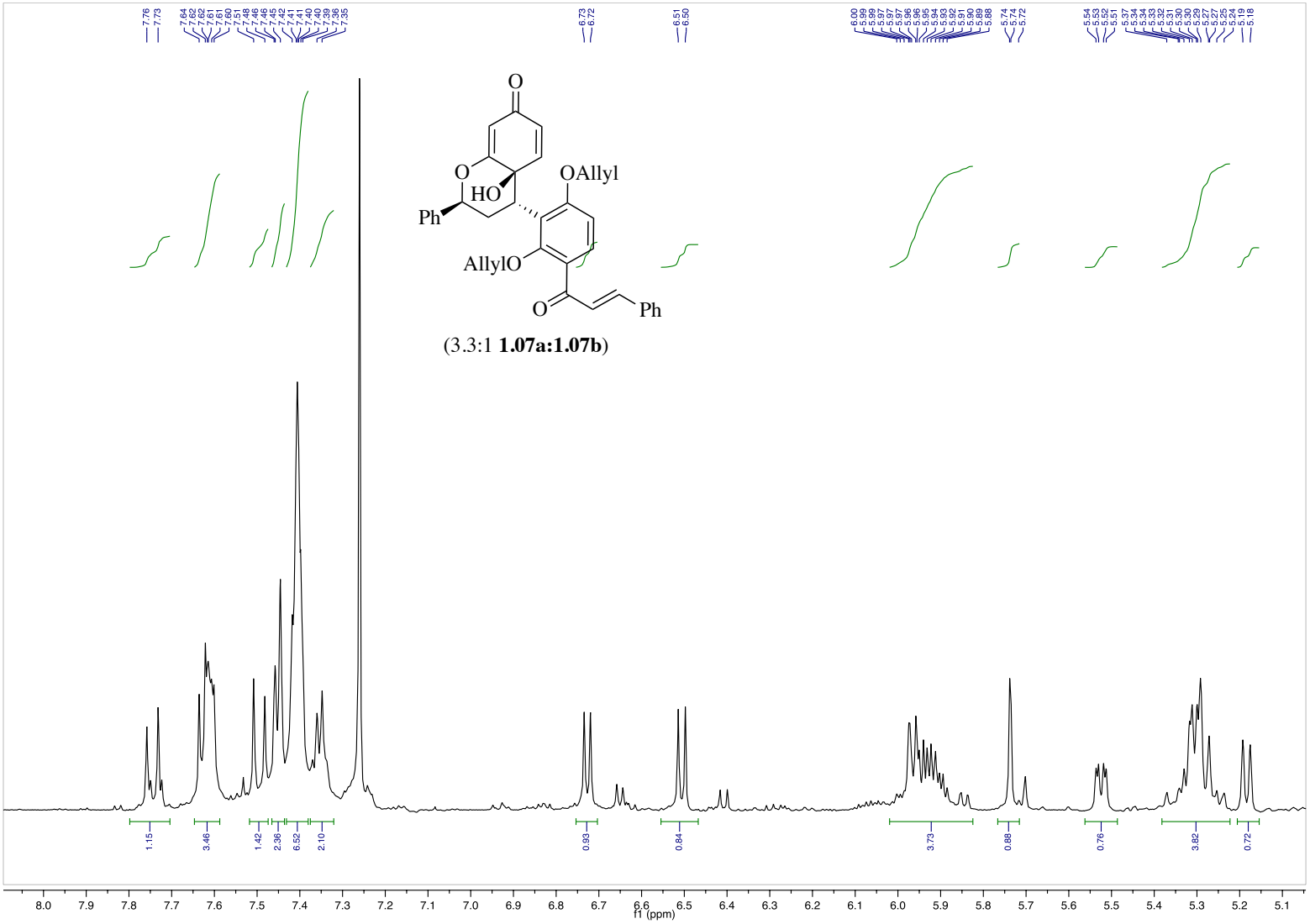

Figure A.53. ^{1}H NMR (600 MHz, $CDCl_3$), **1.07a** (inset)

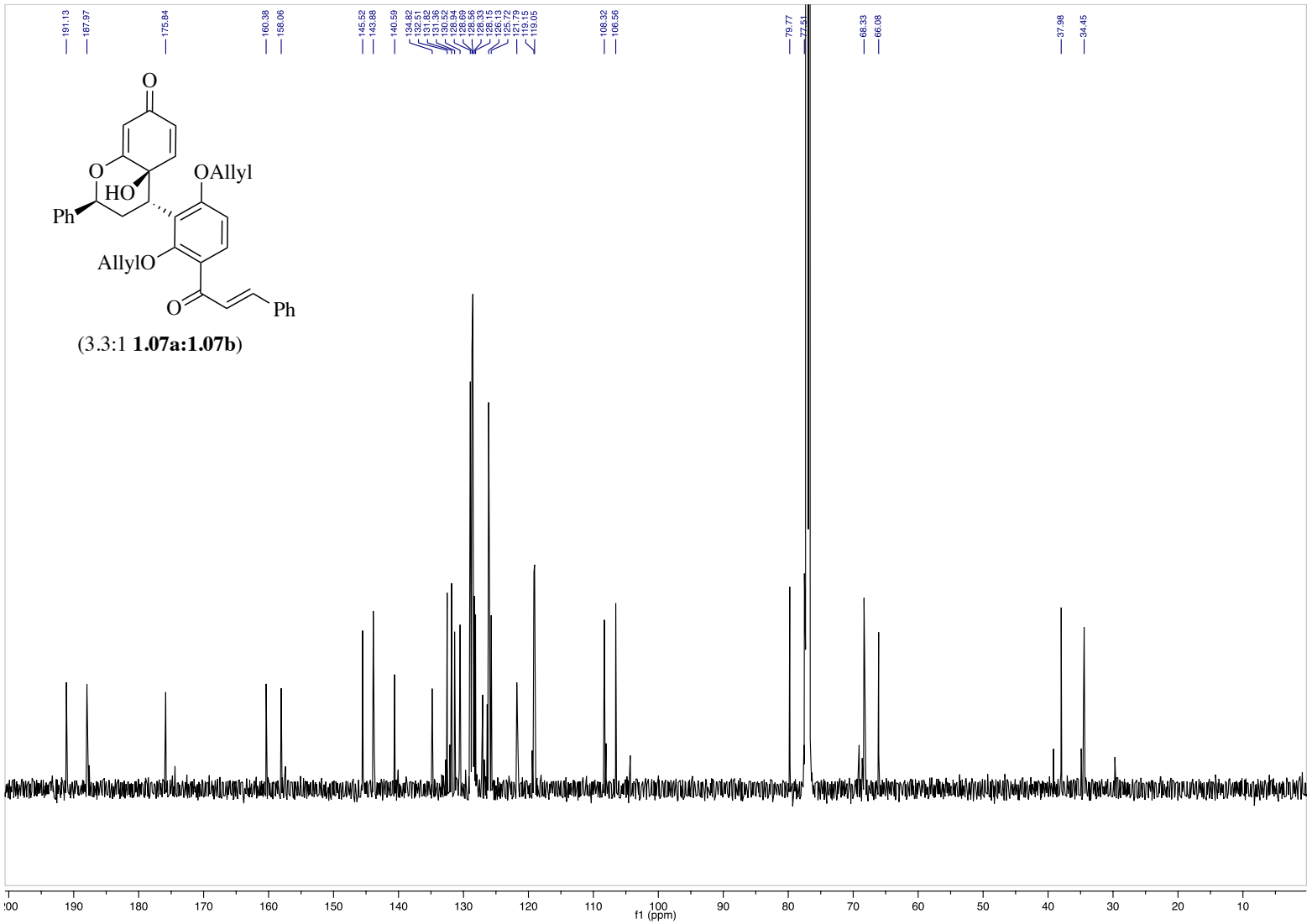

Figure A.54. ^{13}C NMR (151 MHz, $CDCl_3$), **1.07a**

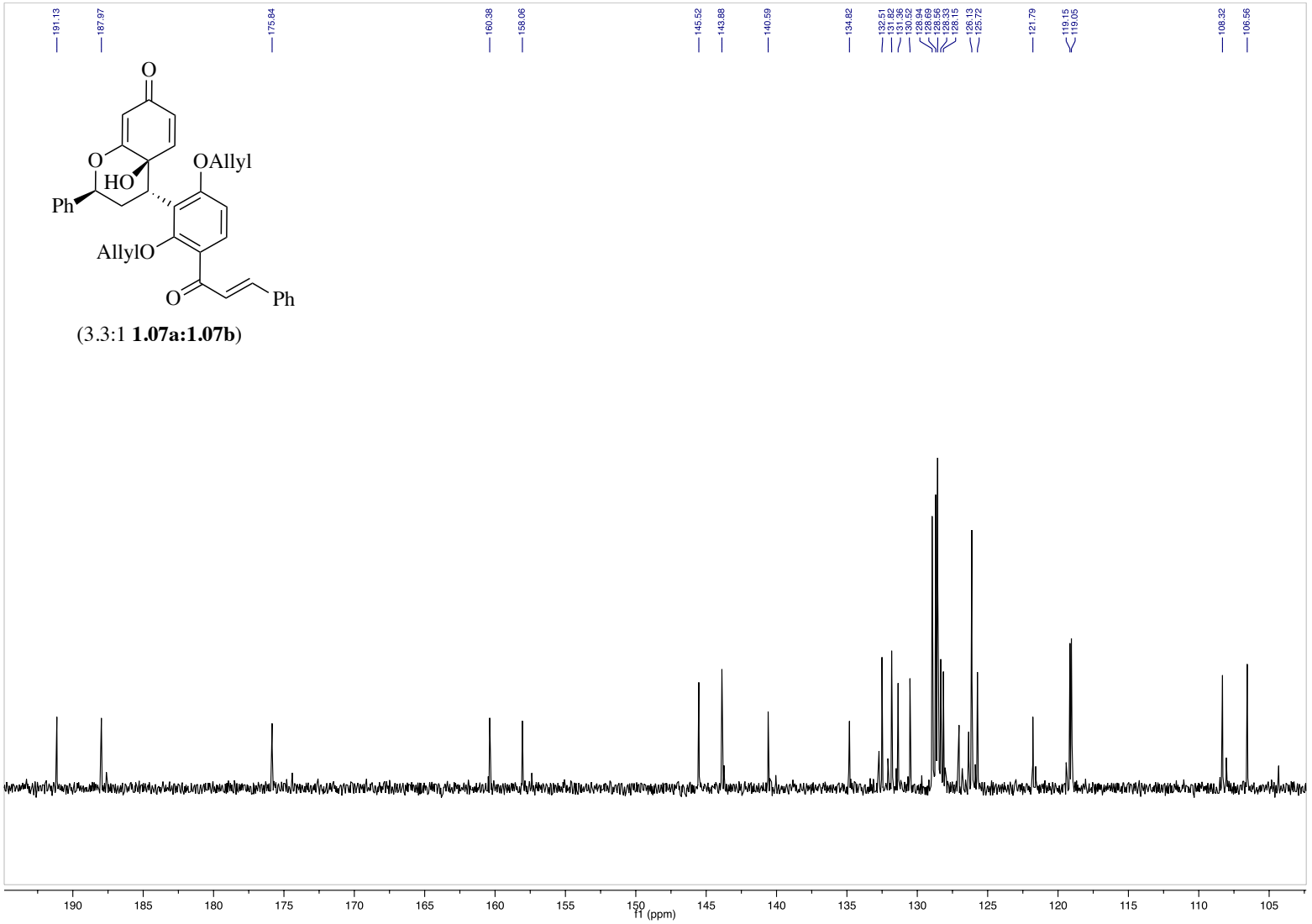

Figure A.55. ^{13}C NMR (151 MHz, $CDCl_3$), **1.07a** (inset)

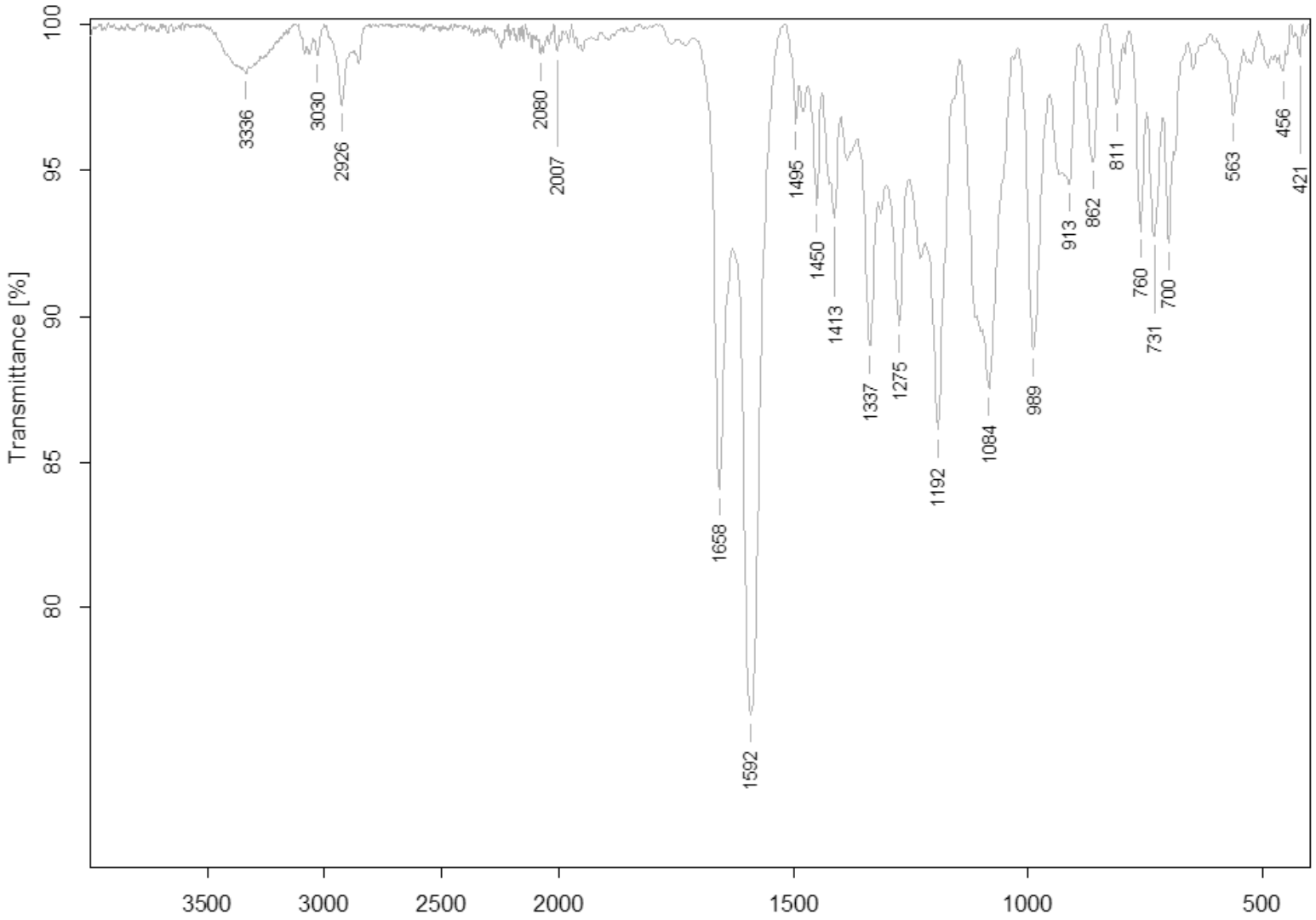

Figure A.56. IR (ATR), **1.07a**

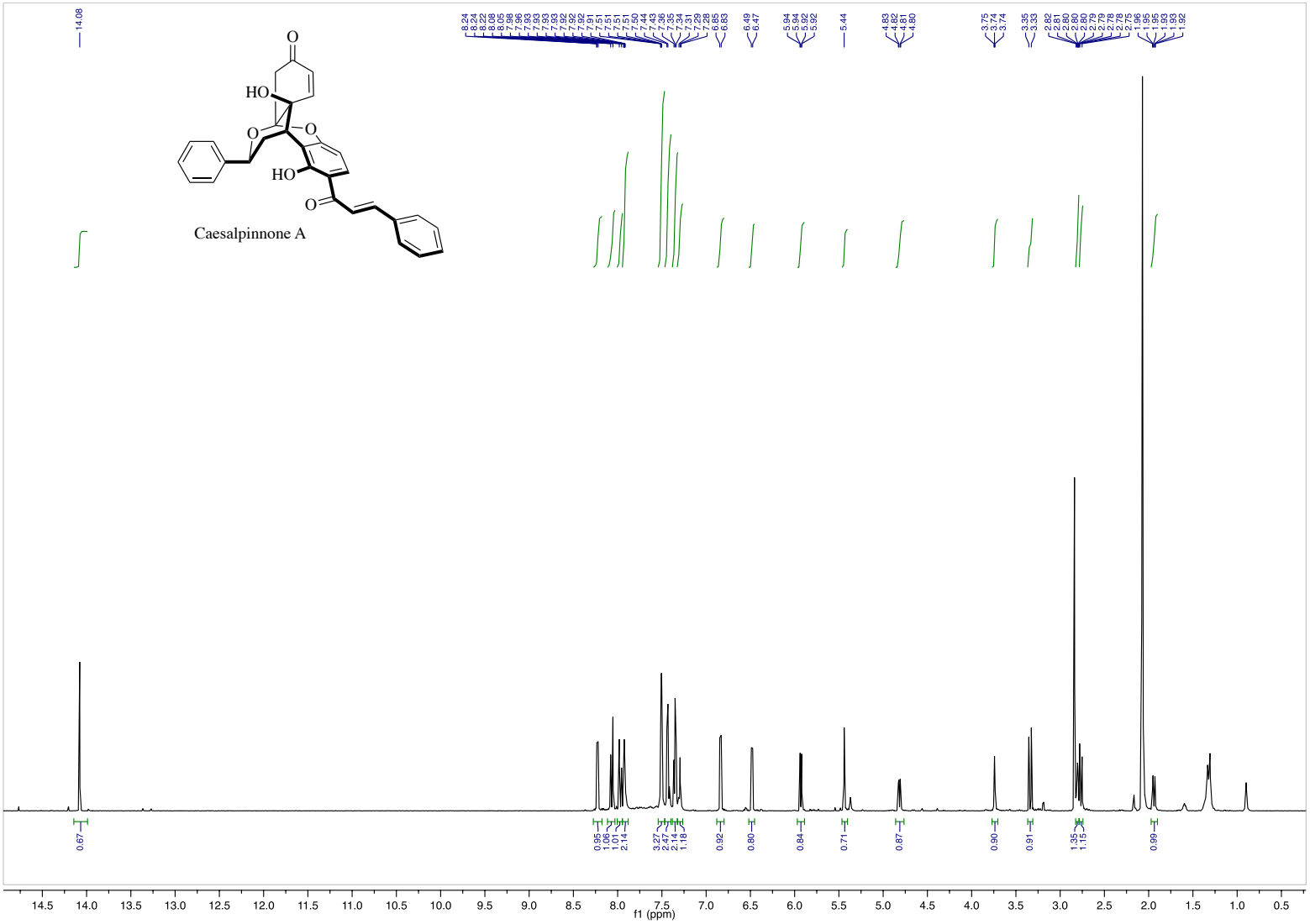

Figure A.57. ^{1}H NMR (600 MHz, acetone-d_6), **1.01**

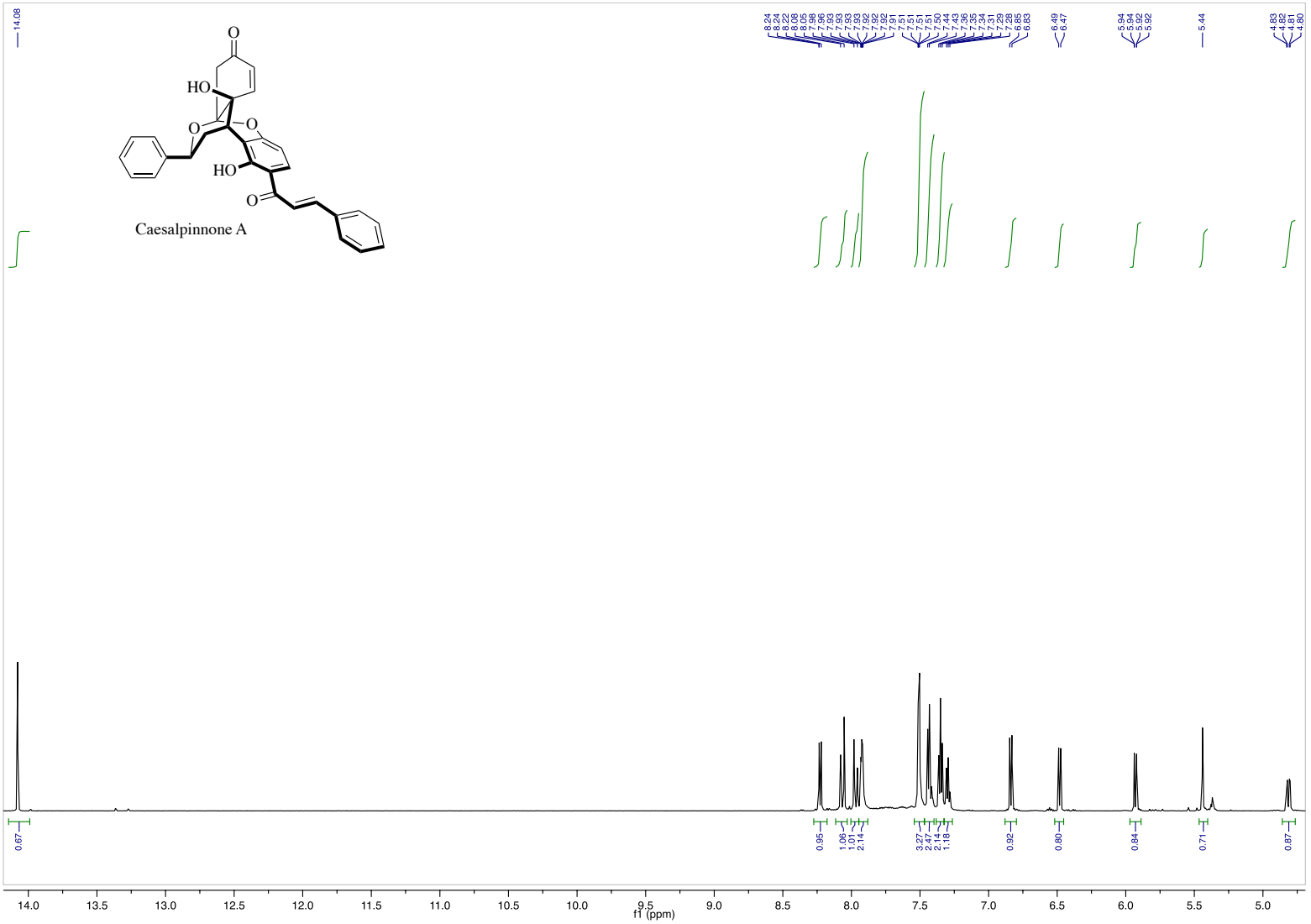

Figure A.58. ^{1}H NMR (600 MHz, acetone-d_6), **1.01** (inset)

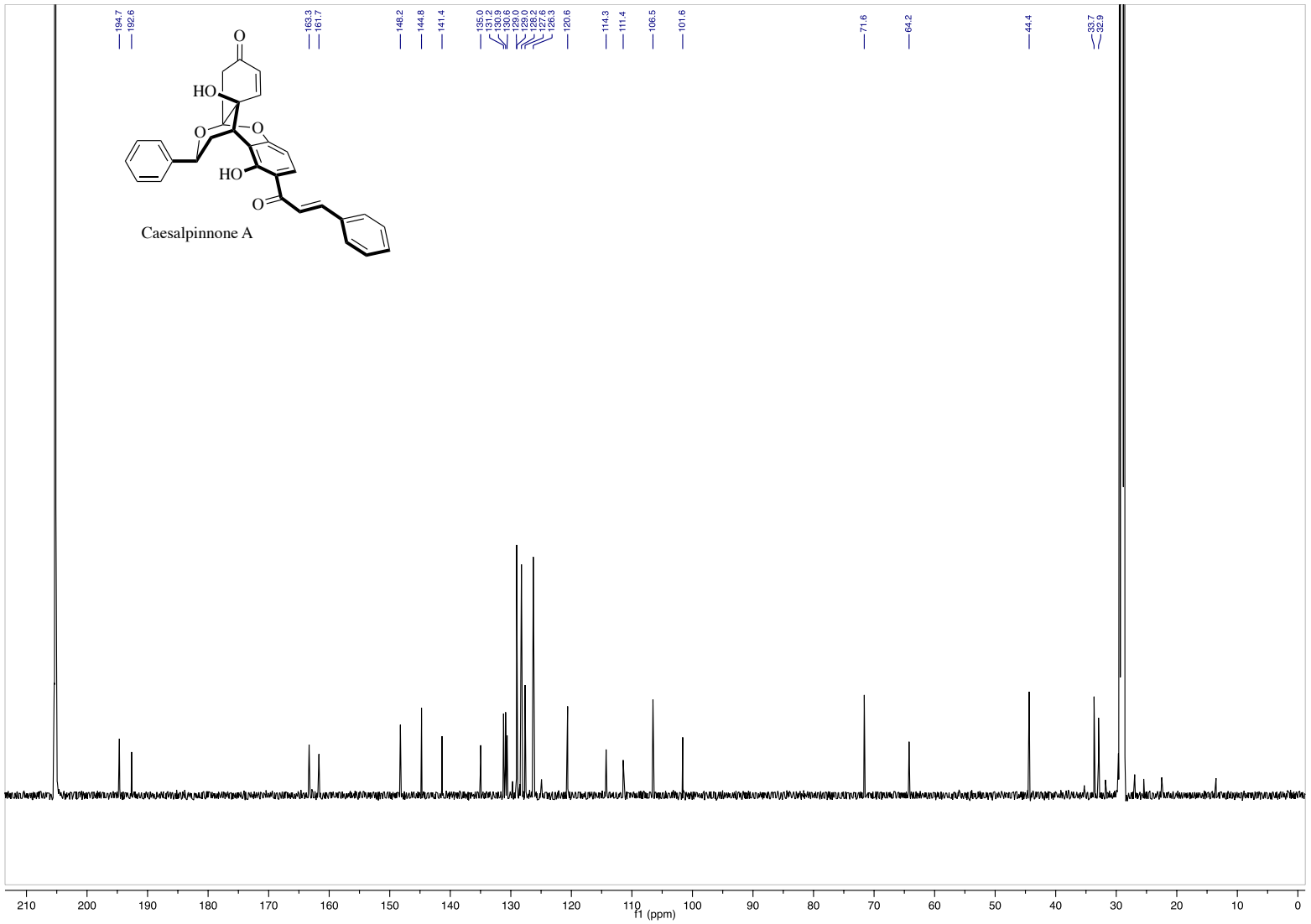

Figure A.59. ^{13}C NMR (151 MHz, acetone-d_6), **1.01**

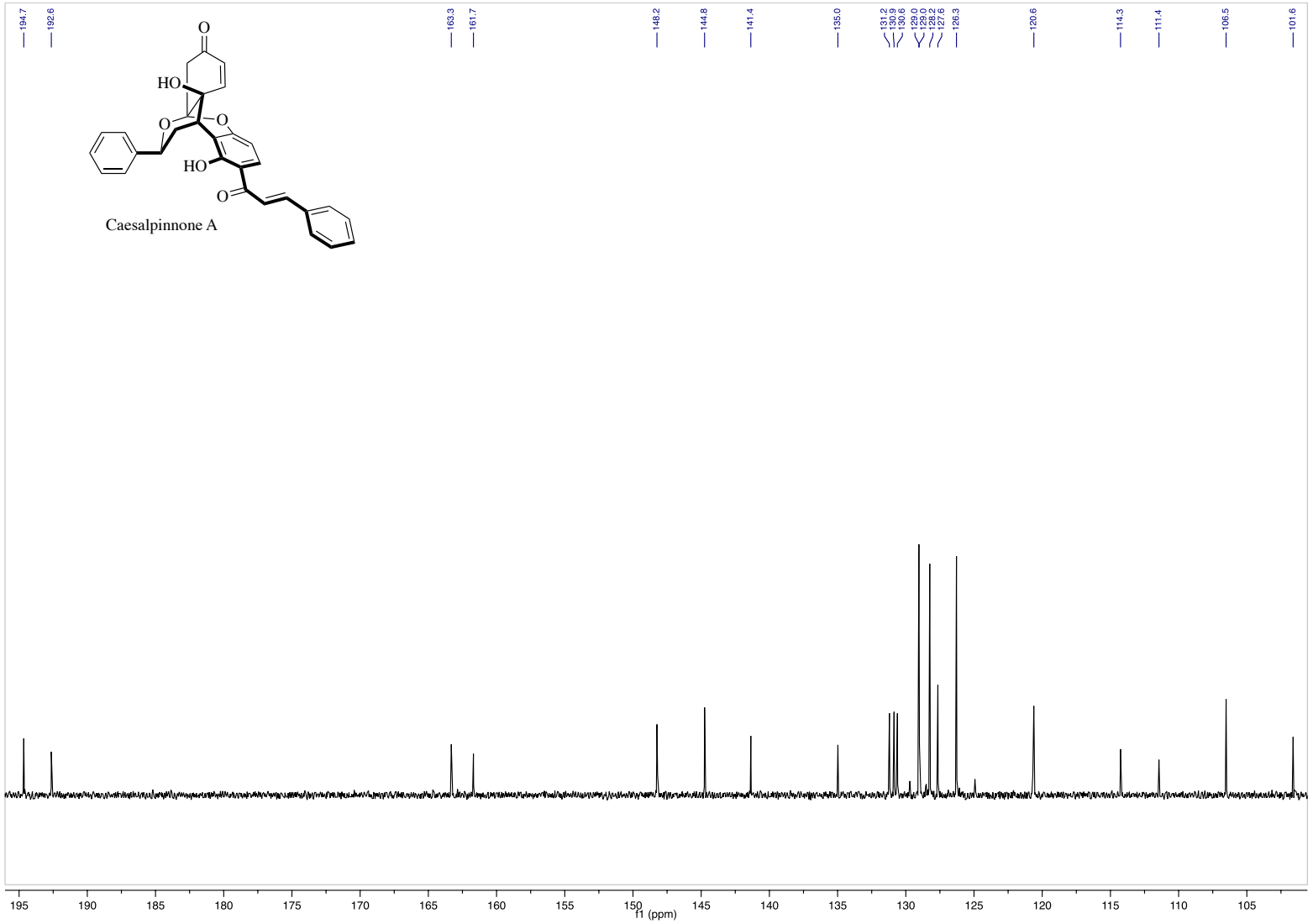

Figure A.60. ^{13}C NMR (151 MHz, acetone-d_6), **1.01** (inset)

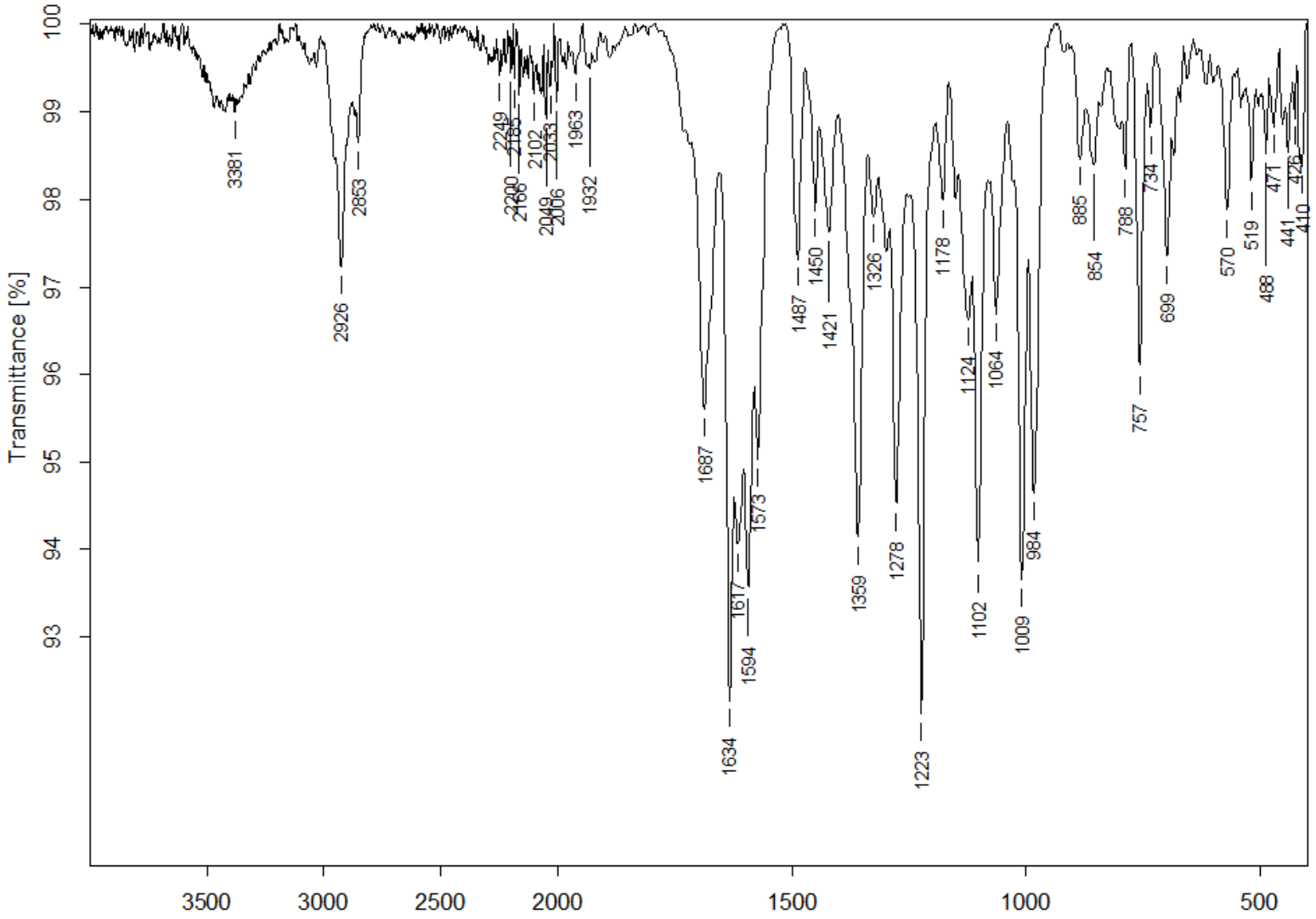

Figure A.61. IR (ATR), **1.01**

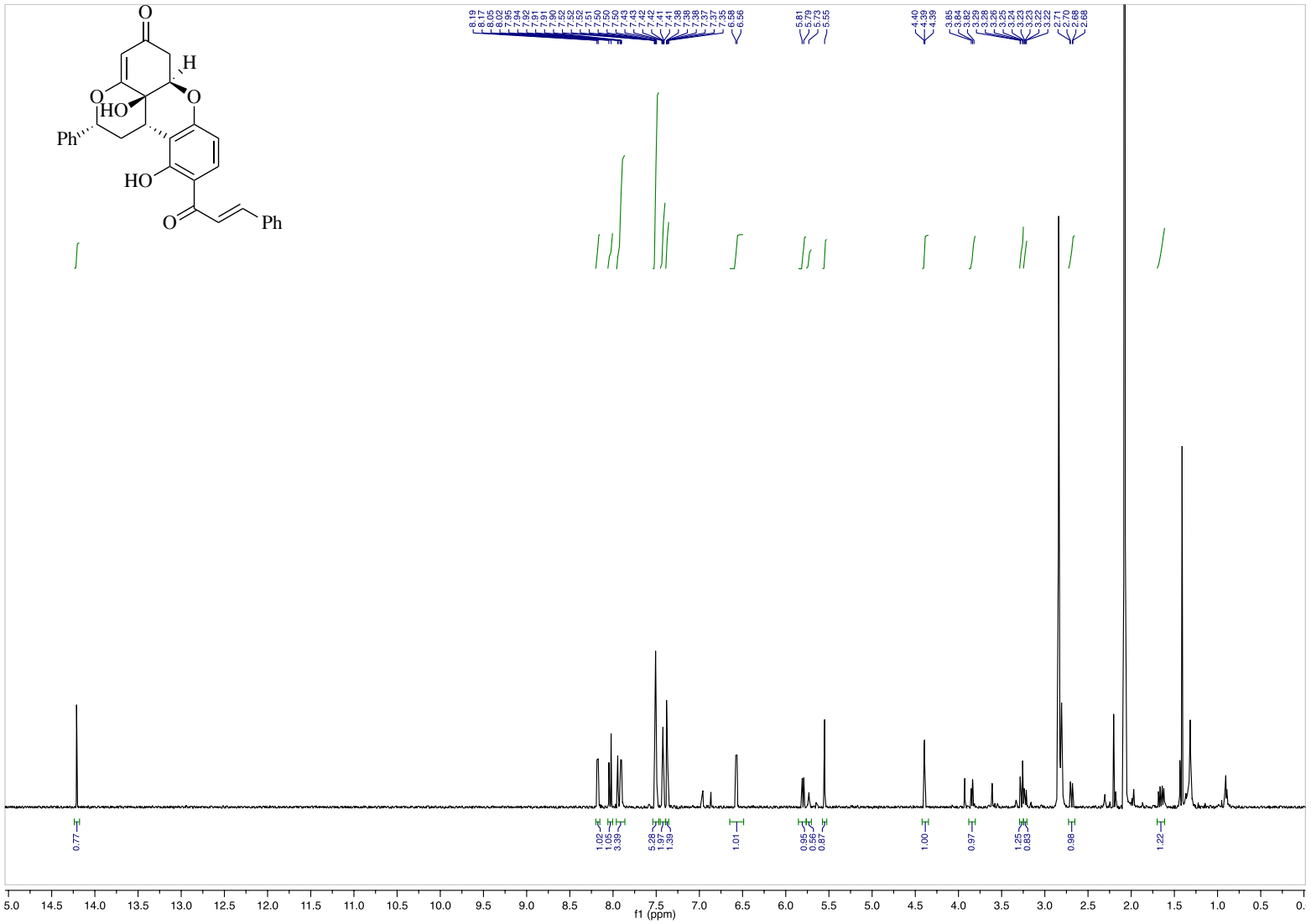

Figure A.62. ^{1}H NMR (600 MHz, acetone-d_6), **1.01a**

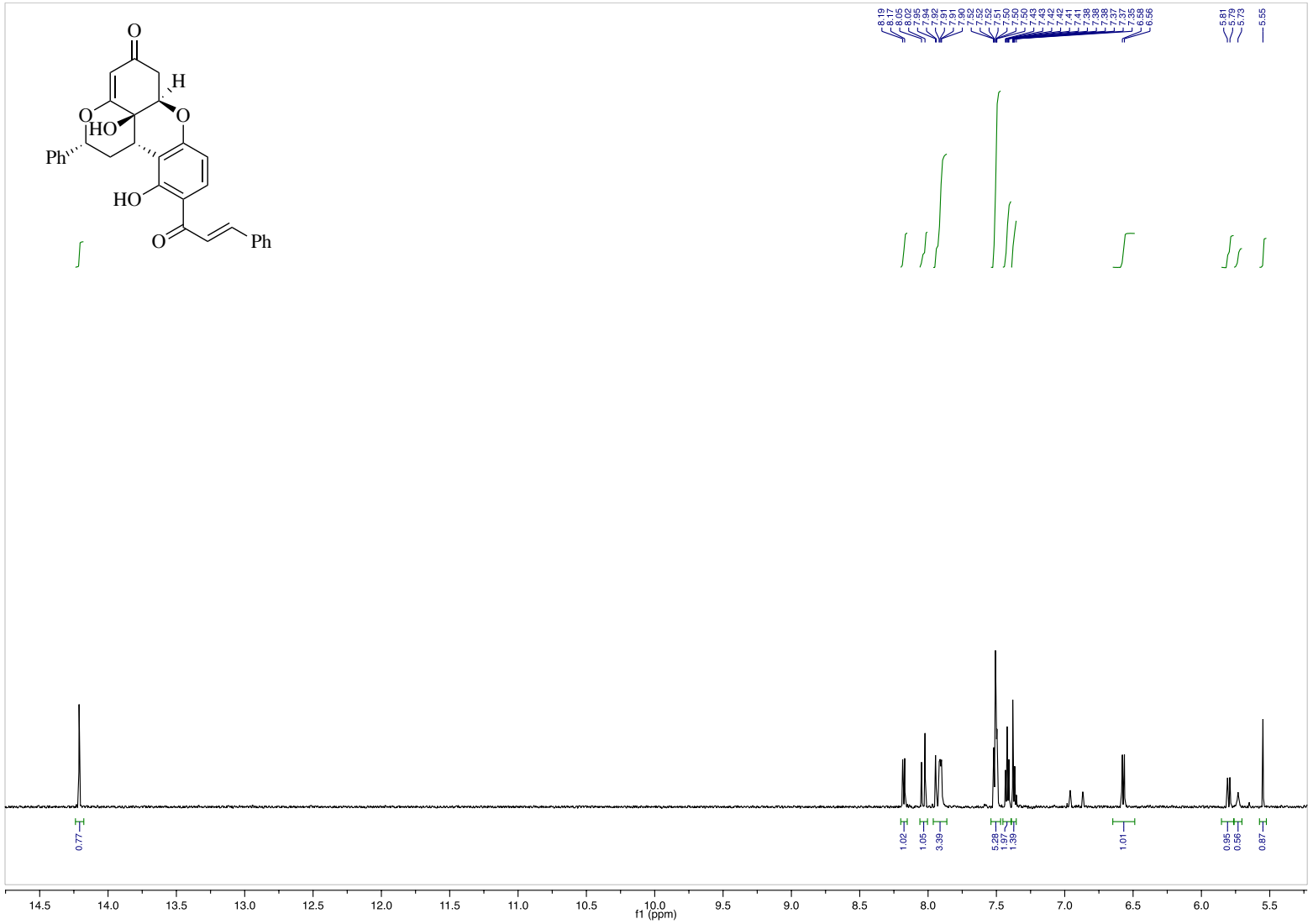

Figure A.63. ^{1}H NMR (600 MHz, acetone-d_6), **1.01a** (inset)

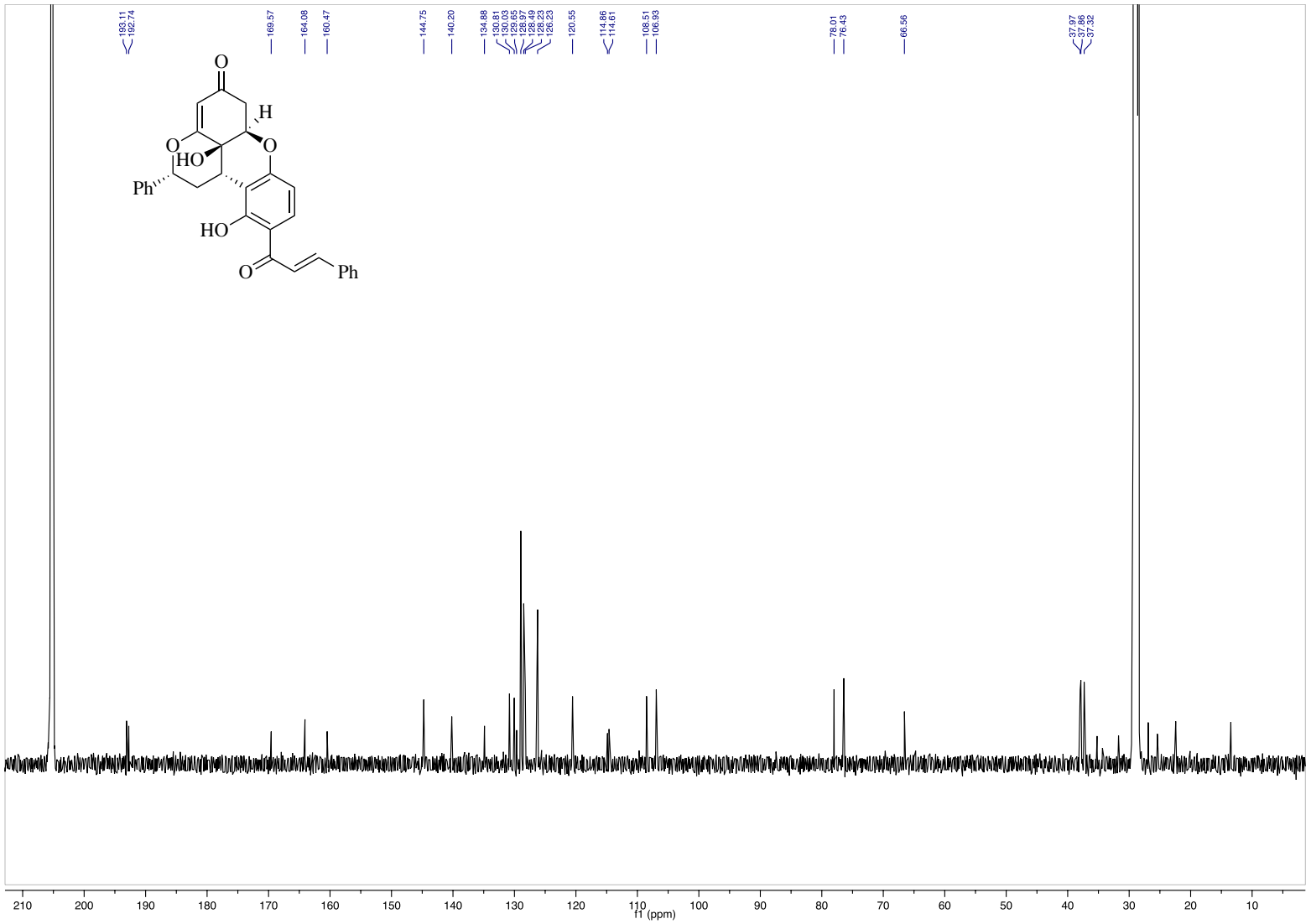

Figure A.64. ^{13}C NMR (151 MHz, acetone-d_6), **1.01a**

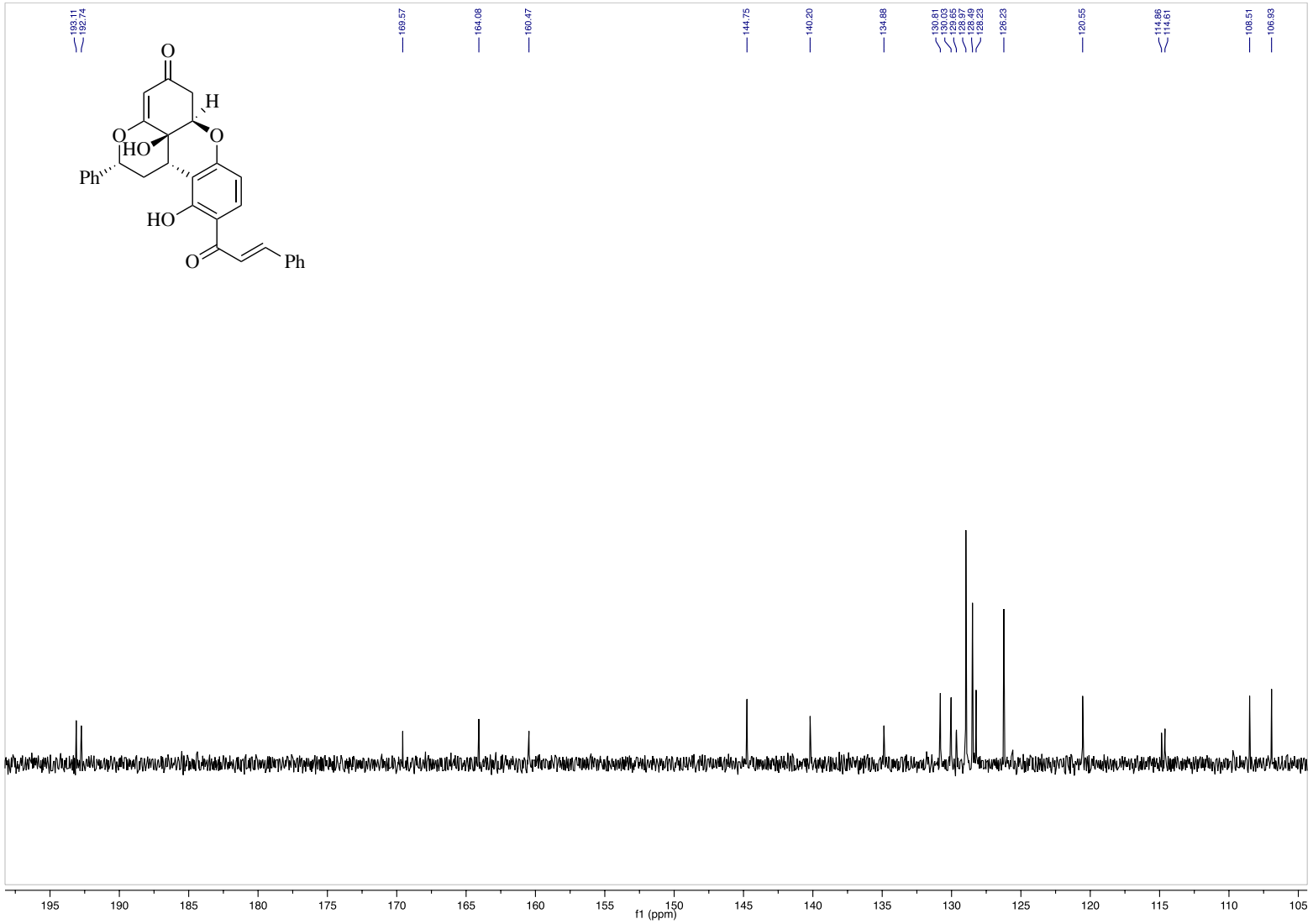

Figure A.65. ^{13}C NMR (151 MHz, acetone-d_6), **1.01a** (inset)

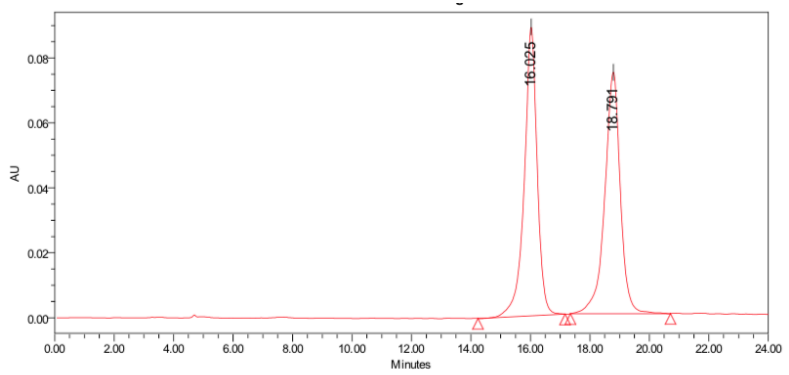

Peak Results

	Name	RT	Area	Height	Amount	Units
1		16.025	2679935	89021		
2		18.791	2703710	74374		

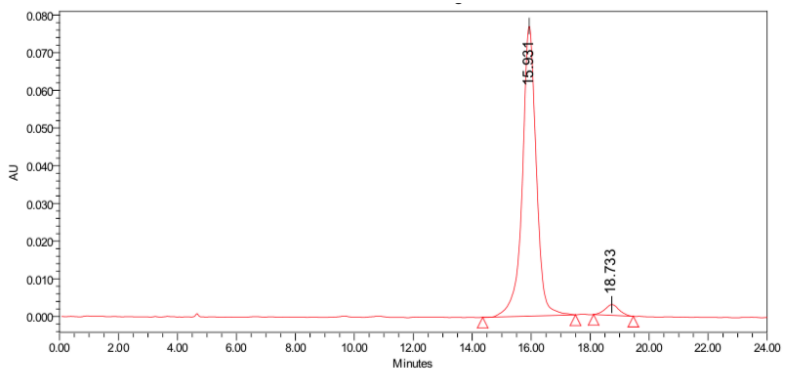

Peak Results

	Name	RT	Area	Height	Amount	Units
1		15.931	2528870	76969		
2		18.733	96925	2885		

Figure A.66. Chiral HPLC traces of racemic **1.14** (top trace) and enantioenriched (*R*)-**1.14** (bottom trace). Phenomenex i-Amylose 1 (4.6 mm x 250 mm, 5 µM), 93:7 hexanes–iPrOH @ 1 mL/min (96.5:3.5 er)

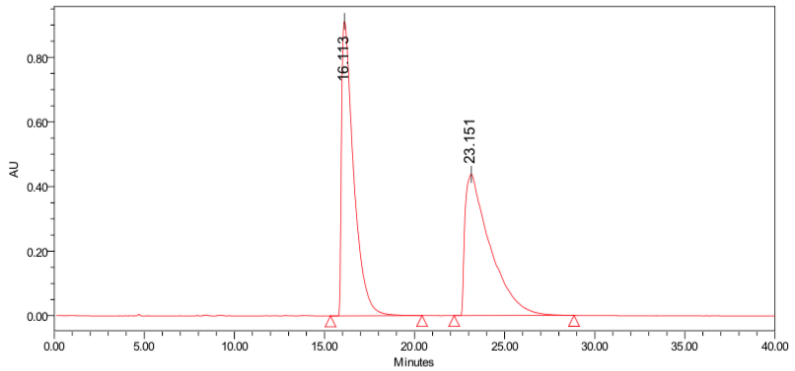

Peak Results

	Name	RT	Area	Height	Amount	Units
1		16.113	42503597	912017		
2		23.151	42468004	437764		

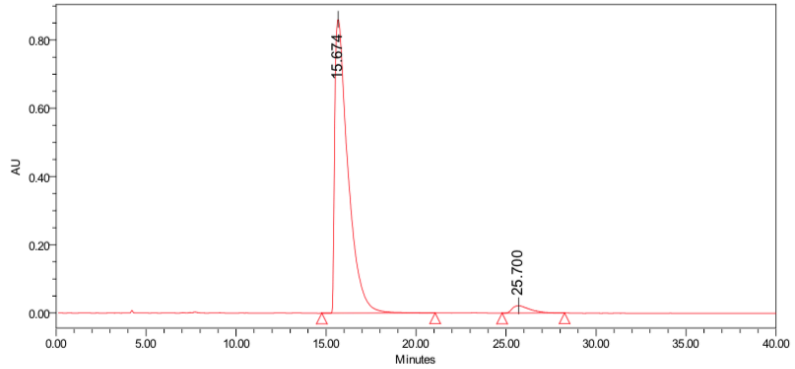

Peak Results

	Name	RT	Area	Height	Amount	Units
1		15.674	43952330	861202		
2		25.700	1491630	21718		

Figure A.67. Chiral HPLC traces of racemic **1.15** (top trace) and enantioenriched **1.15** (bottom trace). Phenomenex i-amylose 1 (4.6 mm x 250 mm, 5 μM), 85:15 hexanes–iPrOH @ 1 mL/min. (96.5:3.5 er)

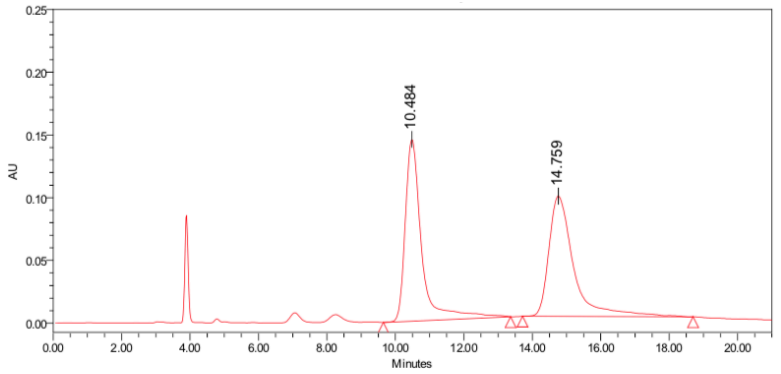

Peak Results

	Name	RT	Area	Height	Amount	Units
1		10.484	4837315	144901		
2		14.759	4846953	96028		

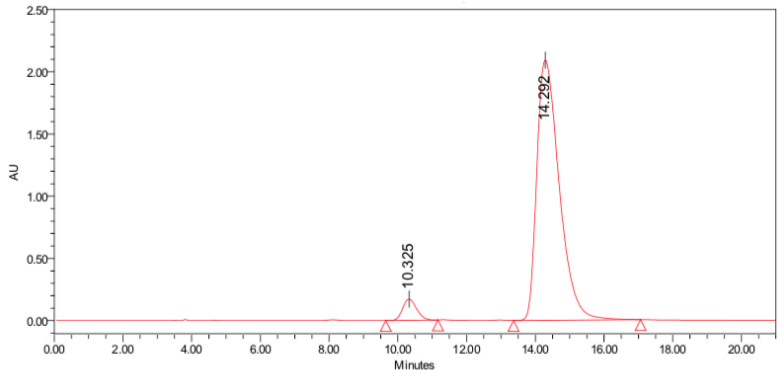

Peak Results

	Name	RT	Area	Height	Amount	Units
1		10.325	4830694	171144		
2		14.292	94749914	2091033		

Figure A.68. Chiral HPLC traces of racemic **1.10** (top trace) and enantioenriched (*R*)-**1.10** (bottom trace). Phenomenex i-Amylose 1 (4.6 mm x 250 mm, 5 μM), 70:30 hexanes–iPrOH @ 1 mL/min. (95:5 er)

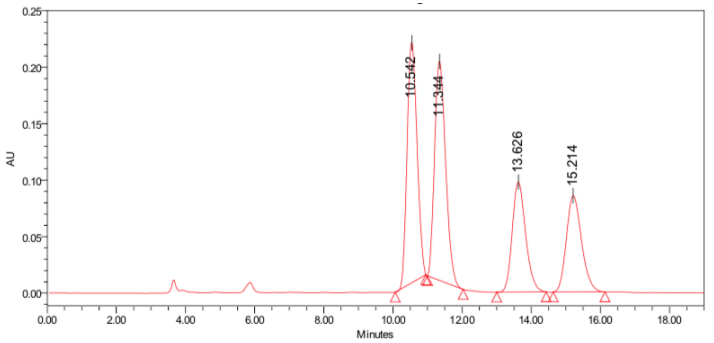

Peak Results

	Name	RT	Area	Height	Amount	Units
1		10.542	4251672	212945		
2		11.344	4308237	194020		
3		13.626	2622137	97534		
4		15.214	2596163	85361		

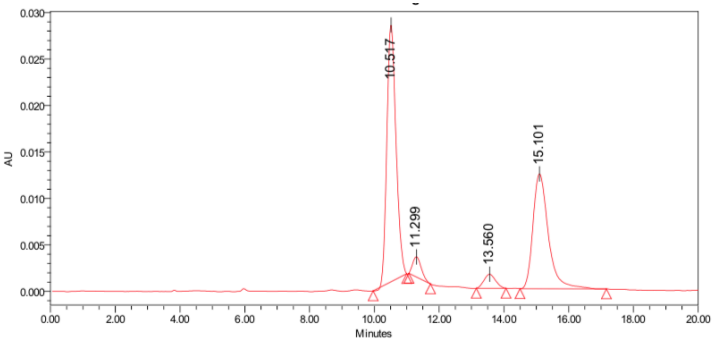

Peak Results

	Name	RT	Area	Height	Amount	Units
1		10.517	542093	27627		
2		11.299	39760	2170		
3		13.560	37501	1516		
4		15.101	408421	12353		

Figure A.69. Chiral HPLC traces of racemic **1.09** (top trace) and enantioenriched 1.0**9** (bottom trace). Phenomenex i-Amylose 1 (4.6 mm x 250 mm, 5 μM), 80:3 hexanes–iPrOH @ 0.83 mL/min. (Major atropisomer: 93:7 er. Minor atropisomer: 91.5:8.5 er)

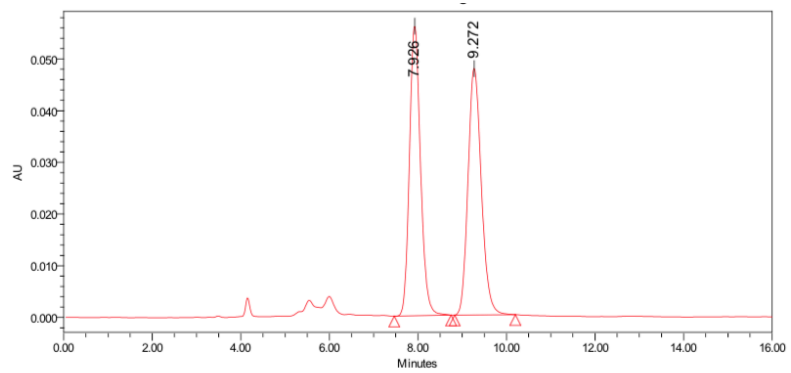

Peak Results

	Name	RT	Area	Height	Amount	Units
1		7.926	970553	56129		
2		9.272	995344	47702		

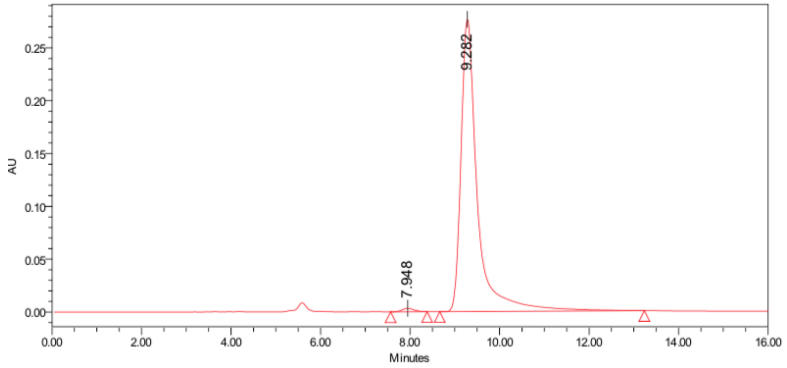

Peak Results

	Name	RT	Area	Height	Amount	Units
1		7.948	61910	3334		
2		9.282	7045968	276766		

Figure A.70. Chiral HPLC traces of racemic **1.17** (top trace) and enantioenriched **1.17** (bottom trace, after recrystallization).

Phenomenex i-Amylose 1 (4.6 mm x 250 mm, 5 μM), 85:15 hexanes–iPrOH @ 1.0 mL/min. (99:1 er)

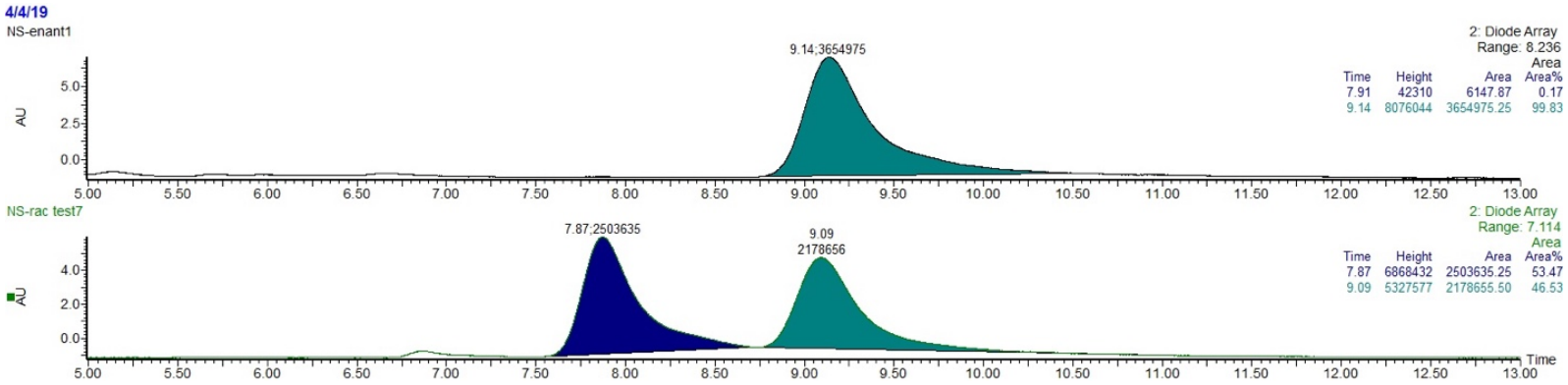

Figure A.71. Chiral UPLC traces of racemic (–)-**1.03** (top trace) and racemic **1.03** (bottom trace). Phenomenex Lux Cellulose-2 (4.6 mm x 150 mm, 3 μM), 40:60(0.2% formic acid) MeCN–Water @ 0.7 mL/min.

APPENDIX B

Spectral Data for Chapter Two

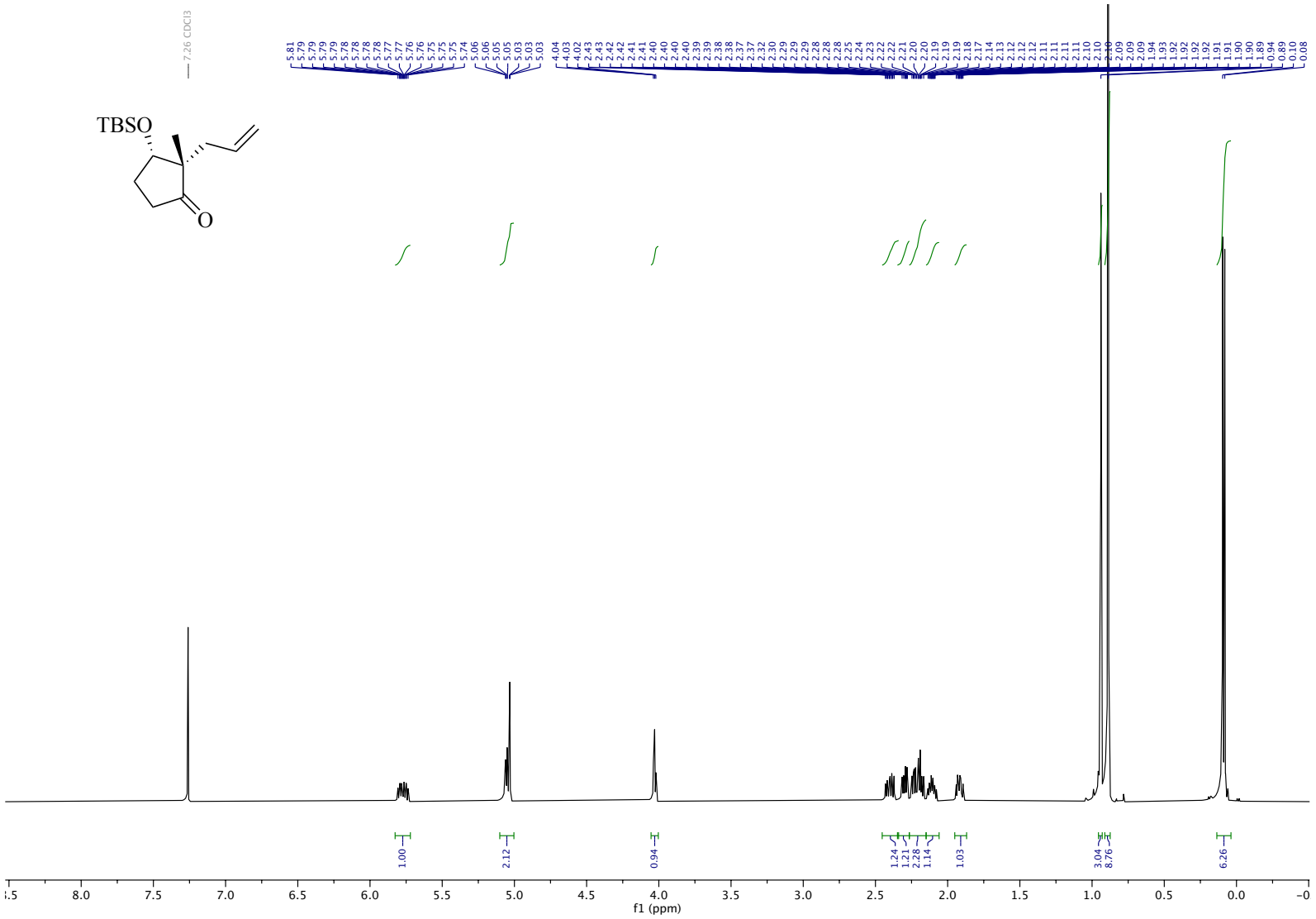

Figure B.1. ^{1}H NMR (600 MHz, $CDCl_3$), **2.12**

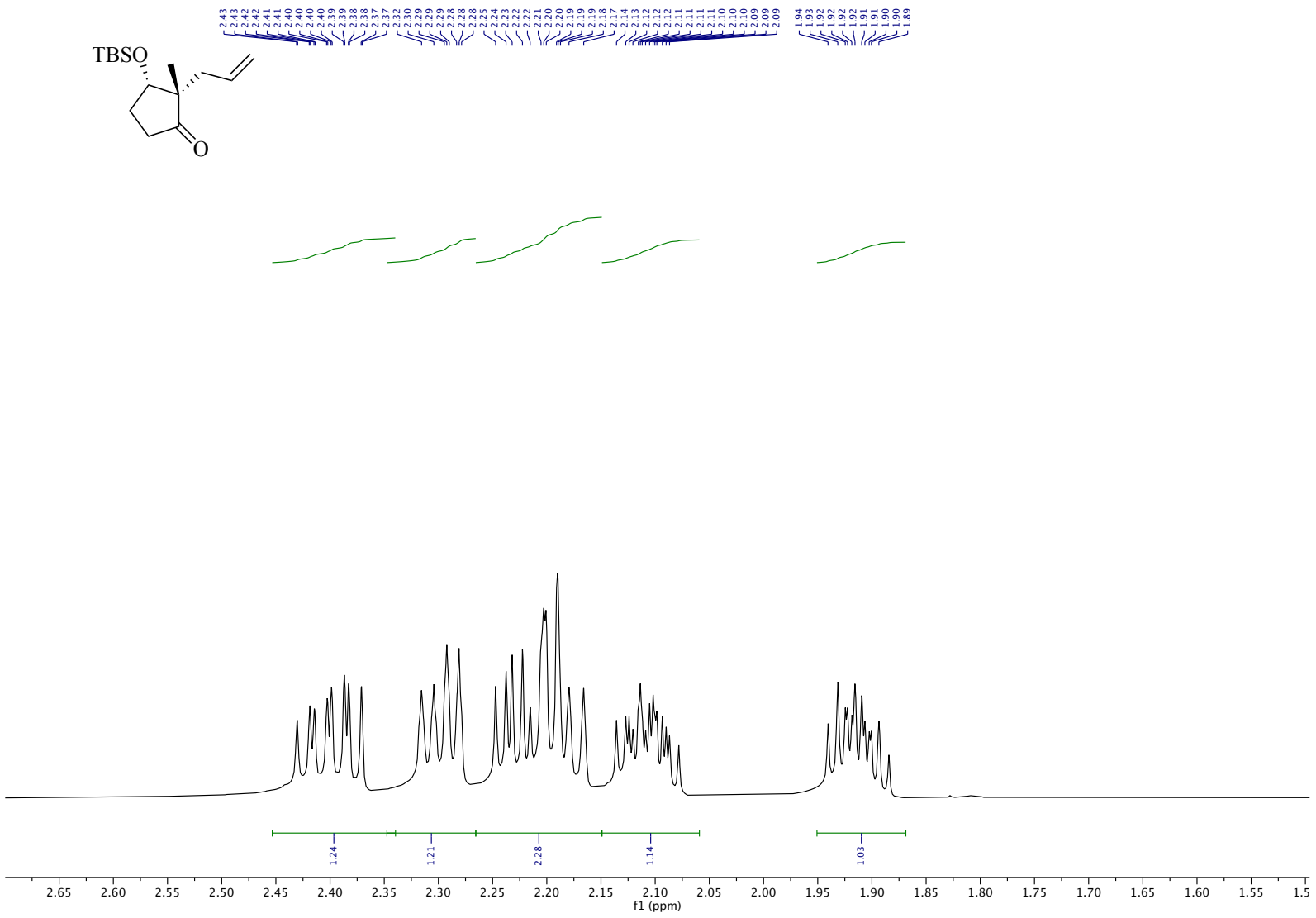

Figure B.2. ^{1}H NMR (600 MHz, $CDCl_3$), **2.12** (inset)

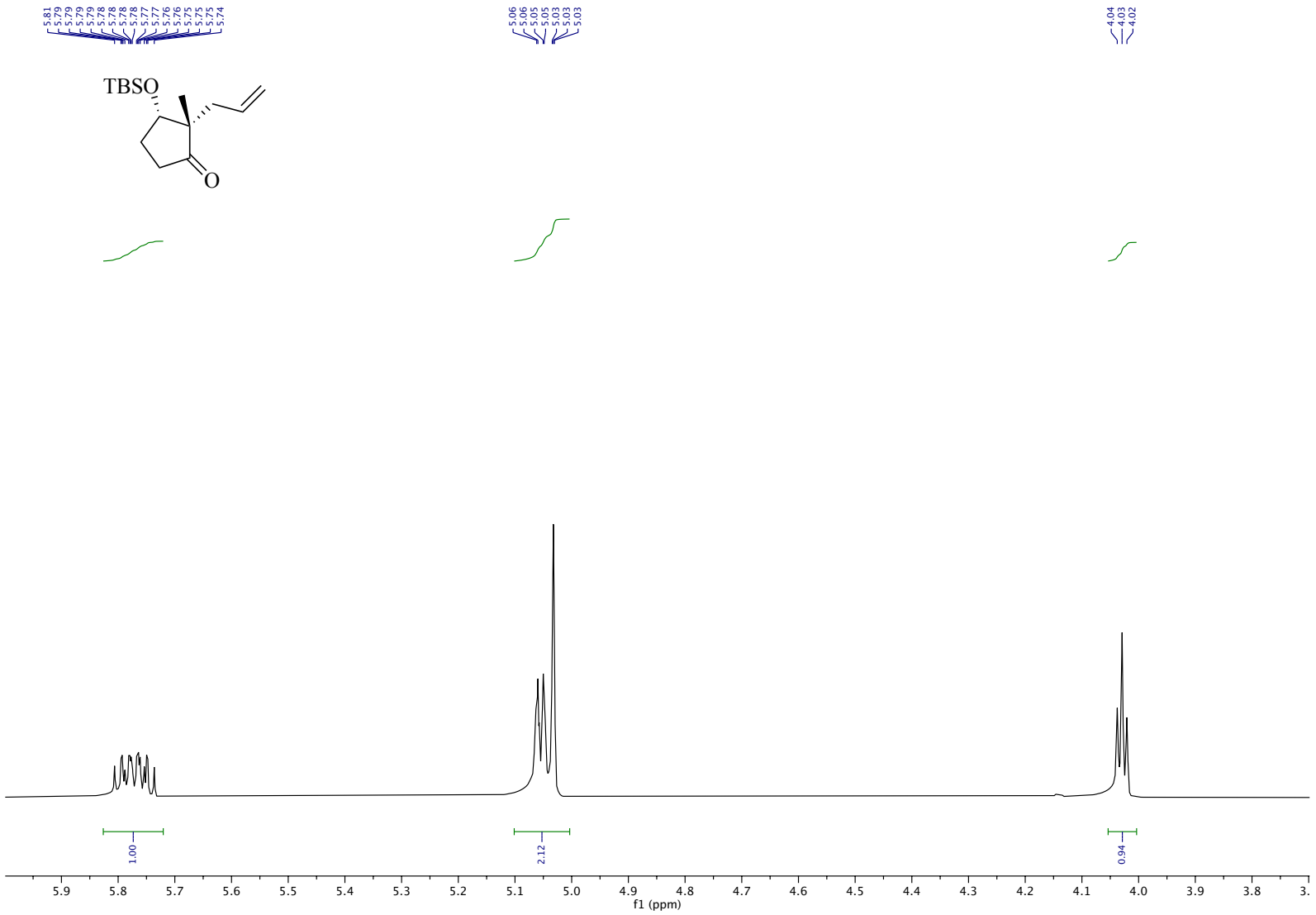

Figure B.3. ^{1}H NMR (600 MHz, $CDCl_3$), **2.12** (inset)

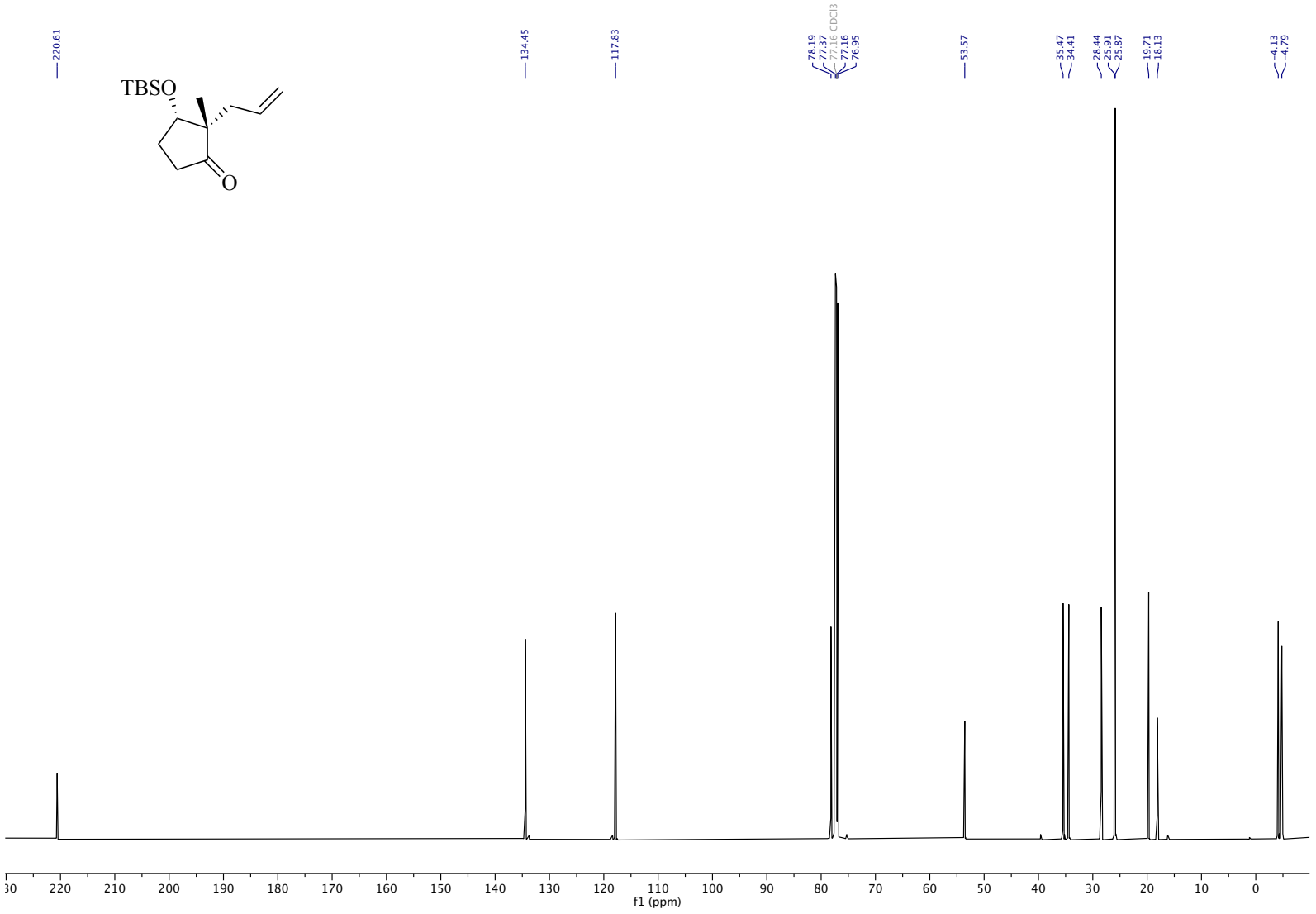

Figure B.4. ^{13}C NMR (151 MHz, $CDCl_3$), **2.12**

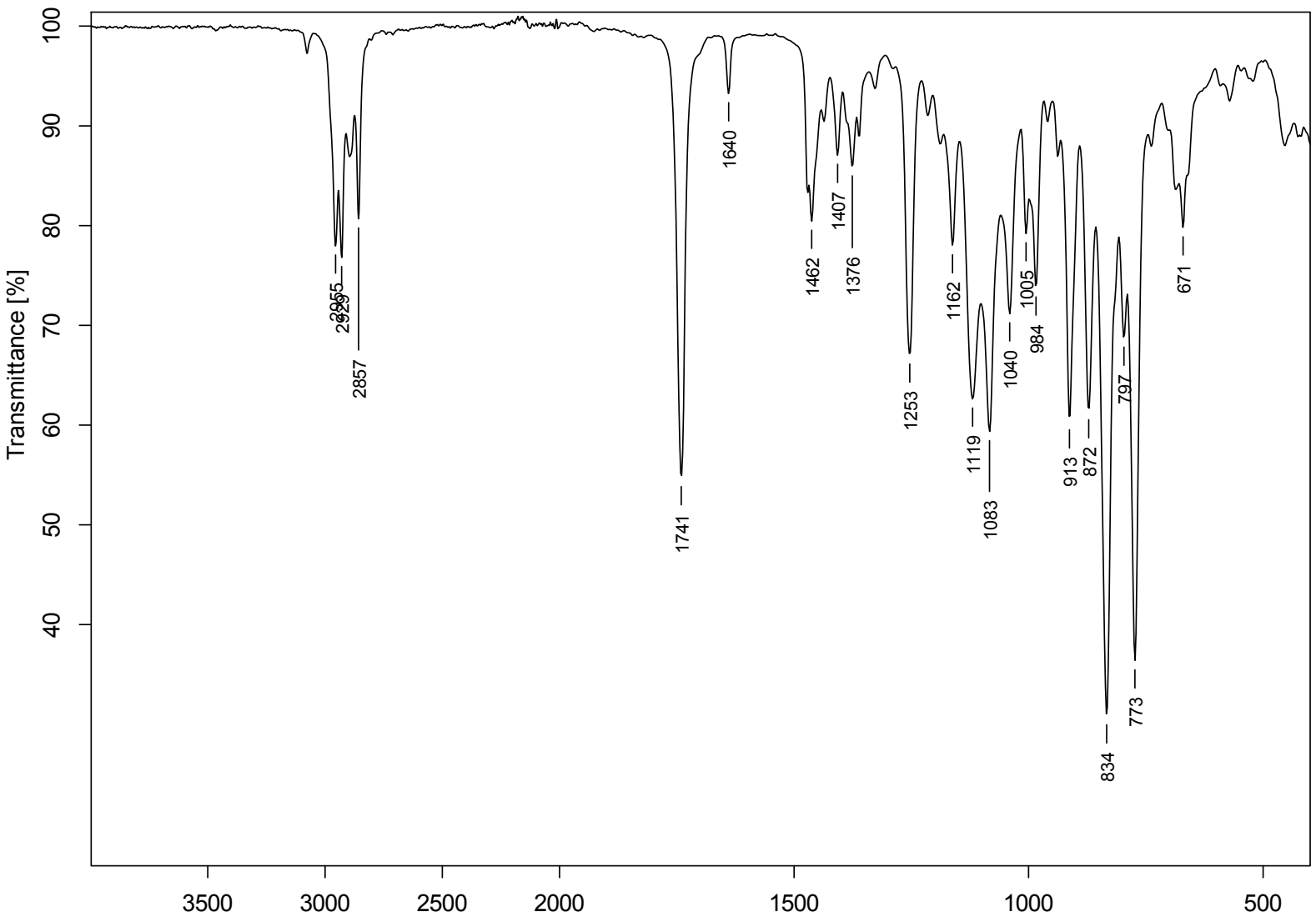

Figure B.5. IR (ATR), **2.12**

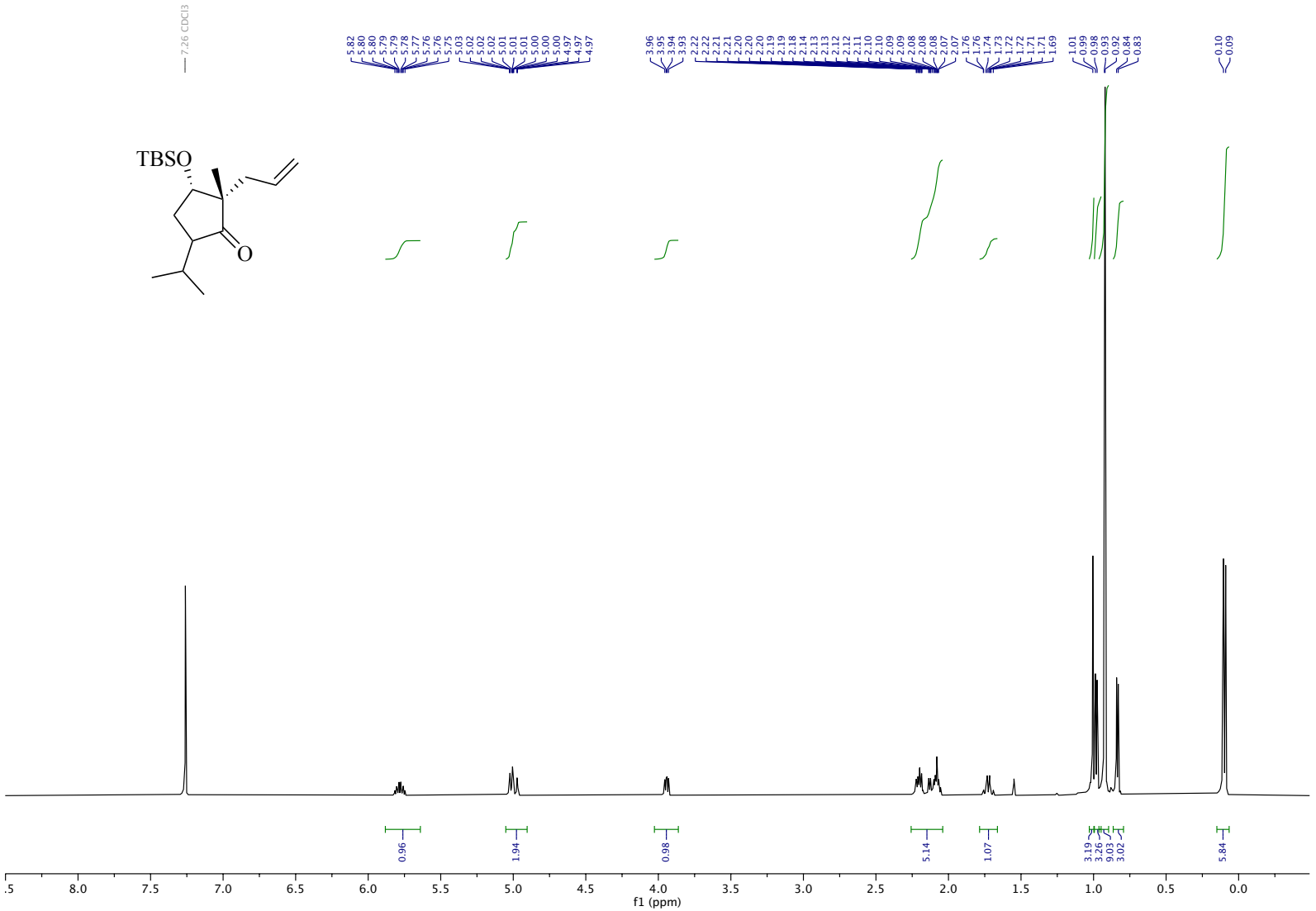

Figure B.6. ^{1}H NMR (600 MHz, $CDCl_3$), **2.13** (major diastereomer)

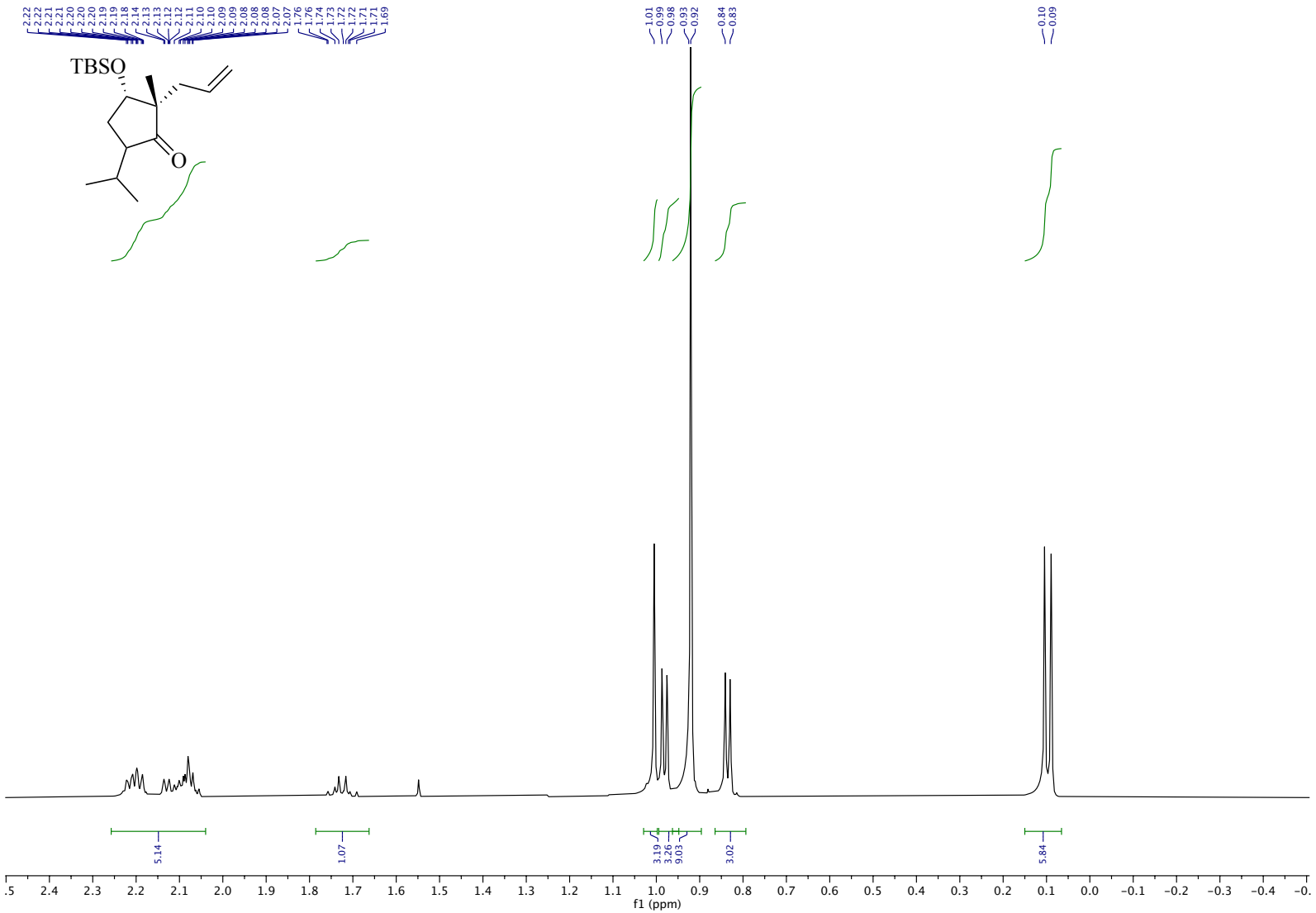

Figure B.7. ^{1}H NMR (600 MHz, $CDCl_3$), **2.13** (major diastereomer, inset)

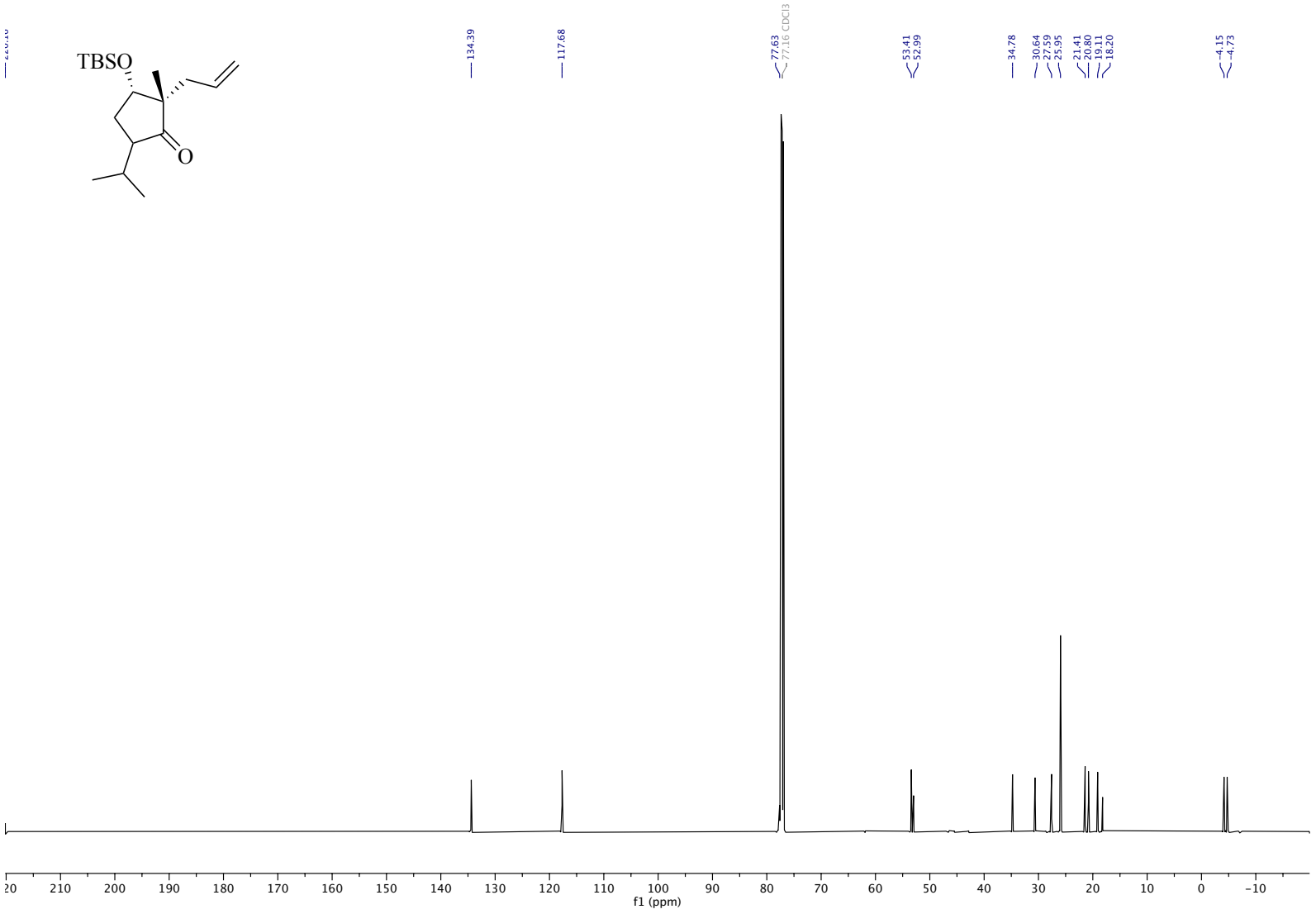

Figure B.8. ^{13}C NMR (151 MHz, $CDCl_3$), **2.13** (major diastereomer)

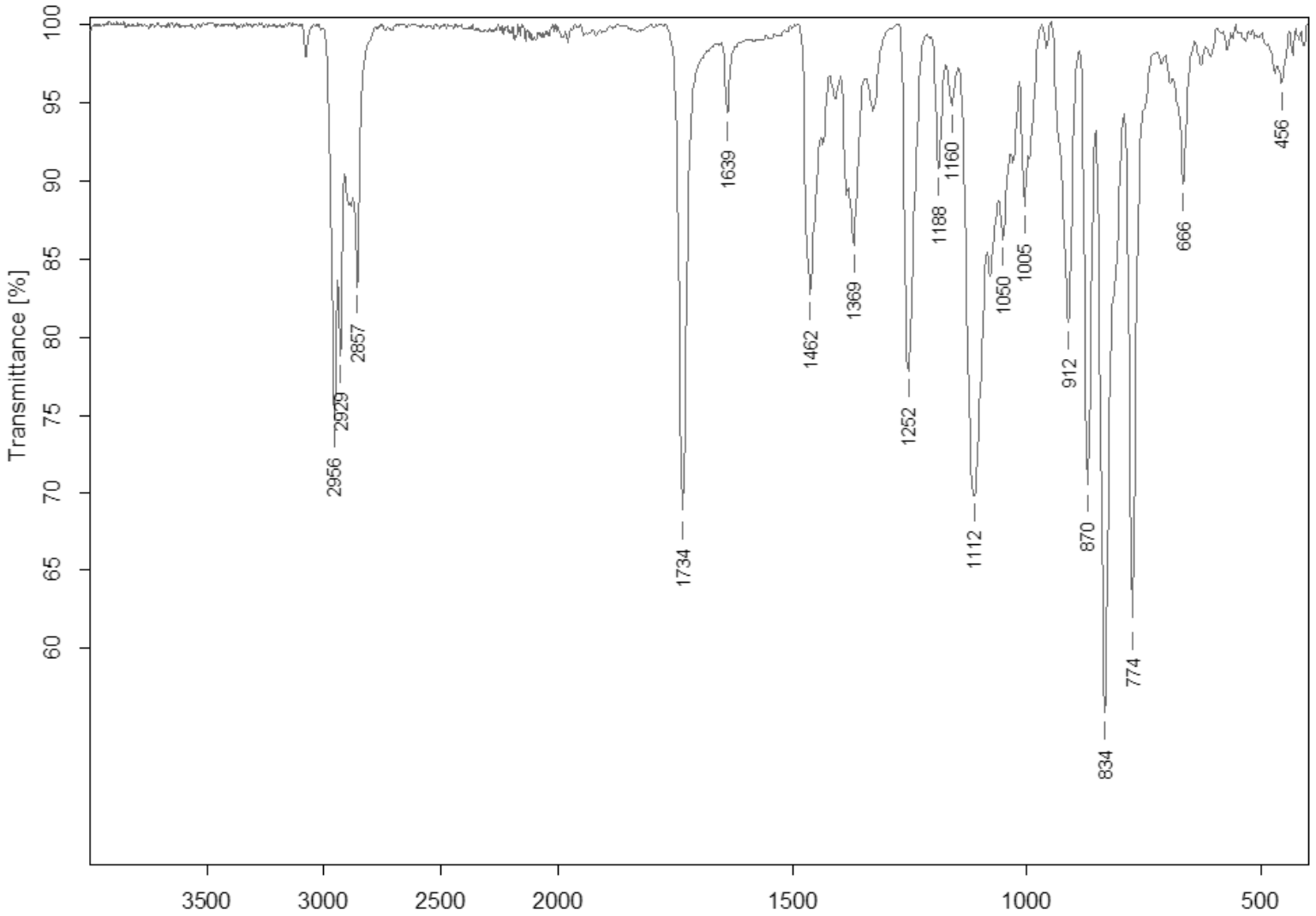

Figure B.9. IR (ATR), **2.13** (major diastereomer)

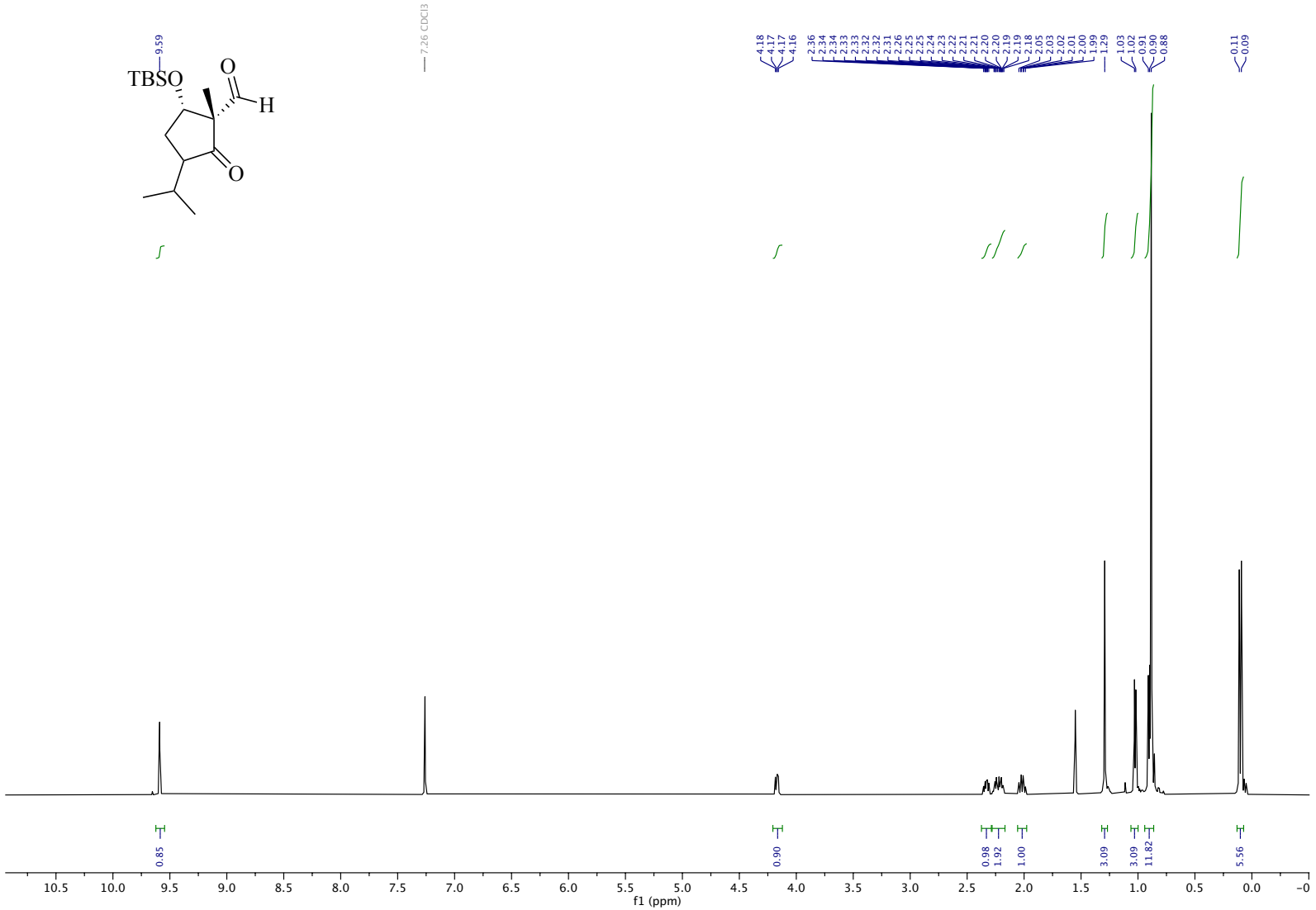

Figure B.10. ^{1}H NMR (600 MHz, $CDCl_3$), **2.08** (major diastereomer)

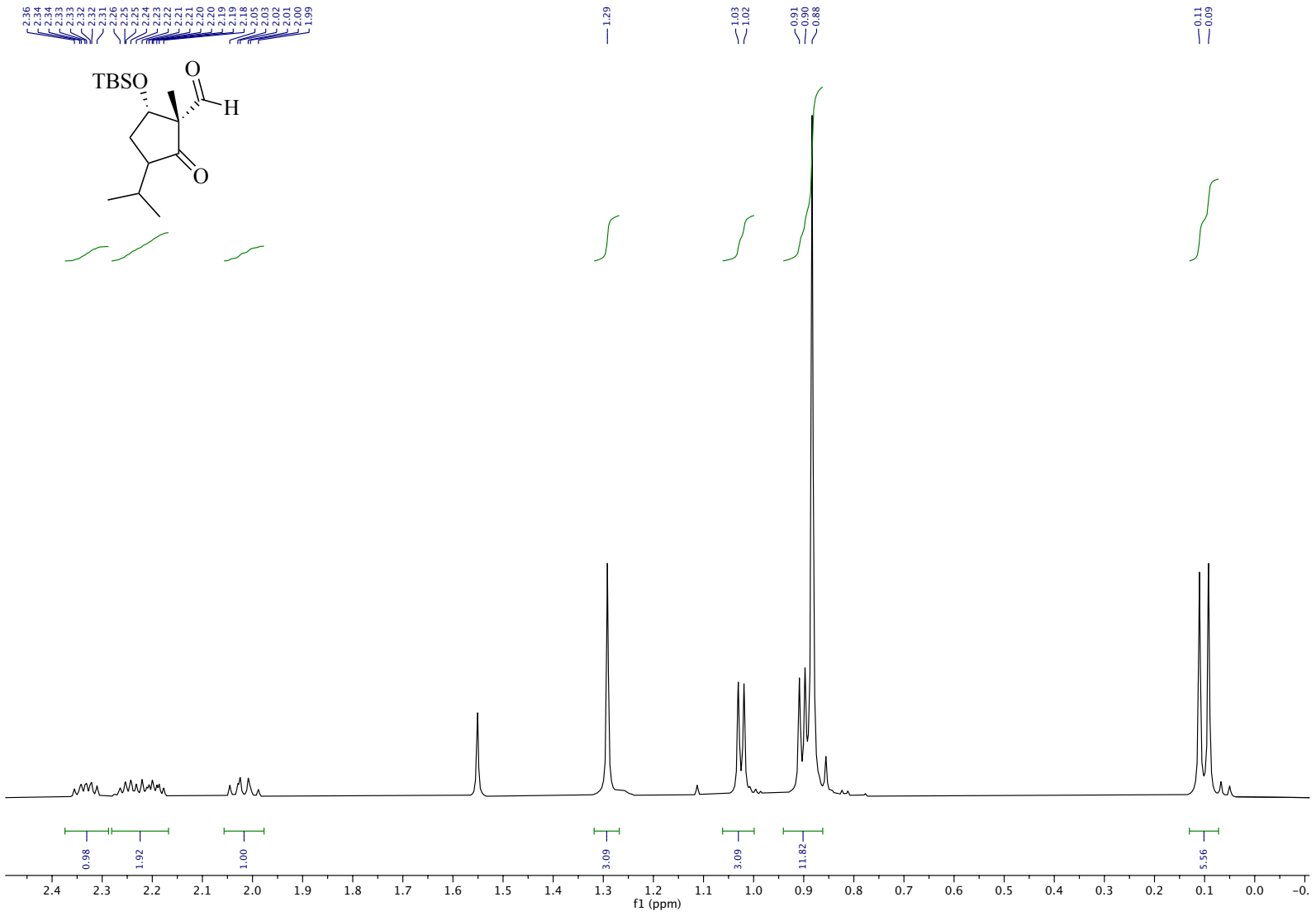

Figure B.11. ^{1}H NMR (600 MHz, $CDCl_3$), **2.08** (major diastereomer, inset)

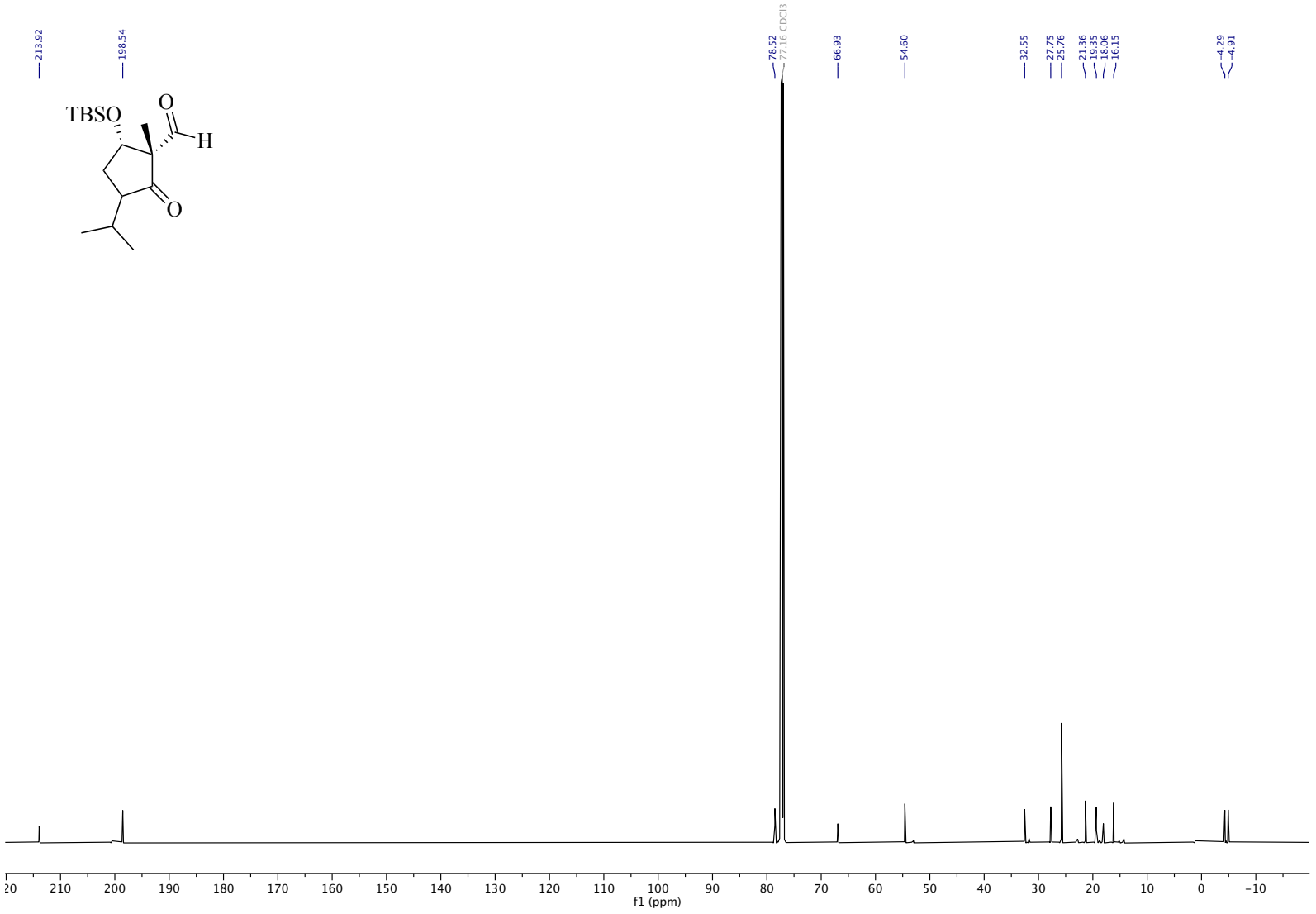

Figure B.12. ^{13}C NMR (151 MHz, $CDCl_3$), **2.08** (major diastereomer)

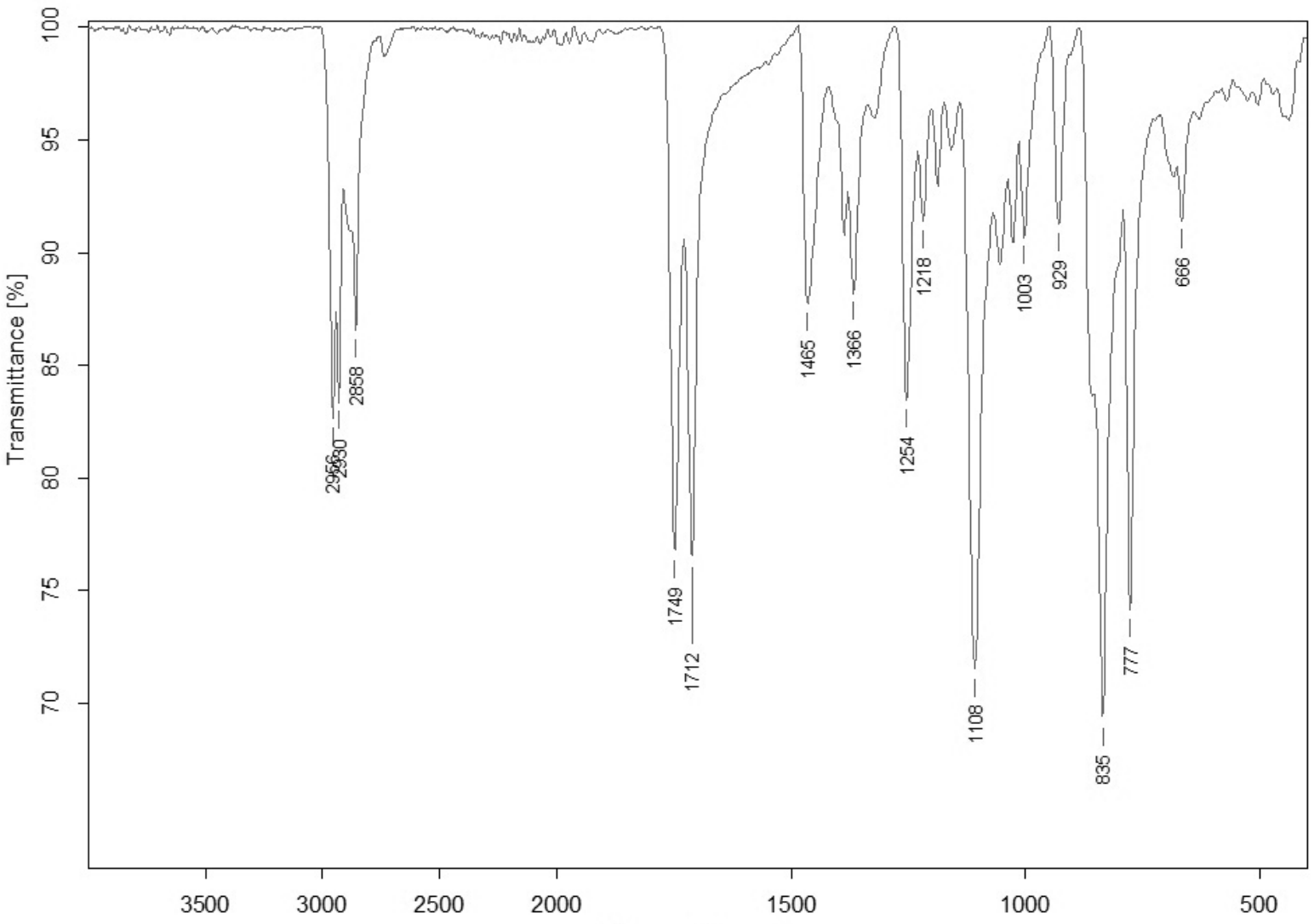

Figure B.13. IR (ATR), **2.08** (major diastereomer)

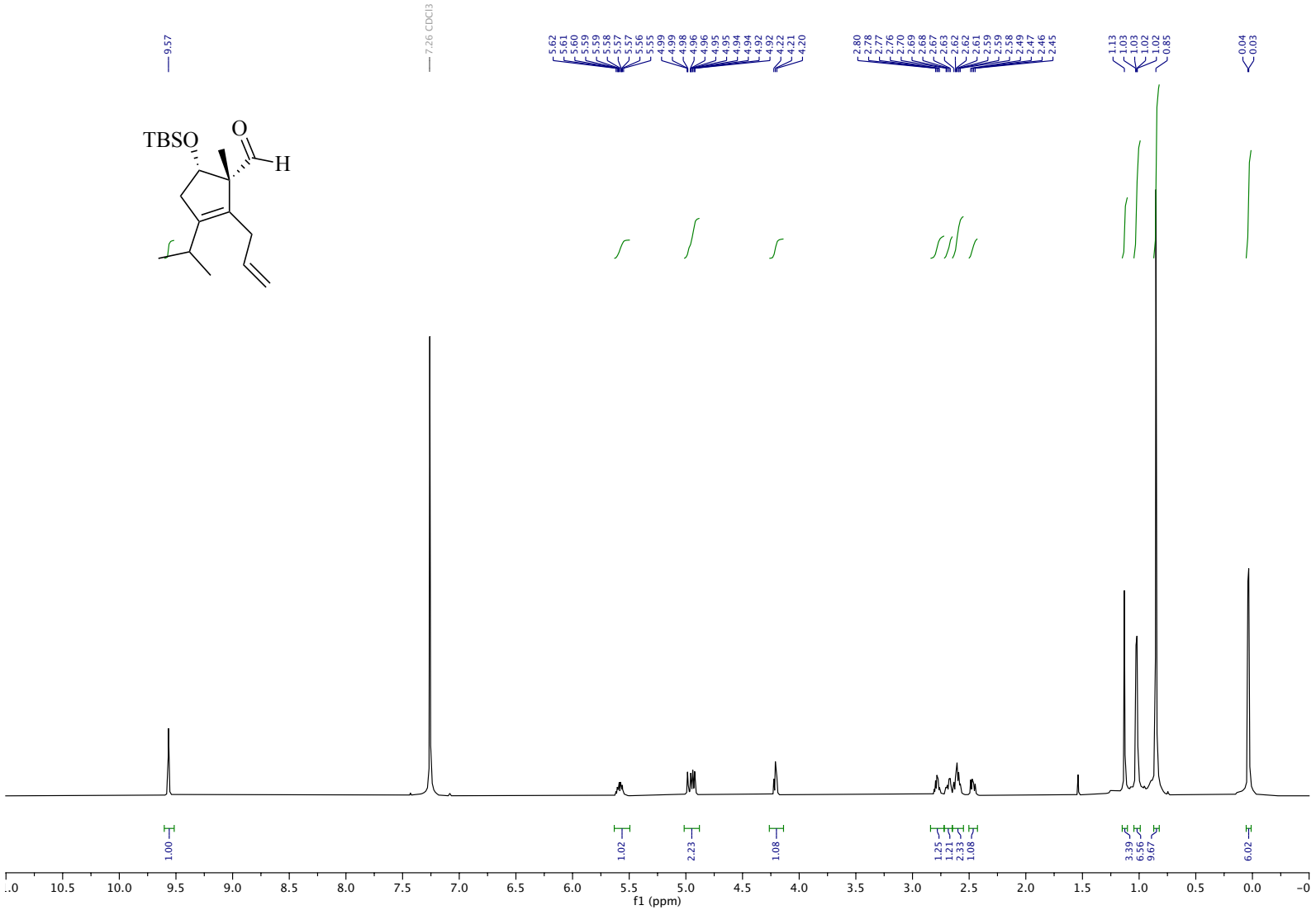

Figure B.14. ^{1}H NMR (600 MHz, $CDCl_3$), **2.06** (inset)

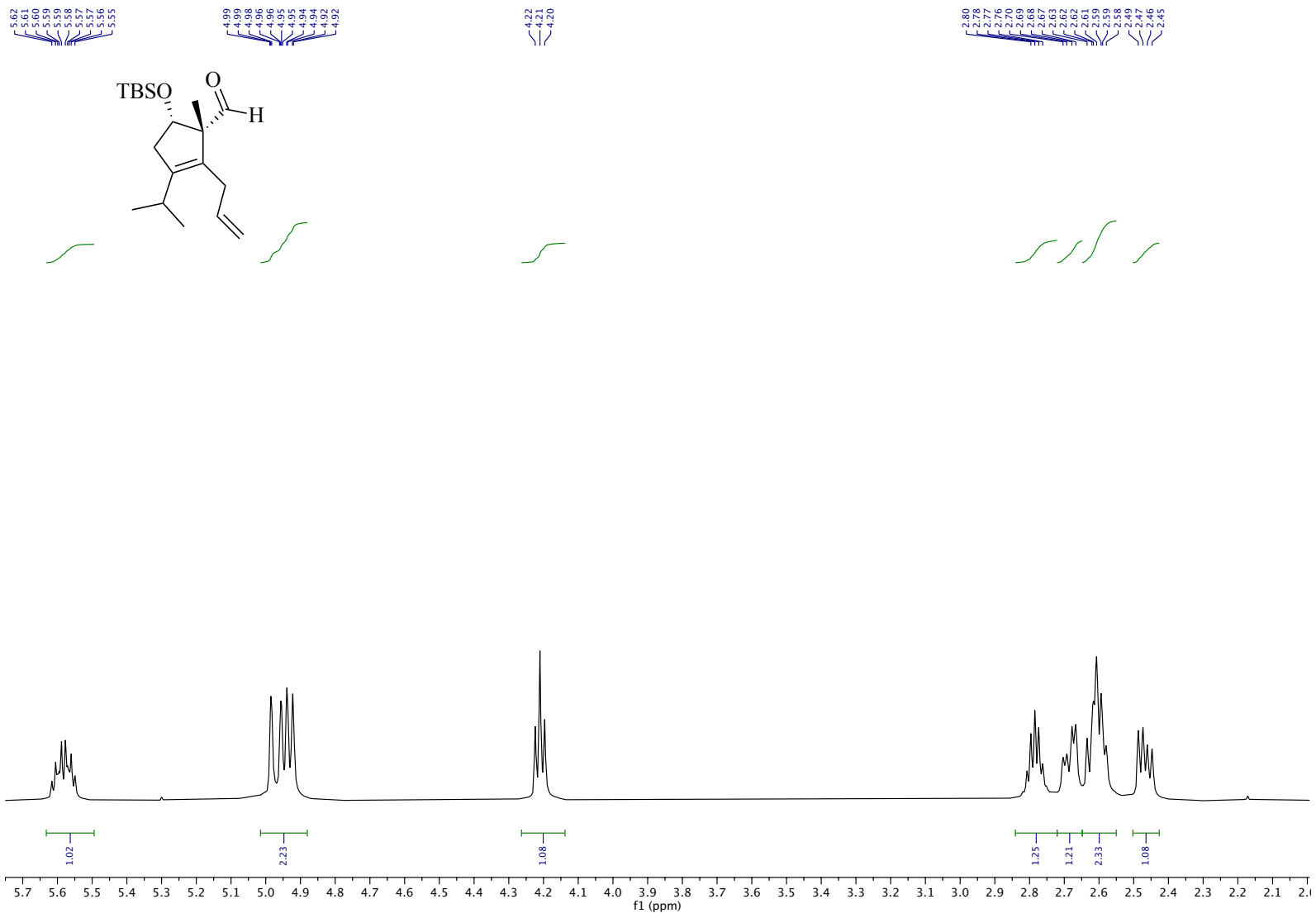

Figure B.15. ^{1}H NMR (600 MHz, $CDCl_3$), **2.06** (inset)

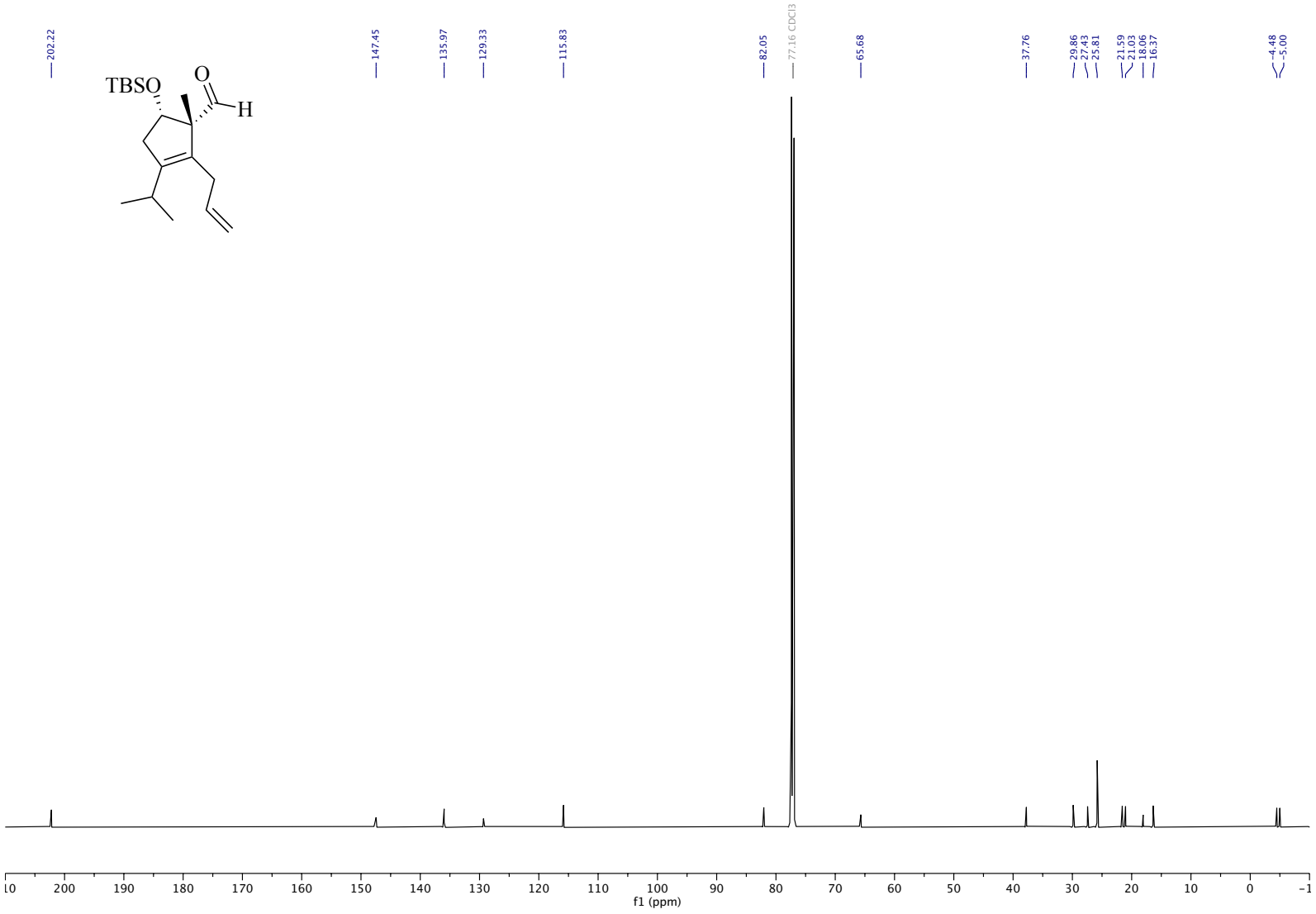

Figure B.16. ^{13}C NMR (151 MHz, $CDCl_3$), **2.06**

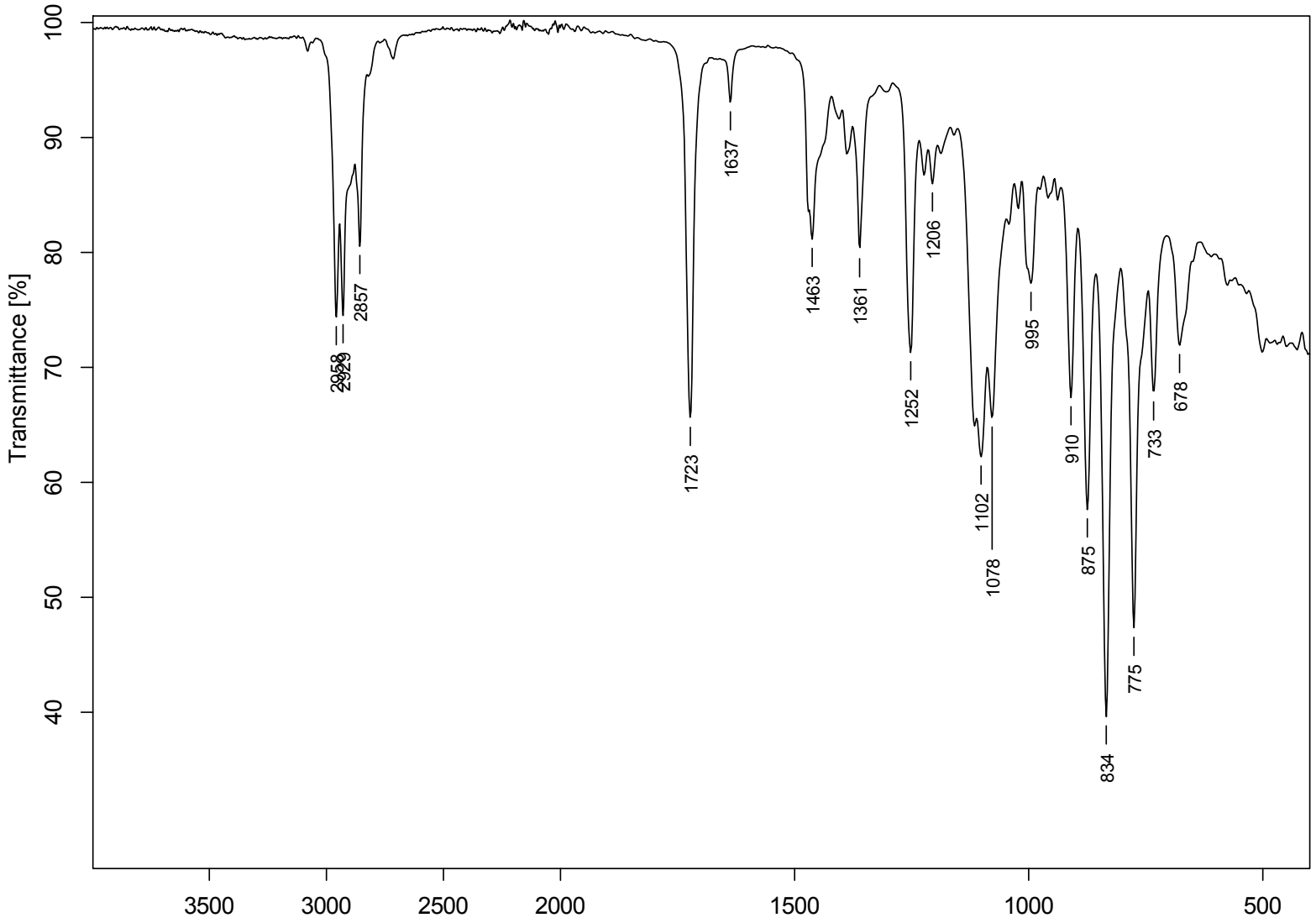

Figure B.17. IR (ATR), **2.06**

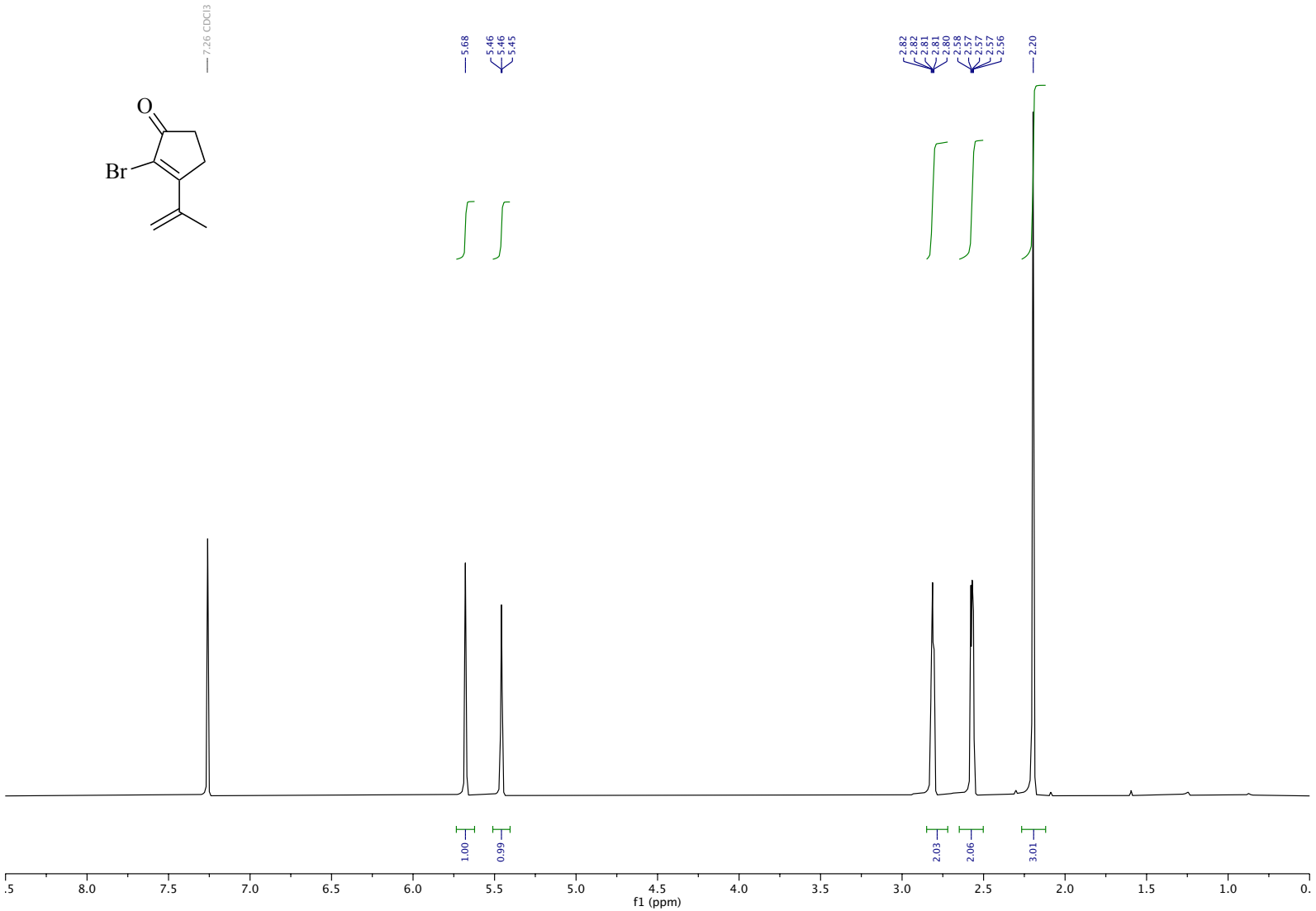

Figure B.18. ^{1}H NMR (600 MHz, $CDCl_3$), **2.16**

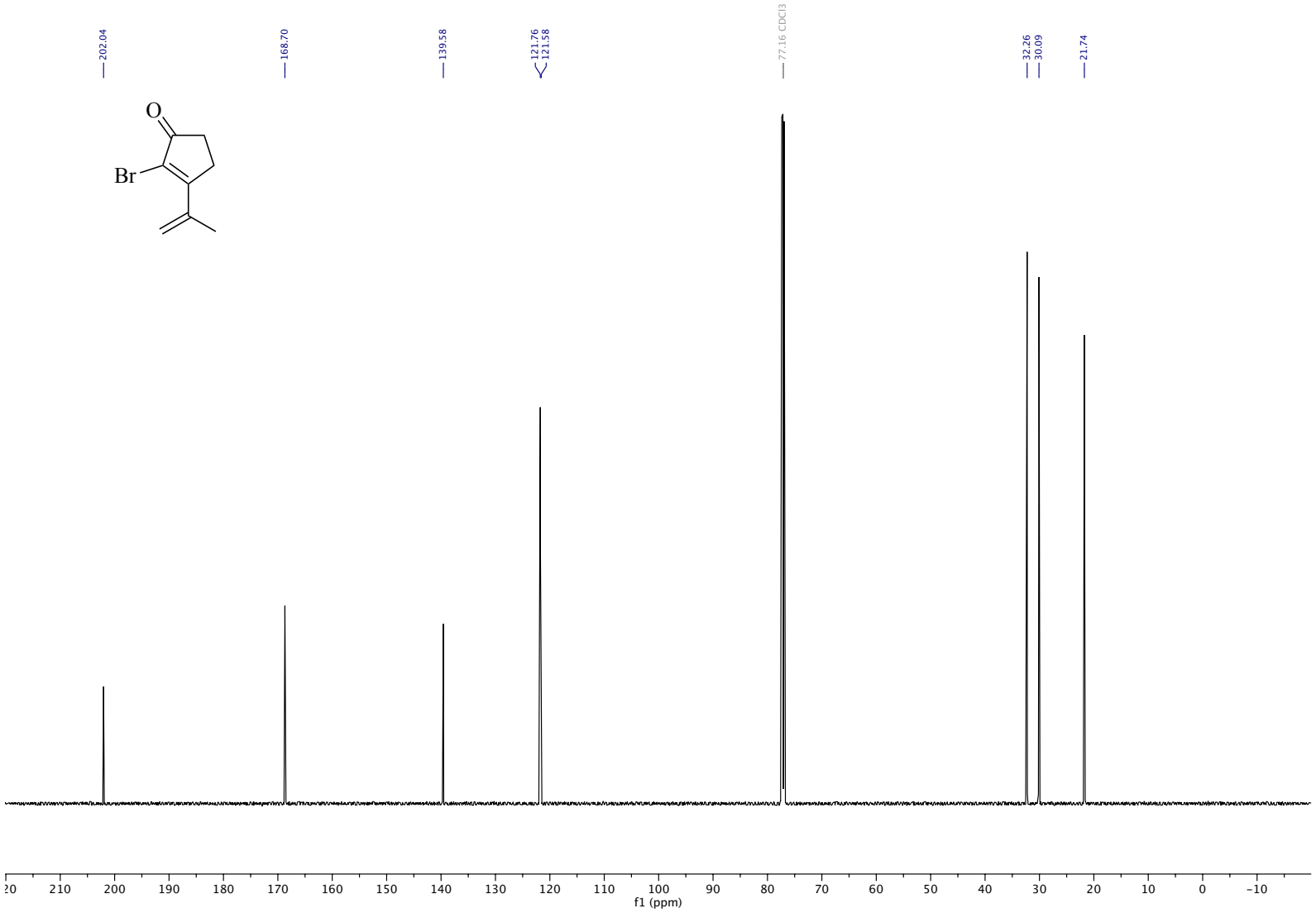

Figure B.19. ^{13}C NMR (151 MHz, $CDCl_3$), **2.16**

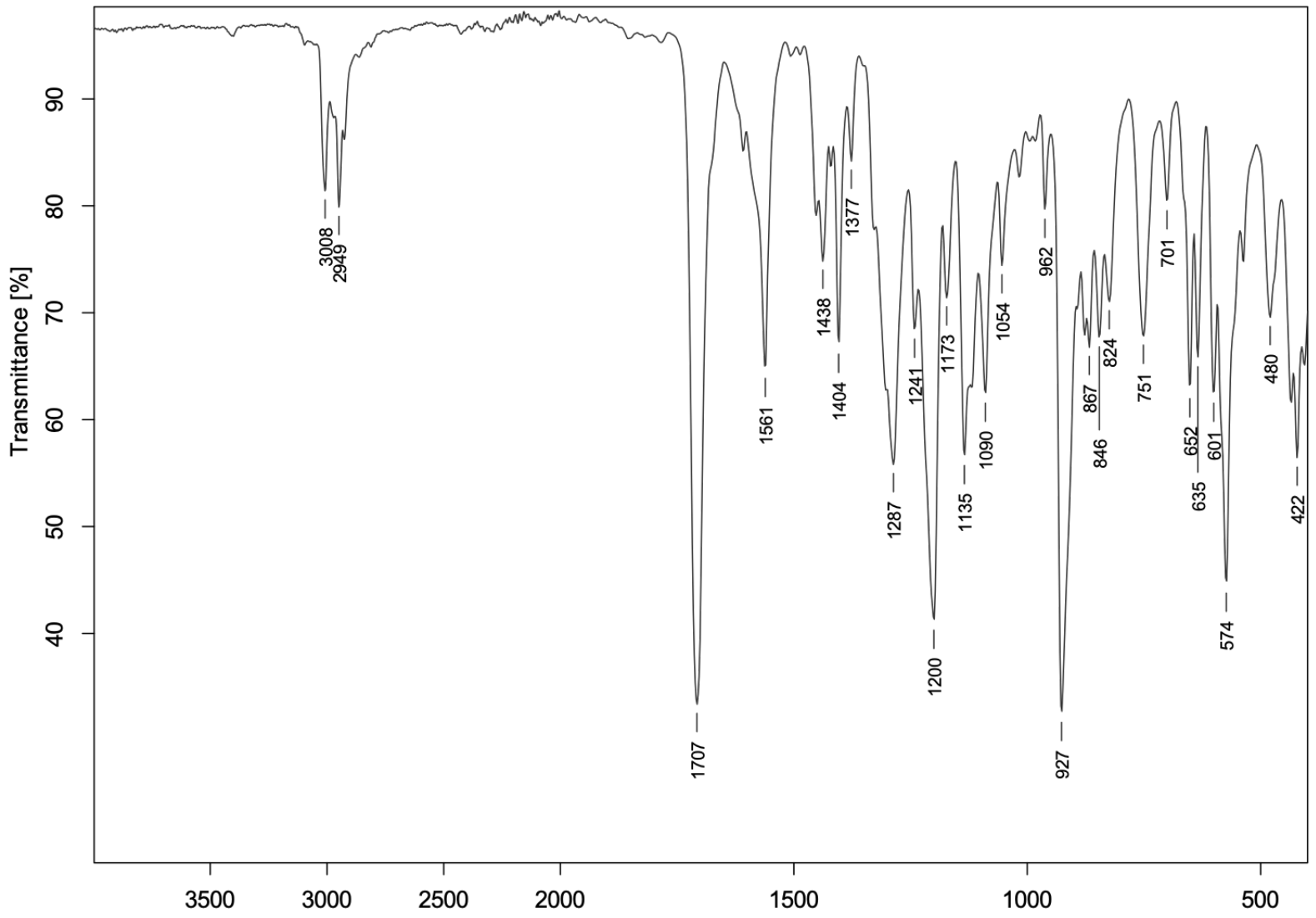

Figure B.20. IR (ATR), **2.16**

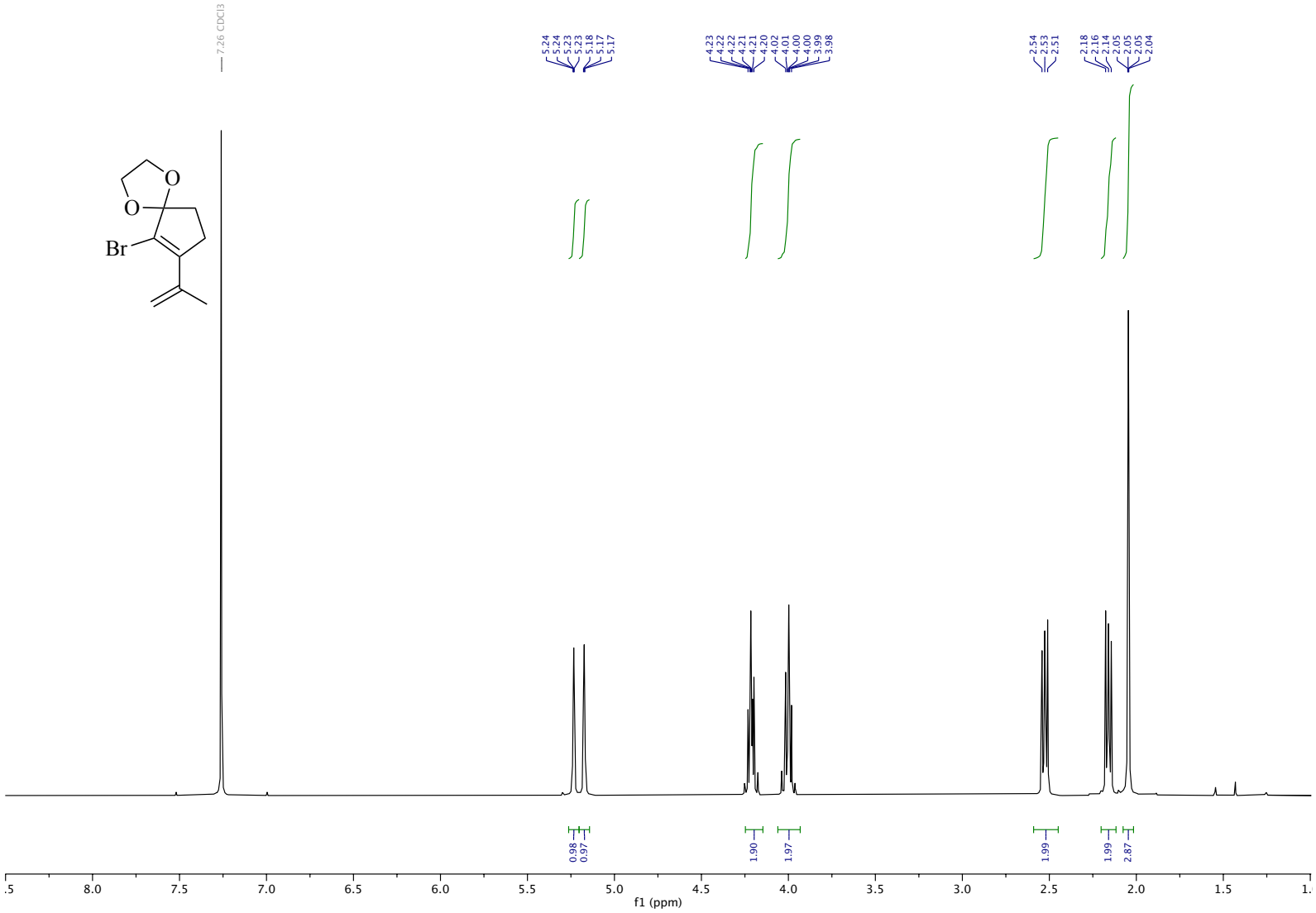

Figure B.21. ^{1}H NMR (400 MHz, $CDCl_3$), **2.07**

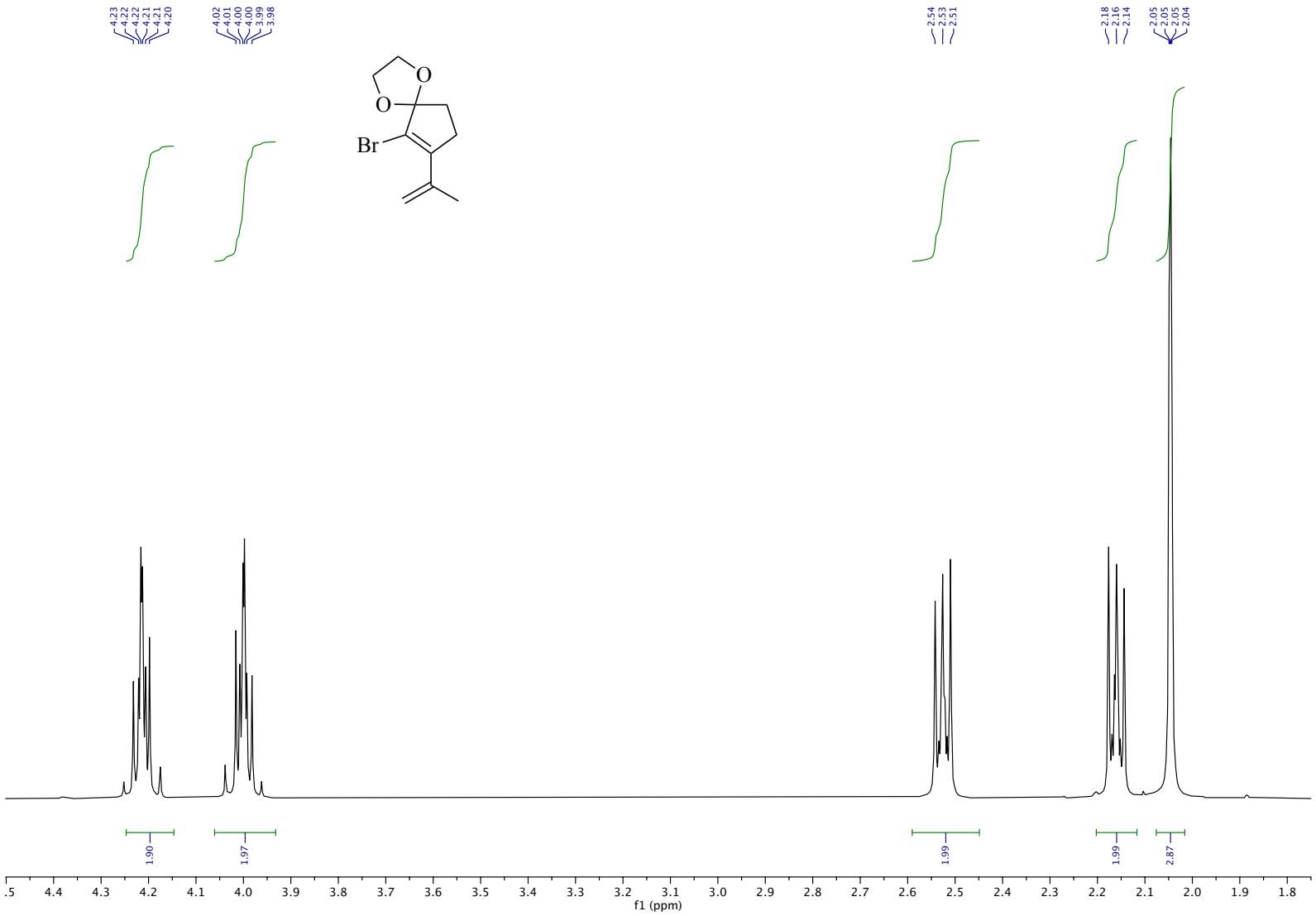

Figure B.22. ^{1}H NMR (400 MHz, $CDCl_3$), **2.07** (inset)

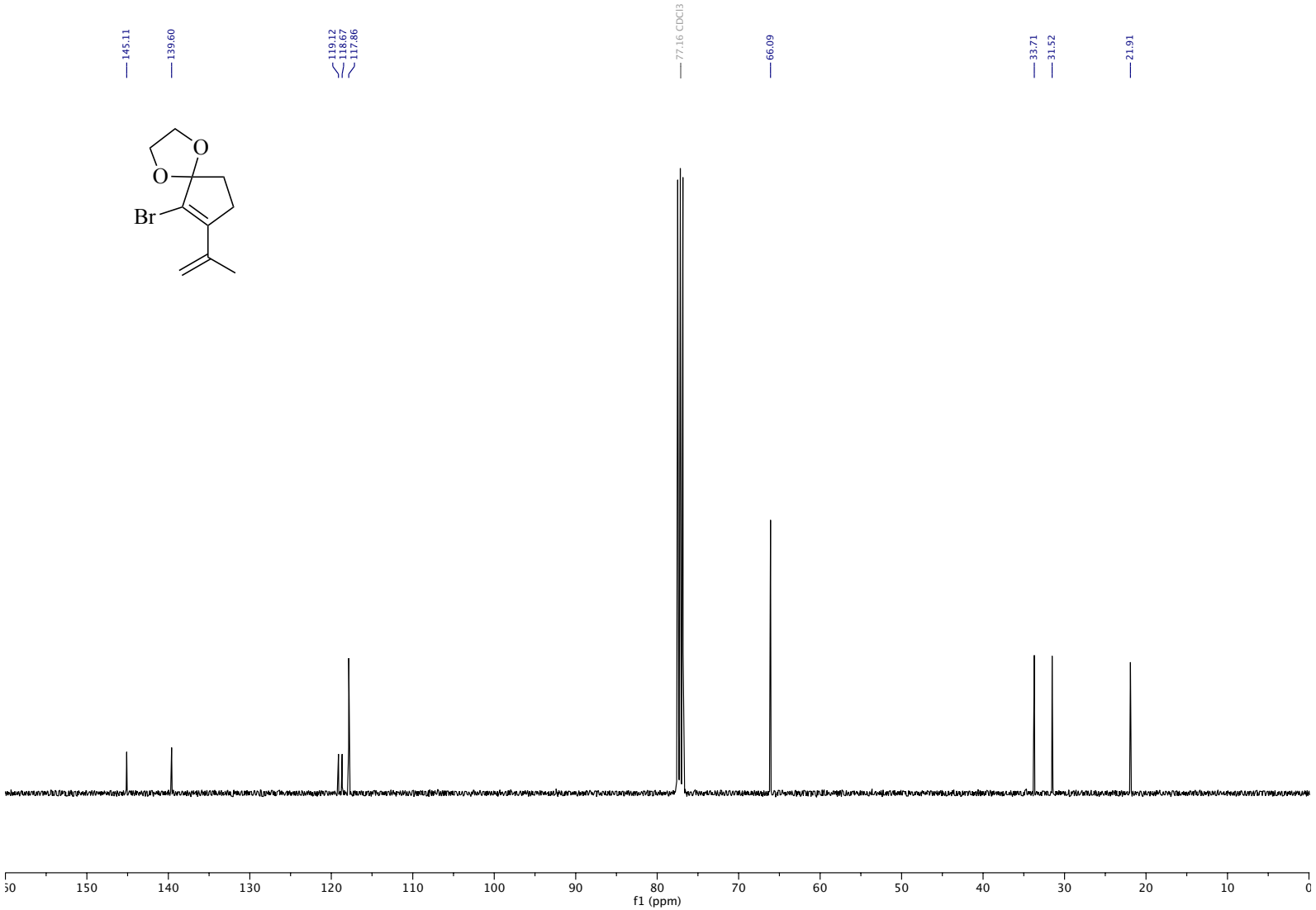

Figure B.23. ^{13}C NMR (101 MHz, $CDCl_3$), **2.07**

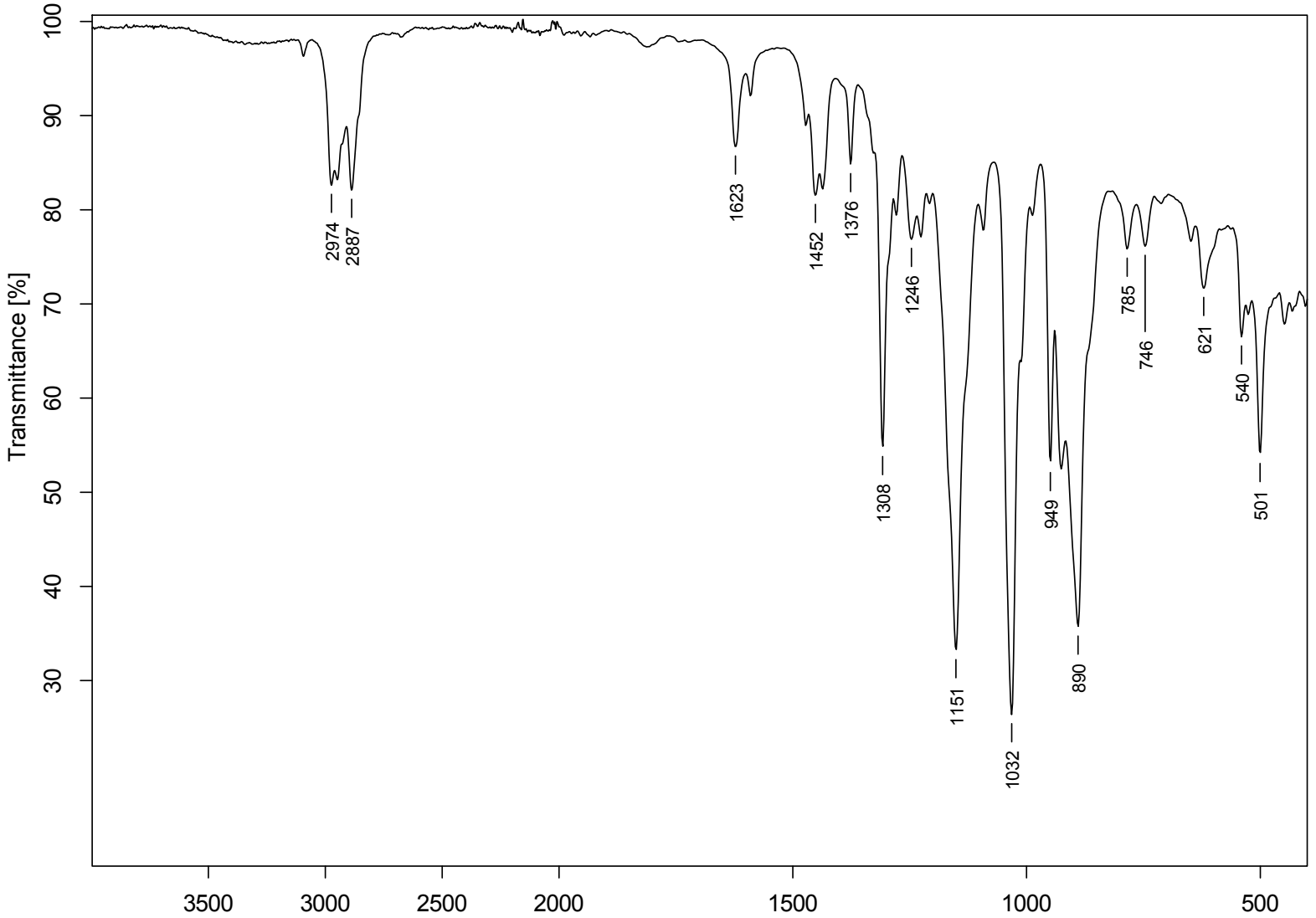

Figure B.24. IR (ATR), **2.07**

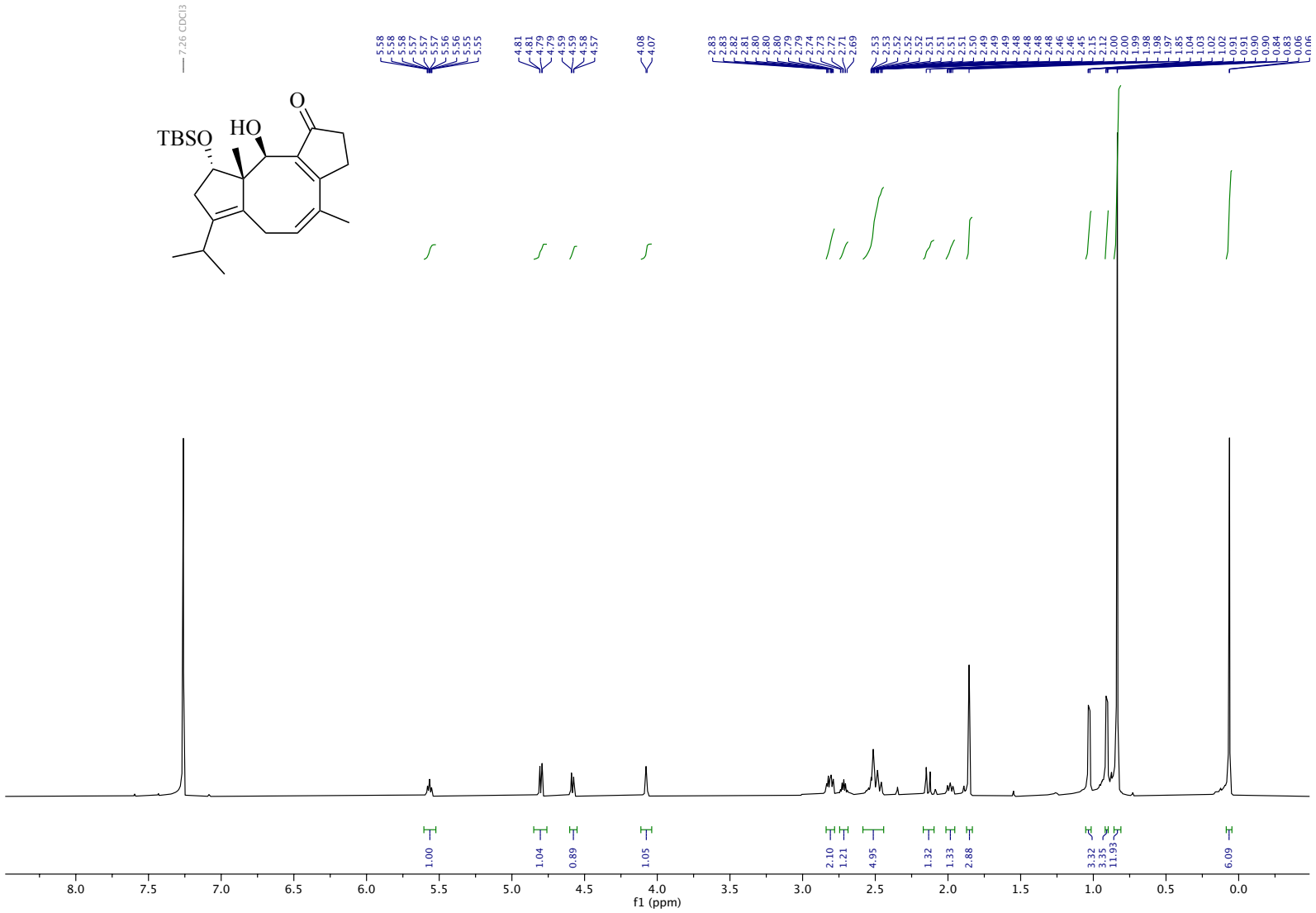

Figure B.25. ^{1}H NMR (400 MHz, $CDCl_3$), **2.04**

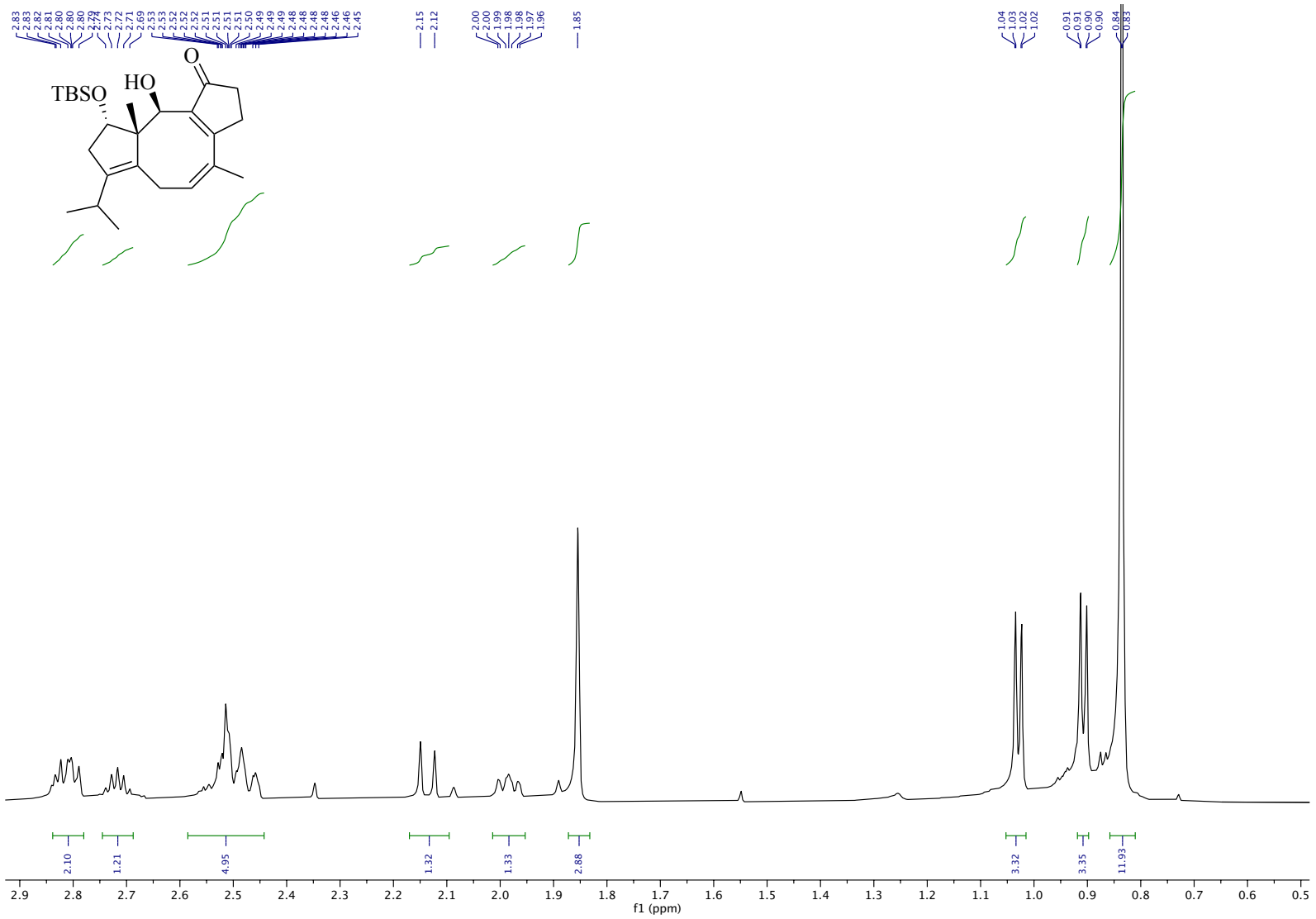

Figure B.26. ^{1}H NMR (400 MHz, $CDCl_3$), **2.04** (inset)

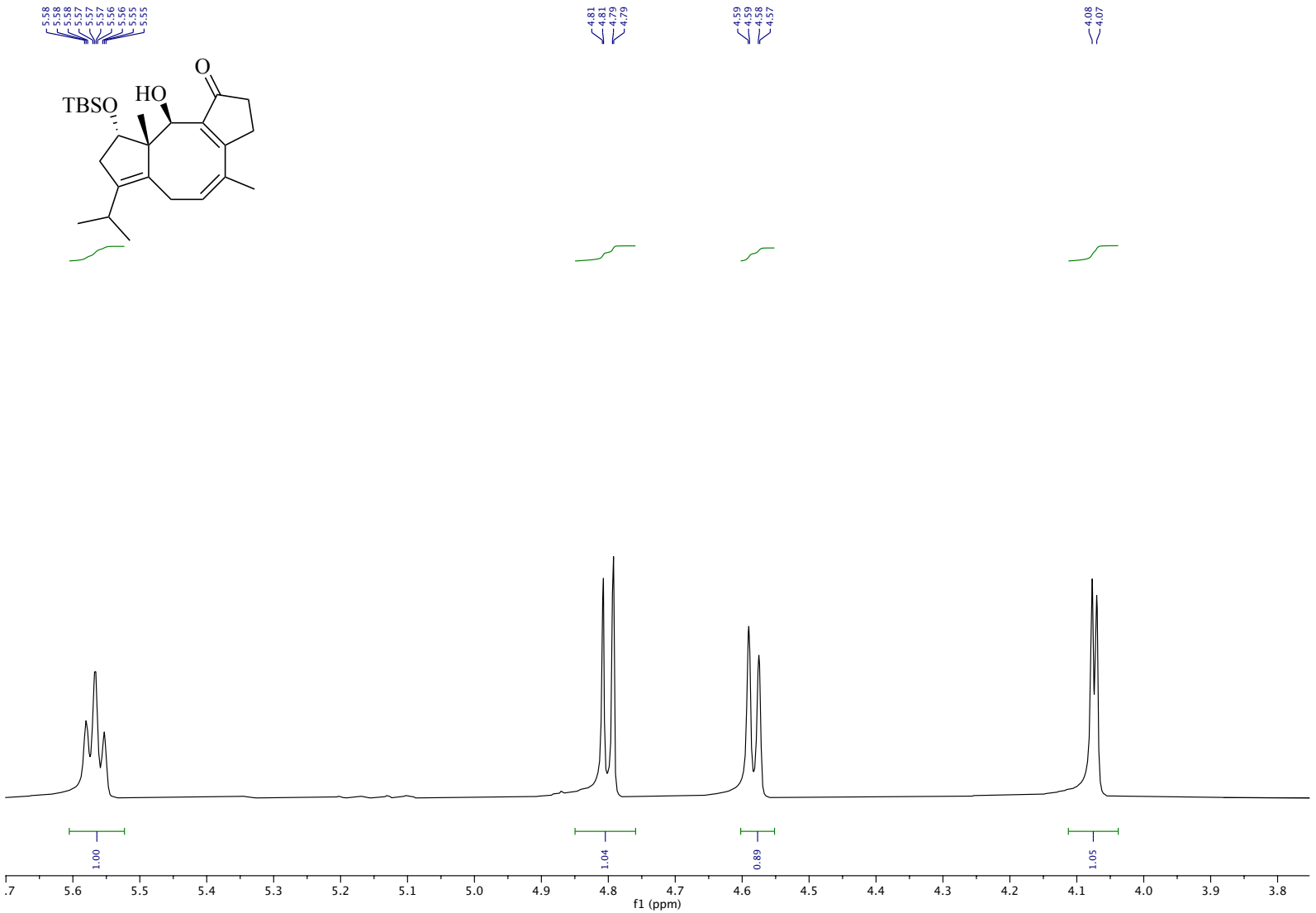

Figure B.27. ^{1}H NMR (400 MHz, $CDCl_3$), **2.04** (inset)

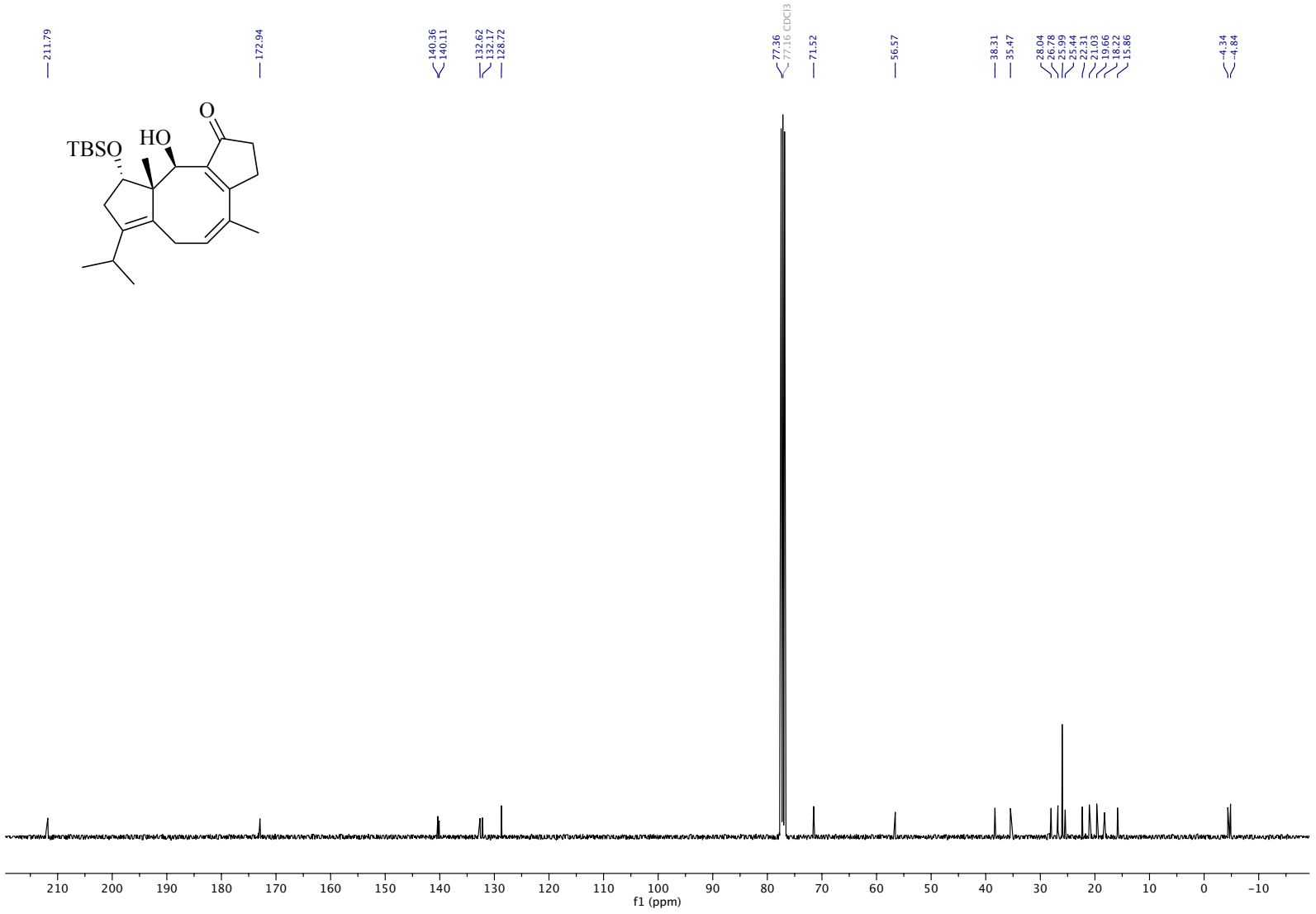

Figure B.28. ^{13}C NMR (151 MHz, $CDCl_3$), **2.04**

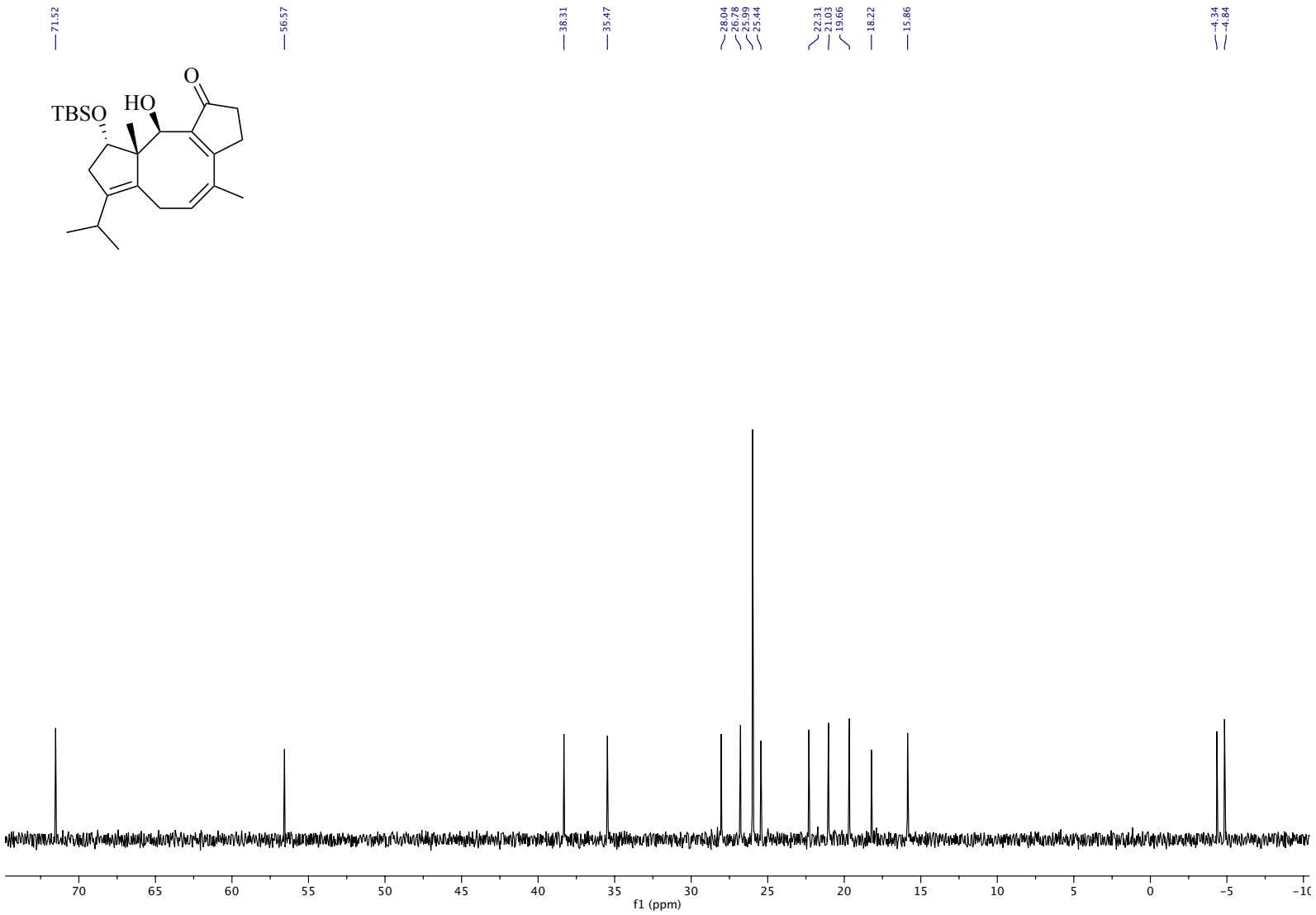

Figure B.29. ^{13}C NMR (151 MHz, $CDCl_3$), **2.04** (inset)

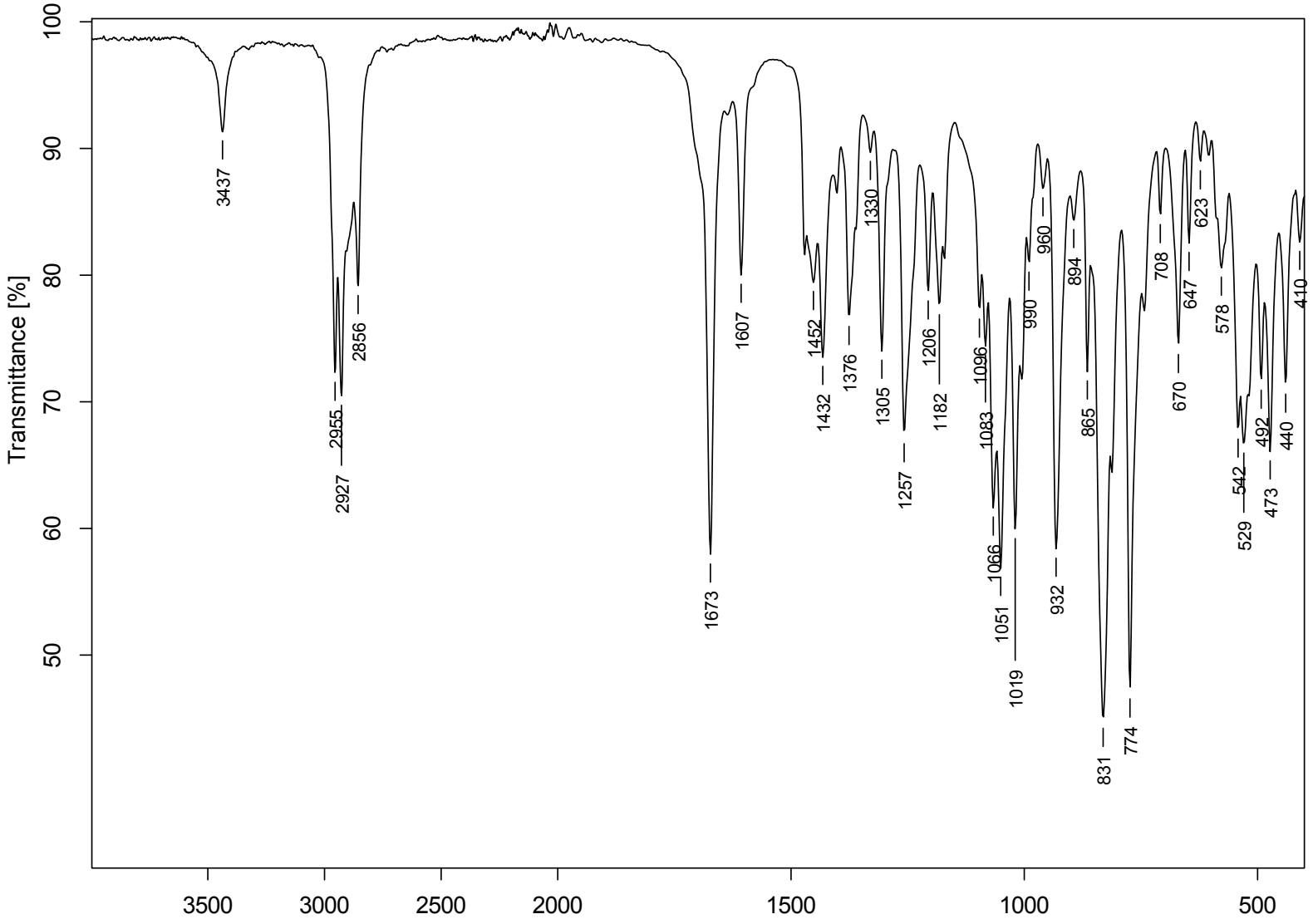

Figure B.30. IR (ATR), **2.04**

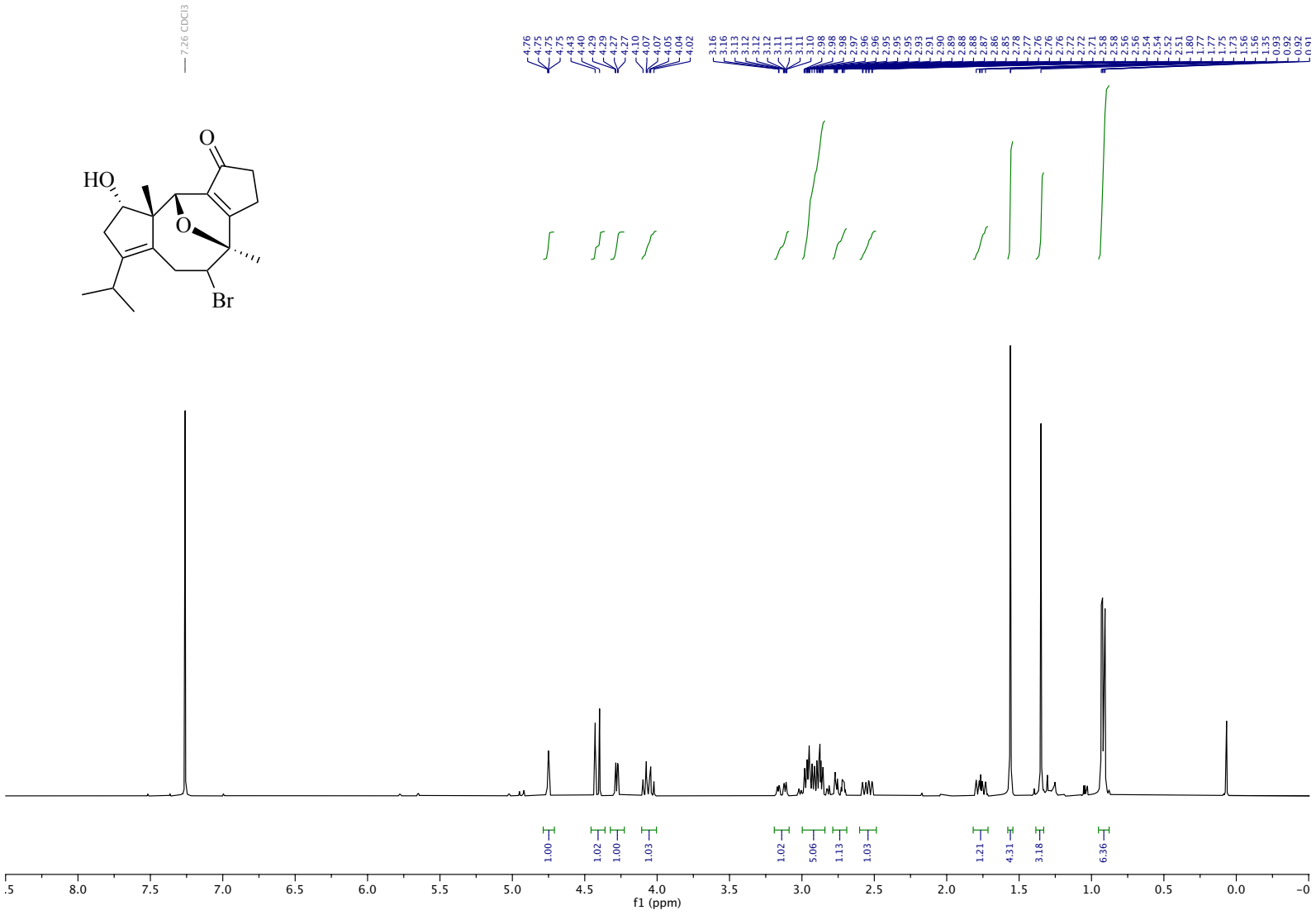

Figure B.31. ^{1}H NMR (400 MHz, $CDCl_3$), **2.19**

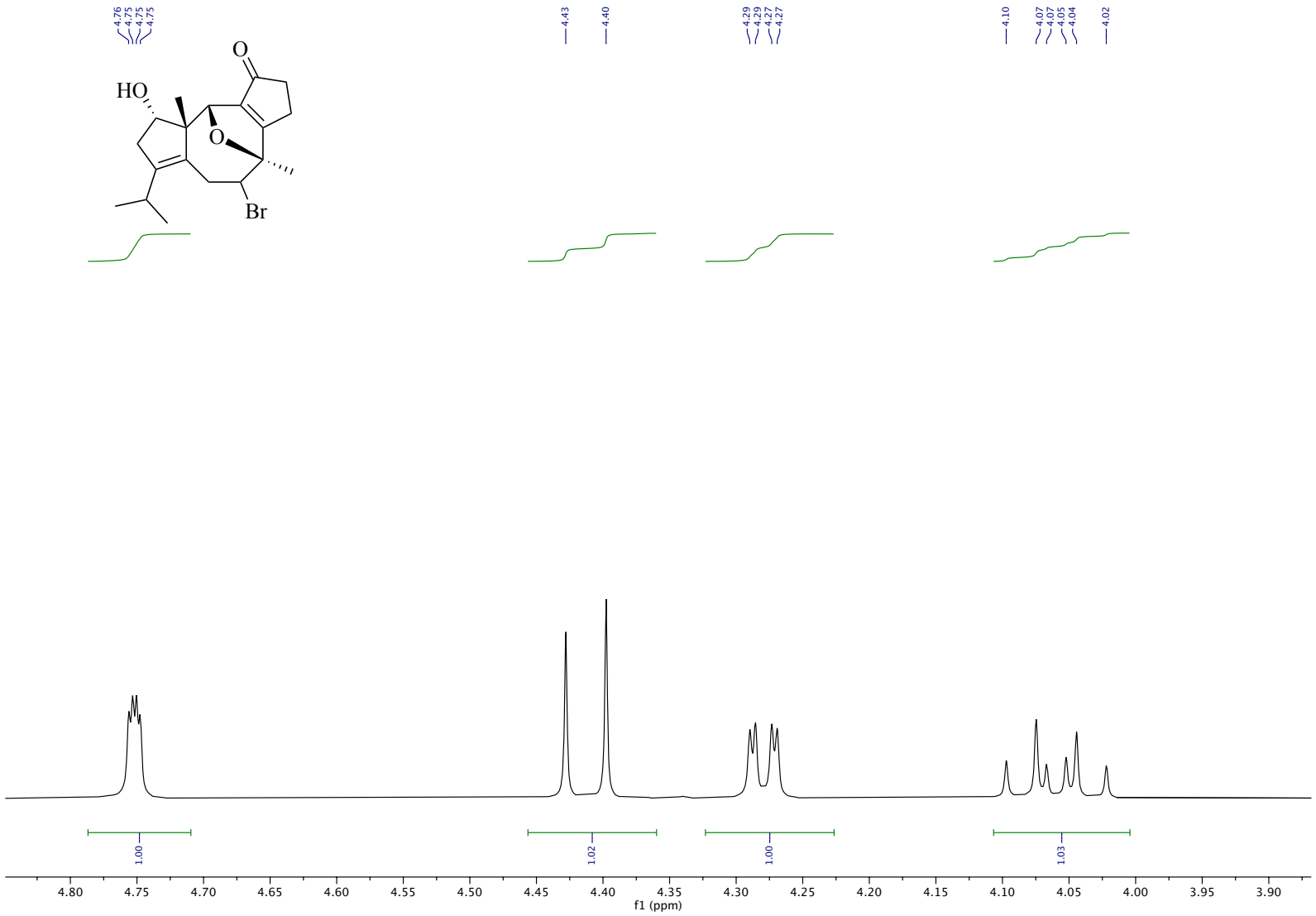

Figure B.32. ^{1}H NMR (400 MHz, $CDCl_3$), **2.19** (inset)

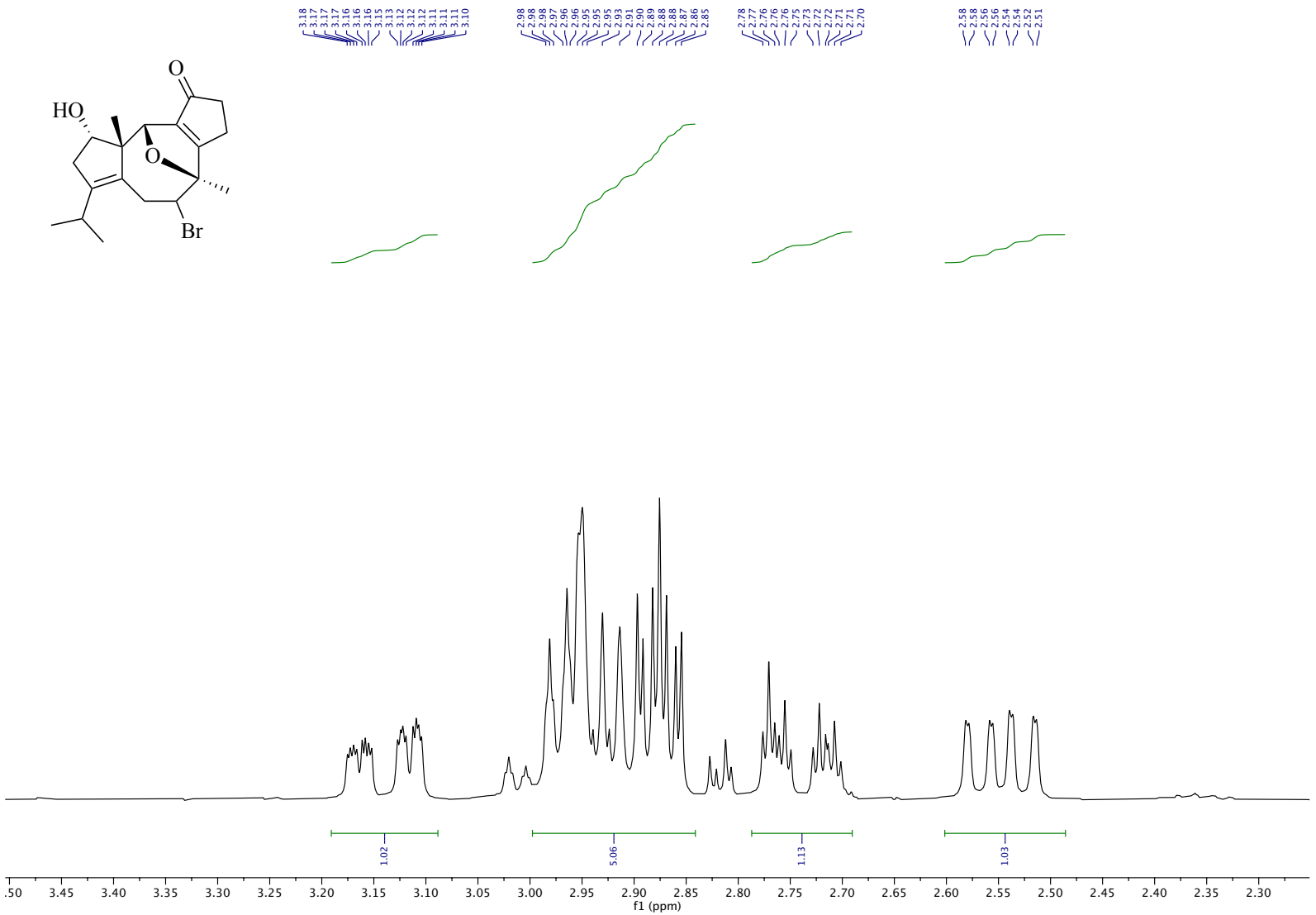

Figure B.33. ^{1}H NMR (400 MHz, $CDCl_3$), **2.19** (inset)

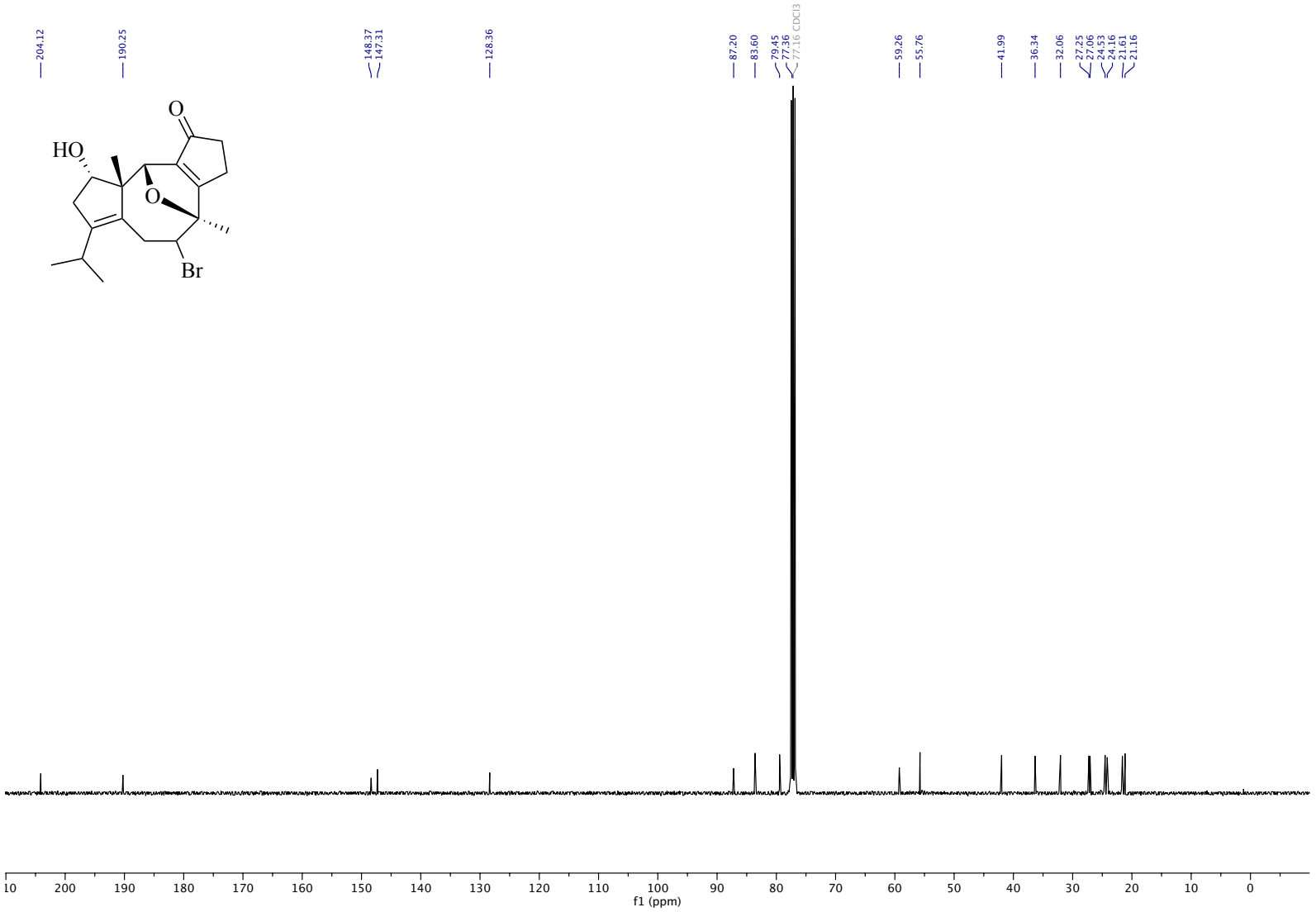

Figure B.34. ^{13}C NMR (101 MHz, $CDCl_3$), **2.19**

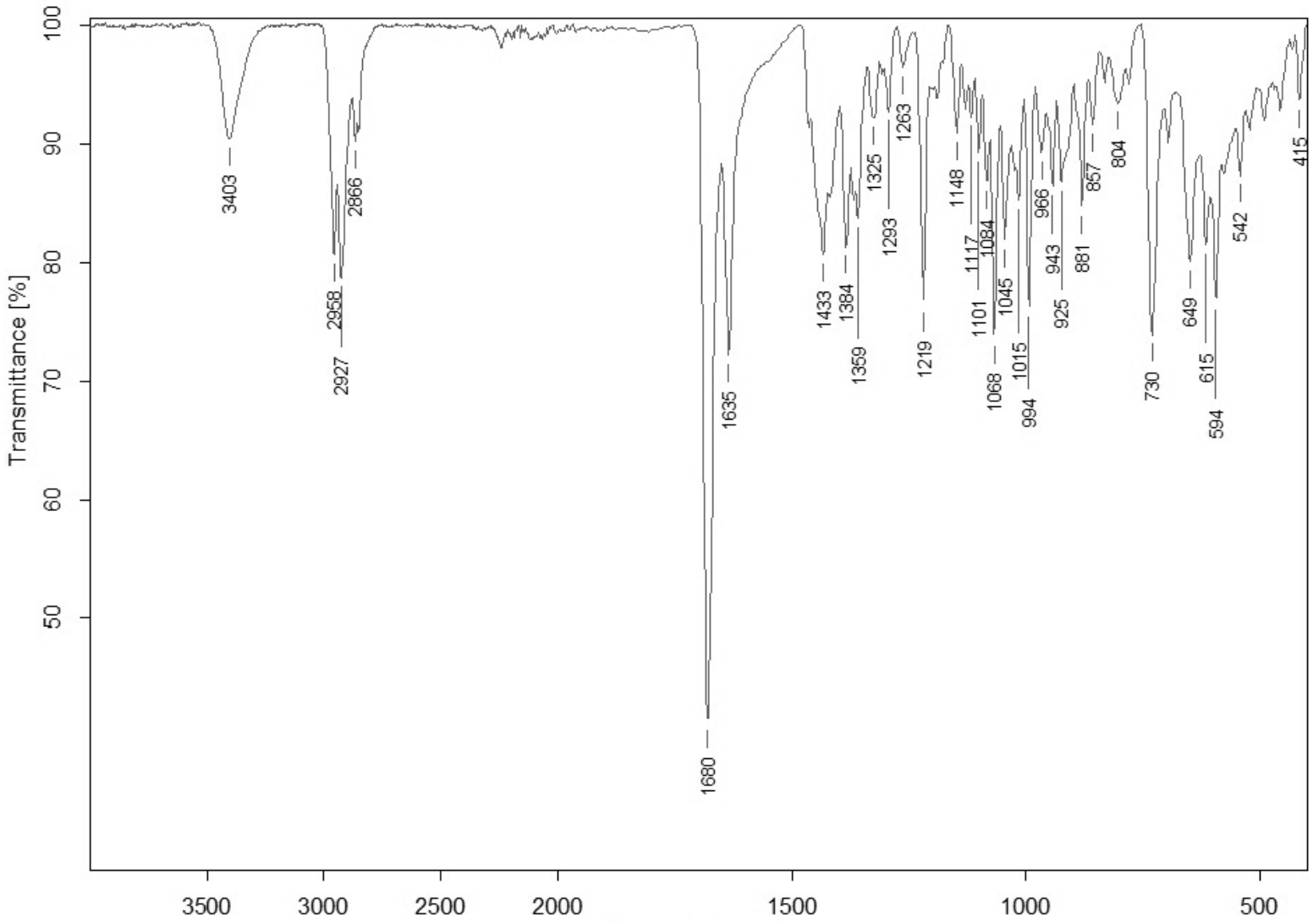

Figure B.35. IR (ATR), **2.19**

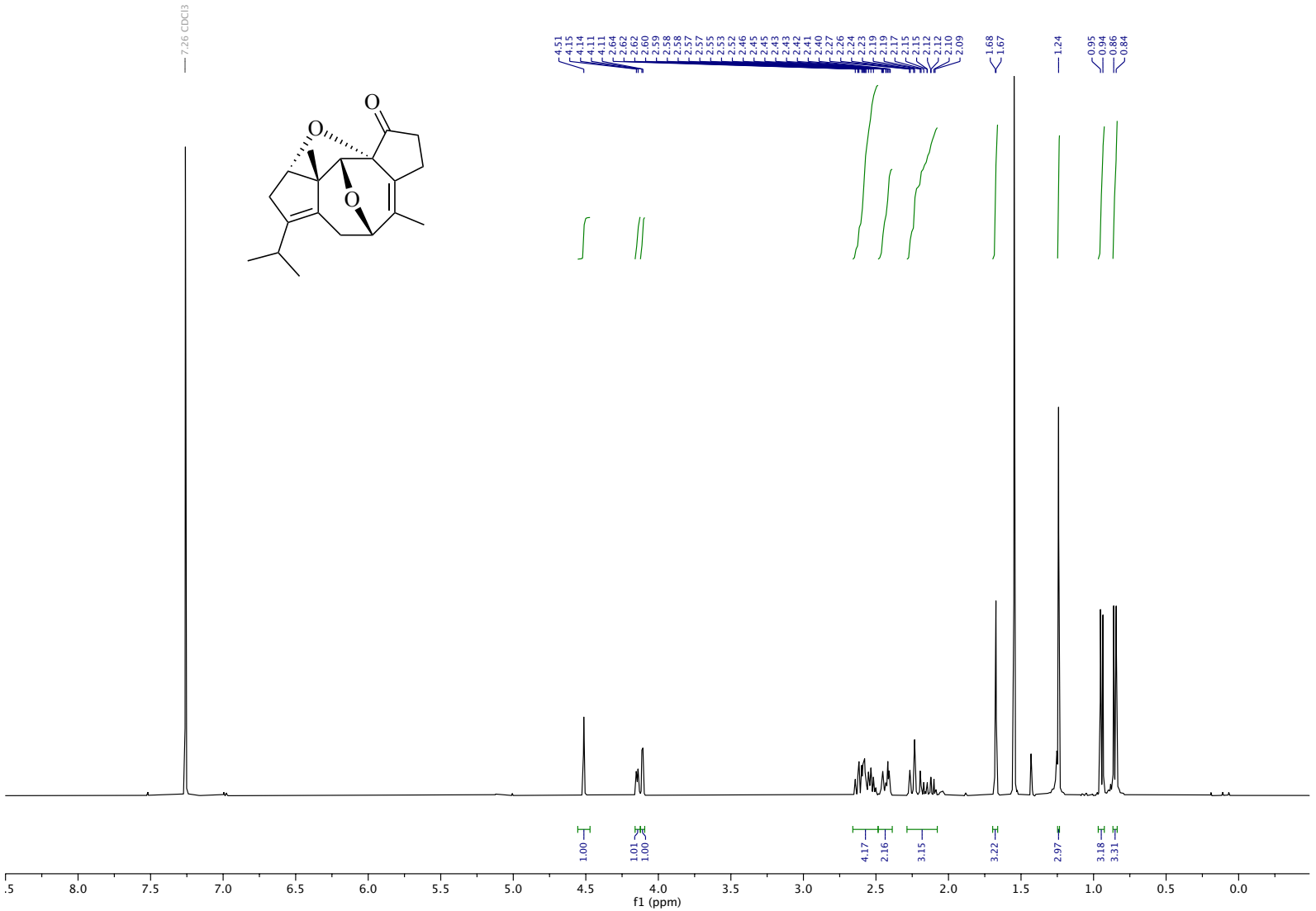

Figure B.36. ^{1}H NMR (400 MHz, $CDCl_3$), **2.20**

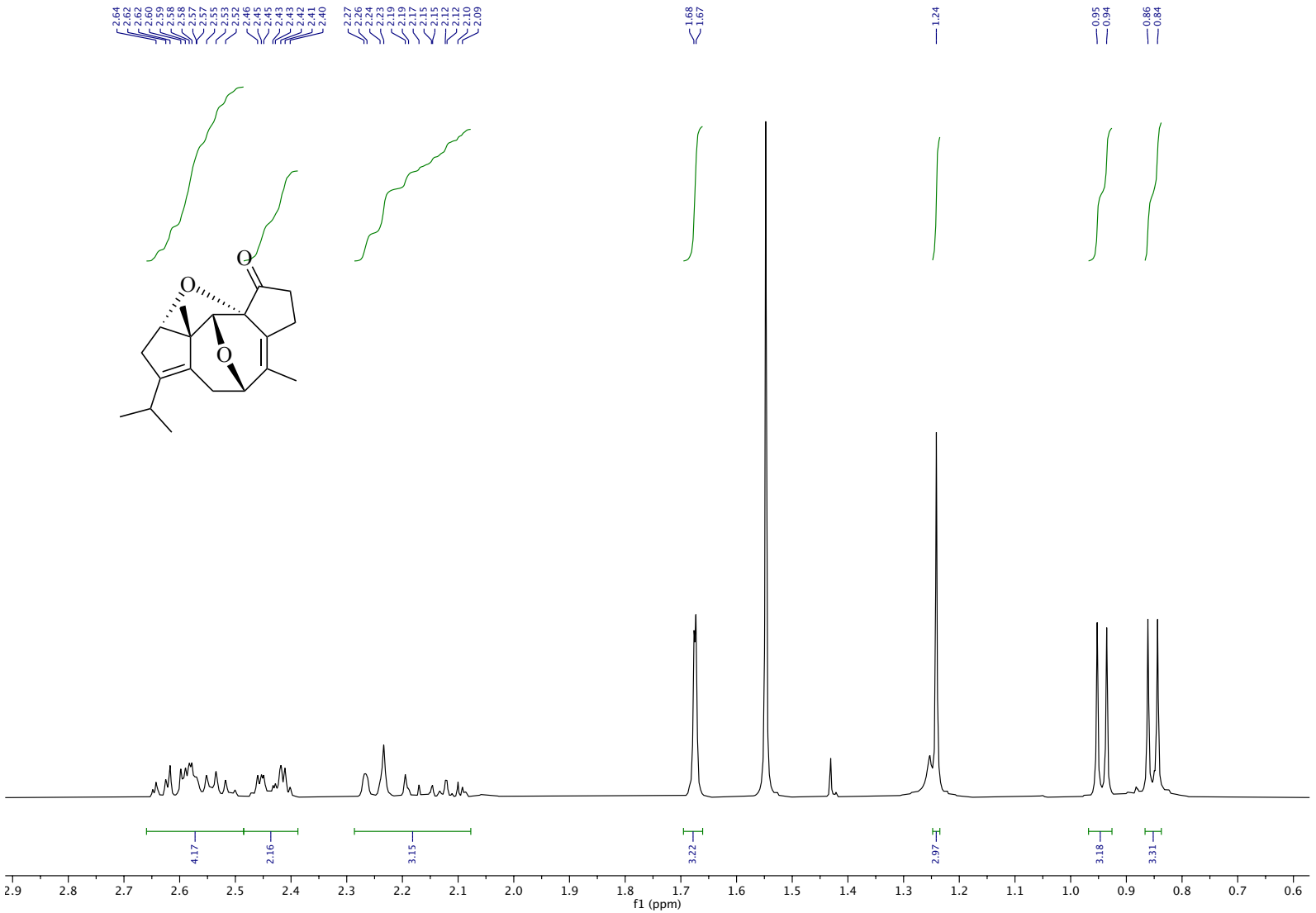

Figure B.37. ^{1}H NMR (400 MHz, $CDCl_3$), **2.20** (inset)

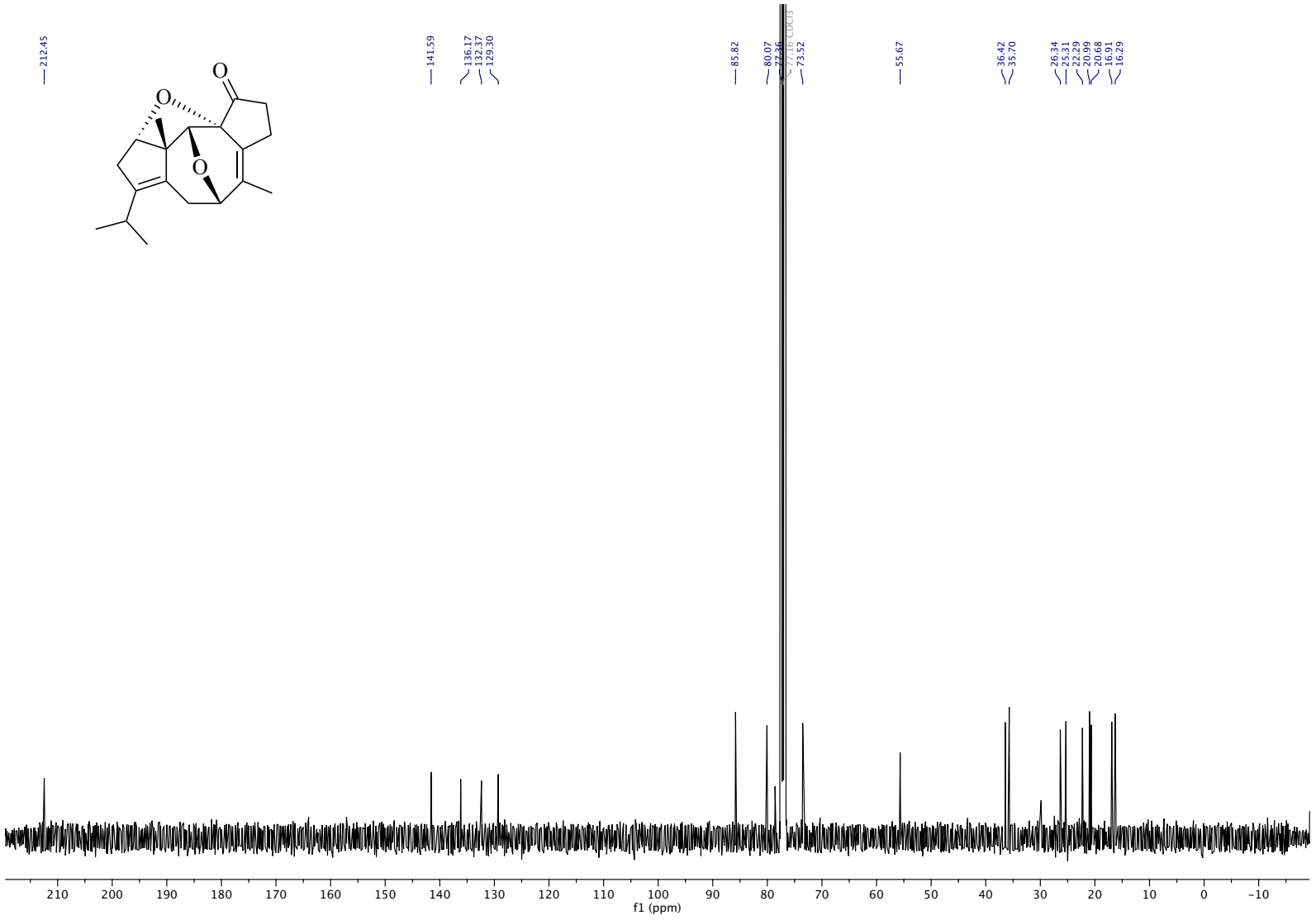

Figure B.38. ^{13}C NMR (101 MHz, $CDCl_3$), **2.20**

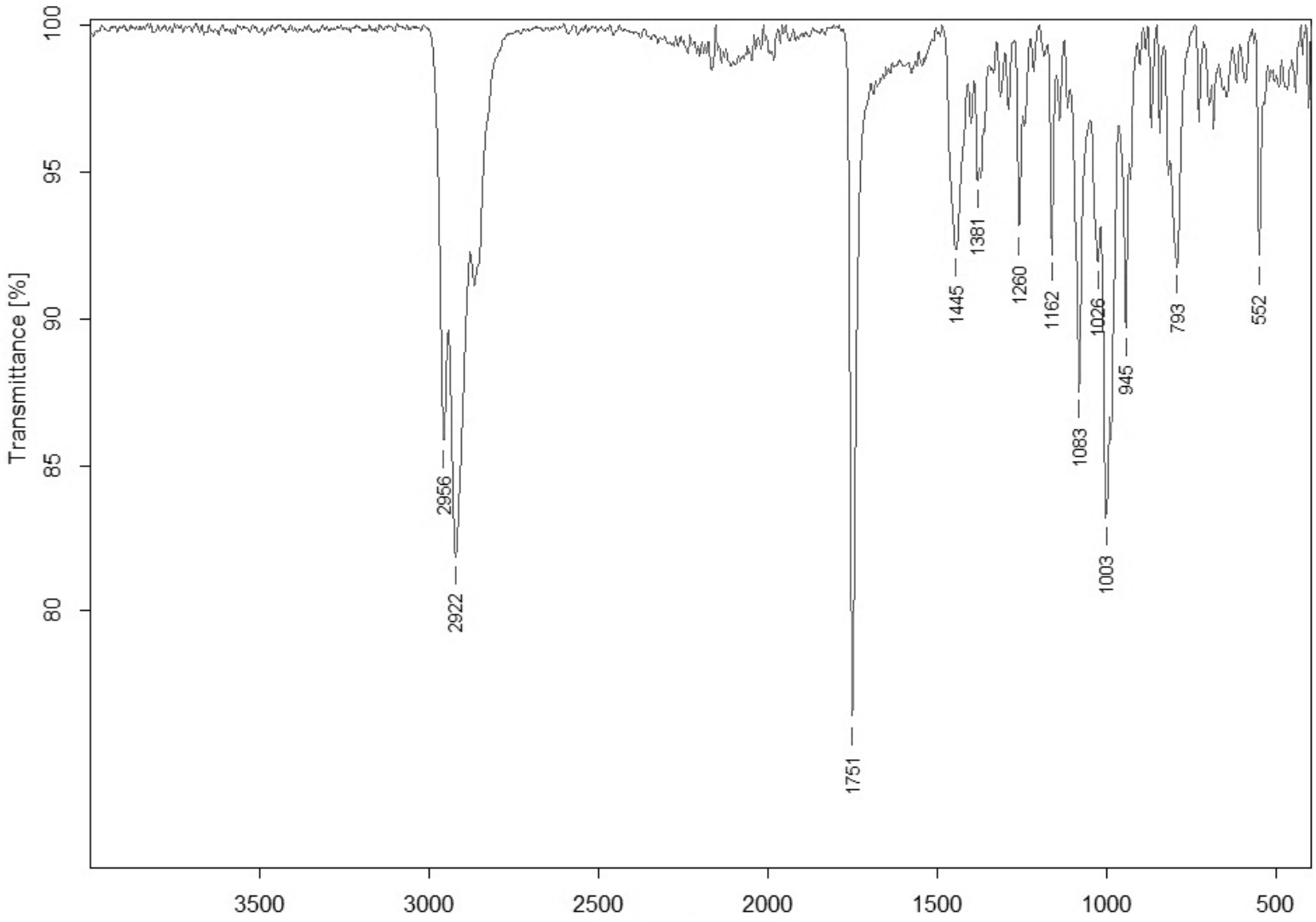

Figure B.39. IR (ATR), **2.20**

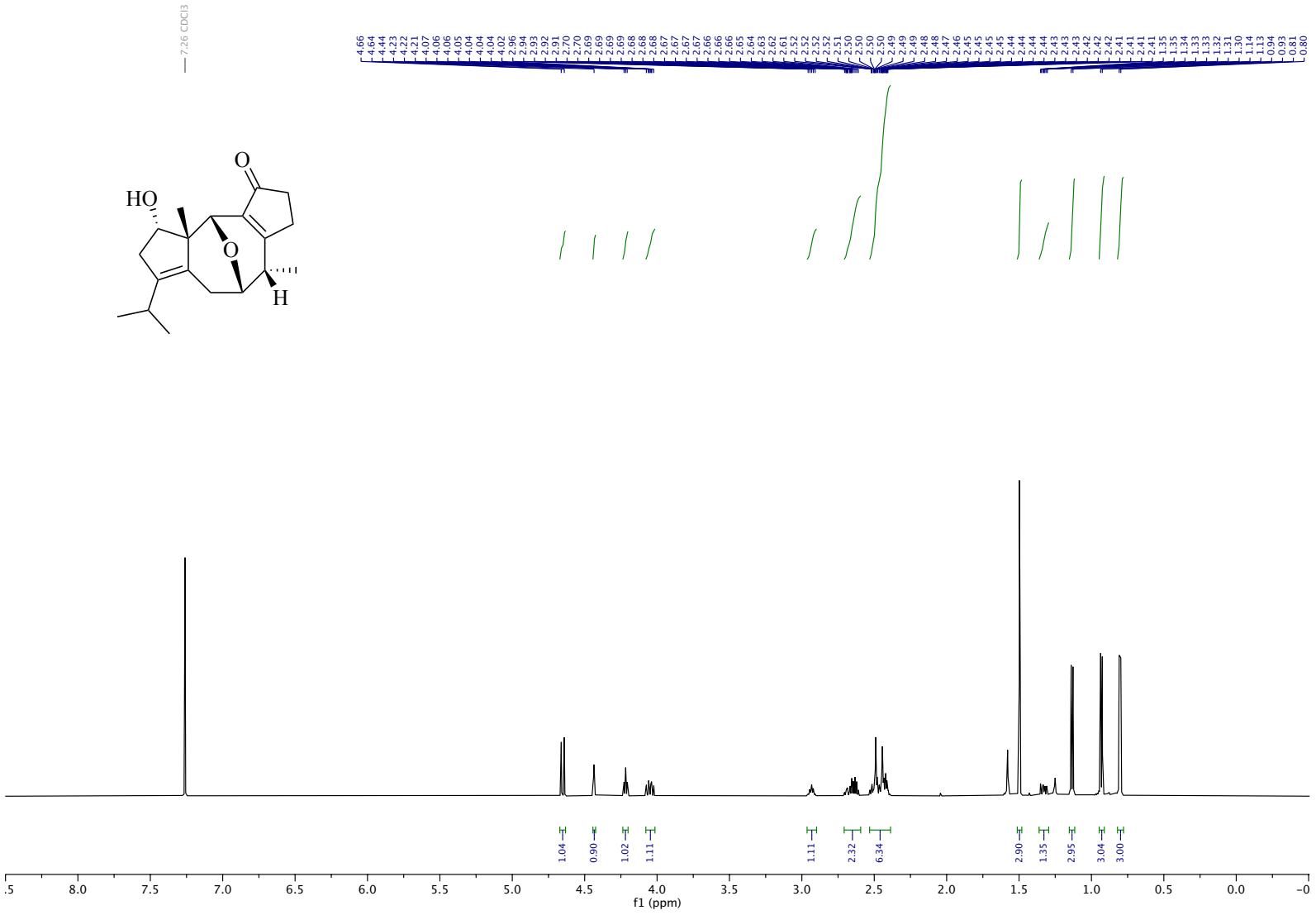

Figure B.40. ^{1}H NMR (600 MHz, $CDCl_3$), **2.21a**

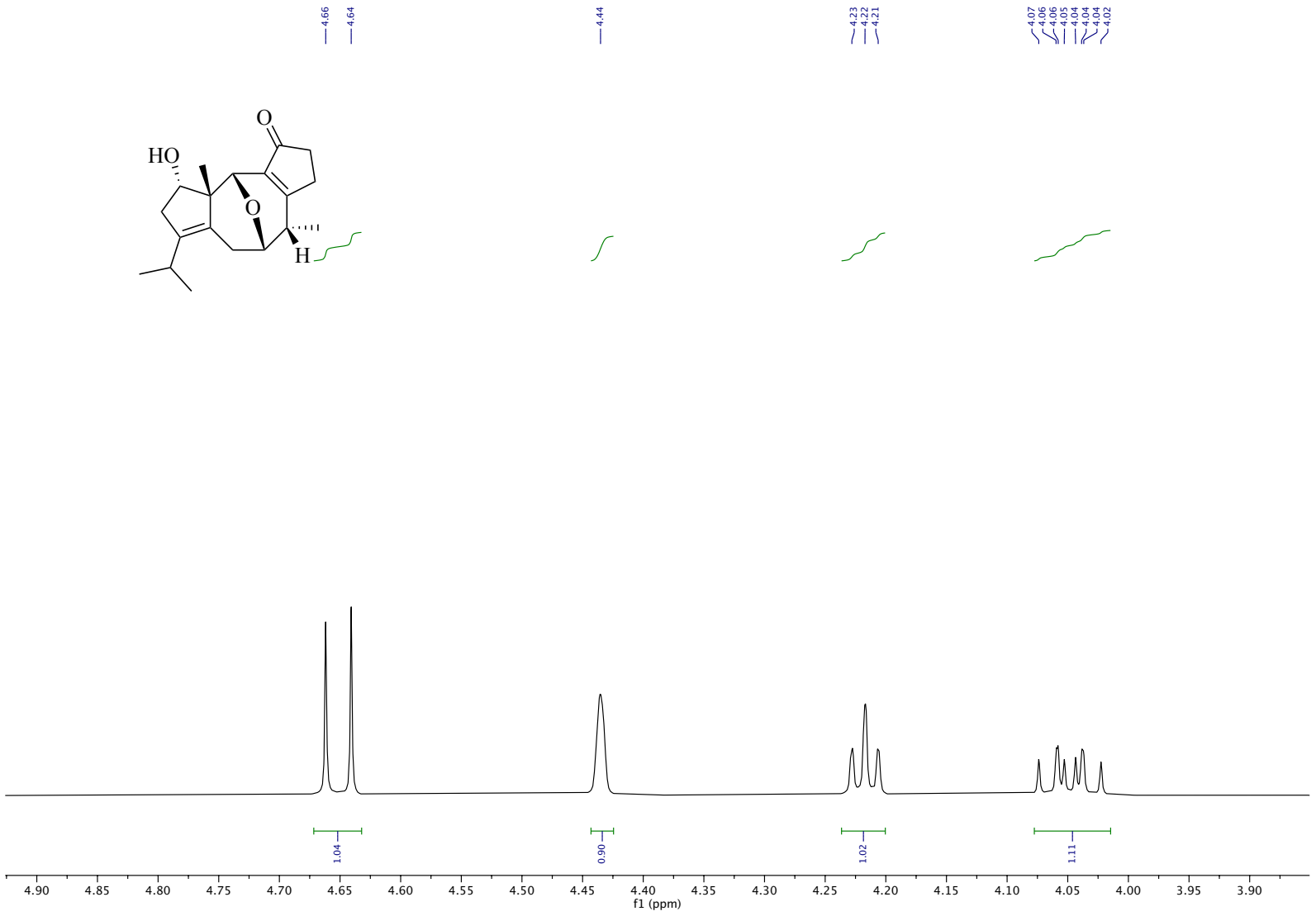

Figure B.41. ^{1}H NMR (600 MHz, $CDCl_3$), **2.21a** (inset)

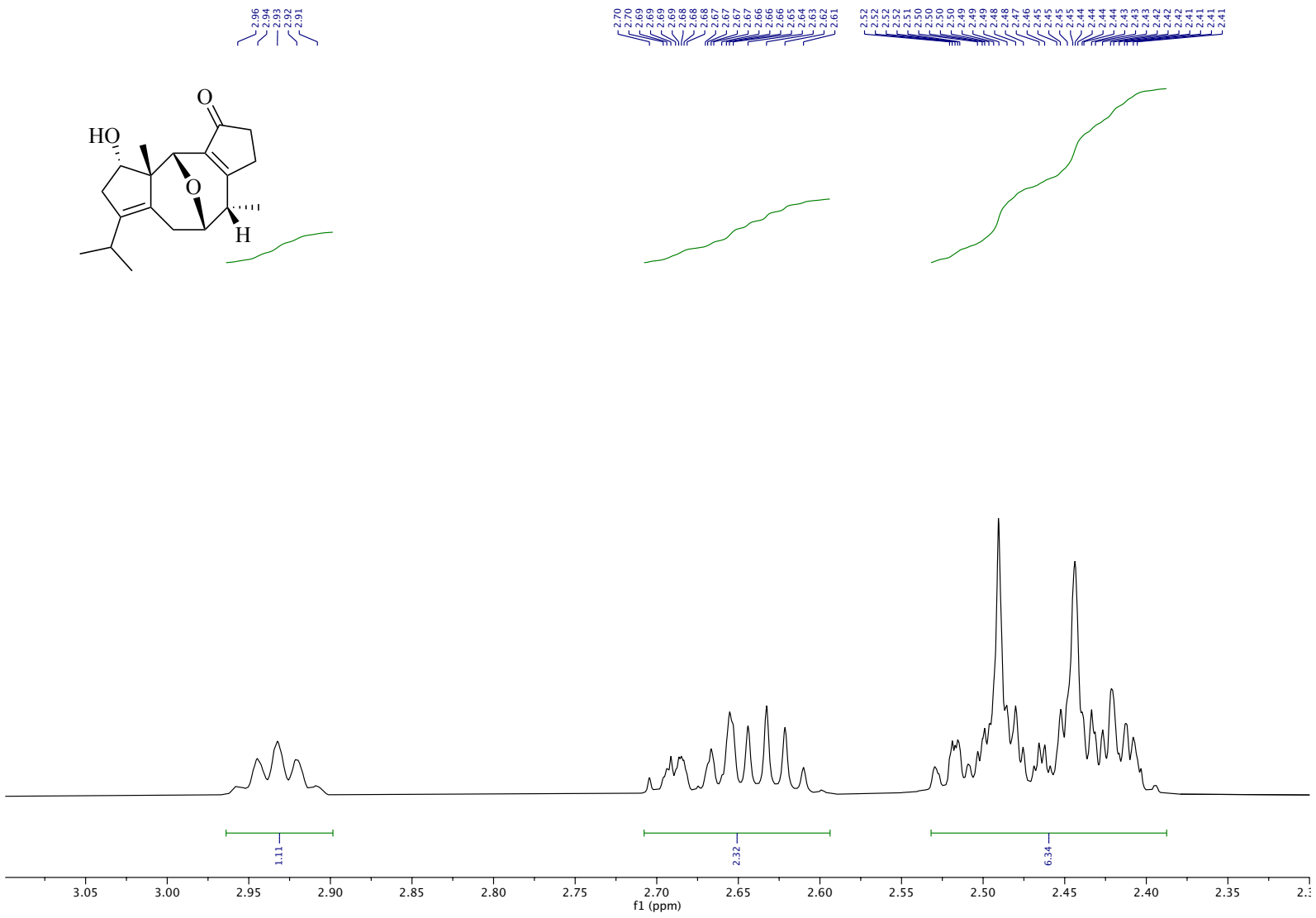

Figure B.42. ^{1}H NMR (600 MHz, $CDCl_3$), **2.21a** (inset)

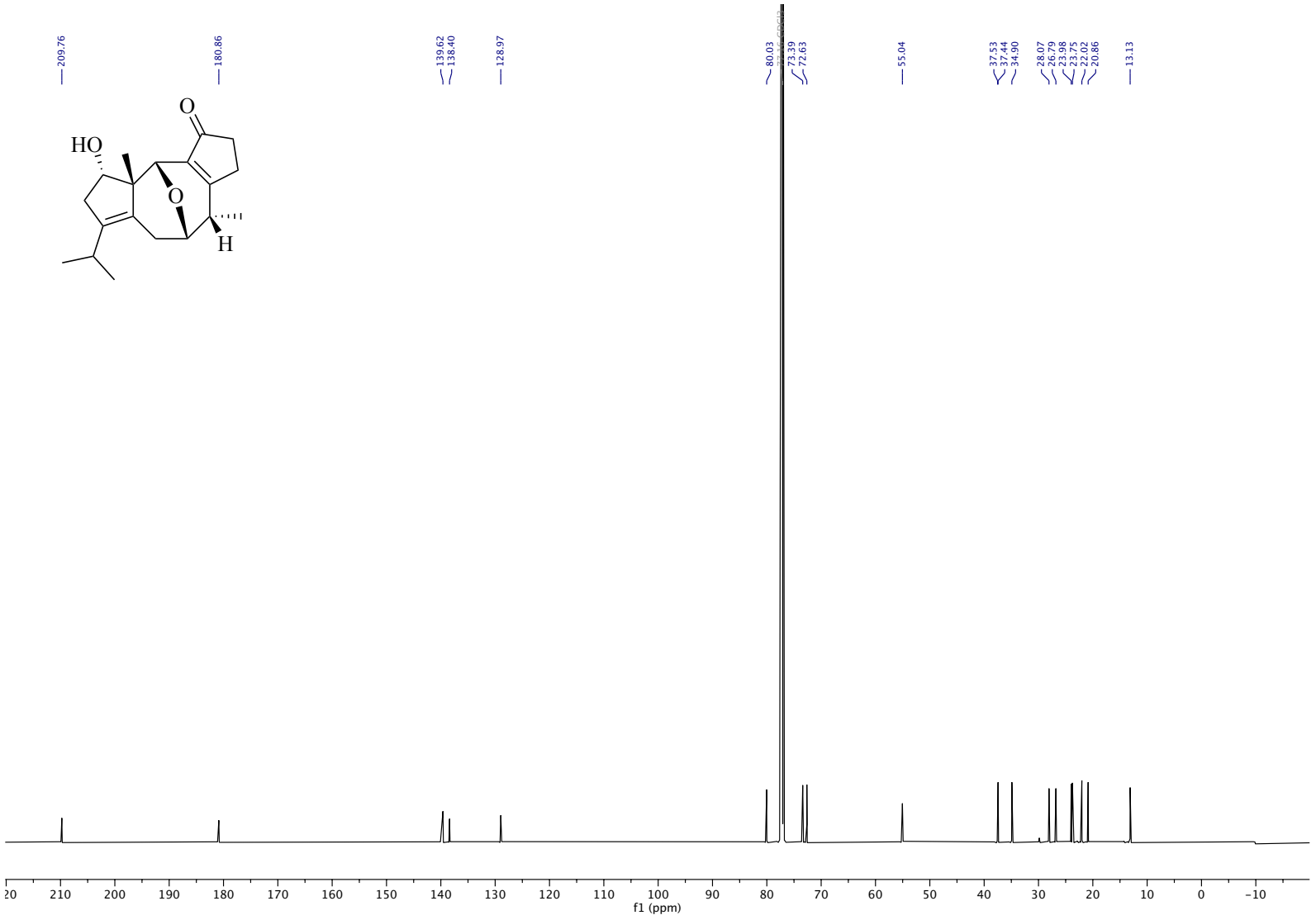

Figure B.43. ^{13}C NMR (151 MHz, $CDCl_3$), **2.21a**

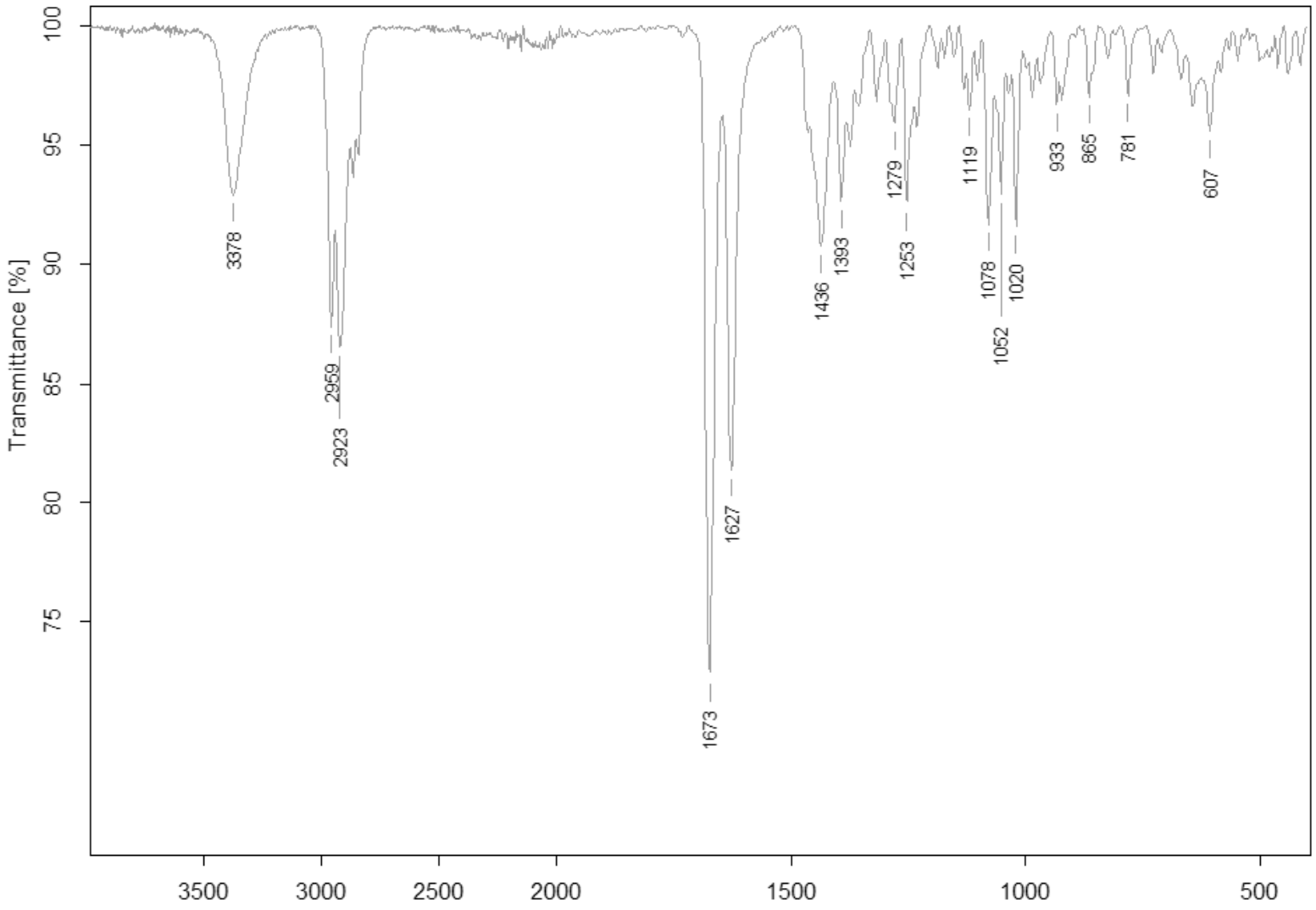

Figure B.44. IR (ATR), **2.21a**

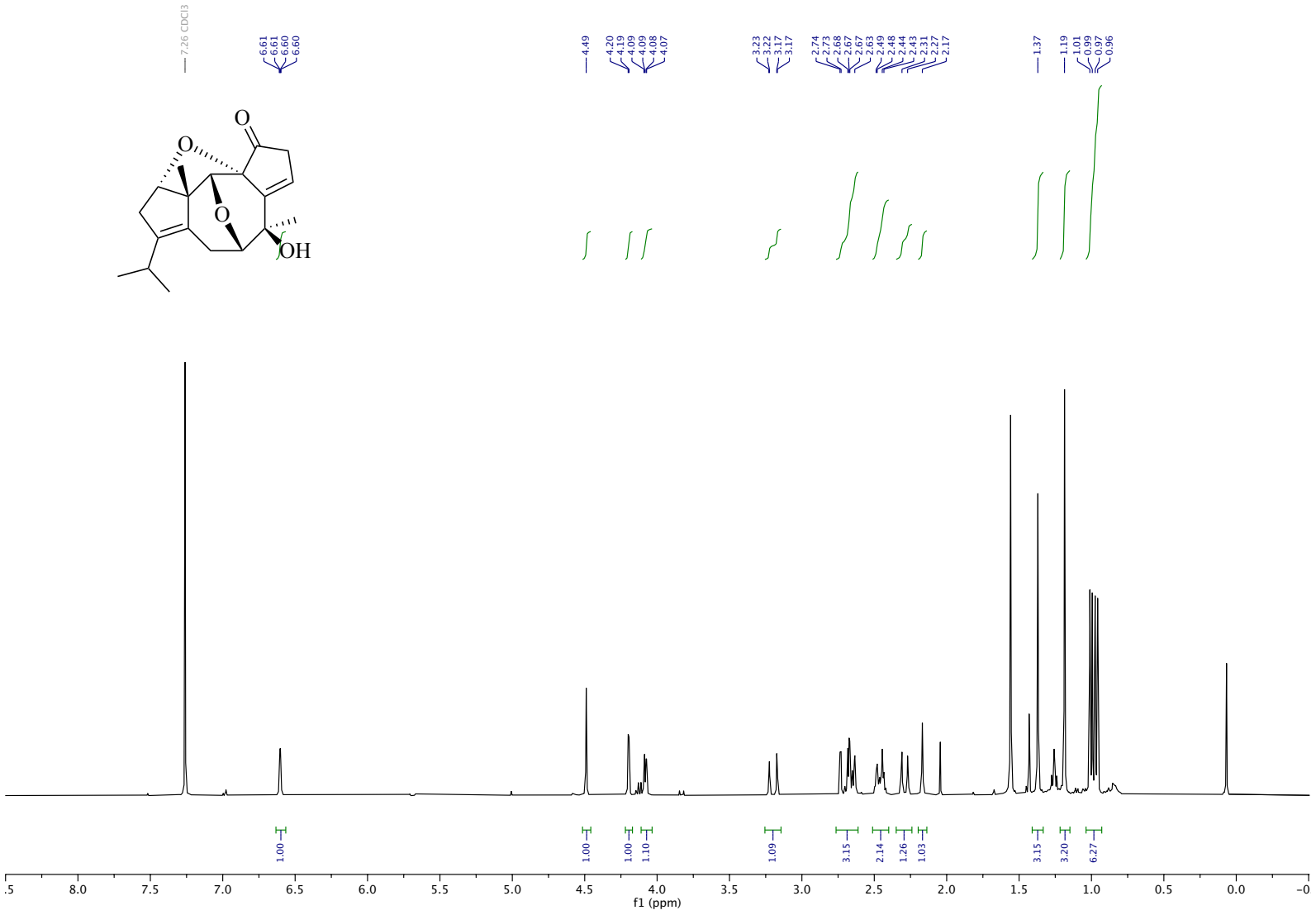

Figure B.45. ^{1}H NMR (400 MHz, $CDCl_3$), **2.23**

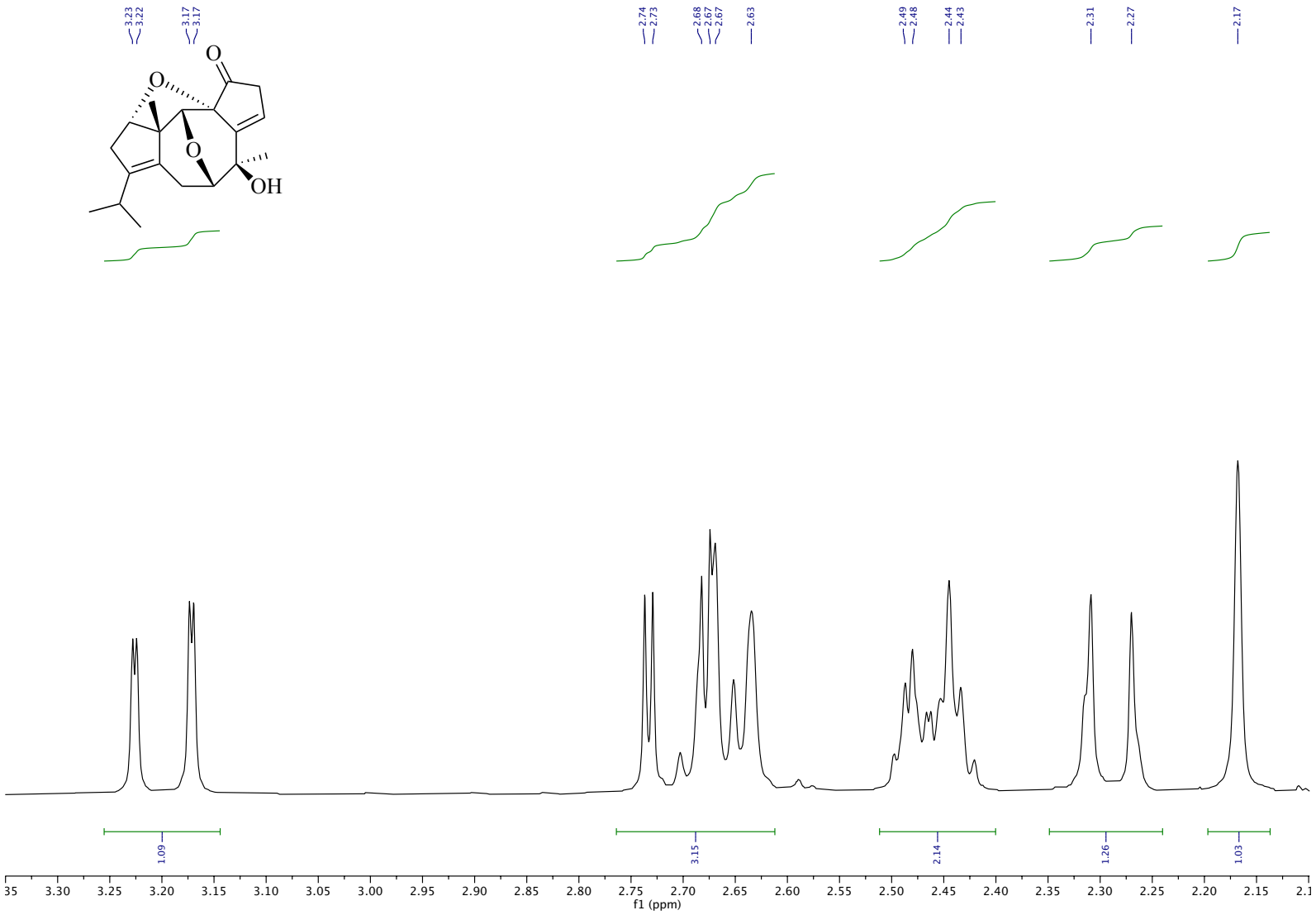

Figure B.46. ^{1}H NMR (400 MHz, $CDCl_3$), **2.23** (inset)

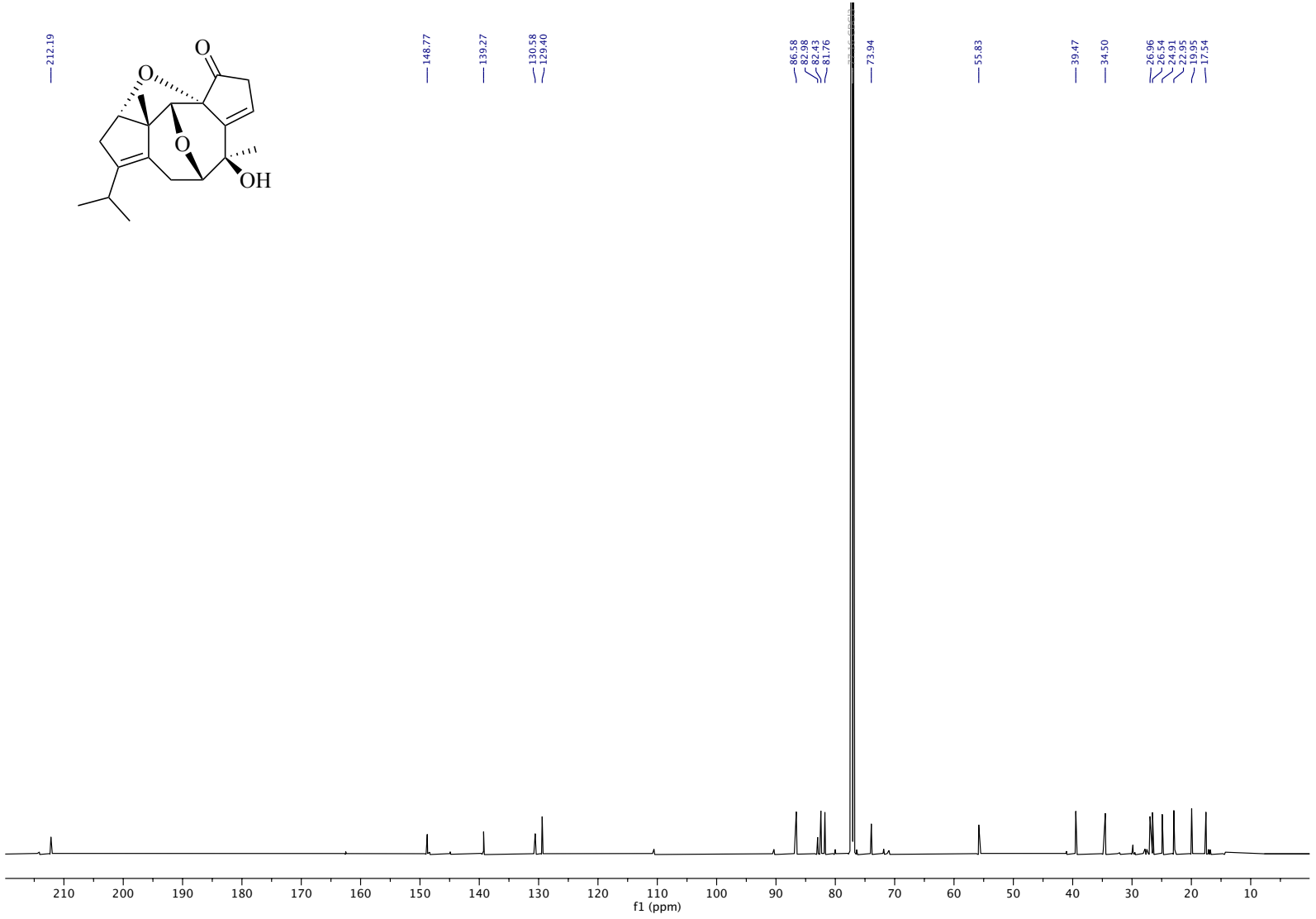

Figure B.47. ^{13}C NMR (151 MHz, $CDCl_3$), **2.23**

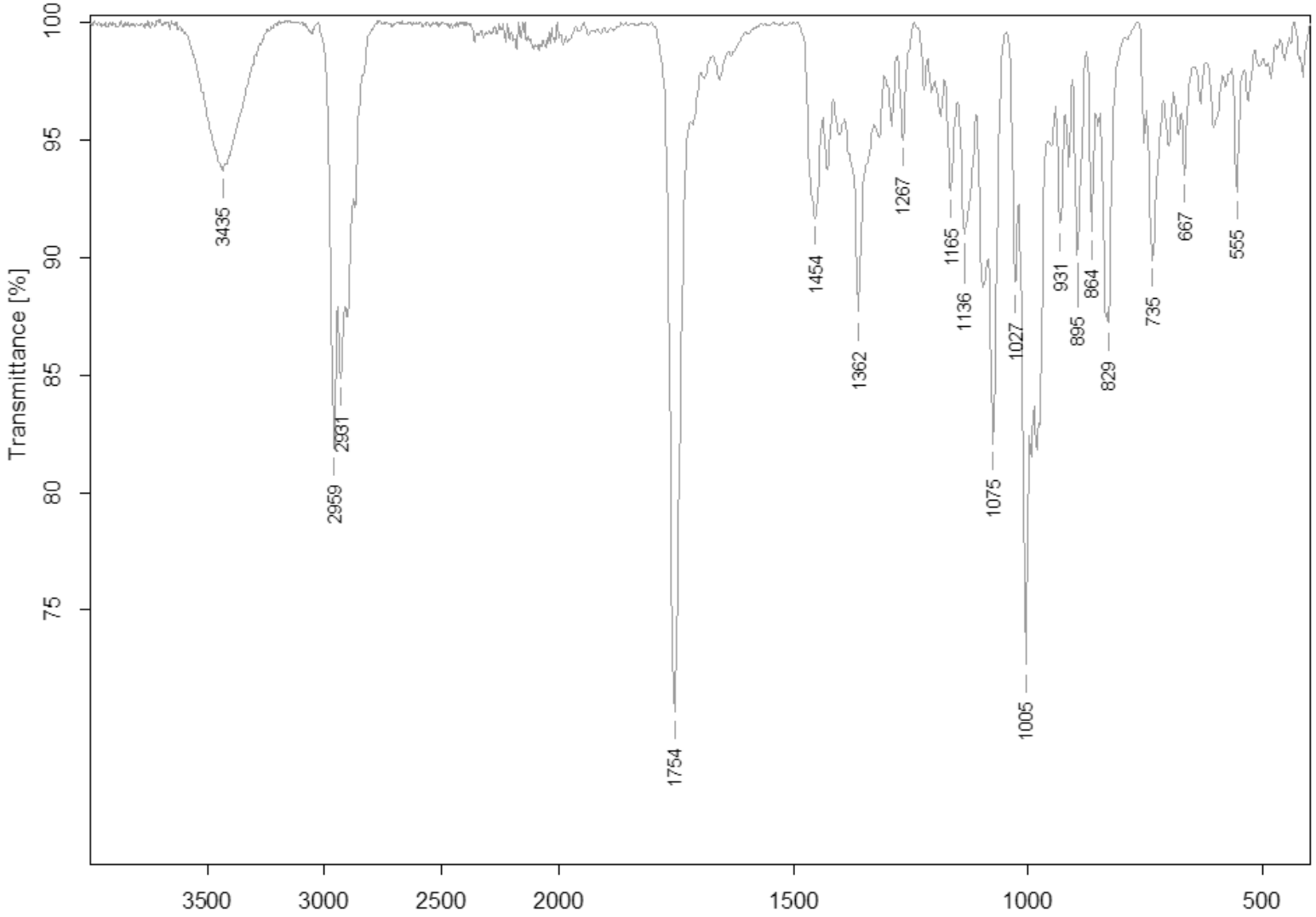

Figure B.48. IR (ATR), **2.23**

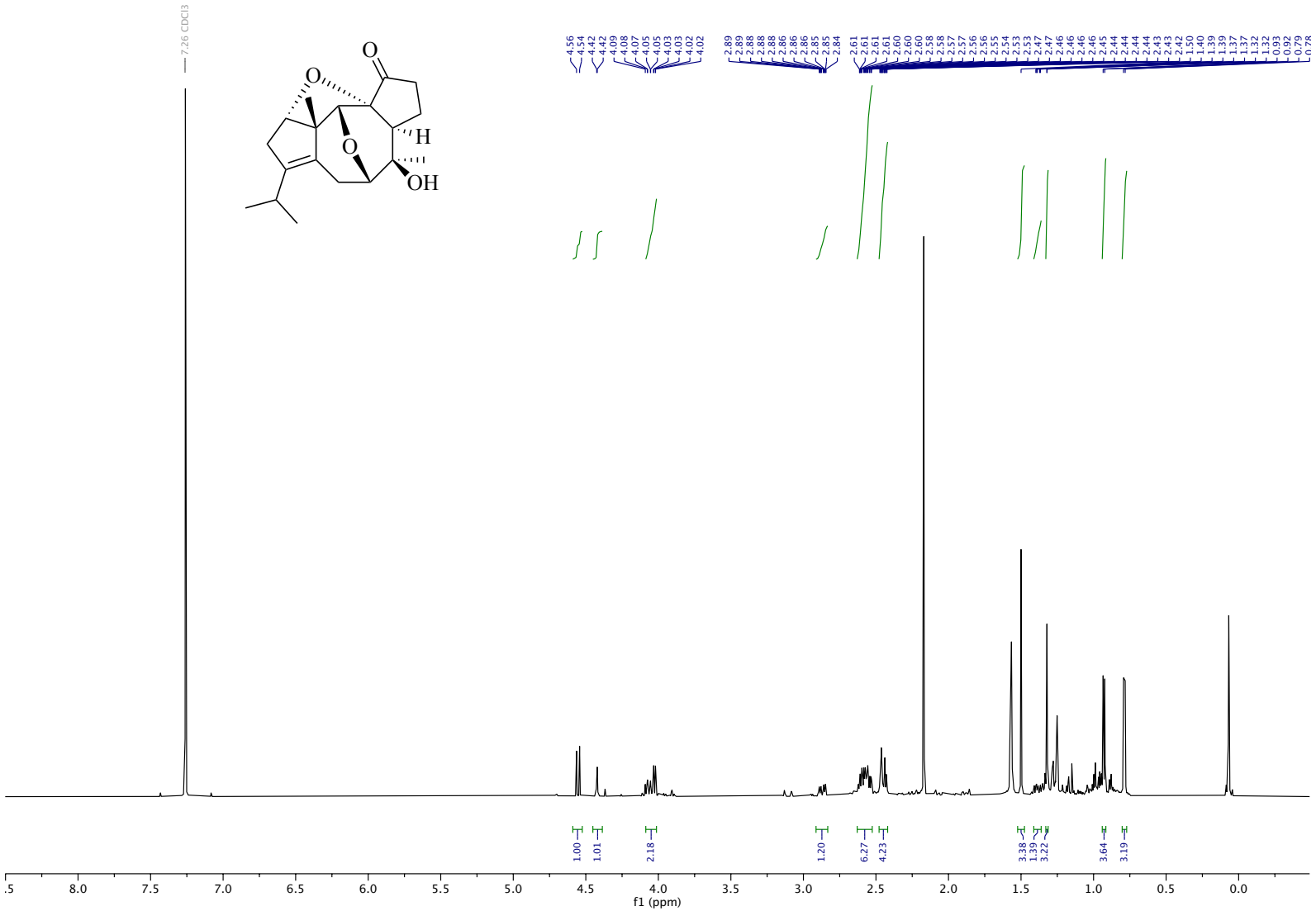

Figure B.49. ^{1}H NMR (600 MHz, $CDCl_3$), **2.24**

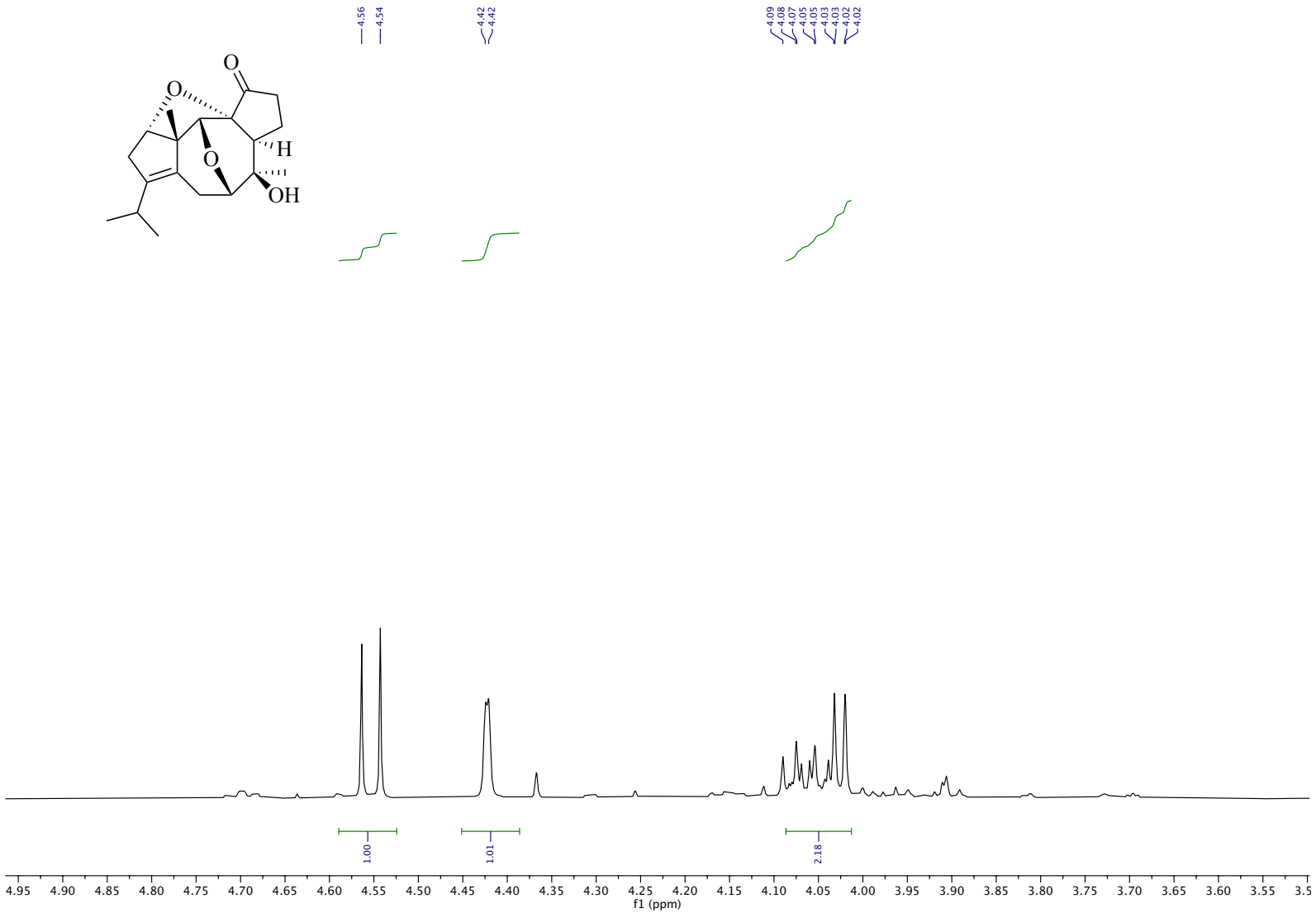

Figure B.50. ^{1}H NMR (600 MHz, $CDCl_3$), **2.24** (inset)

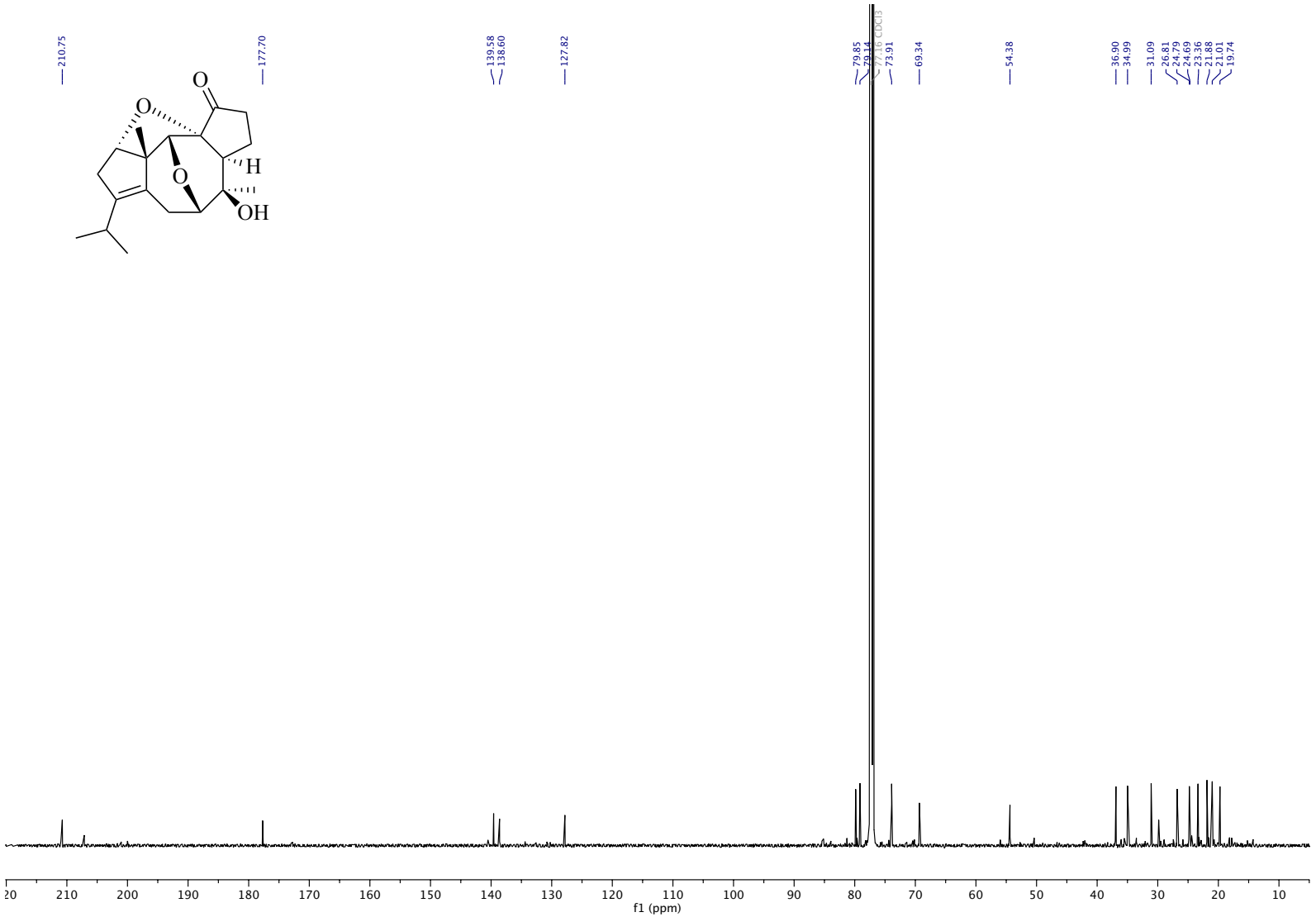

Figure B.51. ^{13}C NMR (151 MHz, $CDCl_3$), **2.24**

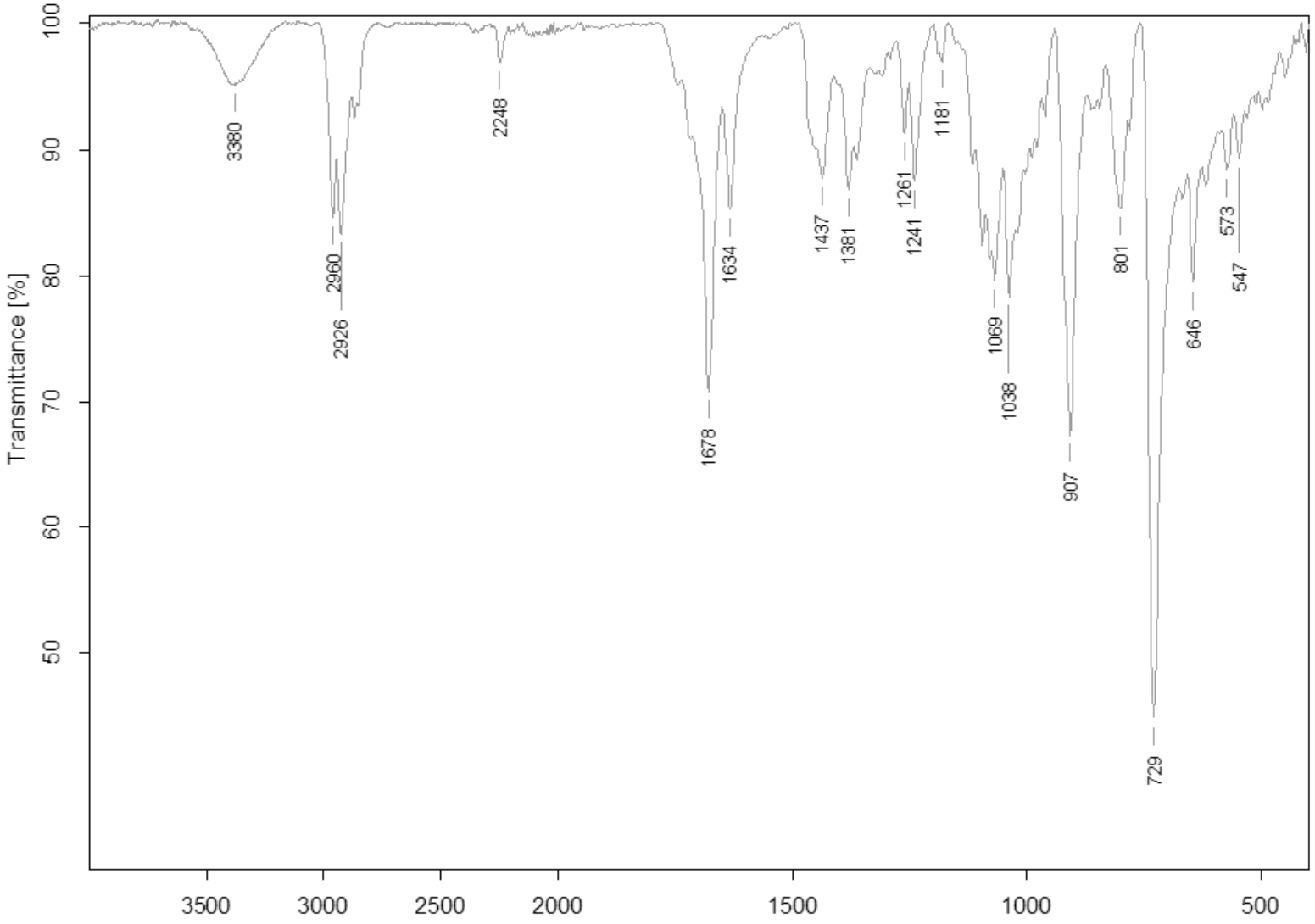

Figure B.52. IR (ATR), **2.24**

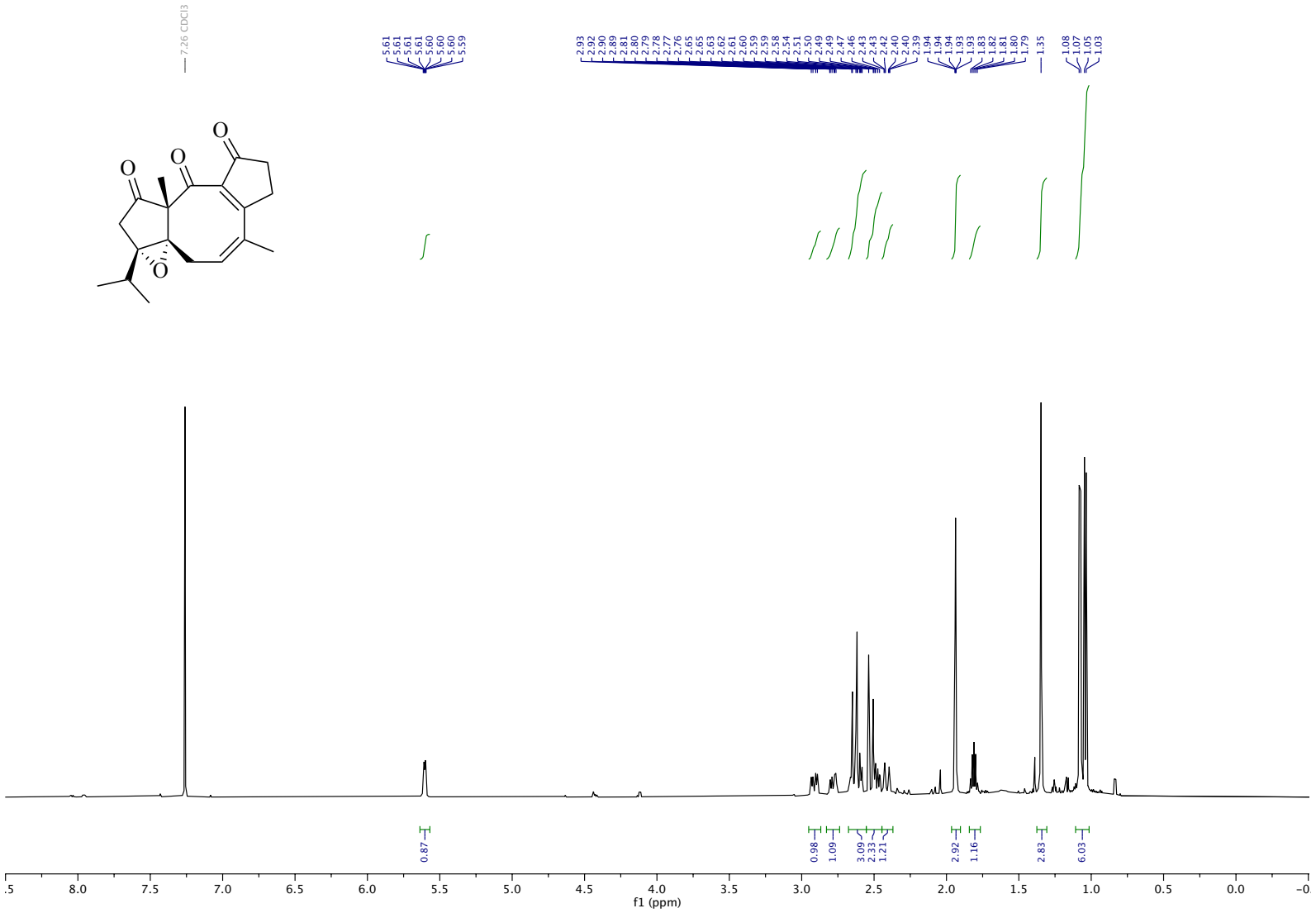

Figure B.53. ^{1}H NMR (600 MHz, $CDCl_3$), **2.29**

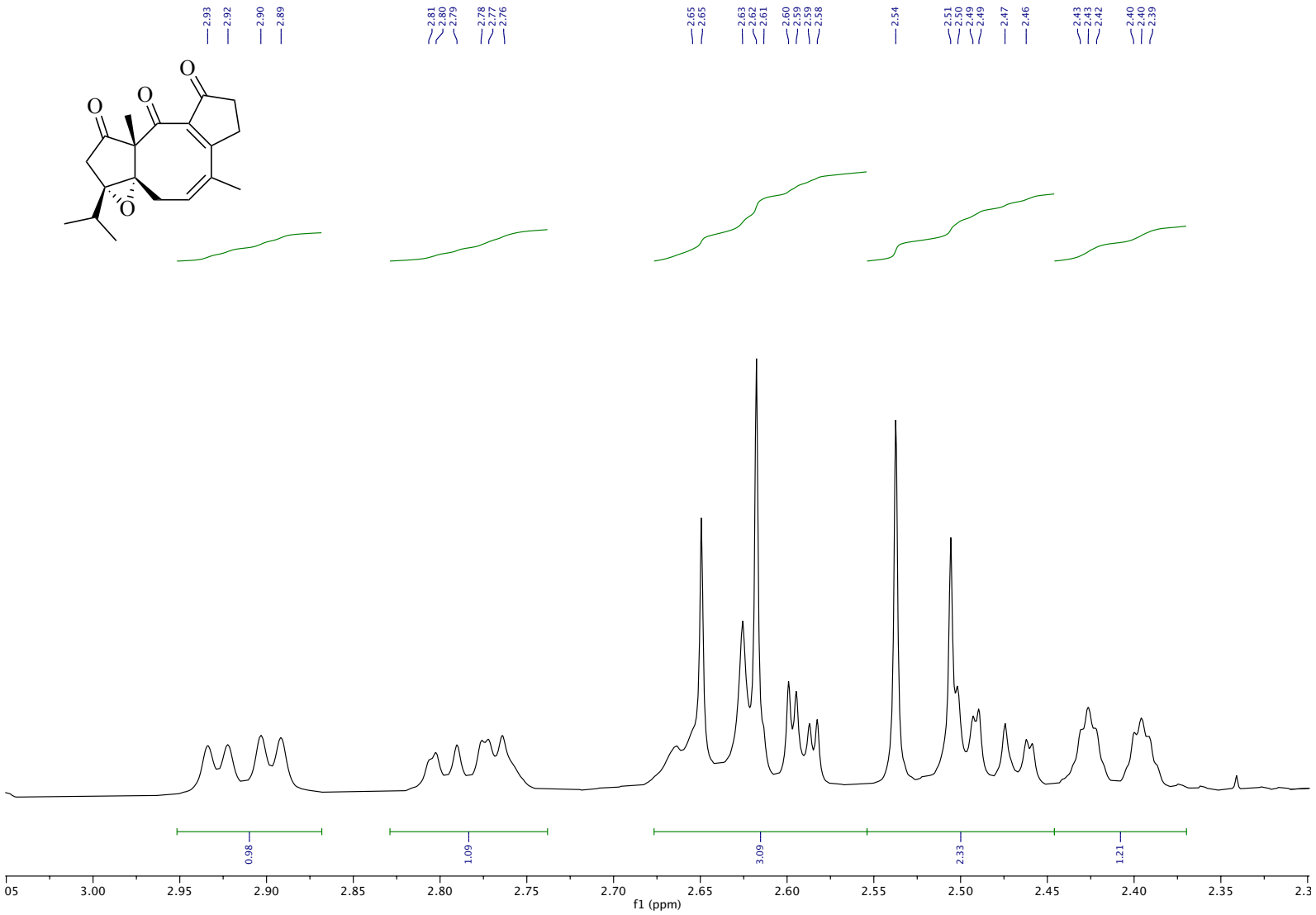

Figure B.54. ^{1}H NMR (600 MHz, $CDCl_3$), **2.29** (inset)

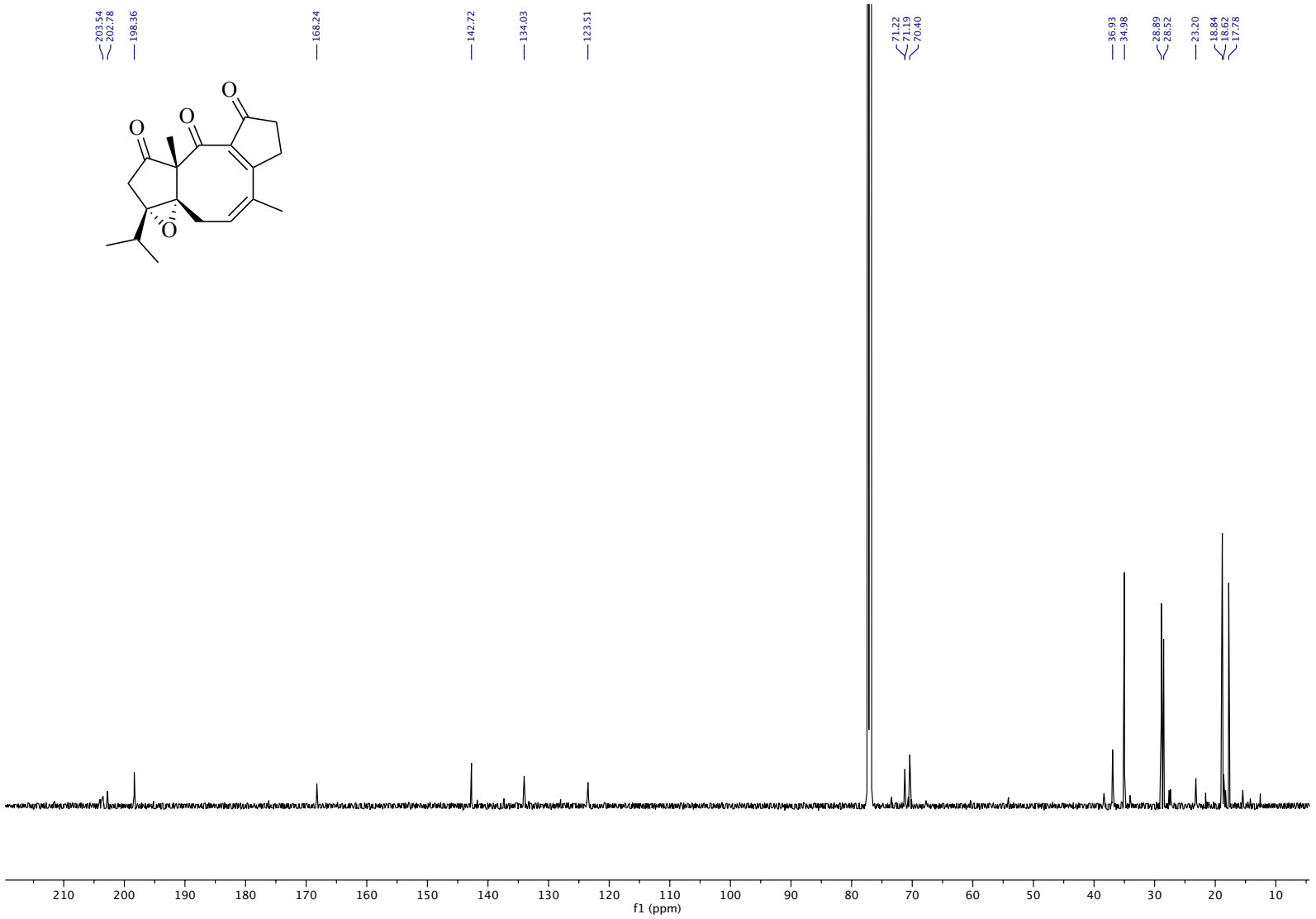

Figure B.55. ^{13}C NMR (151 MHz, $CDCl_3$), **2.29**

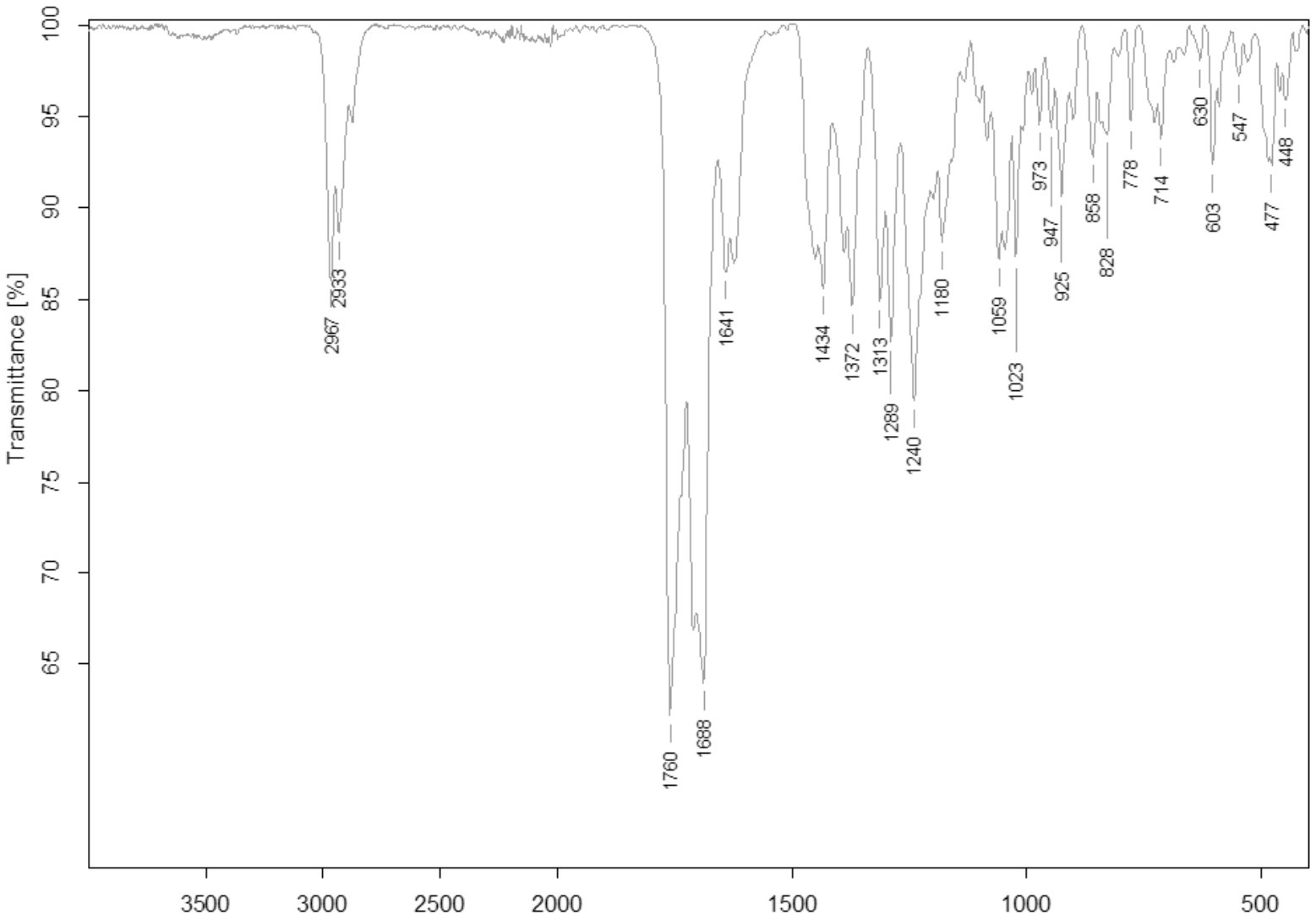

Figure B.56. IR (ATR), **2.29**

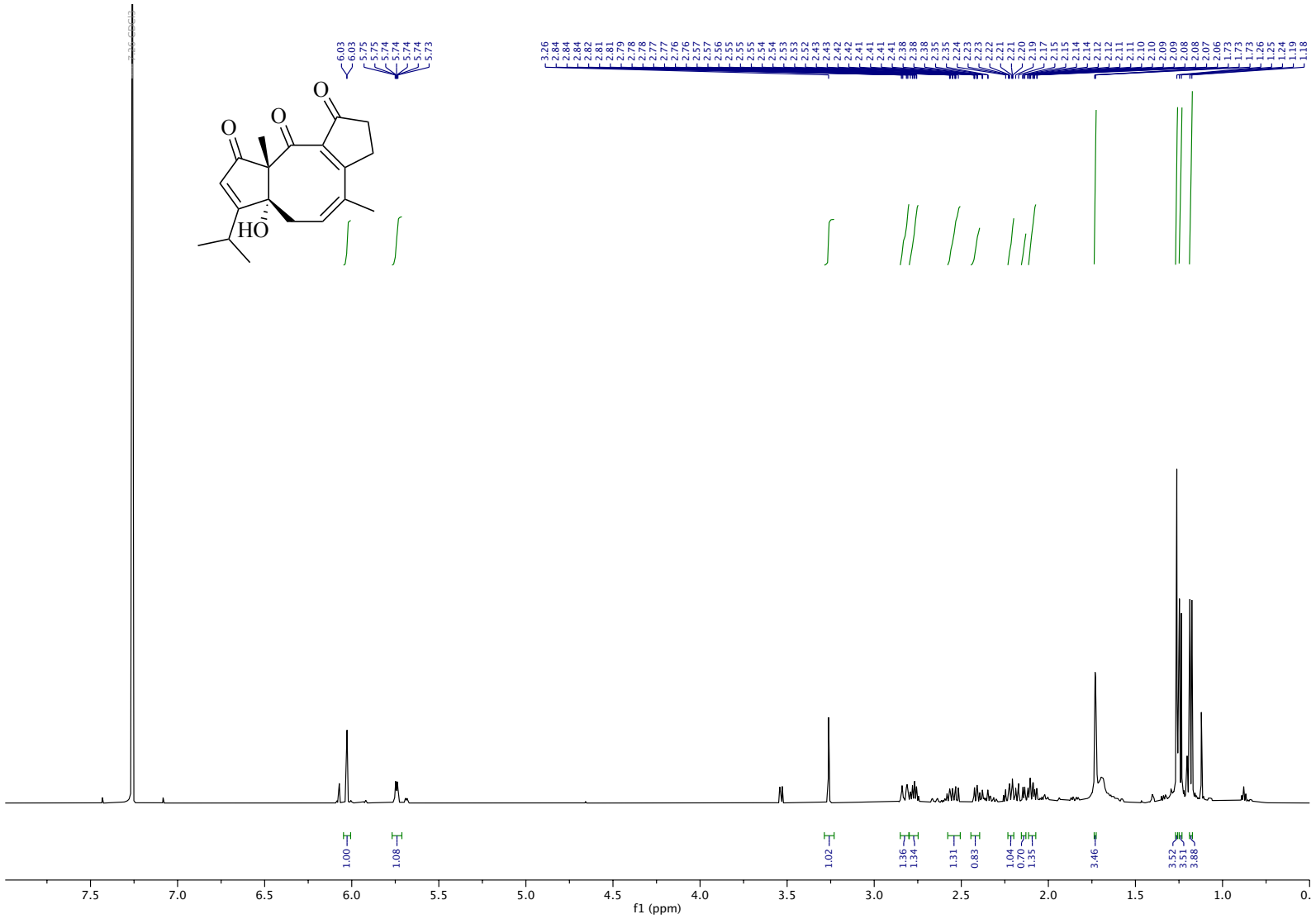

Figure B.57. ^{1}H NMR (600 MHz, $CDCl_3$), **2.26**

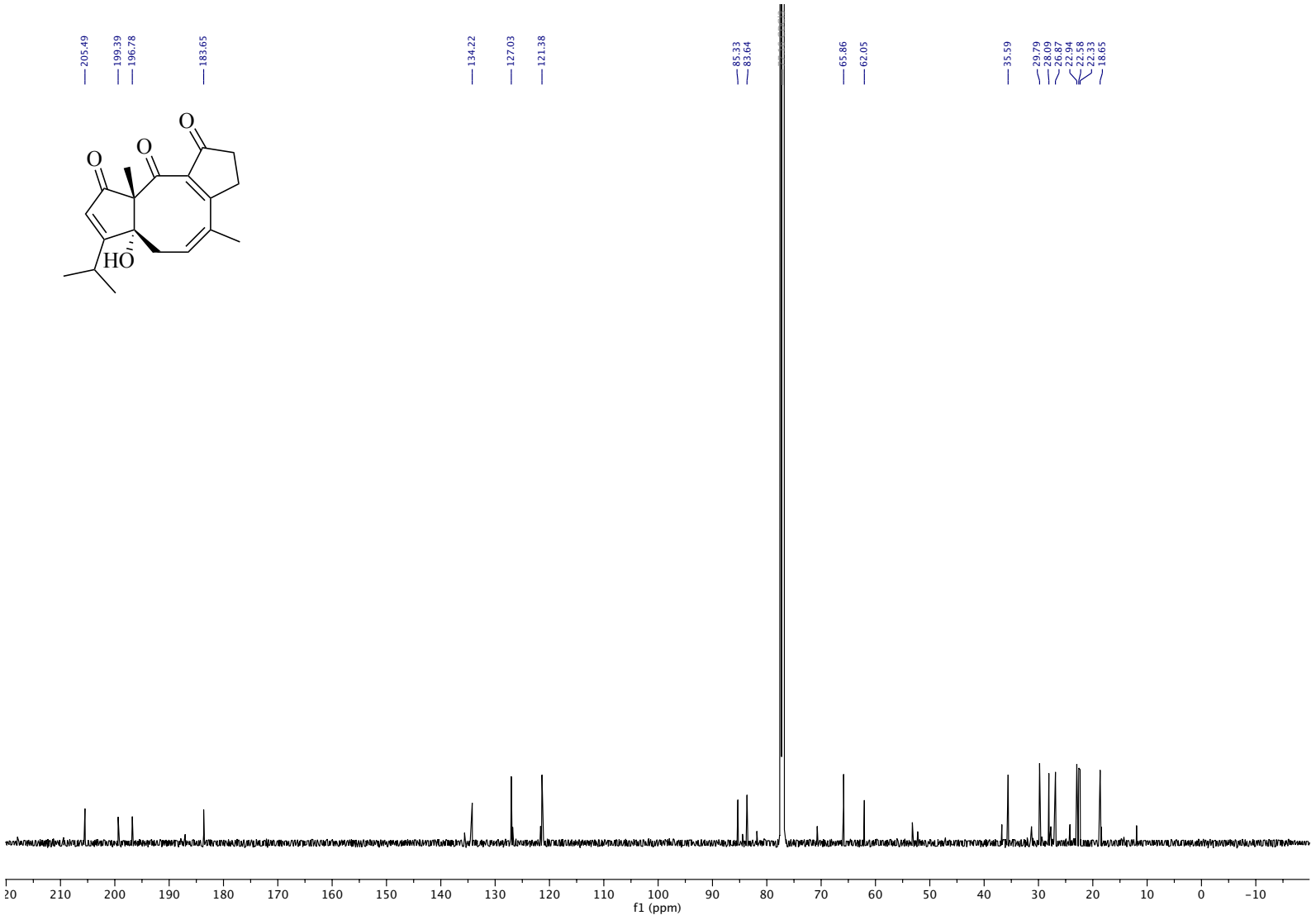

Figure B.58. ^{13}C NMR (151 MHz, $CDCl_3$), **2.26**

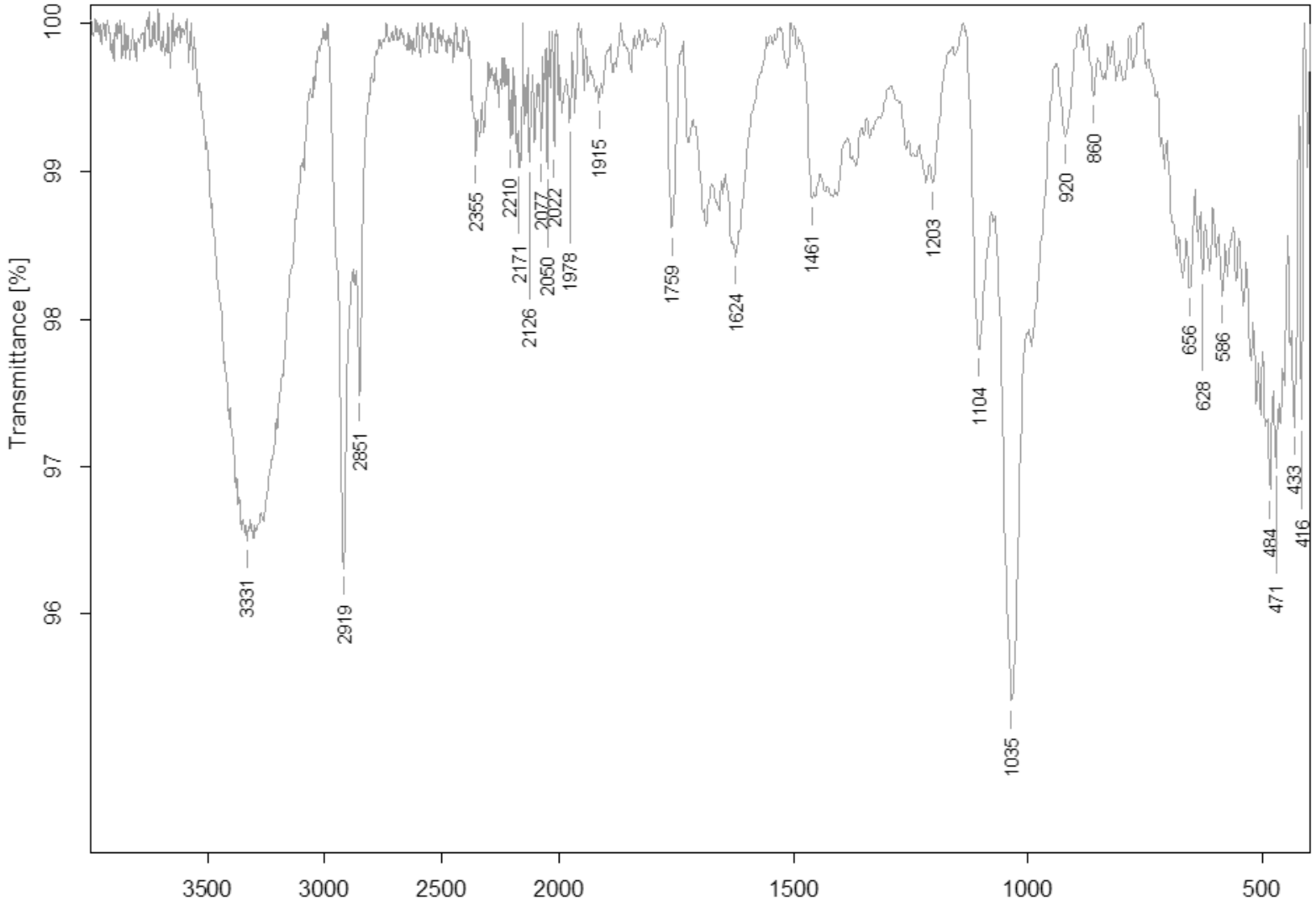

Figure B.59. IR (ATR), **2.26**

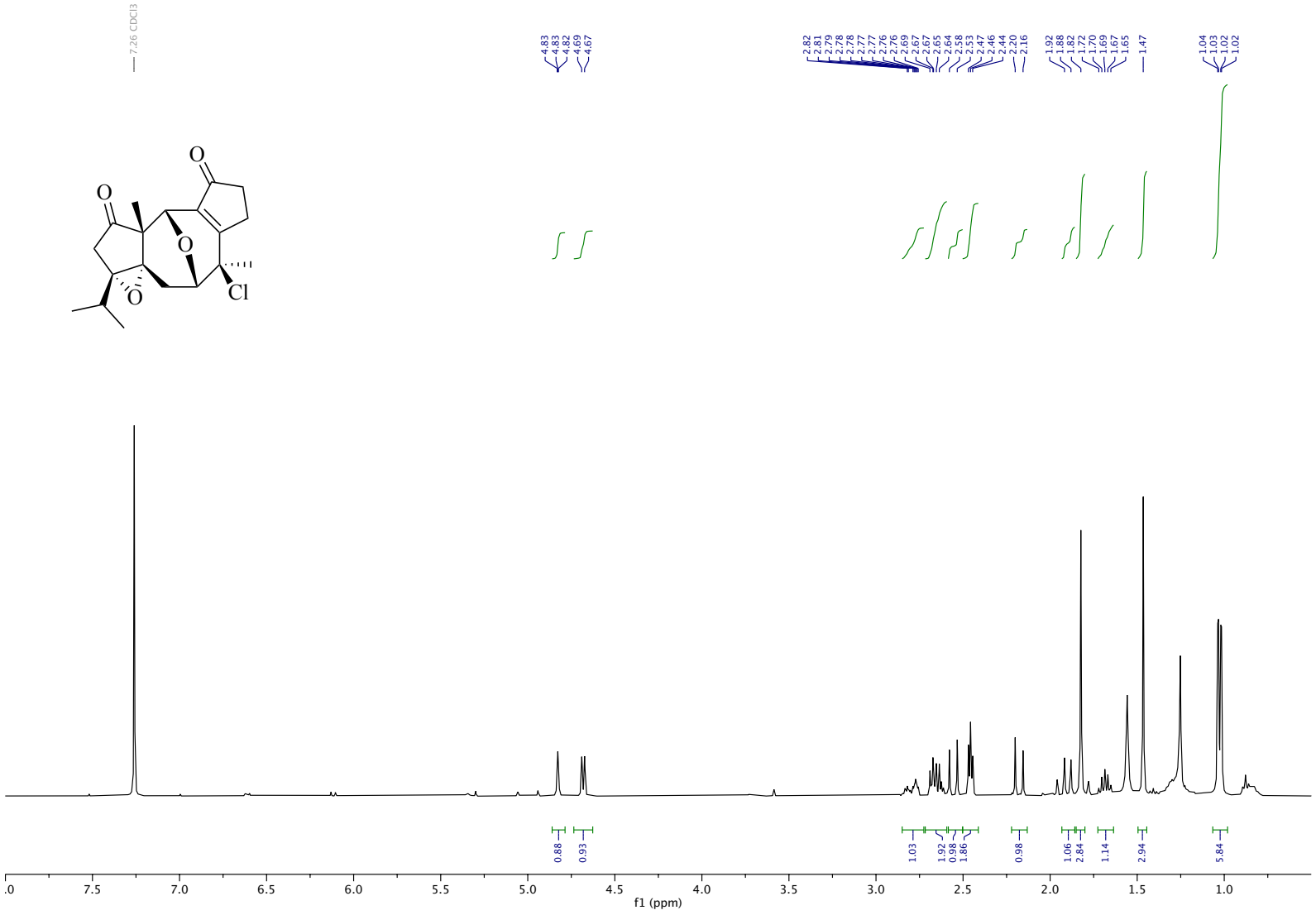

Figure B.60. ^{1}H NMR (400 MHz, $CDCl_3$), **2.32**

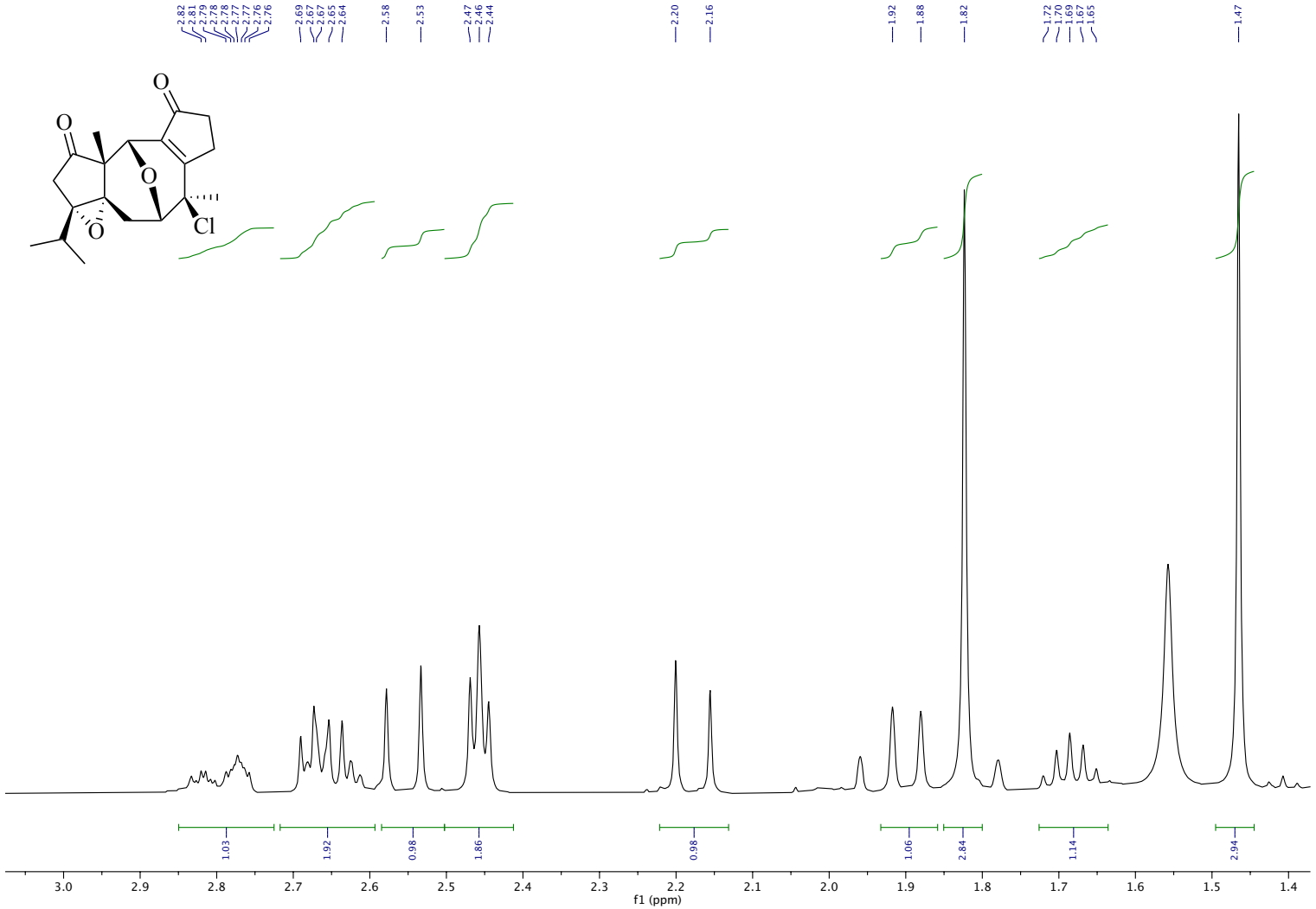

Figure B.61. ^{1}H NMR (400 MHz, $CDCl_3$), **2.32** (inset)

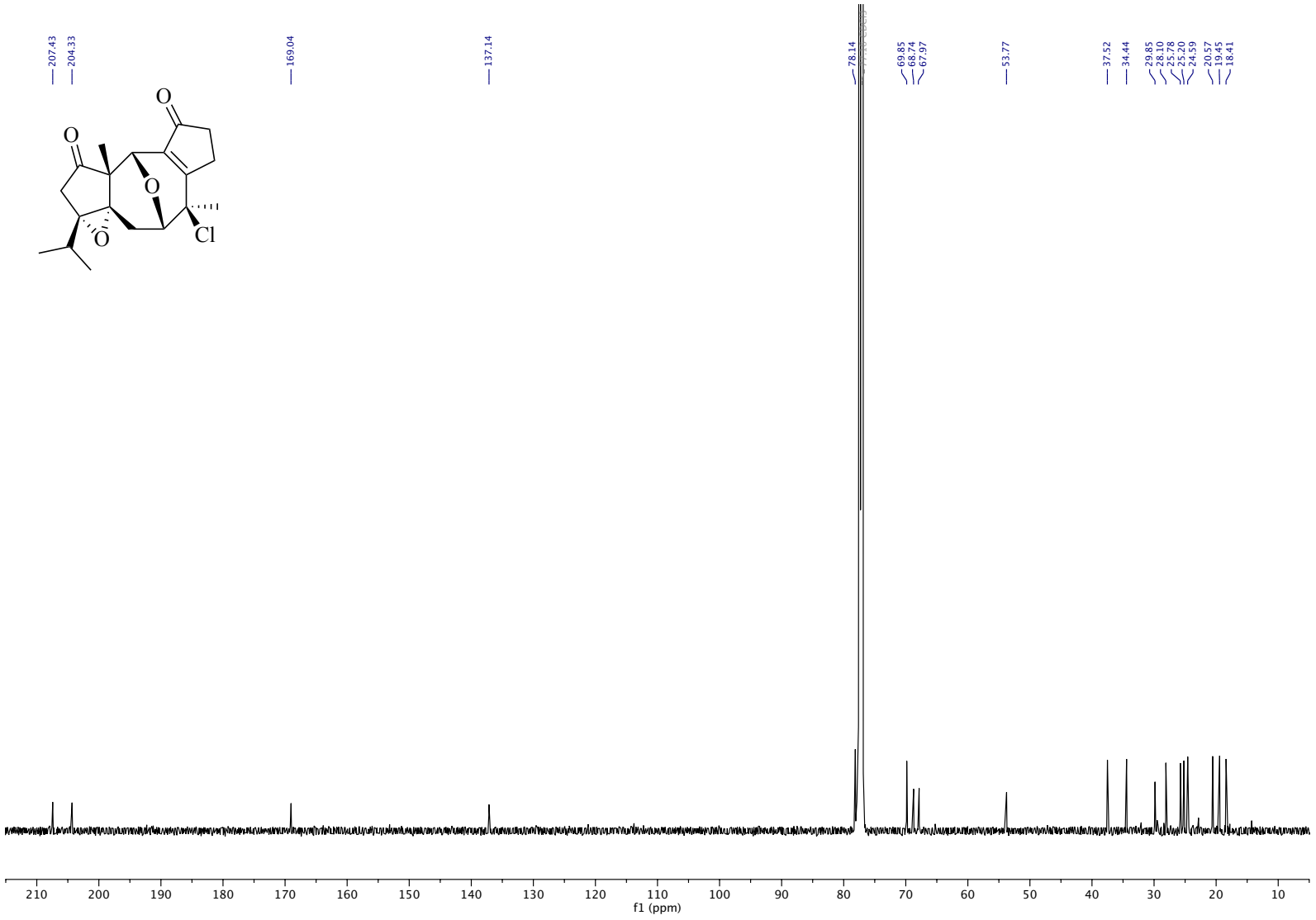

Figure B.62. ^{13}C NMR (151 MHz, $CDCl_3$), **2.32**

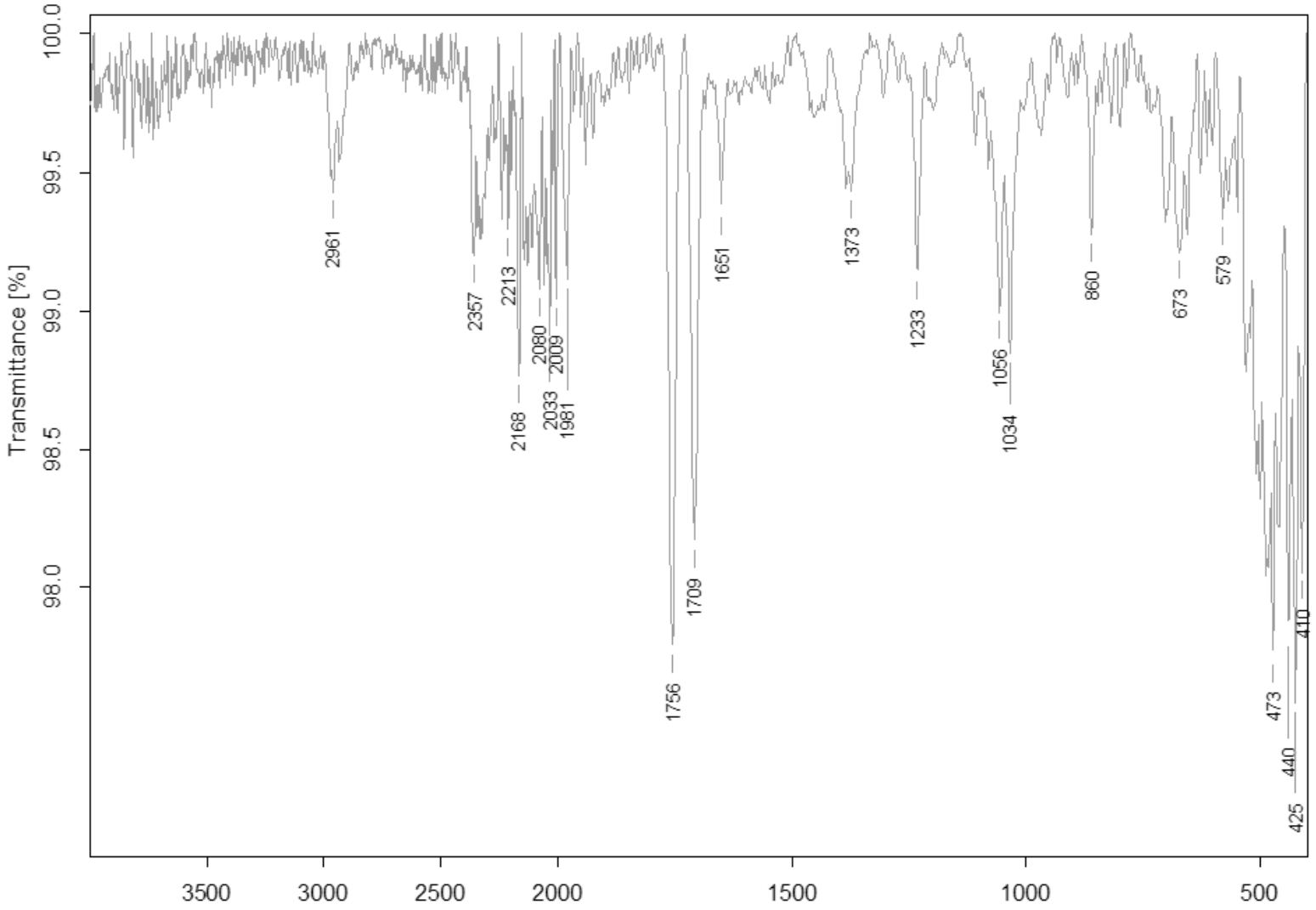

Figure B.63. IR (ATR), **2.32**

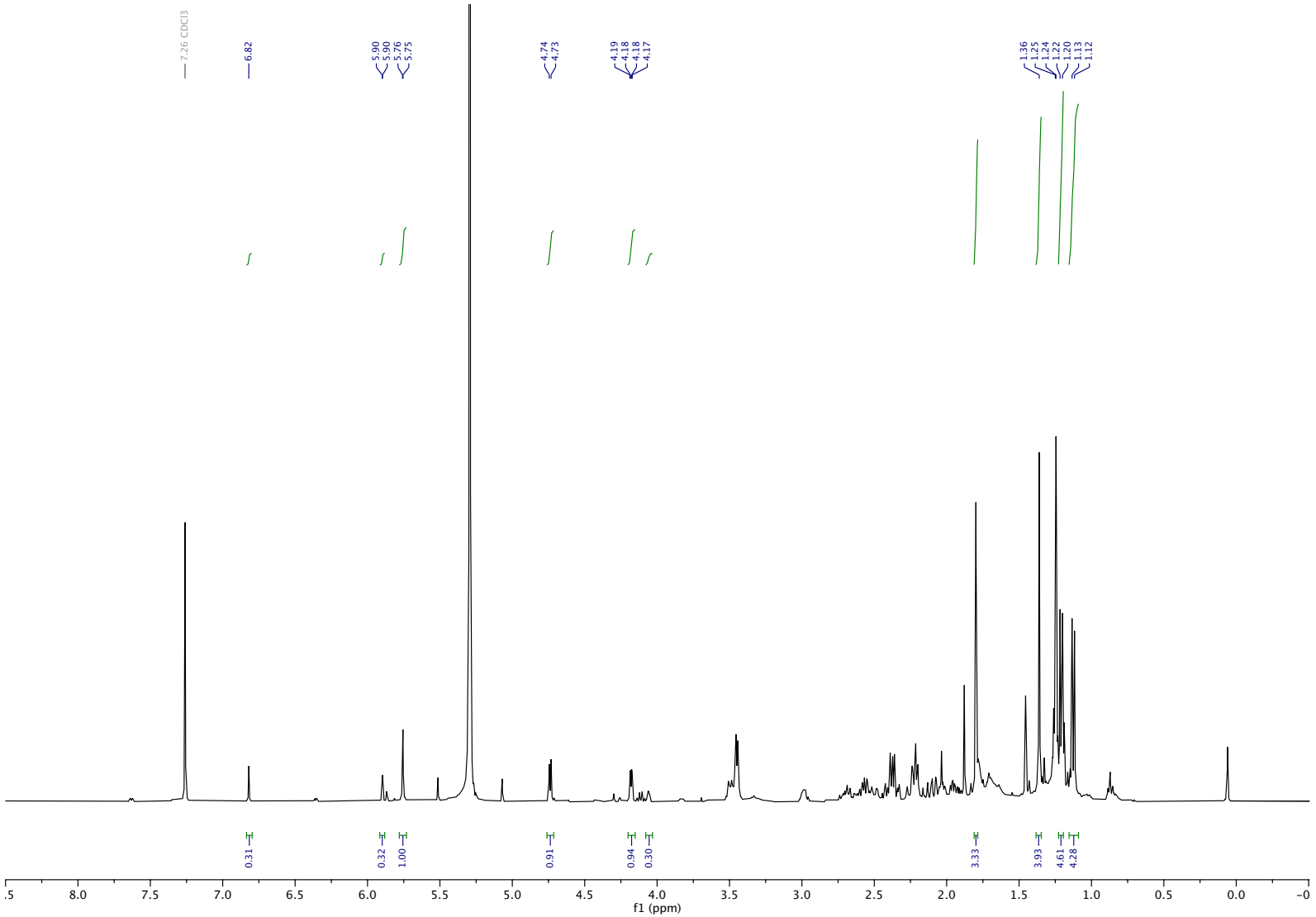

Figure B.64. ^{1}H NMR (400 MHz, $CDCl_3$), Crude **2.34** (Table 2.2, Entry 2)

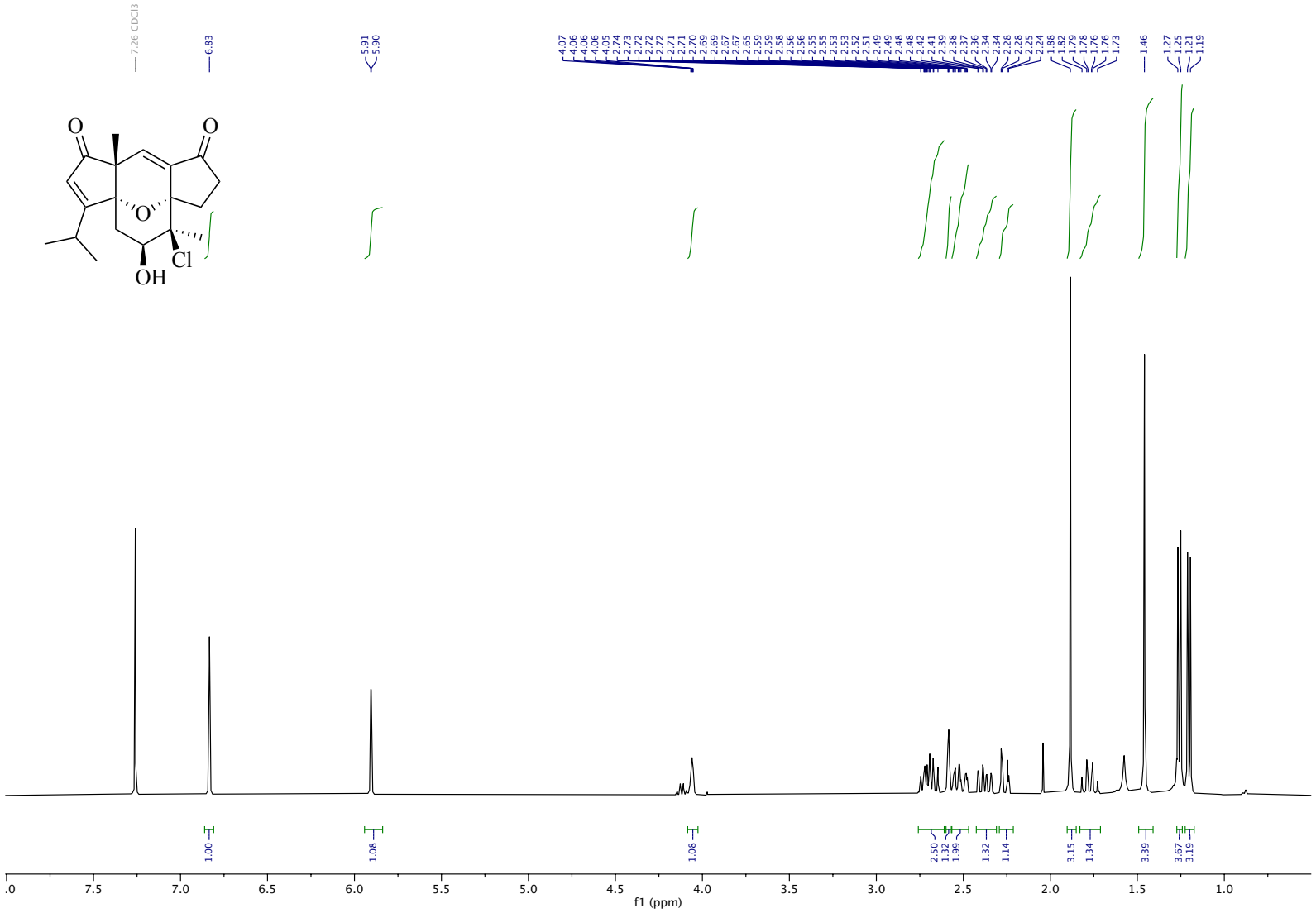

Figure B.65. ^{1}H NMR (400 MHz, $CDCl_3$), **2.34**

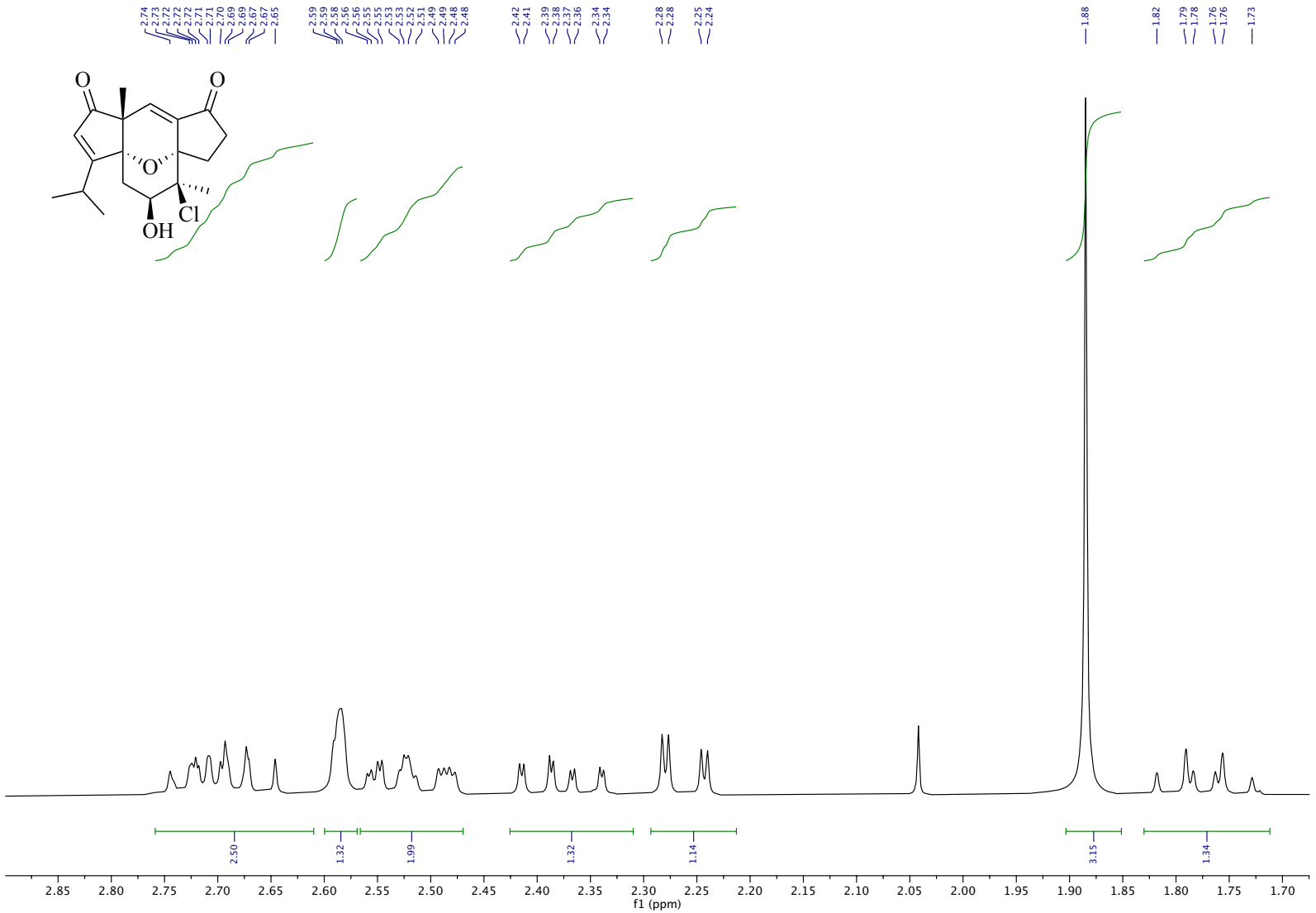

Figure B.66. ^{1}H NMR (400 MHz, $CDCl_3$), **2.34** (inset)

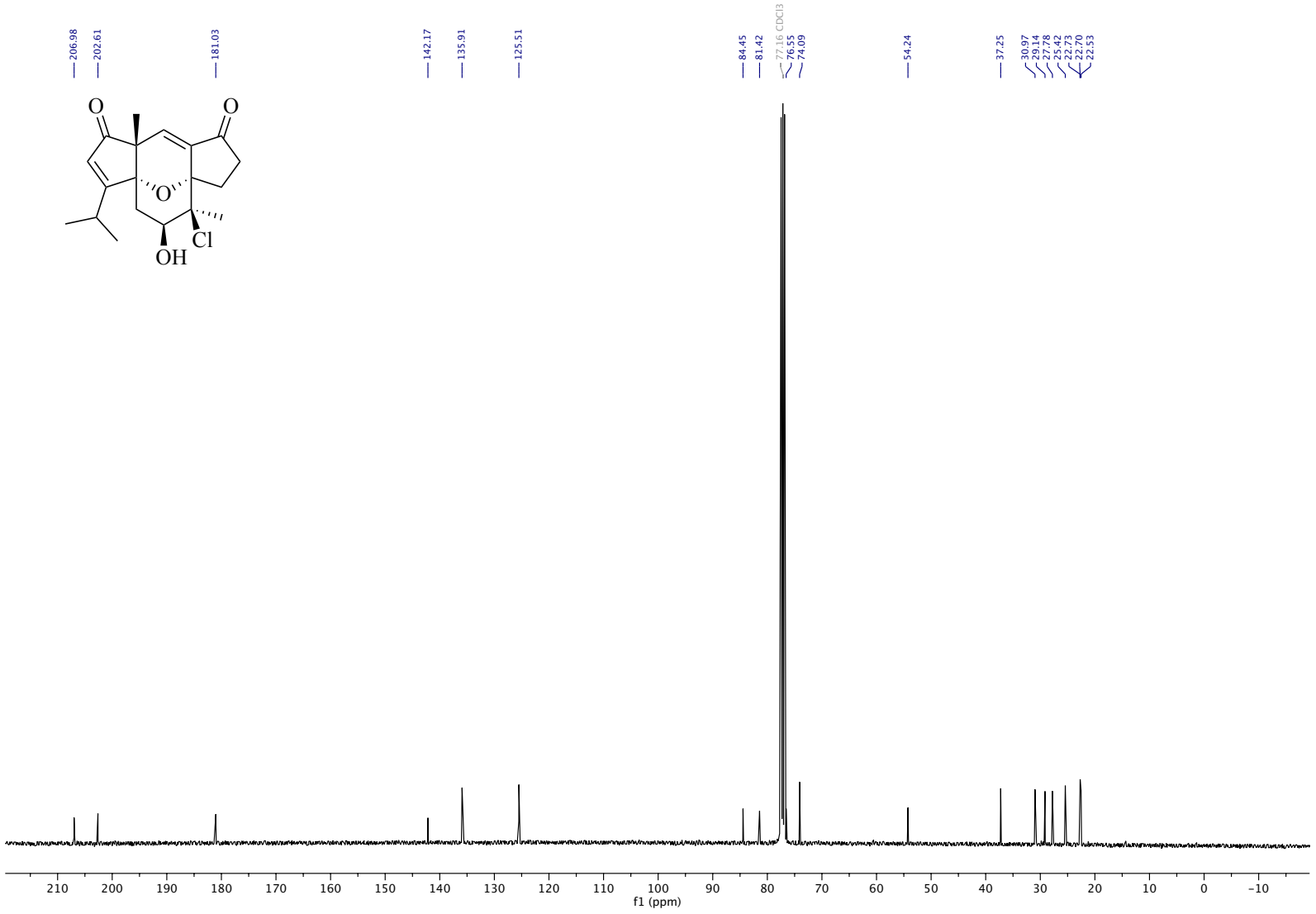

Figure B.67. ^{13}C NMR (101 MHz, $CDCl_3$), **2.34**

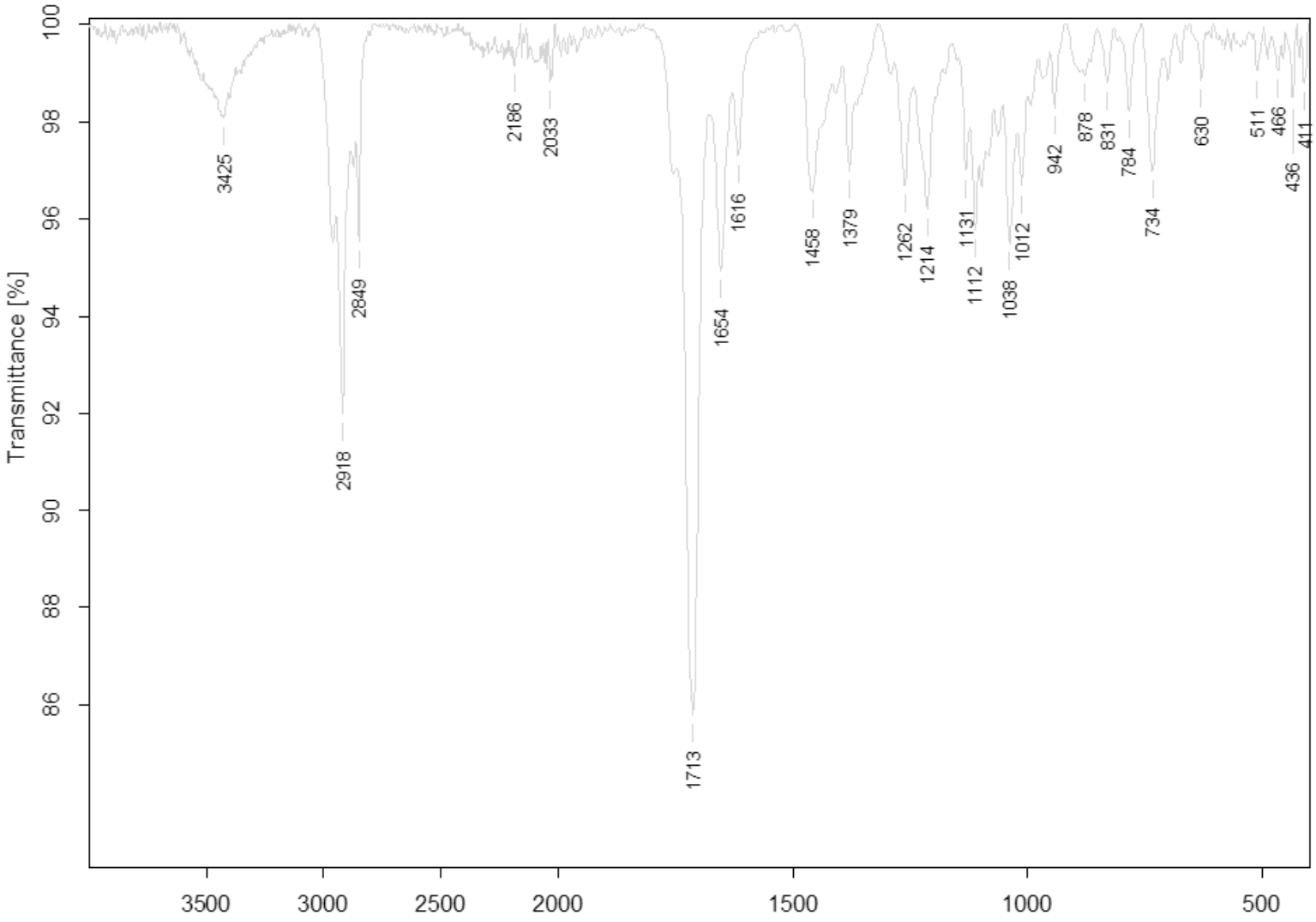

Figure B.68. IR (ATR), **2.32**

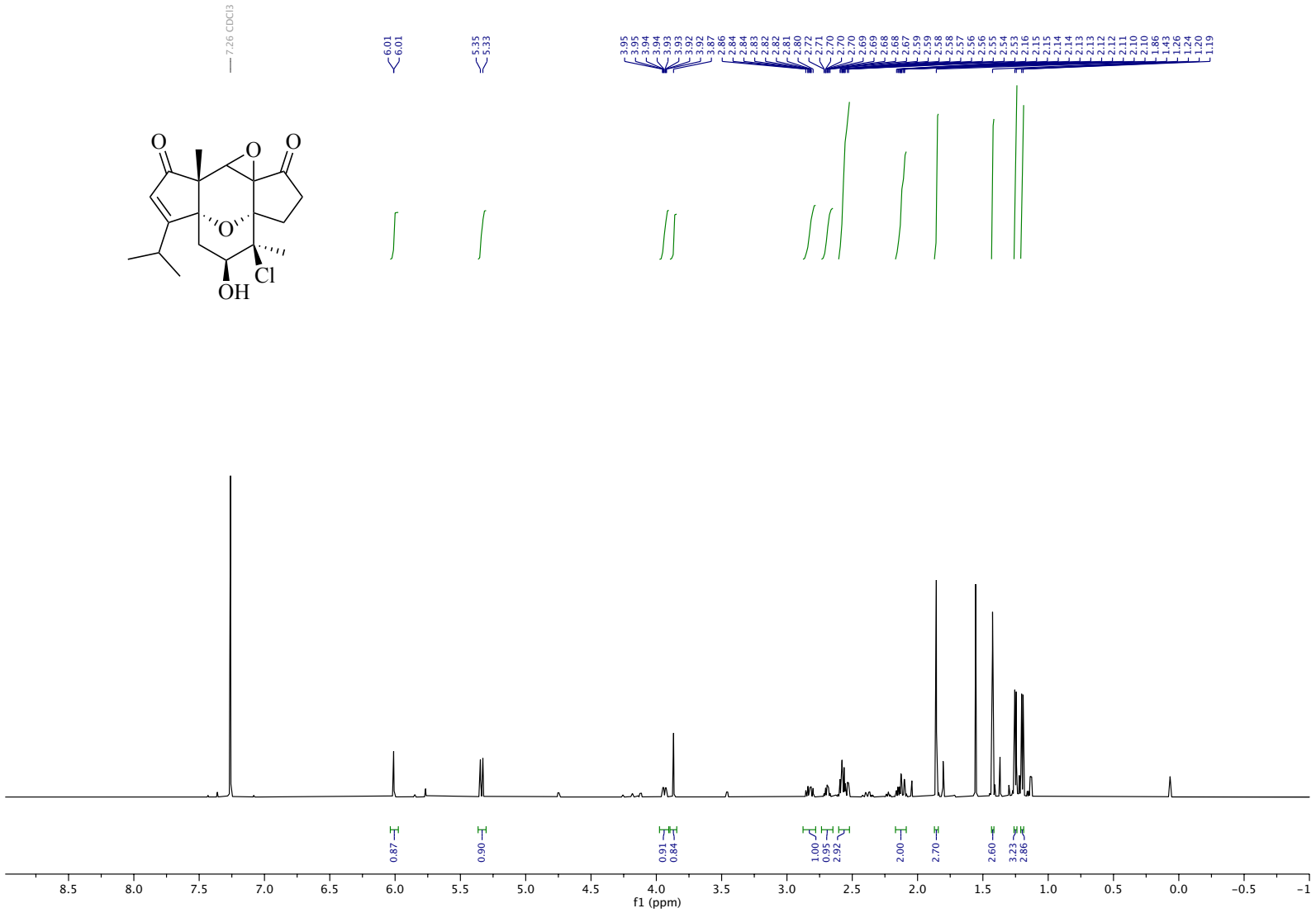

Figure B.69. ^{1}H NMR (600 MHz, $CDCl_3$), **2.37**

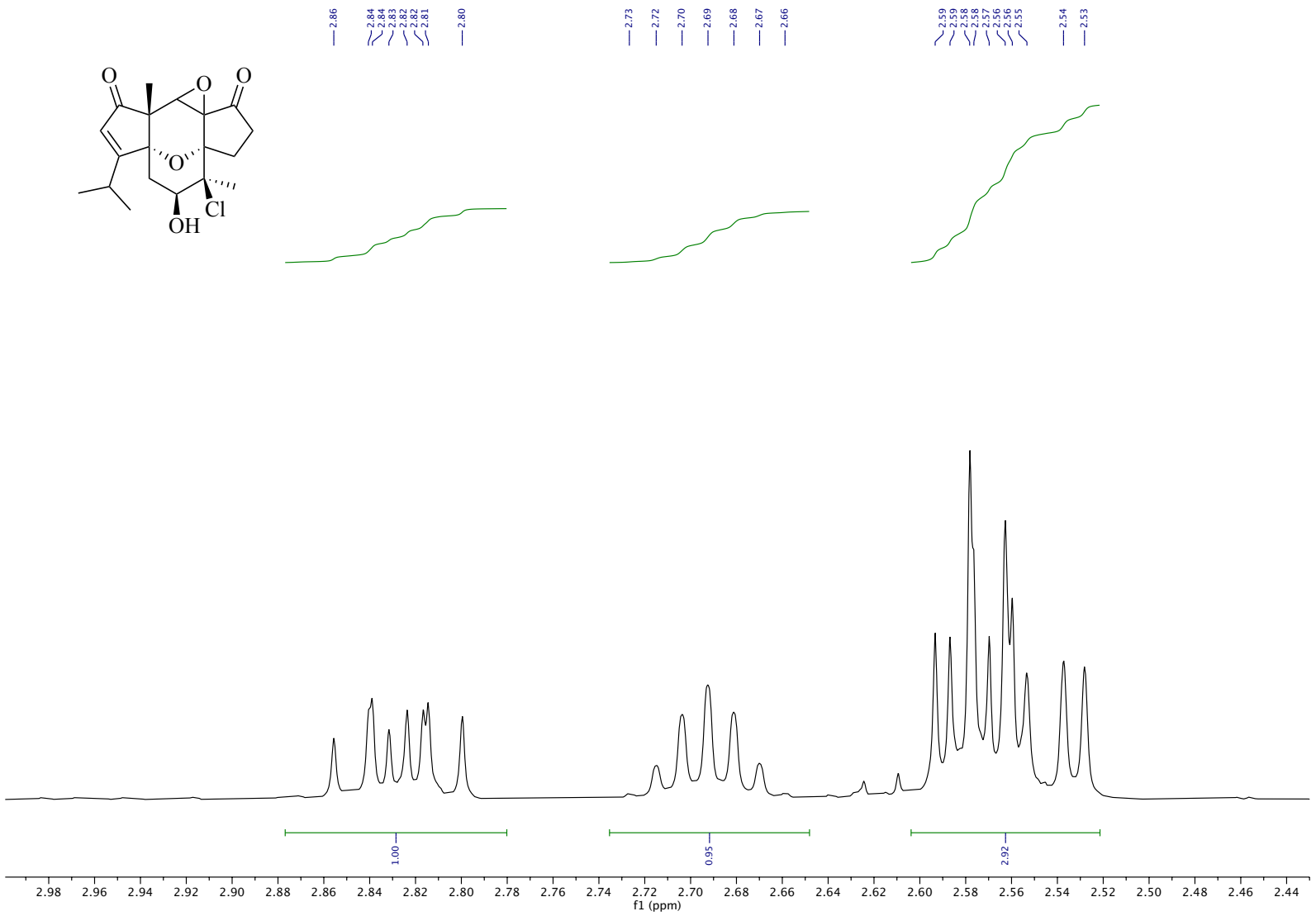

Figure B.70. ^{1}H NMR (600 MHz, $CDCl_3$), **2.37** (inset)

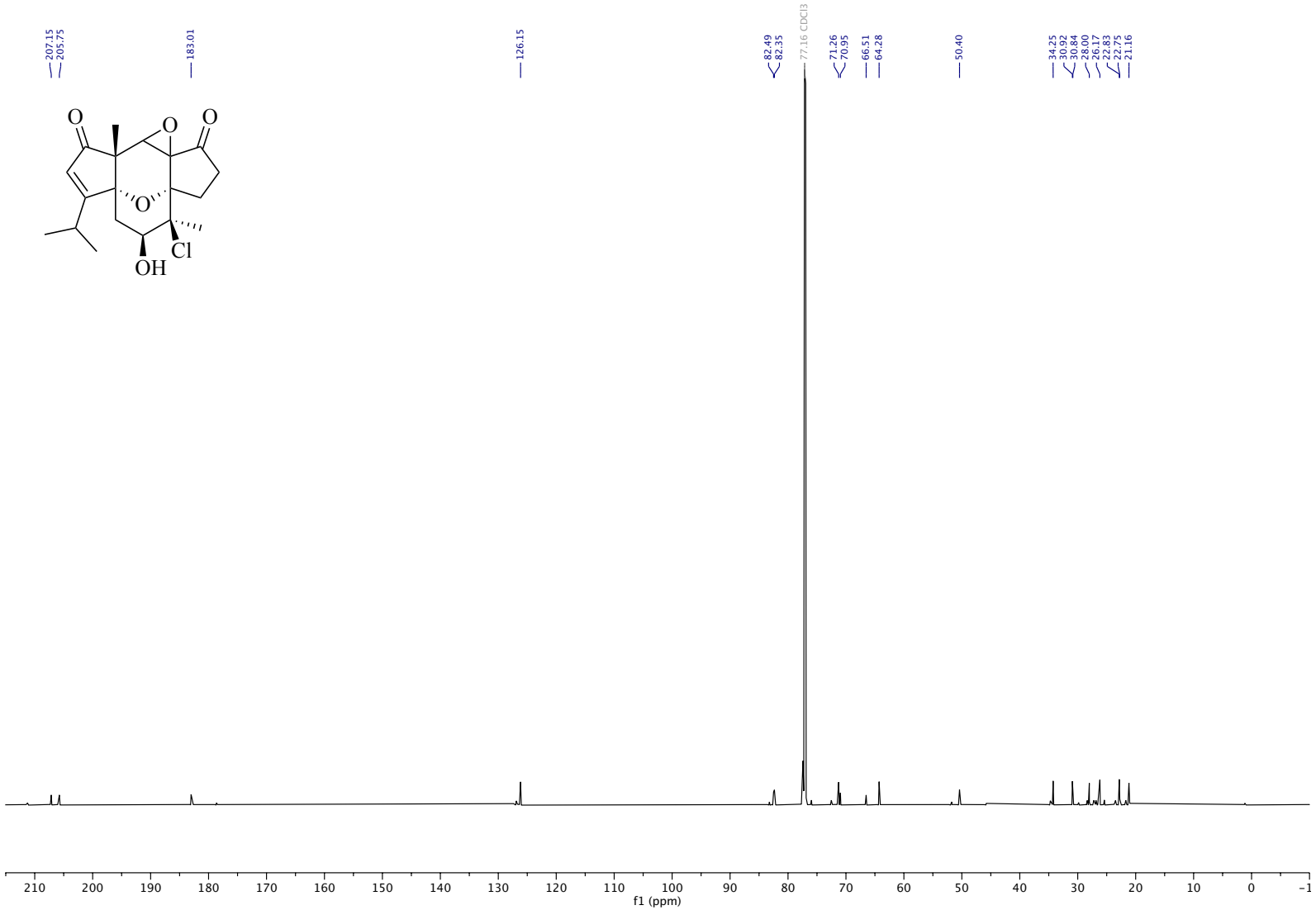

Figure B.71. ^{13}C NMR (151 MHz, $CDCl_3$), **2.37**

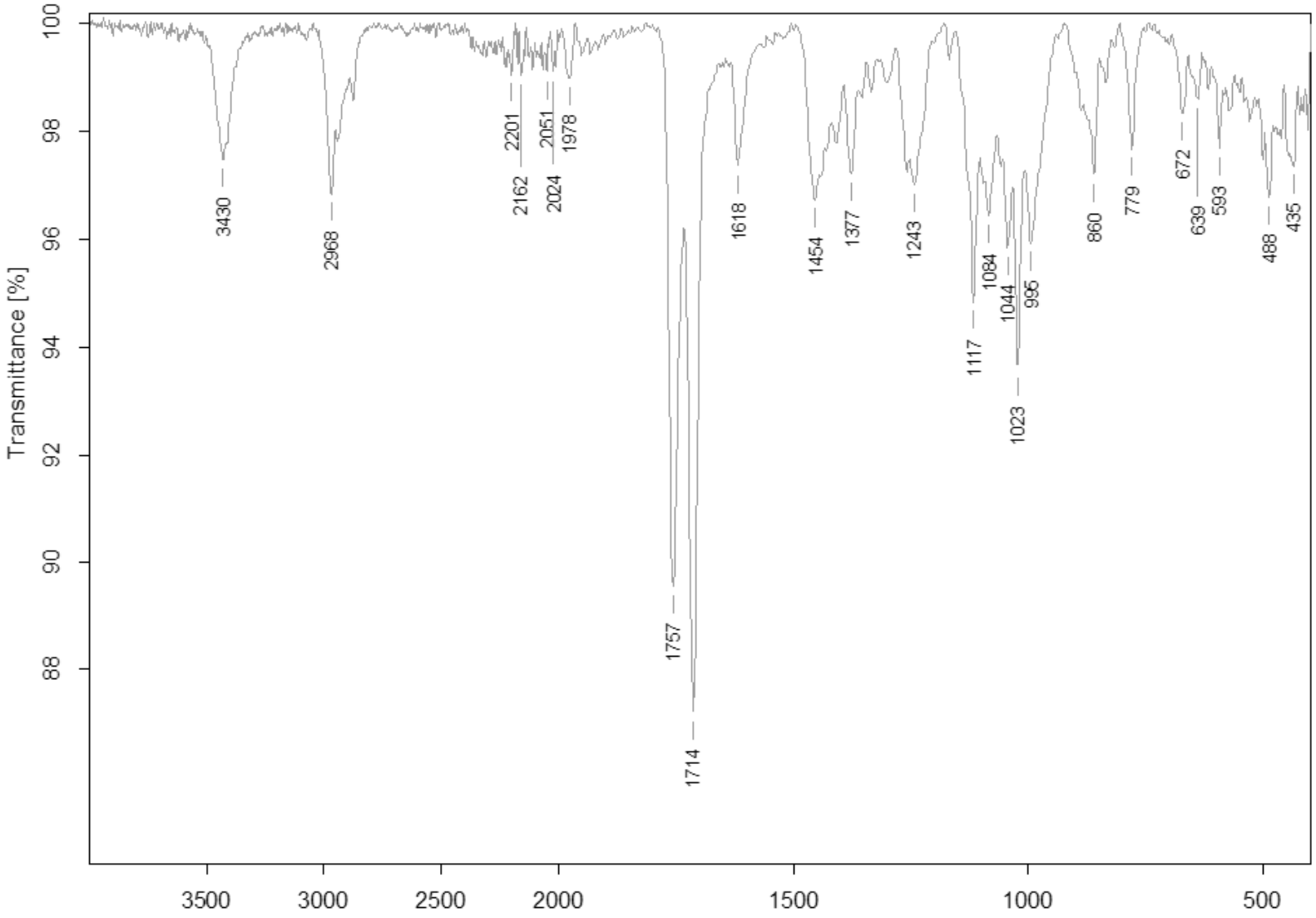

Figure B.72. IR (ATR), **2.37**

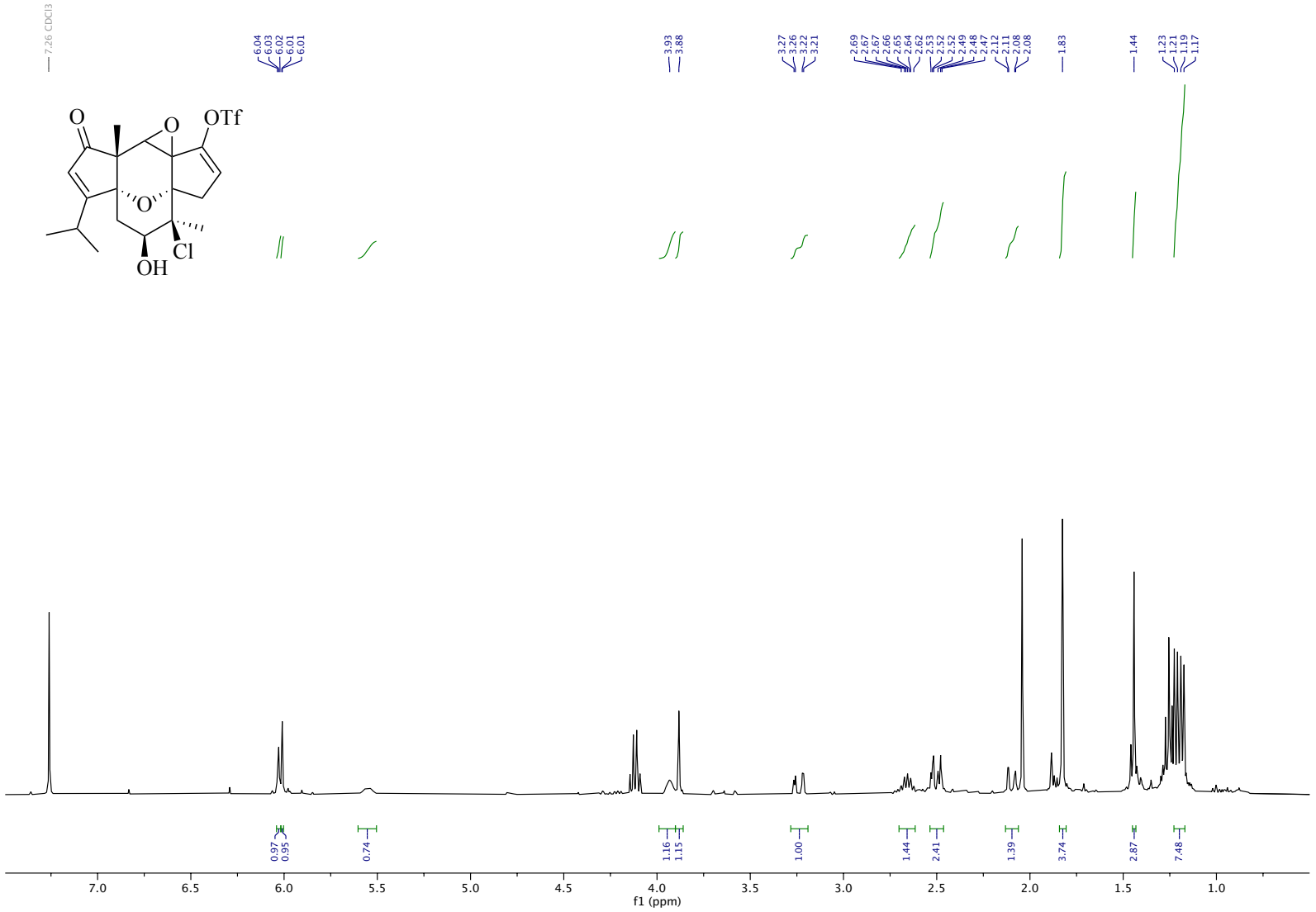

Figure B.73. ^{1}H NMR (600 MHz, $CDCl_3$), **2.39** (Silica plug)

APPENDIX C

X-ray Crystallography Data

*C.1. Crystal Structure Analysis of Cyclooctadiene **2.04***

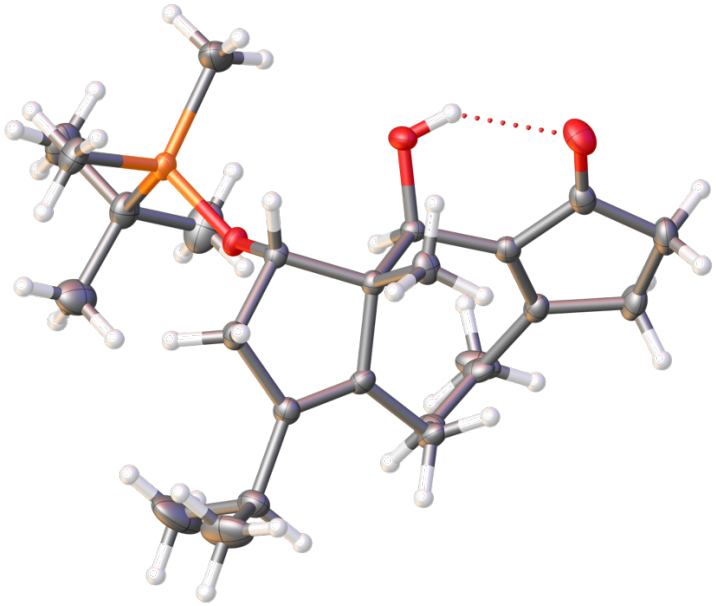

Figure C.1. ORTEP drawing of cyclooctadiene **2.04**

Table C.1. Crystal data and structure refinement for **2.04**.

Identification code	JLW_136	
Empirical formula	C21 H30 O7 Si	
Formula weight	422.54	
Temperature	150(2) K	
Wavelength	0.71073 Å	
Crystal system	Orthorhombic	
Space group	$P2_12_12_1$	
Unit cell dimensions	a = 7.6953(4) Å	a= 90°.
	b = 17.3659(6) Å	b= 90°.
	c = 18.4307(9) Å	g = 90°.
Volume	2463.0(2) $Å^3$	
Z	4	
Density (calculated)	1.139 Mg/m^3	
Absorption coefficient	0.130 mm^{-1}	
F(000)	904	
Crystal size	0.440 x 0.253 x 0.081 mm^3	
Theta range for data collection	2.346 to 26.375°.	
Index ranges	-9<=h<=8, -21<=k<=18, -12<=l<=22	
Reflections collected	5941	
Independent reflections	3911 [R(int) = 0.0612]	
Completeness to theta = 25.242°	90.7 %	
Absorption correction	None	
Max. and min. transmission	0.949 and 0.869	
Refinement method	Full-matrix least-squares on F^2	
Data / restraints / parameters	3911 / 0 / 271	
Goodness-of-fit on F^2	1.212	
Final R indices [I>2sigma(I)]	R1 = 0.0618, wR2 = 0.1559	
R indices (all data)	R1 = 0.1237, wR2 = 0.2560	
Absolute structure parameter	0.02(12)	
Extinction coefficient	n/a	
Largest diff. peak and hole	1.047 and -1.592 $e.Å^{-3}$	

Table C.2. Atomic coordinates (x 10^4) and equivalent isotropic displacement parameters ($Å^2$x 10^3) for **2.04**. U(eq) is defined as one third of the trace of the orthogonalized U^{ij} tensor.

	x	y	z	U(eq)
Si(1)	4877(2)	3467(1)	6556(1)	16(1)
O(1)	3915(5)	6659(3)	4775(3)	27(1)
O(2)	4244(4)	5221(2)	5437(2)	17(1)
O(3)	5884(5)	4296(2)	6634(2)	15(1)
C(1)	5505(7)	6595(3)	4711(3)	18(1)
C(2)	6629(8)	7072(4)	4213(4)	25(1)
C(3)	8431(8)	6699(4)	4256(3)	24(1)
C(4)	8260(7)	6118(3)	4853(3)	15(1)
C(5)	6619(7)	6048(3)	5115(3)	14(1)
C(6)	5977(6)	5447(3)	5641(3)	12(1)
C(7)	5991(6)	5678(3)	6443(3)	12(1)
C(8)	4905(7)	6411(3)	6568(3)	18(1)
C(9)	5271(6)	5013(3)	6909(3)	13(1)
C(10)	3752(8)	3209(4)	7417(4)	26(1)
C(11)	3221(9)	3486(4)	5817(4)	33(2)
C(12)	6732(8)	2788(3)	6342(4)	23(1)
C(13)	7732(10)	3093(4)	5672(5)	41(2)
C(14)	6039(10)	1981(4)	6179(4)	35(2)
C(15)	7978(8)	2749(4)	6988(5)	35(2)
C(16)	6122(6)	5134(3)	7660(3)	15(1)
C(17)	7841(6)	5515(3)	7458(3)	15(1)
C(18)	9327(7)	5541(3)	7989(3)	21(1)
C(19)	10128(12)	4738(5)	8072(7)	61(3)
C(20)	8792(9)	5862(6)	8717(4)	42(2)
C(21)	7791(6)	5792(3)	6788(3)	14(1)
C(22)	9234(7)	6201(3)	6391(3)	17(1)
C(23)	10114(6)	5690(3)	5842(3)	18(1)
C(24)	9726(6)	5661(3)	5144(3)	18(1)
C(25)	10692(7)	5178(4)	4590(4)	28(1)

Table C.3. Bond lengths [Å] and angles [°] for **2.04**.

Si(1)-O(3)	1.641(4)
Si(1)-C(10)	1.862(7)
Si(1)-C(11)	1.865(6)
Si(1)-C(12)	1.893(6)
O(1)-C(1)	1.234(7)
O(2)-C(6)	1.440(6)
O(3)-C(9)	1.426(6)
C(1)-C(5)	1.480(7)
C(1)-C(2)	1.510(8)
C(2)-C(3)	1.533(9)
C(2)-H(14)	0.9900
C(2)-H(19)	0.9900
C(3)-C(4)	1.499(8)
C(3)-H(13)	0.9900
C(3)-H(12)	0.9900
C(4)-C(5)	1.357(8)
C(4)-C(24)	1.480(8)
C(5)-C(6)	1.508(7)
C(6)-C(7)	1.531(7)
C(6)-H(15)	1.0000
C(7)-C(21)	1.536(7)
C(7)-C(8)	1.540(7)
C(7)-C(9)	1.543(7)
C(8)-H(17)	0.9800
C(8)-H(18)	0.9800
C(8)-H(16)	0.9800
C(9)-C(16)	1.545(7)
C(9)-H(29)	1.0000
C(10)-H(10A)	0.9800
C(10)-H(10B)	0.9800
C(10)-H(10C)	0.9800
C(11)-H(11A)	0.9800
C(11)-H(11B)	0.9800
C(11)-H(11C)	0.9800
C(12)-C(14)	1.530(8)
C(12)-C(15)	1.530(9)
C(12)-C(13)	1.549(9)
C(13)-H(7)	0.9800
C(13)-H(8)	0.9800
C(13)-H(9)	0.9800
C(14)-H(1)	0.9800
C(14)-H(3)	0.9800
C(14)-H(30)	0.9800

C(15)-H(4)	0.9800
C(15)-H(6)	0.9800
C(15)-H(5)	0.9800
C(16)-C(17)	1.524(7)
C(16)-H(28)	0.9900
C(16)-H(27)	0.9900
C(17)-C(21)	1.327(8)
C(17)-C(18)	1.506(7)
C(18)-C(20)	1.509(9)
C(18)-C(19)	1.533(10)
C(18)-H(23)	1.0000
C(19)-H(22)	0.9800
C(19)-H(21)	0.9800
C(19)-H(20)	0.9800
C(20)-H(26)	0.9800
C(20)-H(25)	0.9800
C(20)-H(24)	0.9800
C(21)-C(22)	1.506(7)
C(22)-C(23)	1.505(8)
C(22)-H(22A)	0.9900
C(22)-H(22B)	0.9900
C(23)-C(24)	1.323(8)
C(23)-H(23A)	0.9500
C(24)-C(25)	1.515(8)
C(25)-H(11)	0.9800
C(25)-H(10)	0.9800
C(25)-H(2)	0.9800
O(3)-Si(1)-C(10)	110.9(3)
O(3)-Si(1)-C(11)	111.7(3)
C(10)-Si(1)-C(11)	108.0(3)
O(3)-Si(1)-C(12)	102.0(2)
C(10)-Si(1)-C(12)	112.3(3)
C(11)-Si(1)-C(12)	112.0(3)
C(9)-O(3)-Si(1)	129.9(3)
O(1)-C(1)-C(5)	125.7(5)
O(1)-C(1)-C(2)	125.2(5)
C(5)-C(1)-C(2)	109.0(5)
C(1)-C(2)-C(3)	104.8(5)
C(1)-C(2)-H(14)	110.8
C(3)-C(2)-H(14)	110.8
C(1)-C(2)-H(19)	110.8
C(3)-C(2)-H(19)	110.8
H(14)-C(2)-H(19)	108.9
C(4)-C(3)-C(2)	104.1(5)
C(4)-C(3)-H(13)	110.9
C(2)-C(3)-H(13)	110.9

C(4)-C(3)-H(12)	110.9
C(2)-C(3)-H(12)	110.9
H(13)-C(3)-H(12)	109.0
C(5)-C(4)-C(24)	122.2(5)
C(5)-C(4)-C(3)	113.8(5)
C(24)-C(4)-C(3)	124.0(5)
C(4)-C(5)-C(1)	107.6(5)
C(4)-C(5)-C(6)	126.5(5)
C(1)-C(5)-C(6)	125.3(5)
O(2)-C(6)-C(5)	108.9(4)
O(2)-C(6)-C(7)	109.3(4)
C(5)-C(6)-C(7)	115.8(4)
O(2)-C(6)-H(15)	107.5
C(5)-C(6)-H(15)	107.5
C(7)-C(6)-H(15)	107.5
C(6)-C(7)-C(21)	116.0(4)
C(6)-C(7)-C(8)	111.0(4)
C(21)-C(7)-C(8)	108.7(4)
C(6)-C(7)-C(9)	109.8(4)
C(21)-C(7)-C(9)	100.9(4)
C(8)-C(7)-C(9)	109.9(4)
C(7)-C(8)-H(17)	109.5
C(7)-C(8)-H(18)	109.5
H(17)-C(8)-H(18)	109.5
C(7)-C(8)-H(16)	109.5
H(17)-C(8)-H(16)	109.5
H(18)-C(8)-H(16)	109.5
O(3)-C(9)-C(7)	109.7(4)
O(3)-C(9)-C(16)	107.3(4)
C(7)-C(9)-C(16)	104.2(4)
O(3)-C(9)-H(29)	111.8
C(7)-C(9)-H(29)	111.8
C(16)-C(9)-H(29)	111.8
Si(1)-C(10)-H(10A)	109.5
Si(1)-C(10)-H(10B)	109.5
H(10A)-C(10)-H(10B)	109.5
Si(1)-C(10)-H(10C)	109.5
H(10A)-C(10)-H(10C)	109.5
H(10B)-C(10)-H(10C)	109.5
Si(1)-C(11)-H(11A)	109.5
Si(1)-C(11)-H(11B)	109.5
H(11A)-C(11)-H(11B)	109.5
Si(1)-C(11)-H(11C)	109.5
H(11A)-C(11)-H(11C)	109.5
H(11B)-C(11)-H(11C)	109.5
C(14)-C(12)-C(15)	109.3(5)

C(14)-C(12)-C(13)	109.3(6)
C(15)-C(12)-C(13)	108.9(6)
C(14)-C(12)-Si(1)	110.4(4)
C(15)-C(12)-Si(1)	109.7(4)
C(13)-C(12)-Si(1)	109.1(4)
C(12)-C(13)-H(7)	109.5
C(12)-C(13)-H(8)	109.5
H(7)-C(13)-H(8)	109.5
C(12)-C(13)-H(9)	109.5
H(7)-C(13)-H(9)	109.5
H(8)-C(13)-H(9)	109.5
C(12)-C(14)-H(1)	109.5
C(12)-C(14)-H(3)	109.5
H(1)-C(14)-H(3)	109.5
C(12)-C(14)-H(30)	109.5
H(1)-C(14)-H(30)	109.5
H(3)-C(14)-H(30)	109.5
C(12)-C(15)-H(4)	109.5
C(12)-C(15)-H(6)	109.5
H(4)-C(15)-H(6)	109.5
C(12)-C(15)-H(5)	109.5
H(4)-C(15)-H(5)	109.5
H(6)-C(15)-H(5)	109.5
C(17)-C(16)-C(9)	102.0(4)
C(17)-C(16)-H(28)	111.4
C(9)-C(16)-H(28)	111.4
C(17)-C(16)-H(27)	111.4
C(9)-C(16)-H(27)	111.4
H(28)-C(16)-H(27)	109.2
C(21)-C(17)-C(18)	128.0(5)
C(21)-C(17)-C(16)	111.1(4)
C(18)-C(17)-C(16)	120.9(5)
C(17)-C(18)-C(20)	112.4(5)
C(17)-C(18)-C(19)	110.0(5)
C(20)-C(18)-C(19)	110.9(7)
C(17)-C(18)-H(23)	107.8
C(20)-C(18)-H(23)	107.8
C(19)-C(18)-H(23)	107.8
C(18)-C(19)-H(22)	109.5
C(18)-C(19)-H(21)	109.5
H(22)-C(19)-H(21)	109.5
C(18)-C(19)-H(20)	109.5
H(22)-C(19)-H(20)	109.5
H(21)-C(19)-H(20)	109.5
C(18)-C(20)-H(26)	109.5
C(18)-C(20)-H(25)	109.5

H(26)-C(20)-H(25)	109.5
C(18)-C(20)-H(24)	109.5
H(26)-C(20)-H(24)	109.5
H(25)-C(20)-H(24)	109.5
C(17)-C(21)-C(22)	127.0(5)
C(17)-C(21)-C(7)	111.4(4)
C(22)-C(21)-C(7)	121.6(5)
C(23)-C(22)-C(21)	112.4(4)
C(23)-C(22)-H(22A)	109.1
C(21)-C(22)-H(22A)	109.1
C(23)-C(22)-H(22B)	109.1
C(21)-C(22)-H(22B)	109.1
H(22A)-C(22)-H(22B)	107.9
C(24)-C(23)-C(22)	125.1(5)
C(24)-C(23)-H(23A)	117.4
C(22)-C(23)-H(23A)	117.4
C(23)-C(24)-C(4)	120.2(5)
C(23)-C(24)-C(25)	124.5(5)
C(4)-C(24)-C(25)	115.3(5)
C(24)-C(25)-H(11)	109.5
C(24)-C(25)-H(10)	109.5
H(11)-C(25)-H(10)	109.5
C(24)-C(25)-H(2)	109.5
H(11)-C(25)-H(2)	109.5
H(10)-C(25)-H(2)	109.5

Table C.4. Anisotropic displacement parameters ($Å^2 x\ 10^3$) for **2.04**. The anisotropic displacement factor exponent takes the form: $-2p^2[\ h^2\ a^{*2}U^{11} + ...\ + 2\ h\ k\ a^*\ b^*\ U^{12}\ ]$

	U^{11}	U^{22}	U^{33}	U^{23}	U^{13}	U^{12}
Si(1)	22(1)	11(1)	15(1)	1(1)	-2(1)	-4(1)
O(1)	25(2)	27(2)	28(2)	4(2)	-4(2)	9(2)
O(2)	12(2)	21(2)	18(2)	1(2)	-4(1)	-5(1)
O(3)	19(2)	8(2)	20(2)	1(2)	0(1)	-1(1)
C(1)	25(3)	13(2)	16(3)	0(2)	-2(2)	1(2)
C(2)	35(3)	21(3)	20(3)	8(2)	-2(2)	0(2)
C(3)	30(3)	24(3)	16(3)	5(2)	4(2)	-6(2)
C(4)	20(2)	13(2)	12(2)	0(2)	1(2)	-3(2)
C(5)	17(2)	12(2)	13(2)	0(2)	-1(2)	-1(2)
C(6)	9(2)	13(2)	14(2)	1(2)	-2(2)	-1(2)
C(7)	13(2)	10(2)	12(2)	0(2)	0(2)	1(2)
C(8)	23(2)	12(2)	19(3)	-1(2)	2(2)	4(2)
C(9)	13(2)	12(2)	13(2)	1(2)	0(2)	1(2)
C(10)	29(3)	23(3)	27(3)	5(3)	5(2)	-7(2)
C(11)	38(3)	24(3)	37(4)	0(3)	-20(3)	-6(3)
C(12)	33(3)	14(2)	22(3)	-1(2)	1(2)	0(2)
C(13)	45(4)	32(3)	45(5)	2(3)	22(4)	2(3)
C(14)	50(4)	16(3)	40(4)	-4(3)	-1(3)	0(3)
C(15)	27(3)	31(3)	46(4)	-3(3)	-11(3)	9(3)
C(16)	16(2)	17(2)	11(2)	2(2)	2(2)	-1(2)
C(17)	17(2)	14(2)	12(2)	-3(2)	-1(2)	-3(2)
C(18)	20(2)	26(3)	16(3)	1(2)	-5(2)	-4(2)
C(19)	53(5)	43(4)	86(8)	2(5)	-47(5)	16(4)
C(20)	34(3)	78(6)	16(3)	-12(3)	-5(3)	-8(4)
C(21)	14(2)	12(2)	14(2)	-2(2)	2(2)	-3(2)
C(22)	16(2)	20(2)	15(3)	1(2)	1(2)	-10(2)
C(23)	11(2)	24(3)	18(3)	-4(2)	1(2)	-5(2)
C(24)	10(2)	25(3)	19(3)	-1(2)	0(2)	-5(2)
C(25)	16(3)	44(4)	23(3)	-12(3)	-1(2)	7(2)

C.2. Crystal Structure Analysis of Cage **2.20**

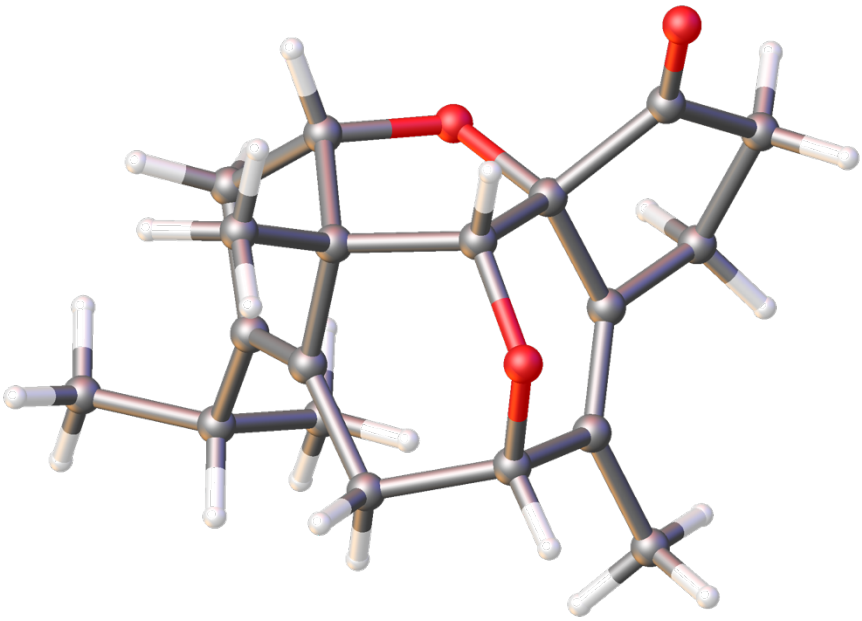

Figure C.2. ORTEP drawing of cage **2.20**

Table C.5. Crystal data and structure refinement for **2.20**.

Identification code	JLW_219	
Empirical formula	C19 H24 O3	
Formula weight	300.38	
Temperature	150(2) K	
Wavelength	0.71073 Å	
Crystal system	Triclinic	
Space group	P -1	
Unit cell dimensions	a = 9.2917(9) Å	a= 97.335(4)°.
	b = 9.3805(9) Å	b= 93.296(4)°.
	c = 9.5697(9) Å	g = 104.993(4)°.
Volume	795.54(13) $Å^3$	
Z	2	
Density (calculated)	1.254 Mg/m^3	
Absorption coefficient	0.083 mm^{-1}	
F(000)	324	
Crystal size	0.297 x 0.270 x 0.240 mm^3	
Theta range for data collection	2.273 to 29.594°.	
Index ranges	-12<=h<=12, -13<=k<=13, -13<=l<=13	
Reflections collected	28538	
Independent reflections	4416 [R(int) = 0.0356]	
Completeness to theta = 25.242°	98.9 %	
Absorption correction	Semi-empirical from equivalents	
Max. and min. transmission	0.929 and 0.925	
Refinement method	Full-matrix least-squares on F^2	
Data / restraints / parameters	4416 / 0 / 203	
Goodness-of-fit on F^2	0.974	
Final R indices [I>2sigma(I)]	R1 = 0.0405, wR2 = 0.1130	
R indices (all data)	R1 = 0.0432, wR2 = 0.1157	
Extinction coefficient	n/a	
Largest diff. peak and hole	0.415 and -0.170 $e.Å^{-3}$	

Table C.6. Atomic coordinates (x 10^4) and equivalent isotropic displacement parameters ($Å^2$x 10^3) for **2.20**. U(eq) is defined as one third of the trace of the orthogonalized U^{ij} tensor.

	x	y	z	U(eq)
O(1)	3887(1)	1805(1)	10081(1)	41(1)
O(2)	5326(1)	1133(1)	7313(1)	19(1)
O(3)	7964(1)	4029(1)	9705(1)	21(1)
C(1)	4189(1)	2377(1)	9043(1)	24(1)
C(2)	3229(1)	3145(1)	8239(1)	28(1)
C(3)	4148(1)	3741(1)	7043(1)	27(1)
C(4)	5731(1)	3830(1)	7593(1)	19(1)
C(5)	5645(1)	2487(1)	8326(1)	16(1)
C(6)	6978(1)	4942(1)	7686(1)	20(1)
C(7)	8362(1)	4838(1)	8539(1)	20(1)
C(8)	9387(1)	4123(1)	7637(1)	20(1)
C(9)	8561(1)	2525(1)	7155(1)	16(1)
C(10)	8147(1)	1776(1)	5844(1)	16(1)
C(11)	7086(1)	254(1)	5893(1)	18(1)
C(12)	6561(1)	444(1)	7373(1)	16(1)
C(13)	7850(1)	1619(1)	8270(1)	16(1)
C(14)	7063(1)	2543(1)	9240(1)	17(1)
C(15)	7129(1)	6330(1)	7013(1)	29(1)
C(16)	8953(1)	995(1)	9085(1)	22(1)
C(17)	8540(1)	2333(1)	4472(1)	21(1)
C(18)	7260(1)	2855(2)	3819(1)	34(1)
C(19)	8917(2)	1148(1)	3422(1)	34(1)

Table C.7. Bond lengths [Å] and angles [°] for **2.20**.

O(1)-C(1)	1.2019(13)
O(2)-C(5)	1.4489(10)
O(2)-C(12)	1.4570(10)
O(3)-C(14)	1.4270(11)
O(3)-C(7)	1.4414(11)
C(1)-C(2)	1.5165(15)
C(1)-C(5)	1.5383(13)
C(2)-C(3)	1.5433(16)
C(3)-C(4)	1.5120(13)
C(4)-C(6)	1.3335(13)
C(4)-C(5)	1.5049(12)
C(5)-C(14)	1.5239(12)
C(6)-C(15)	1.5029(13)
C(6)-C(7)	1.5136(13)
C(7)-C(8)	1.5427(13)
C(8)-C(9)	1.4953(12)
C(9)-C(10)	1.3394(12)
C(9)-C(13)	1.5232(12)
C(10)-C(17)	1.5045(12)
C(10)-C(11)	1.5190(12)
C(11)-C(12)	1.5278(12)
C(12)-C(13)	1.5311(12)
C(13)-C(16)	1.5276(12)
C(13)-C(14)	1.5321(12)
C(17)-C(19)	1.5251(14)
C(17)-C(18)	1.5294(15)
C(5)-O(2)-C(12)	110.70(6)
C(14)-O(3)-C(7)	112.05(6)
O(1)-C(1)-C(2)	126.30(9)
O(1)-C(1)-C(5)	125.31(10)
C(2)-C(1)-C(5)	108.37(8)
C(1)-C(2)-C(3)	105.66(8)
C(4)-C(3)-C(2)	102.72(8)
C(6)-C(4)-C(5)	122.26(8)
C(6)-C(4)-C(3)	130.25(9)
C(5)-C(4)-C(3)	106.56(8)
O(2)-C(5)-C(4)	111.12(7)
O(2)-C(5)-C(14)	106.62(7)
C(4)-C(5)-C(14)	114.70(7)
O(2)-C(5)-C(1)	104.32(7)
C(4)-C(5)-C(1)	101.29(7)
C(14)-C(5)-C(1)	118.33(8)
C(4)-C(6)-C(15)	124.98(9)

C(4)-C(6)-C(7)	118.85(8)
C(15)-C(6)-C(7)	116.17(9)
O(3)-C(7)-C(6)	110.96(7)
O(3)-C(7)-C(8)	109.71(7)
C(6)-C(7)-C(8)	112.96(7)
C(9)-C(8)-C(7)	107.46(7)
C(10)-C(9)-C(8)	130.16(8)
C(10)-C(9)-C(13)	111.77(8)
C(8)-C(9)-C(13)	117.35(7)
C(9)-C(10)-C(17)	127.28(8)
C(9)-C(10)-C(11)	110.37(8)
C(17)-C(10)-C(11)	122.22(8)
C(10)-C(11)-C(12)	102.34(7)
O(2)-C(12)-C(11)	108.44(7)
O(2)-C(12)-C(13)	105.26(7)
C(11)-C(12)-C(13)	105.38(7)
C(9)-C(13)-C(16)	113.02(7)
C(9)-C(13)-C(12)	101.29(7)
C(16)-C(13)-C(12)	115.06(7)
C(9)-C(13)-C(14)	109.68(7)
C(16)-C(13)-C(14)	112.97(7)
C(12)-C(13)-C(14)	103.86(7)
O(3)-C(14)-C(5)	112.85(7)
O(3)-C(14)-C(13)	112.74(7)
C(5)-C(14)-C(13)	103.11(7)
C(10)-C(17)-C(19)	111.79(8)
C(10)-C(17)-C(18)	110.43(8)
C(19)-C(17)-C(18)	110.13(9)

Table C.8 Anisotropic displacement parameters ($Å^2 x\ 10^3$) for **2.20**. The anisotropic displacement factor exponent takes the form: $-2p^2[\ h^2\ a^{*2}U^{11} + ... + 2\ h\ k\ a^*\ b^*\ U^{12}\ ]$

	U^{11}	U^{22}	U^{33}	U^{23}	U^{13}	U^{12}
O(1)	38(1)	55(1)	38(1)	22(1)	21(1)	16(1)
O(2)	16(1)	18(1)	21(1)	-2(1)	-1(1)	6(1)
O(3)	26(1)	19(1)	15(1)	-2(1)	-1(1)	4(1)
C(1)	22(1)	24(1)	25(1)	2(1)	8(1)	7(1)
C(2)	21(1)	29(1)	37(1)	2(1)	6(1)	11(1)
C(3)	24(1)	29(1)	32(1)	8(1)	0(1)	13(1)
C(4)	22(1)	19(1)	18(1)	4(1)	3(1)	10(1)
C(5)	18(1)	16(1)	16(1)	2(1)	3(1)	6(1)
C(6)	26(1)	17(1)	19(1)	2(1)	5(1)	9(1)
C(7)	23(1)	15(1)	19(1)	-1(1)	1(1)	3(1)
C(8)	18(1)	18(1)	21(1)	0(1)	1(1)	2(1)
C(9)	15(1)	16(1)	16(1)	2(1)	1(1)	5(1)
C(10)	16(1)	18(1)	16(1)	1(1)	2(1)	6(1)
C(11)	18(1)	16(1)	18(1)	-1(1)	0(1)	5(1)
C(12)	17(1)	14(1)	18(1)	2(1)	0(1)	5(1)
C(13)	18(1)	16(1)	14(1)	2(1)	0(1)	5(1)
C(14)	20(1)	17(1)	14(1)	2(1)	1(1)	5(1)
C(15)	37(1)	20(1)	34(1)	10(1)	9(1)	10(1)
C(16)	23(1)	24(1)	21(1)	4(1)	-3(1)	10(1)
C(17)	23(1)	24(1)	16(1)	2(1)	4(1)	6(1)
C(18)	40(1)	42(1)	26(1)	14(1)	4(1)	20(1)
C(19)	43(1)	42(1)	22(1)	0(1)	12(1)	19(1)

C.3. Crystal Structure Analysis of Allylic Alcohol **2.23**

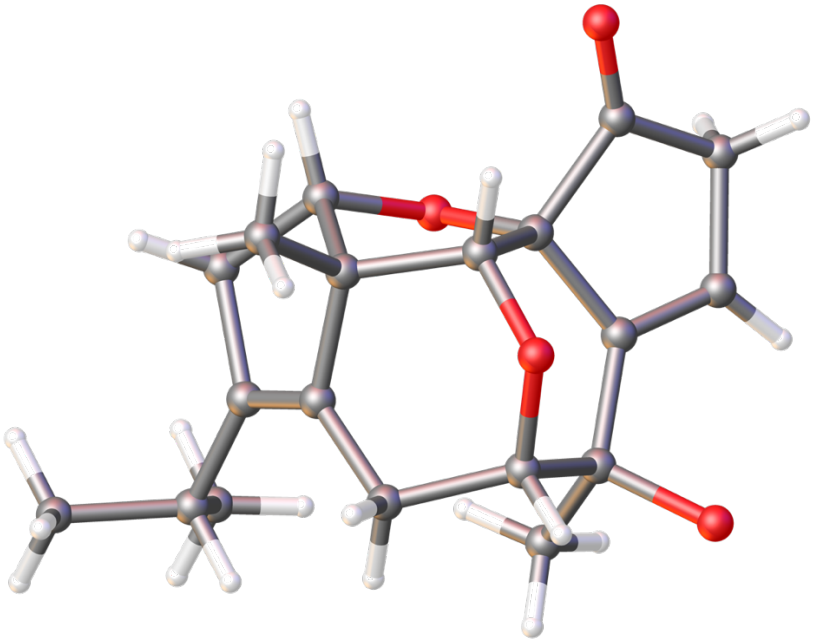

Figure C.3. ORTEP drawing of poor-diffracting allylic alcohol **2.23**

BIBLIOGRAPHY

Zhang, L.-J.; Bi, D.-W.; Hu, J.; Mu, W.-H.; Li, Y.-P.; Xia, G.-H.; Yang, L.; Li, X.-N.; Liang, X.-S.; Wang, L.-Q. *Org. Lett.* **2017**, *19*, 4315–4318.

Wollenweber, E.; Seigler, D. S. *Phytochem.* **1982**, *21*, 1063–1066.

Tanrisever, N.; Fronczek, F. R.; Fischer, N. H.; Williamson, G. B. *Phytochem.* **1986**, *26*, 175–179.

Pescitelli, G. *Marine Drugs* **2018**, *16*, 388.

Barluenga, J.; Valdés, C. *Angew. Chem., Int. Ed.* **2011**, *50*, 7486–7500.

Bamford, W. R.; Stevens, T. S. 924. *J. Chem.l Soc.* **1952**, 4735.

Pawar, G. G.; Tiwari, V. K.; Jena, H. S.; Kapur, M. *Chem. Eur. J.* **2015**, *21*, 9905

Barton, D. H.; McCombie, S. W. *J. Chem. Soc., Perkin Trans.* **1975**, 16, 1574.

Iwasaki, K.; Wan, K. K.; Oppedisano, A.; Crossley, S. W.; Shenvi, R. *J. Am. Chem. Soc.* **2014**, *136*, 1300–1303.

Pearlman,W. M. *Tetrahedron Lett.* **1967**, 8 , 1663 —1664

Van De Water, R. W.; Hoarau, C.; Pettus, T. R. R. *Tetrahedron Lett.* **2003**, *44*, 5109–5113.

Timmerman, J. C.; Sims, N. J.; Wood, J. L. *J. Am. Chem. Soc.* **2019**, *141*, 10082– 10090

Holder, J. C.; Marziale, A. N.; Gatti, M.; Mao, B.; Stoltz, B. M. *Chem. Eur. J.* **2013**, *19*, 74

Tsuji, J.; Takahashi, H.; Morikawa, M. *Tetrahedron Lett.* **1965**, *6*, 4387–4388.

Li, F.; Lin, S.; Zhang, S.; Pan, L.; Chai, C.; Su, J.-C.; Yang, B.; Liu, J.; Wang, J.; Hu, Z.; Zhang, Y. *J. Nat. Prod.* **2020**, *83*, 1931–1938.

Cordovilla, C.; Bartolomé, C.; Martínez-Ilarduya, J. M.; Espinet, P. *ACS Catal.* **2015**, *5*, 3040–3053.

Brooks, D. W.; Grothaus, P. G.; Irwin, W. L. *J. Org. Chem.* **1982**, *47*, 2820–2821.

Carr, J. M.; Snowden, T. S. *Tetrahedron* **2008**, *64*, 2897–2905.

Liu, L. L.; Chiu, P. *Chem. Comm.* **2011**, *47* (12), 3416.

Wu, G.-J.; Zhang, Y.-H.; Tan, D.-X.; He, L.; Cao, B.-C.; He, Y.-P.; Han, F.-S. *J. Org. Chem.* **2019**, *84*, 3223–3238.

Krueger, A. C.; Warren, K. M.; Carroll, W. M.; Pratt, J. K.; Hutchins, D. K. WO2012083170A1, 2012.

He, F.; Bo, Y.; Altom, J. D.; Corey, E. J. *J. Am. Chem. Soc.* **1999**, *121*, 6771–6772.

Smith, A. B.; Branca, S. J.; Pilla, N. N.; Guaciaro, M. A. *J. Org. Chem.* **1982**, *47*, 1855–1869.

Bader, S. J.; Snapper, M. L. *J. Am. Chem. Soc.* **2005**, *127*, 1201–1205.

Tsuna, K.; Noguchi, N.; Nakada, M. *Chem. Eur. J.* **2013**, *19*, 5476–5486.

Paquette, L. A.; Romine, J. L.; Lin, H.-S. *Tetrahedron Lett.* **1987**, *28*, 31–34.

Bartlett, P. A.; Mori, I.; Bose, J. A. *J. Org. Chem.* **1989**, *54*, 3236–3239.

Mander, L. N. *Comp. Org. Syn.* **1991**, 489–521.

Stork, G.; Sher, P. M.; Chen, H. L. *J. Am. Chem. Soc.* **1986**, *108*, 6384–6385.

Hoveyda, A. H.; Evans, D. A.; Fu, G. C. *Chem. Rev.* **1993**, *93*, 1307–1370.

Kolb, H. C.; VanNieuwenhze, M. S.; Sharpless, K. B. *Chem. Rev.* **1994**, *94*, 2483–2547.

Xue, Y.; Dong, G. *J. Am. Chem. Soc.* **2021**, *143* (22), 8272–8277.

Nagata, W.; Yoshioka, M. *Tetrahedron Lett.* **1966**, *7*, 1913–1918.

Hafeman, N. J.; Loskot, S. A.; Reimann, C. E.; Pritchett, B. P.; Virgil, S. C.; Stoltz, B. M. *J. Am. Chem. Soc.* **2020**, *142*, 8585–8590.

ABOUT THE AUTHOR

Noah J. Sims was born in Syracuse, NY on October 18th, 1996 to Jeffrey and Stacey Sims. Spending most of his early and late childhood in a small urban area outside of Syracuse, he was homeschooled until 4th grade. His love for science and experimentation was fostered greatly by curiosity as well as his parents support. In 4th grade he went to public school, for the first time, at Fabius-Pompey Elementary. He would then remain at the Fabius-Pompey school district until his graduation in 2014. While in high-school he had his first chemistry class where he instantly fell in love. It was the perfect combination of math, logic, problem-solving, and creativity. He would then later take AP chemistry to further his knowledge. Upon graduation, he then went to the University of Rochester where he initially was a biology major on a pre-med track. After the first year, he was unsure if that was the right track for him, and after taking organic chemistry his sophomore year – he knew he wanted to investigate this field more. Eventually switching to a chemistry major late in his college career, he went on to do research under the supervision of Robert K. Boeckman Jr. He was exposed to total synthesis for the first time working on projects like apoptolidin A and nakadormain A. Recommended by Professor Boeckman, he went on to apply to Baylor University in hopes of working under the tutelage of John L. Wood. To his glee, his goals came to fruition and he started at Baylor University in 2018 after receiving his B.S. in Chemistry. At Baylor University, Noah worked on more total synthesis – specifically on caesalpinnone A, and a family of fusicoccane terpenoids. Upon completion

of his graduate work, he defended in September of 2022. He is excited about his future in learning new types of chemistry and beyond.